Conference Program

January 20-22 | DoubleTree by Hilton Orlando at Sea World® | Orlando, Florida USA

ELECTRONIC MATERIALS AND APPLICATIONS 2016

Electronic Materials and Applications 2016 addresses emerging needs, opportunities and key challenges in the field of electronic materials and applications. Technical presentations highlight advancements in materials and devices for electronics, sensors, energy generation and storage, photovoltaics, and LEDs.

Scan for meeting app.

ceramics.org/ema2016

The American Ceramic Society
www.ceramics.org

Welcome

Welcome to Electronic Materials and Applications 2016. Jointly programmed by the Electronics Division and Basic Science Division of The American Ceramic Society, EMA 2016 is the seventh in a series of annual international meetings focused on electroceramic materials and their applications in electronic, magnetic, dielectric and optical components, devices and systems.

The 2016 meeting features symposia focused on structure-processing-property relationships; composites; computational design; functional thin films; ionic conductors; LEDs and photovoltaics; multiferroics; superconductors; multi-scale structure in perovskites; thermoelectrics; and thin film and interface stability. In addition to the technical symposia, EMA 2016 also features a poster and networking session (Wed, 5:30-7:30 p.m., Arctic/Atlantic), Basic Science Division tutorial. (Wed evening, 7:45-9:45 p.m., Coral A) and lunchtime sessions featuring the finalists for the best student presentation awards (Wed and Thurs 12:40-1:50 p.m., Coral A) with boxed lunches provided for the first 32 attendees, thanks to our generous sponsors. The conference continues with the dinner and awards banquet (Thurs, 7:00-9:00 p.m., Arctic/Atlantic) and the grand finale of the meeting: a light-hearted session on Learning from Failure (Fri, 5:45-6:45 p.m., Indian). All of these activities are included in the meeting registration, and everyone is encouraged to attend!

The meeting also features plenary lectures by distinguished scientists, including Darrell Schlom, Herbert Fisk Johnson Professor of Industrial Chemistry, Cornell University; James Warren, technical program director for materials genomics, Material Measurement Laboratory, National Institute of Standards and Technology; and Thomas Detzel, senior manager, GaN Technology Development, Infineon Technologies Austria AG. The technical program, which includes invited lectures, contributed papers, and poster presentations, will provide ample opportunity for the exchange of information and ideas on the latest developments in the theory, experimental investigation and applications of electroceramic materials. The participants represent an international mix of industrial, university, and federal laboratory researchers, engineers, technologists and leaders.

We are pleased to build on the previous successes of this conference series in providing a distinctive forum to address emerging needs, opportunities and key challenges in the field of electronic materials and applications. We anticipate that this year's meeting will continue to highlight the most recent scientific advances and technological innovations in the field, and to facilitate the interactions and collaborations that will help to shape its future.

The Electronics Division, Basic Science Division, symposium organizers, and staff from The American Ceramic Society thank you for joining us for EMA 2016. We hope you have a rewarding and beneficial meeting experience and very much look forward to your continued participation in future EMA meetings.

Organizers

Brady Gibbons
Electronics Division

John Blendell
Basic Science Division

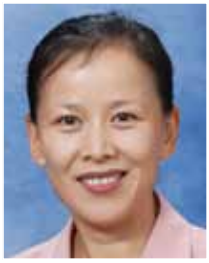

Haiyan Wang
Electronics Division

Dominique Chatain
Basic Science Division

Table of Contents

Final Program

Basic Science Division Officers

Chair: Shen Dillon, University of Illinois, USA
Chair-Elect: Xingbo Liu, West Virginia University, USA
Vice Chair: Dunbar Birnie, Rutgers University, USA
Secretary: Paul Salvador, Carnegie Mellon University, USA

Electronics Division Officers

Trustee: Winnie Wong-Ng
Chair: Haiyan Wang, Texas A&M University, USA
Chair Elect: Geoff Brennecka, Colorado School of Mines, USA
Vice Chair: Brady Gibbons, Oregon State University; USA
Secretary: Rick Ubic, Boise State University, USA
Secretary-Elect: Jon Ihlefeld, Sandia National Laboratories, USA

Schedule At A Glance

Tuesday, January 19		
Registration	5:00 p.m. – 6:30 p.m.	Oceans Ballroom Foyer
Wednesday, January 20		
Registration	7:30 a.m. – 6:00 p.m.	Oceans Ballroom Foyer
Plenary session I – Darrell Schlom, Cornell University	8:30 a.m. – 9:30 a.m.	Indian
Coffee break	9:30 a.m. – 10:00 a.m.	Atlantic
Concurrent technical sessions	10:00 a.m. – 12:30 p.m.	Indian, Pacific, Coral A & B, Mediterranean A, B, C
Poster session set-up	12:00 p.m. – 5:00 p.m.	Arctic/Atlantic
Lunch on own	12:30 p.m. – 2:00 p.m.	
Student award finalist presentations	12:45 p.m. – 1:50 p.m.	Coral A
Concurrent technical sessions	2:00 p.m. – 5:30 p.m.	Indian, Pacific, Coral A & B, Mediterranean A, B, C
Coffee break	3:30 p.m. – 4:00 p.m.	Atlantic
Poster session & reception	5:30 p.m. – 7:30 p.m.	Arctic/Atlantic
BSD Tutorial: Structure and Kinetics of Interfaces in Ceramics	7:45 p.m. – 9:45 p.m.	Coral A
Thursday, January 21		
Registration	7:30 a.m. – 5:30 p.m.	Oceans Ballroom Foyer
Plenary session II – James Warren, NIST	8:30 a.m. – 9:30 a.m.	Indian
Coffee break	9:30 a.m. – 10:00 a.m.	Atlantic
Concurrent technical sessions	10:00 a.m. – 12:30 p.m.	Indian, Pacific, Coral A & B, Mediterranean A, B, C
Lunch on own	12:30 p.m. – 2:00 p.m.	
Student award finalist presentations	12:45 p.m. – 1:45 p.m.	Coral A
Concurrent technical sessions	2:00 p.m. – 5:30 p.m.	Indian, Pacific, Coral A & B, Mediterranean A, B, C
Coffee break	3:30 p.m. – 4:00 p.m.	Atlantic
YP Reception	5:30 p.m. – 6:30 p.m.	Barefoot Bar
Conference dinner	7:00 p.m. – 9:00 p.m.	Arctic/Atlantic
Friday, January 22		
Registration	7:30 a.m. – 5:30 p.m.	Oceans Ballroom Foyer
Plenary session III – Thomas Detzel, Infineon	8:30 a.m. – 9:30 a.m.	Indian
Coffee break	9:30 a.m. – 10:00 a.m.	Atlantic
Concurrent technical sessions	10:00 a.m. – 12:30 p.m.	Indian, Pacific, Coral A & B, Mediterranean A, B, C
Lunch on own	12:30 p.m. – 2:00 p.m.	
Concurrent technical sessions	2:00 p.m. – 5:30 p.m.	Indian, Pacific, Coral A & B, Mediterranean A, B, C
Coffee break	3:30 p.m. – 4:00 p.m.	Atlantic
Failure—The Greatest Teacher	5:45 p.m. – 6:45 p.m.	Indian

2016 Conference Sponsors

Special thanks to our sponsors for their generosity

3M

MTI KJ GROUP

SCIENCE TO SHAPE THE FUTURE OF THE ARMY
ARMY RESEARCH OFFICE
1951

Center for Integrated Nanotechnologies
CINT
Sandia
Los Alamos

RADIANT TECHNOLOGIES, INC.

Media Sponsors

AMERICAN CERAMIC SOCIETY bulletin
emerging ceramics & glass technology

CeramicTechToday
FROM THE AMERICAN CERAMIC SOCIETY

CERAMIC APPLICATIONS
Components for high performance

The Center for Integrated Nanotechnologies

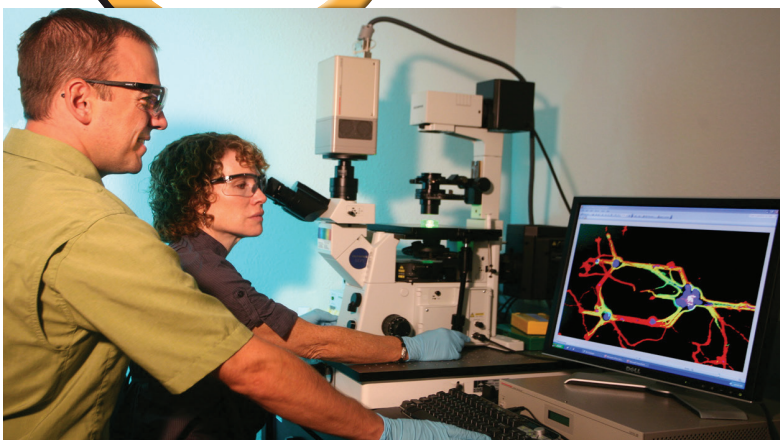

One Scientific Community Focused on Nanoscience Integration

The Center for Integrated Nanotechnologies (CINT) is a Department of Energy/ Office of Science Nanoscale Science Research Center (NSRC) operating as a national user facility devoted to establishing the scientific principles that govern the design, performance, and integration of nanoscale materials. Through its Core Facility in Albuquerque and Gateway to Los Alamos Facility, CINT provides open access to tools and expertise needed to explore the continuum from scientific discovery to the integration of nanostructures into the micro- and macro world.

Science Thrusts

Integration is the key to exploiting the novel properties of nanoscale materials and subsequently creating new nanotechnologies to benefit society. Hence, the CINT scientific community is built around nanomaterials integration. The scientific staff and capabilities at CINT are organized into four interdisciplinary Science Thrusts:

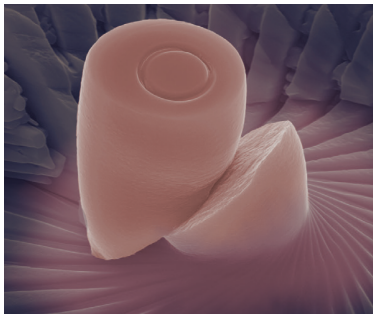

Nanoscale Electronics & Mechanics

Control of electronic transport and wave functions, and mechanical coupling and properties using nanomaterials and integrated structures.

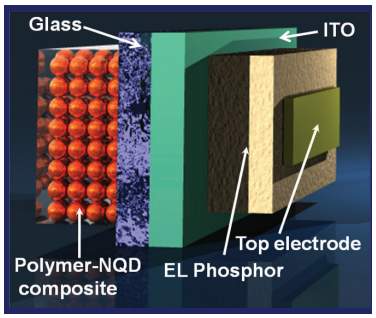

Nanophotonics & Optical Nanomaterials

Synthesis, excitation and energy transformations of optically active nano materials and collective or emergent electromagnetic phenomena (plasmonics, metamaterials, photonic lattices).

Soft, Biological & Composite Nanomaterials

Solution-based materials synthesis and assembly of soft, composite and artificial bio-mimetic nanosystems.

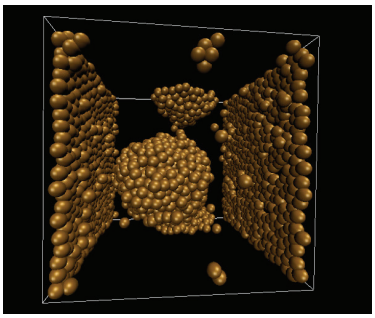

Theory & Simulation of Nanoscale Phenomena

Assembly, interfacial interactions, and emergent properties of nanoscale systems, including their electronic, magnetic, and optical properties.

User Program

CINT operates as a national user facility providing access to state-of-the-art facilities staffed by laboratory scientists, post-doctoral fellows and technical support personnel who are leaders in the CINT scientific thrust areas. Access is via peer-reviewed technical proposals, for independent or collaborative research, submitted in response to semi-annual Calls for User Proposals. Pre-competitive research that will be published in the open literature can be approved for no-fee access to CINT. Proprietary research may be conducted in accord with Federal regulations for full-cost recovery. CINT cannot provide funding to users.

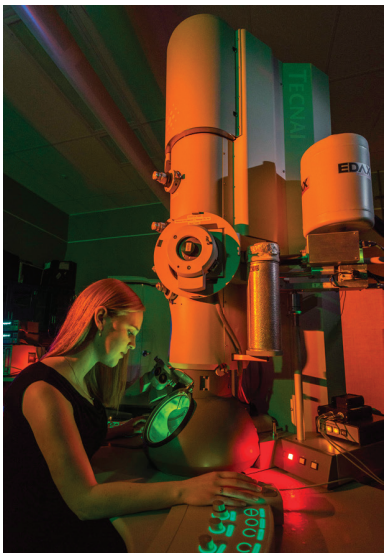

Selected CINT Capabilities

Synthesis and fabrication

- Quantum dots, nanoparticles
- Biomolecular composites
- Semiconductor nanowires
- Metamaterials and plasmonic nanomaterials
- Semiconductor molecular beam epitaxy
- Epitaxial nanocomposite films pulsed laser deposition, laser molecular beam epitaxy
- CVD for 2D nanostructured films
- Dip-pen nanolithography
- Integration lab: A suite of processing tools for fabrication

Characterization

- 3D tracking images
- Ultrafast optical spectroscopies
- In situ transmission electron microscopy
- Optomechanics
- Quantum transport
- Nanomechanics and nanomanipulator
- Discovery platforms
- Holographic optical trapping

Theory

- Molecular dynamics and Monte Carlo simulations
- Classical and quantum density functional theory
- First-principles density-functional theory + dynamical mean-field theory for strongly correlated electronic systems
- Exact-diagonalization approach
- Quantum dynamics and pump-probe spectroscopy in coupled and strongly correlated electronic systems
- Non-adiabatic excited state molecular dynamics in molecules

2016 Plenary Speakers INDIAN ROOM

8:30 a.m. – 9:30 a.m. | Wednesday, January 20

Darrell Schlom, Herbert Fisk Johnson professor of industrial chemistry, Cornell University

Title: *Thin-Film Alchemy: Using Strain and Dimensionality to Unleash the Hidden Properties of Oxides*

Biography: Darrell Schlom is the Herbert Fisk Johnson professor of Industrial Chemistry in the Department of Materials Science and Engineering at Cornell University. After receiving a B.S. degree from Caltech, he did graduate work at Stanford University, receiving an M.S. in Electrical Engineering and a Ph.D. in Materials Science and Engineering. He was then a post-doc at IBM's research lab in Zurich, Switzerland in the oxide superconductors and novel materials group managed by Nobel Prize winners J. Georg Bednorz and K. Alex Müller. He has received various awards including an Alexander von Humboldt Research Fellowship and the MRS Medal. He has published over 500 papers and 8 patents resulting in an h-index of 68 and over 21,000 citations. He is a Fellow of both the American Physical Society and the Materials Research Society.

8:30 a.m. – 9:30 a.m. | Thurday, January 21

James Warren, technical program director for materials genomics material measurement lab, National Institute of Standards and Technology

Title: *The Materials Genome Initiative: NIST, Data, and Open Science*

Biography: James A. Warren is the director of the materials genome program in the Materials Measurement Laboratory of NIST. After receiving his Ph.D. in theoretical physics at the University of California, Santa Barbara, which was preceded by an A.B. (also in Physics) from Dartmouth College in 1992, he took a position as an NRC post-doc in the metallurgy division at NIST. In 1995, with three other junior NIST staff members, he co-founded the NIST Center for Theoretical and Computational Materials Science, which he has directed since 2001. From 2005-2013 he was the leader of the thermodynamics and kinetics group. His research has been broadly concerned with developing both models of materials phenomena, and the tools to enable the solution of these models. Specific foci over the years has included solidification, pattern formation, grain structures, creep, diffusion, wetting, and spreading in metals. In 2010-11, Warren was part of the ad hoc committee within the National Science and Technology Council (NSTC) that crafted the founding whitepaper on the administration's Materials Genome Initiative (MGI), and has served as the executive secretary of the NSTC MGI subcommittee since 2012.

8:30 a.m. – 9:30 a.m. | Friday, January 22

Thomas Detzel, senior manager GaN technology development, Infineon Technologies Austria AG

Title: *Power Semiconductors*

Biography: Thomas Detzel received the M.S. degree in physics from the University of Konstanz, Konstanz, Germany, and the Ph.D. degree in surface and thin-film physics in 1994 from the Max-Planck-Institute Garching near Munich, Germany. Afterwards he was a Postdoc with the Institut de Physique et Chimie des Matériaux de Strasbourg, Strasbourg, France. In 1995, he was with Rodel Europe GmbH, where he was an application manager for chemical–mechanical polishing. In 1999, he joined Infineon Technologies Austria AG, Villach, Austria, where he was responsible for the metallization development of power integrated circuits. He has been the project manager of different power device developments since 2004, and was leading the research project robust metallization and interconnect at the Competence Center for Automotive and Industrial Electronics from 2006-2011. Since 2011 he has been managing the technology development group for GaN power devices at Infineon Villach. Detzel is an alumnus of the German National Academic Foundation and a member of the German Physical Society.

Symposia

The 2016 Organizing Committee:
Brady Gibbons, Electronics Division John Blendell, Basic Science Division
Haiyan Wang, Electronics Division Dominique Chatain, Basic Science Division

S1. Multiferroic Materials and Multilayer Ferroic Heterostructures: Properties and Applications
S. Pamir Alpay, University of Connecticut, USA; Daniel Shreiber, U.S. ARL, USA; Ichiro Takeuchi, University of Maryland, USA; Timothy Haugan, U.S. Air Force Research Laboratory, USA

S2. Functional Materials: Synthesis Science, Properties, and Integration
Jon-Paul Maria, North Carolina State University, USA; Jon Ihlefeld, Sandia National Laboratories, USA; Ronald Polcawich, U.S. Army Research Laboratory, USA

S3. Use of Thermal Energy for Electrical Power Generation and Refrigeration: Fundamental Science, Materials Development and Devices
Alp Sehirlioglu, Case Western Reserve University, USA; David Singh, Oak Ridge National Laboratory, USA; Antoine Maignan, CrisMat, France; Winnie Wong-Ng, NIST, USA; Anke Weidenkaff, University of Stuttgart, Germany; Patrick Hopkins, University of Virginia, USA; Edward P. Gorzkowski, Naval Research Laboratory, USA

S4. Ion-conducting Ceramics
Jon Ihlefeld, Sandia National Laboratories, USA; Frank Chen, University of South Carolina, USA; Jeff Sakamoto, University of Michigan, USA; Erik Spoerke, Sandia National Laboratories, USA; Hui (Claire) Xiong, Boise State University, USA

S5. Multifunctional Nanocomposites
Roman Engel-Herbert, Pennsylvania State University, USA; Aiping Chen, Los Alamos National Laboratory, USA; Judith L. MacManus-Driscoll, University of Cambridge, UK; James Rondinelli, Northwestern University, USA; Bharat Jalan, University of Minnesota, USA; Junwoo Son, Pohang University of Science and Technology, South Korea; Oliver Bierwagen, Paul Drude Insitute for Solid State Electronics, Germany

S6. Computational Design of Electronic Materials
Mina Yoon, Oak Ridge National Laboratory, USA; Wolfgang Windl, Ohio State University, USA; Ghanshyam Pilania, Los Alamos National Laboratory, USA; James Rondinelli, Northwestern University, USA; Emmanouil Kioupakis, University of Michigan, USA

S7. Processing and Microstructure of Functional Ceramics: Sintering, Grain Growth and Their Impact on the Materials Properties
Wolfgang Rheinheimer, Karlsruhe Institute of Technology, Germany; Michael Hoffmann, Karlsruhe Institute of Technology, Germany

S8. Interface Structure, Orientation, and Composition: Influence on Properties and Kinetics
Dominique Chatain, CINaM, France; Wayne Kaplan, Technion, Israel; John Blendell, Purdue University, USA; Carol Handwerker, Purdue University, USA

S9. Recent Developments in Superconducting Materials and Applications
Gang Wang, Institute of Physics, Chinese Academy of Sciences, China; Xingjiang Zhou, Institute of Physics, Chinese Academy of Sciences, China; Tim Haugan, Air Force Research Laboratory, USA; Haiyan Wang, Texas A&M University, USA

S10. Emerging Functionalities in Layered-Oxide and Related Materials
Serge M. Nakhmanson, University of Connecticut, USA; Bharat Jalan, University of Minnesota, USA; Edward Gorzkowski, U.S. Naval Research Laboratory, USA

S11. Advanced Electronic Materials: Processing, Structures, Properties and Applications
Shujun Zhang, The Pennsylvania State University, USA; Xiaoli Tan, Iowa State University, USA; Kyle Webber, Technische Universität Darmstadt, Germany; Satoshi Wada, University of Yamanashi, Japan

Doubletree by Hilton Floor Plan

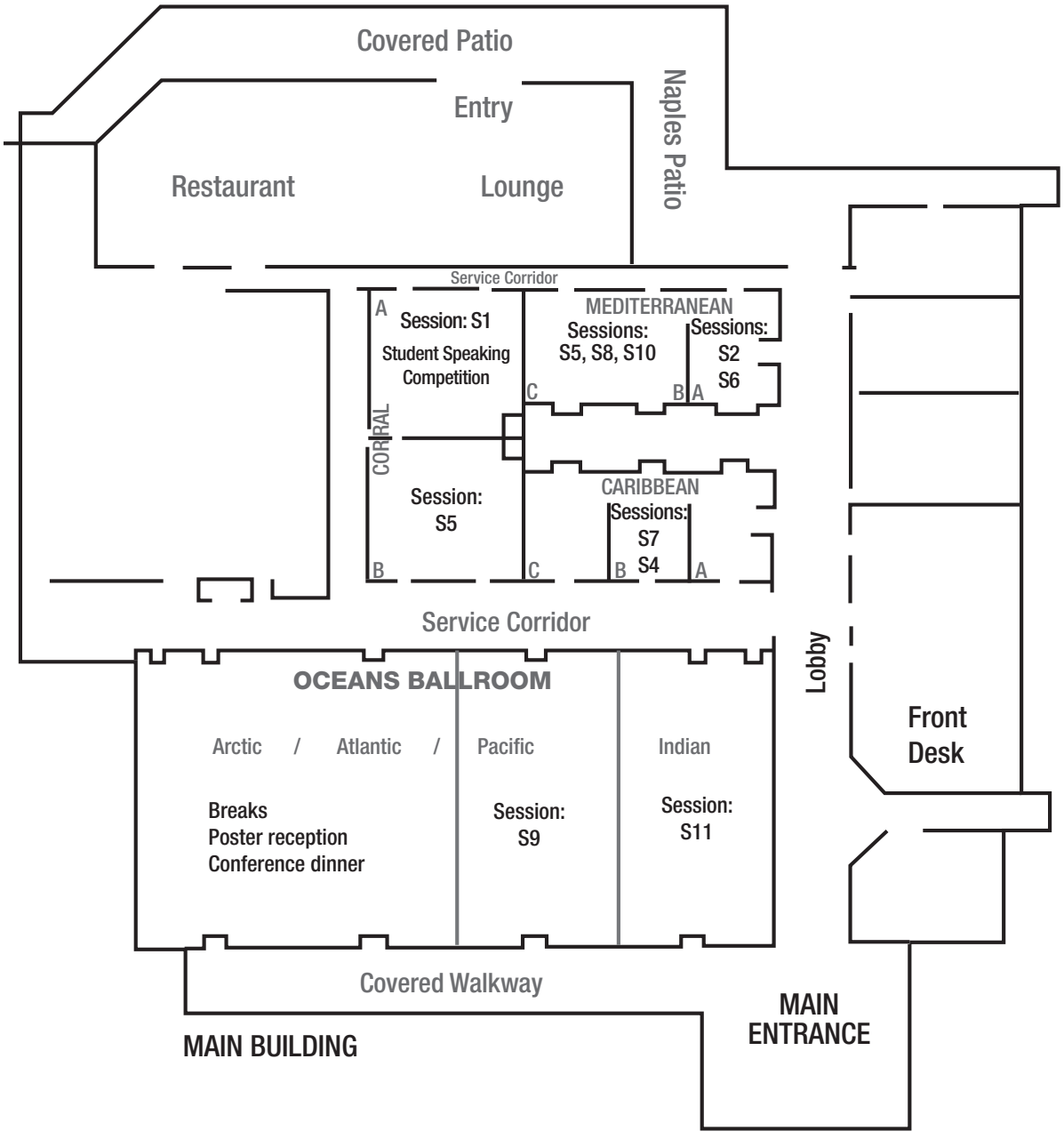

MTI Desktop Film Coaters

For Research of New Generation Materials

MTI Corporation manufacture and supply various types of compact film coaters for material research, such as Perovskite solar cell, thin rechargeable battery, Ferro-magnetic film, and etc. Please visit our website (www.mtixtl.com) for detailed specifications of each product, along with video demo and product options.

Spin Coating 	Dip Coating 	Tape Casting 
Screen Printing 	Plasma Sputtering 	Plasma Cleaning 
PECVD 	CSS & Thermal Evaporation 	Spray Pyrolysis Coating 

For inquiries or questions, please contact MTI Corp at info@mtixtl.com or call toll free at **1-888-525-3070**

Direct product purchase available on our secured online store.

MTI Corporation --- Since 1994

860 South 19th Street, Richmond, CA 94804, USA

Tel: 510-525-3070 Fax: 510-525-4705

E-mail: info@mtixtl.com Website: www.mtixtl.com

Best Student Award Finalist Presentations

In recognition of their outstanding contributions to our field, each year the ACerS Electronics Division selects the top three presentations and top three posters presented by students at EMA. While all of the student posters are judged during the poster session as part of this competition, logistical restraints dictate that only a subset of the oral presentations be fully judged. Thus, the Awards Committee of the ACerS Electronics Division pores over all submitted student abstracts and selects 10 finalists for the best presentation awards. These finalists are then given the opportunity to speak in the special lunchtime sessions to compete for this award in addition to or in place of speaking in the regular symposium to which they submitted their abstract. Only those students who speak in during the lunchtime sessions are eligible for the awards and they are listed below. However, all of the finalists should be congratulated! Look for their titles in gray call-out boxes throughout the program. Please join us over lunch on Wednesday and Thursday to celebrate these students and their work.

Boxed lunches for the first 32 attendees each day are provided.

Wednesday
Room: Coral A

12:50-1:05 p.m.	Jilai Ding	Oak Ridge National Lab
1:05-1:20 p.m.	Matthew Cabral	North Carolina State University
1:20-1:35 p.m.	Hadar Nahor	Technion - Israel Institute of Technology
1:35-1:50 p.m.	Steven Brewer	Georgia Institute of Technology

Thursday
Room: Coral A

12:45-1:00 p.m.	Peng Gao	Alfred University
1:00-1:15 p.m.	Jeffrey Braun	University of Virginia
1:15-1:30 p.m.	Guangqing Liu	University of New South Wales
1:30-1:45 p.m.	Kyle Kelley	North Carolina State University

Young Professionals who were awarded registration support:

Symposium 1	Deepam Maurya	Symposium 8	Ming Tang
Symposium 3	Jon Mackey	Symposium 9	Dr. Yifeng Yang
Symposium 4	Sandrine Ricote	Symposium 10	James Neilson
Symposium 6	Changwon Park		

MEETING REGULATIONS

The American Ceramic Society is a nonprofit scientific organization that facilitates the exchange of knowledge meetings and publication of papers for future reference. The Society owns and retains full right to control its publications and its meetings. The Society has an obligation to protect its members and meetings from intrusion by others who may wish to use the meetings for their own private promotion purpose. Literature found not to be in agreement with the Society's goals, in competition with Society services or of an offensive nature will not be displayed anywhere in the vicinity of the meeting. Promotional literature of any kind may not be displayed without the Society's permission and unless the Society provides tables for this purpose. Literature not conforming to this policy or displayed in other than designated areas will be disposed. The Society will not permit unauthorized scheduling of activities during its meeting by any person or group when those activities are conducted at its meeting place in interference with its programs and scheduled activities. The Society does not object to appropriate activities by others during its meetings if it is consulted with regard to time, place, and suitability. Any person or group wishing to conduct any activity at the time and location of the Society meeting must obtain permission from the Executive Director or Director of Meetings, giving full details regarding desired time, place and nature of activity.

Diversity Statement: The American Ceramic Society values diverse and inclusive participation within the field of ceramic science and engineering. ACerS strives to promote involvement and access to leadership opportunity regardless of race, ethnicity, gender, religion, age, sexual orientation, nationality, disability, appearance, geographic location, career path or academic level.

The American Ceramic Society plans to take photographs and video at the conference and reproduce them in educational, news or promotional materials, whether in print, electronic or other media, including The American Ceramic Society's website. By participating in the conference, you grant The American Ceramic Society the right to use your name and photograph for such purposes. All postings become the property of The American Ceramic Society.

During oral sessions conducted during Society meetings, **unauthorized photography, videotaping and audio recording is prohibited.** Failure to comply may result in the removal of the offender from the session or from the remainder of the meeting.

Registration Requirements: Attendance at any meeting of the Society shall be limited to duly registered persons.

Disclaimer: Statements of fact and opinion are the responsibility of the authors alone and do not imply an opinion on the part of the officers, staff or members of The American Ceramic Society. The American Ceramic Society assumes no responsibility for the statements and opinions advanced by the contributors to its publications or by the speakers at its programs; nor does The American Ceramic Society assume any liability for losses or injuries suffered by attendees at its meetings. Registered names and trademarks, etc. used in its publications, even without specific indications thereof, are not to be considered unprotected by the law. Mention of trade names of commercial products does not constitute endorsement or recommendations for use by the publishers, editors or authors.

Final determination of the suitability of any information, procedure or products for use contemplated by any user, and the manner of that use, is the sole responsibility of the user. Expert advice should be obtained at all times when implementation is being considered, particularly where hazardous materials or processes are encountered.

Presenting Author List

Oral Presenters

Name	Date	Time	Room	Page Number
		A		
Abraham, A.	22-Jan	5:00PM	Indian	30
Ahmad, M.M.	20-Jan	4:30PM	Caribbean B	17
Ahmad, M.M.	22-Jan	11:45AM	Caribbean B	26
Akrobetu, R.	21-Jan	11:30AM	Mediterranean B/C	22
Albe, K.	21-Jan	2:00PM	Mediterranean A	24
Alpay, P.	22-Jan	4:30PM	Mediterranean A	29
Anandan, V.	22-Jan	10:00AM	Caribbean B	26
Anton, E.	20-Jan	5:45PM	Pacific	18
		B		
Balachandran, B.	22-Jan	11:45AM	Coral A	28
Baldini, M.	21-Jan	5:15PM	Coral B	24
Bassiri-Gharb, N.	21-Jan	2:00PM	Coral A	23
Bayer, T.J.	20-Jan	3:00PM	Indian	18
Becker, C.R.	22-Jan	11:15AM	Caribbean B	26
Bell, A.J.	21-Jan	2:00PM	Indian	25
Bell, N.S.	21-Jan	11:30AM	Caribbean B	21
Binder, J.R.	20-Jan	4:00PM	Caribbean B	17
Binomran, S.	22-Jan	3:00PM	Indian	30
Birol, T.	20-Jan	11:00AM	Coral B	14
Brant, J.	20-Jan	3:00PM	Pacific	17
Braun, J.L.	20-Jan	3:15PM	Mediterranean B/C	16
Braun, J.L.	21-Jan	1:00PM	Coral A	23
Brewer, S.	20-Jan	1:35PM	Coral A	15
Brewer, S.	21-Jan	5:30PM	Mediterranean B/C	25
Brinkman, K.	21-Jan	2:00PM	Caribbean B	23
Butt, D.P.	22-Jan	1:30PM	Caribbean B	28
		C		
Cabral, M.J.	20-Jan	1:05PM	Coral A	15
Cabral, M.J.	20-Jan	3:15PM	Indian	18
Cann, D.	20-Jan	10:30AM	Indian	15
Cann, D.	22-Jan	5:45PM	Mediterranean B/C	30
Cantoni, C.	20-Jan	10:30AM	Pacific	14
Cao, G.	22-Jan	10:30AM	Caribbean B	26
Carter, J.	20-Jan	2:30PM	Indian	18
Ceh, M.	20-Jan	5:00PM	Mediterranean B/C	16
Chambers, S.	20-Jan	10:00AM	Coral B	14
Chan, J.H.	20-Jan	5:45PM	Mediterranean B/C	16
Chen, J.	22-Jan	4:15PM	Coral B	29
Chen, X.	22-Jan	10:30AM	Indian	28
Cheng, S.	21-Jan	2:30PM	Coral B	24
Choi, H.	20-Jan	12:15PM	Mediterranean A	13
Choi, S.	20-Jan	4:30PM	Coral B	17
Chu, Y.	21-Jan	10:00AM	Coral B	21
Civale, L.	20-Jan	4:45PM	Pacific	18
Comes, R.B.	20-Jan	2:30PM	Coral B	17
		D		
Dai, X.	21-Jan	4:30PM	Pacific	25
Damjanovic, D.	21-Jan	2:30PM	Indian	26
Daw, M.	22-Jan	2:45PM	Mediterranean A	29
Dawber, M.	20-Jan	2:00PM	Coral B	17
De Souza, R.A.	22-Jan	10:30AM	Coral B	26
Dean, J.S.	20-Jan	12:00PM	Indian	15
Deluca, M.	20-Jan	2:00PM	Indian	18
Detzel, T.	22-Jan	8:40AM	Indian	26
Dickey, E.C.	21-Jan	2:00PM	Mediterranean B/C	25
Ding, J.	20-Jan	12:50PM	Coral A	15
Ding, J.	21-Jan	4:30PM	Caribbean B	24
Dkhil, B.	20-Jan	10:30AM	Coral A	13
Dkhil, B.	20-Jan	11:45AM	Mediterranean B/C	14
Donovan, B.F.	22-Jan	11:30AM	Coral A	28
		E		
Eastman, J.A.	21-Jan	11:15AM	Coral B	21
Ederer, C.	22-Jan	3:45PM	Mediterranean B/C	30
Eom, C.	20-Jan	11:30AM	Pacific	14
Espinal, Y.	21-Jan	10:30AM	Coral A	20
Esteves, G.	21-Jan	10:45AM	Mediterranean A	21
Evans, J.T.	21-Jan	11:15AM	Mediterranean A	21
Evans, P.G.	21-Jan	11:30AM	Coral A	20
		F		
Faghaninia, A.	22-Jan	5:15PM	Mediterranean A	29
Fancher, C.	21-Jan	11:30AM	Indian	22
Farghadany, E.	20-Jan	3:00PM	Mediterranean B/C	16
Feneberg, M.	21-Jan	4:00PM	Coral B	24
Feng, P.	22-Jan	12:15PM	Coral A	28
Fleurial, J.	20-Jan	2:00PM	Mediterranean B/C	16
Foley, B.M.	20-Jan	11:00AM	Mediterranean B/C	13
Funahashi, S.	20-Jan	4:45PM	Mediterranean B/C	16
Funakubo, H.	22-Jan	1:30PM	Mediterranean B/C	29
Furman, E.	22-Jan	3:45PM	Indian	30
		G		
Gao, P.	21-Jan	12:45PM	Coral A	23
Gao, P.	22-Jan	2:30PM	Mediterranean B/C	29
Gelbstein, Y.	20-Jan	10:00AM	Mediterranean B/C	13
Gerhardt, R.A.	20-Jan	3:00PM	Caribbean B	17
Gerhardt, R.A.	21-Jan	10:00AM	Mediterranean B/C	22
Gheorghiu, N.	22-Jan	12:15PM	Pacific	27
Goldacker, W.	22-Jan	10:30AM	Pacific	27
Gorzkowski, E.	21-Jan	10:45AM	Indian	22
Grande, T.	20-Jan	2:00PM	Caribbean B	17
Gregg, M.	20-Jan	11:30AM	Coral A	13
Grimley, E.D.	20-Jan	2:45PM	Indian	18
Gu, Z.	21-Jan	10:45AM	Coral A	20
Gubb, T.A.	22-Jan	11:00AM	Mediterranean B/C	27
Gulgun, M.A.	21-Jan	10:30AM	Caribbean B	21
Gupta, S.K.	22-Jan	2:30PM	Mediterranean A	29
		H		
Hai, G.	21-Jan	5:00PM	Pacific	25
Haile, S.M.	20-Jan	4:00PM	Coral B	17
Haugan, T.J.	22-Jan	11:45AM	Pacific	27
Heinonen, O.	20-Jan	4:30PM	Coral A	15
Henkelman, G.	22-Jan	10:00AM	Mediterranean A	27
Hennig, R.G.	22-Jan	1:30PM	Mediterranean A	29
Heron, J.T.	20-Jan	12:00PM	Coral A	13
Herrera, G.M.	20-Jan	5:00PM	Caribbean B	17
Hill, M.D.	20-Jan	5:00PM	Coral A	15
Hopkins, P.E.	22-Jan	10:00AM	Coral B	26
Hosokura, T.	21-Jan	10:00AM	Indian	22
Hsing, H.	20-Jan	2:45PM	Coral B	17
Hu, J.	21-Jan	2:00PM	Pacific	25
Hu, J.	22-Jan	2:15PM	Coral B	28
Huang, B.	22-Jan	10:30AM	Mediterranean A	27
Huang, J.	20-Jan	12:00PM	Pacific	14
Huey, B.D.	21-Jan	4:00PM	Coral A	23
Huey, B.D.	22-Jan	4:30PM	Indian	30
Huo, X.	22-Jan	12:00PM	Coral A	28
		I		
Ihlefeld, J.	21-Jan	4:45PM	Caribbean B	24
Inclan, E.	21-Jan	3:15PM	Mediterranean A	24
		J		
Jackson, T.	20-Jan	10:00AM	Mediterranean A	13
Janotti, A.	21-Jan	2:00PM	Coral B	24
Jensen, C.	22-Jan	12:30PM	Pacific	27
Jia, J.	20-Jan	10:00AM	Pacific	14
Jia, Q.X.	21-Jan	10:45AM	Coral B	21
Johnson, S.D.	21-Jan	11:00AM	Indian	22
Jones, J.L.	20-Jan	4:00PM	Indian	18
		K		
Kalkur, T.S.	21-Jan	5:15PM	Coral A	23
Kaplan, W.D.	20-Jan	10:00AM	Caribbean B	14
Keeney, L.	21-Jan	3:00PM	Coral A	23
Kelley, K.	20-Jan	12:00PM	Mediterranean A	13

Oral Presenters

Presenting Author List

Oral Presenters

Name	Date	Time	Room	Page Number
Spoerke, E.	21-Jan	3:15PM	Caribbean B	23
Spreitzer, M.	21-Jan	5:30PM	Indian	26
Stanek, C.	21-Jan	4:30PM	Mediterranean A	24
Sternlicht, H.	21-Jan	3:00PM	Mediterranean B/C	25
Sushko, P.	21-Jan	5:00PM	Mediterranean B/C	25
Sushko, P.	22-Jan	2:30PM	Caribbean B	28
Suvorov, D.	22-Jan	2:45PM	Indian	30
T				
Takeda, H.	21-Jan	3:15PM	Indian	26
Tan, X.	21-Jan	10:30AM	Indian	22
Tang, M.	21-Jan	4:30PM	Mediterranean B/C	25
Tran, T.	22-Jan	10:00AM	Mediterranean B/C	27
Trenkle, A.	20-Jan	11:45AM	Caribbean B	14
Trolier-McKinstry, S.	20-Jan	10:00AM	Coral A	13
Trolier-McKinstry, S.	21-Jan	10:30AM	Mediterranean A	21
Tsurumi, T.	20-Jan	10:00AM	Indian	15
U				
Uehara, M.	20-Jan	2:30PM	Mediterranean B/C	16
V				
van Benthem, K.	21-Jan	10:00AM	Caribbean B	21
van Benthem, K.	21-Jan	10:45AM	Mediterranean B/C	22
Viehland, D.	22-Jan	1:30PM	Coral B	28
von Wenckstern, H.	21-Jan	4:45PM	Coral B	24
W				
Wang, G.	20-Jan	4:30PM	Pacific	18
Wang, H.	21-Jan	12:00PM	Coral B	21
Wang, N.	20-Jan	2:00PM	Pacific	17
Warren, J.A.	21-Jan	8:40AM	Indian	20
Wasa, K.	21-Jan	3:00PM	Indian	26
Weidenkaff, A.	21-Jan	12:15PM	Mediterranean A	21
Weng, H.	20-Jan	11:00AM	Pacific	14
Werfel, F.N.	22-Jan	10:00AM	Pacific	27
Wiley, J.B.	22-Jan	10:30AM	Mediterranean B/C	27
Wilke, R.H.	22-Jan	4:15PM	Indian	30
Woodward, P.	22-Jan	2:00PM	Mediterranean B/C	29
Wu, J.	21-Jan	11:00AM	Pacific	22
Wu, L.	22-Jan	4:45PM	Indian	30
X				
Xue, D.	22-Jan	2:45PM	Coral B	29
Y				
Yamaura, K.	20-Jan	4:00PM	Pacific	18
Yan, J.	20-Jan	5:15PM	Pacific	18
Yang, K.	22-Jan	12:15PM	Mediterranean A	27
Yang, S.	22-Jan	3:45PM	Coral B	29
Yang, Y.	21-Jan	5:30PM	Pacific	25
Yaya, A.S.	21-Jan	12:15PM	Caribbean B	21
Ye, L.	20-Jan	5:00PM	Mediterranean A	16
Ye, Z.	21-Jan	4:30PM	Indian	26
Ye, Z.	22-Jan	2:30PM	Indian	30
Yim, K.	22-Jan	5:00PM	Mediterranean A	29
Yoon, H.	21-Jan	3:00PM	Coral B	24
Z				
Zapol, P.	20-Jan	4:30PM	Mediterranean A	16
Zhang, G.	22-Jan	11:00AM	Coral A	28
Zhang, H.	21-Jan	3:15PM	Coral B	24
Zhang, W.	21-Jan	10:30AM	Coral B	21
Zhou, X.	21-Jan	4:00PM	Pacific	25
Zhu, J.	22-Jan	11:45AM	Mediterranean A	27

Poster Presenters

Name	Date	Time	Room	Page Number
Anton, E.	20-Jan	5:30PM	Atlantic/Arctic	19
Brant, J.	20-Jan	5:30PM	Atlantic/Arctic	19
Cho, N.	20-Jan	5:30PM	Atlantic/Arctic	19
Cruvinel dos Reis, I.	20-Jan	5:30PM	Atlantic/Arctic	20
de los Santos Guerra, J.	20-Jan	5:30PM	Atlantic/Arctic	19
Dogan, A.	20-Jan	5:30PM	Atlantic/Arctic	20
Gheorghiu, N.	20-Jan	5:30PM	Atlantic/Arctic	19
Guerrier, J.	20-Jan	5:30PM	Atlantic/Arctic	18
Gui, Z.	20-Jan	5:30PM	Atlantic/Arctic	19
Gurdal, A.E.	20-Jan	5:30PM	Atlantic/Arctic	19
Haugan, T.J.	20-Jan	5:30PM	Atlantic/Arctic	19
Hori, S.	20-Jan	5:30PM	Atlantic/Arctic	19
Hormadaly, J.	20-Jan	5:30PM	Atlantic/Arctic	18
Hou, D.	20-Jan	5:30PM	Atlantic/Arctic	19
Huo, X.	20-Jan	5:30PM	Atlantic/Arctic	19
Imbrenda, D.	20-Jan	5:30PM	Atlantic/Arctic	19
Ivy, J.	20-Jan	5:30PM	Atlantic/Arctic	19
Jeon, S.	20-Jan	5:30PM	Atlantic/Arctic	19
Khatua, D.K.	20-Jan	5:30PM	Atlantic/Arctic	18
Kim, S.	20-Jan	5:30PM	Atlantic/Arctic	19, 20
Kryvobok, R.V.	20-Jan	5:30PM	Atlantic/Arctic	19
Lai, J.A.	20-Jan	5:30PM	Atlantic/Arctic	19
Leng, C.	20-Jan	5:30PM	Atlantic/Arctic	19
Li, E.	20-Jan	5:30PM	Atlantic/Arctic	18
Li, L.	20-Jan	5:30PM	Atlantic/Arctic	19
Liu, M.	20-Jan	5:30PM	Atlantic/Arctic	18
Long, D.	20-Jan	5:30PM	Atlantic/Arctic	20
Ma, Y.	20-Jan	5:30PM	Atlantic/Arctic	19
Madhuri, W.	20-Jan	5:30PM	Atlantic/Arctic	20
Maung, Y.M.	20-Jan	5:30PM	Atlantic/Arctic	19
McCue, C.S.	20-Jan	5:30PM	Atlantic/Arctic	20
Mitic, V.	20-Jan	5:30PM	Atlantic/Arctic	19
Park, J.	20-Jan	5:30PM	Atlantic/Arctic	19
Piercy, B.D.	20-Jan	5:30PM	Atlantic/Arctic	18
Rodriguez Hernandez, G.	20-Jan	5:30PM	Atlantic/Arctic	20
Saito, A.	20-Jan	5:30PM	Atlantic/Arctic	19
Sebastian, M.P.	20-Jan	5:30PM	Atlantic/Arctic	19
Tange, M.	20-Jan	5:30PM	Atlantic/Arctic	19
Usher, T.	20-Jan	5:30PM	Atlantic/Arctic	19
Wagner, N.	20-Jan	5:30PM	Atlantic/Arctic	19
Win, T.T.	20-Jan	5:30PM	Atlantic/Arctic	19
Yuksel Price, B.	20-Jan	5:30PM	Atlantic/Arctic	19, 20
Zerihun, N.	20-Jan	5:30PM	Atlantic/Arctic	20

Wednesday, January 20, 2016

Plenary Session

Plenary I

Room: Indian

8:30 AM

Opening Remarks

8:40 AM

(EMA-PL-001-2016) Thin-Film Alchemy: Using Strain and Dimensionality to Unleash the Hidden Properties of Oxides

D. Schlom*[1]; 1. Cornell University, USA

9:30 AM

Break

S1. Multiferroic Materials and Multilayer Ferroic Heterostructures: Properties and Applications

Synthesis, Processing, and Properties

Room: Coral A

Session Chair: Nazanin Bassiri-Gharb, Georgia Institute of Technology

10:00 AM

(EMA-S1-001-2016) Piezoelectrics on Magnetic Metal Foil (Invited)

S. Trolier-McKinstry*[1]; 1. Pennsylvania State University, USA

10:30 AM

(EMA-S1-002-2016) Strain-tuning in multiferroics (Invited)

B. Dkhil*[1]; 1. CentraleSupélec-CNRS, France

11:00 AM

(EMA-S1-003-2016) Functionally graded ferroelectric and multiferroic thin film heterostructures (Invited)

D. Maurya*[1]; S. Priya[1]; 1. Virginia Tech, USA

11:30 AM

(EMA-S1-004-2016) The Nature of Magnetoelectric Coupling in the Room Temperature Multiferroic Pb(Zr,Ti)O3-Pb(Fe,Ta)O3 (Invited)

M. Gregg*[1]; D. Evans[1]; J. F. Scott[2]; M. Alexe[3]; A. Schilling[1]; 1. Queen's University Belfast, United Kingdom; 2. University of St Andrews, United Kingdom; 3. University of Warwick, United Kingdom

12:00 PM

(EMA-S1-005-2016) Pathways to low energy control of magnetism using multiferroics (Invited)

J. T. Heron*[1]; 1. University of Michigan, USA

S2. Functional Materials: Synthesis Science, Properties, and Integration

Functional Materials: Oxide Semiconductor Synthesis, Integration, and Properties

Room: Mediterranean A

Session Chair: Jon-Paul Maria, North Carolina State University

10:00 AM

(EMA-S2-001-2016) PEALD ZnO Thin Film Transistors for Electroceramic Device Integration (Invited)

T. Jackson*[1]; 1. Penn State University, USA

10:30 AM

(EMA-S2-002-2016) VO_2 Thin Film for Smart Nano Biosensor

D. Kim*[1]; B. Kim[1]; S. Han[1]; C. Kang[1]; S. Nahm[1]; 1. Korea University, The Republic of Korea

10:45 AM

(EMA-S2-003-2016) Step-free GaN substrates for oxide heteroepitaxy

C. T. Shelton*[1]; I. Bryan[1]; E. A. Paisley[2]; E. Sachet[1]; N. Lavrik[3]; M. Biegalski[3]; J. LeBeau[1]; R. Collazo[1]; Z. Sitar[1]; J. Maria[1]; 1. NCSU, USA; 2. Sandia National Laboratories, USA; 3. Oak Ridge National Lab, USA

11:00 AM

(EMA-S2-004-2016) Gate oxide band offset dependence on nitride surface chemistry for GaN power electronics

E. A. Paisley*[1]; C. T. Shelton[2]; M. Brumbach[1]; M. D. Losego[3]; C. Rost[2]; S. Atcitty[1]; J. Maria[2]; J. Ihlefeld[1]; 1. Sandia National Laboratories, USA; 2. North Carolina State University, USA; 3. Georgia Institute of Technology, USA

11:15 AM

(EMA-S2-005-2016) Physical properties of doped $BaSnO_3$ semiconductors with high electrical mobility and optical transparency at room temperature (Invited)

K. Kim*[1]; 1. Seoul National University, The Republic of Korea

11:45 AM

(EMA-S2-006-2016) High Mobility Conductive Oxides for Optoelectronic Components in the mid-IR

E. Sachet*[1]; K. Kelley[1]; C. T. Shelton[1]; S. Franzen[1]; J. Maria[1]; 1. North Carolina State University, USA

12:00 PM

(EMA-S2-007-2016) Doping control in epitaxial thin films via reactive RF co-sputtering

K. Kelley*[1]; E. Sachet[1]; H. Kham[1]; S. Franzen[1]; J. Maria[1]; 1. North Carolina State University, USA

12:15 PM

(EMA-S2-008-2016) A Study on The Transparent and Flexible EMI Shielding Film Manufactured by Impringting Method

H. Choi*[1]; G. Lee[1]; 1. Changsung Corporation, The Republic of Korea

S3. Use of thermal energy for electrical power generation and refrigeration: Fundamental science, materials development and devices

Conversion of Thermal Energy

Room: Mediterranean B/C

Session Chair: Jon Mackey, University of Akron

10:00 AM

(EMA-S3-001-2016) Novel thermoelectric optimization methods (Invited)

Y. Gelbstein*[1]; 1. Ben-Gurion University of the Negev, Israel

10:30 AM

(EMA-S3-002-2016) Thermoelectric modules for Efficient Power Generation (Invited)

N. Pryds*[1]; 1. Technical University of Denmark, Denmark

11:00 AM

(EMA-S3-016-2016) Experimental Investigation of the Ferroelectric Proximity Effect in Bilayer PZT Heterostructures via Thermal Transport Measurements

B. M. Foley*[1]; D. Scrymgeour[2]; E. A. Paisley[2]; J. Michael[2]; B. McKenzie[2]; M. Wallace[3]; D. Medlin[2]; S. Trolier-McKinstry[3]; J. Ihlefeld[2]; P. Hopkins[1]; 1. University of Virginia, USA; 2. Sandia National Laboratories, USA; 3. Pennsylvania State University, USA

11:15 AM

(EMA-S3-004-2016) DRREAM: Drastically Reduced Use of Rare Earths in Applications of Magnetocalorics (Invited)

K. G. Sandeman*[1]; 1. Brooklyn College of The City University of New York, USA

11:45 AM

(EMA-S3-005-2016) Strategies for enhancing caloric responses using ferroelectric oxides

B. Dkhil*[1]; 1. CentraleSupélec-CNRS, France

12:00 PM

(EMA-S3-006-2016) Multicaloric ferroelectrics (Invited)

X. Moya*[1]; 1. University of Cambridge, United Kingdom

S5. Multifunctional Nanocomposites

Multifunctional Nanocomposites I

Room: Coral B

Session Chair: Roman Engel-Herbert, The Pennsylvania State University

10:00 AM

(EMA-S5-001-2016) Magnetism and Nanoscale Structural and Compositional Irregularities in MBE-grown La_2MnNiO_6 on $SrTiO_3$(001) (Invited)

S. Chambers*[1]; 1. Pacific Northwest National Laboratory, USA

10:30 AM

(EMA-S5-002-2016) Templated Self-assembly of Multiferroic Oxide Nanocomposites (Invited)

C. Ross*[1]; 1. Massachusetts Institute of Technology, USA

11:00 AM

(EMA-S5-003-2016) First Principles Design of High T_c Superconductors (Invited)

T. Birol*[1]; 1. Rutgers University, USA

11:30 AM

(EMA-S5-004-2016) Electron Pairing Without Superconductivity (Invited)

J. Levy*[1]; 1. University of Pittsburgh, USA

12:00 PM

(EMA-S5-005-2016) Detangling Extrinsic and Intrinsic Hysteresis for Detecting Dynamic Switch of Electric Dipoles using Graphene Field-Effect Transistors

C. Ma*[1]; Y. Gong[2]; R. Lu[2]; E. Brown[3]; B. Ma[4]; J. Li[3]; J. Wu[2]; 1. Xi\'an Jiaotong University, China; 2. University of Kansas, USA; 3. Kansas Sate University, USA; 4. Argonne National Laboratory, USA

S7. Processing and microstructure of functional ceramics: Sintering, grain growth and their impact on the materials properties

Grain Growth and Abnormal Grain Growth

Room: Caribbean B

Session Chair: Wolfgang Rheinheimer, Karlsruhe Institute of Technology

10:00 AM

(EMA-S7-001-2016) Adsorption, Fields and Grain Boundary Mobility (Invited)

W. D. Kaplan*[1]; 1. Technion - Israel Institute of Technology, Israel

10:30 AM

(EMA-S7-002-2016) Grain Boundary Character Distributions in Perovskite Ceramics (Invited)

G. Rohrer*[1]; S. Ratanaphan[2]; 1. Carnegie Mellon University, USA; 2. King Mongkut's University of Technology Thonburi, Thailand

11:00 AM

(EMA-S7-003-2016) Triggering abnormal grain growth by pressure assisted sintering in $BaLa_4Ti_4O_{15}$ (Invited)

A. M. Senos*[1]; M. Fernandes[1]; N. Selvaraj[1]; J. Abrantes[2]; P. Vilarinho[1]; 1. University of Aveiro/CICECO, Portugal; 2. UIDM, ESTG, Instituto Politecnico de Viana do Castelo, Portugal

11:30 AM

(EMA-S7-004-2016) The Influence of Impurities on the Microstructural Evolution of Alumina

R. Moshe*[1]; W. D. Kaplan[1]; 1. Technion - Israel Institute of Technology, Israel

11:45 AM

(EMA-S7-005-2016) 3D Microstructure Evolution in Strontium Titanate with Non-destructive Imaging

A. Trenkle*[1]; M. Syha[1]; W. Rheinheimer[1]; M. Echlin[3]; W. Lenthe[3]; W. Ludwig[2]; D. Weygand[1]; P. Gumbsch[1]; 1. Karlsruhe Institute of Technology, Germany; 2. European Synchrotron Radiation Facility, France; 3. University of California - Santa Barbara, USA

12:00 PM

(EMA-S7-006-2016) Influence of an electric field on grain growth and sintering in strontium titanate

W. Rheinheimer*[1]; M. J. Hoffmann[1]; 1. Karlsruhe Institute of Technology, Germany

S9. Recent Developments in Superconducting Materials and Applications

New Superconductor 1- New Superconducting Materials and Phenomena

Room: Pacific

Session Chairs: Gang Wang, Institute of Physics, Chinese Academy of Sciences; Claudia Cantoni, Oak Ridge National Laboratory

10:00 AM

(EMA-S9-001-2016) Growth of Stanene and single-layer FeSe on $SrTiO_3$ with a superconducting T_c above 100 K (Invited)

J. Jia*[1]; 1. Shanghai Jiao Tong University, China

10:30 AM

(EMA-S9-002-2016) 2D interfacial superconductivity by local manipulation of atoms and electron spins (Invited)

C. Cantoni*[1]; 1. Oak Ridge National Laboratory, USA

11:00 AM

(EMA-S9-003-2016) Two-Dimensional Oxide Topological Insulator With Iron-Pnictide Superconductor LiFeAs Structure (Invited)

H. Weng*[1]; 1. Institute of Physics, Chinese Academy of Sciences, China

11:30 AM

(EMA-S9-004-2016) Artificially engineered superlattices of pnictide superconductor (Invited)

C. Eom*[1]; 1. University of Wisconsin-Madison, USA

12:00 PM

(EMA-S9-005-2016) Growth of iron chalcogenide thin films on various substrates and pinning enhancement by incorporated nanolayers

J. Huang*[1]; L. Chen[1]; J. Jian[1]; L. Li[1]; H. Wang[1]; 1. Texas A&M University, USA

S11. Advanced electronic Materials: Processing, structures, properties and applications

Advanced Electronic Materials: Dielectrics I

Room: Indian

Session Chairs: David Cann, Oregon State Univ; Takaaki Tsurumi, Tokyo Institute of Technology

10:00 AM

(EMA-S11-001-2016) Concept of Solid State Ionic Capacitor for Future MLCCs (Invited)

T. Tsurumi*[1]; R. Ishikawa[1]; T. Hoshina[1]; H. Takeda[1]; Y. Sakabe[1]; 1. Tokyo Institute of Technology, Japan

10:30 AM

(EMA-S11-002-2016) Non-Stoichiometry in Bismuth Perovskites (Invited)

D. Cann*[1]; N. Prasertpalichatr[1]; N. Kumar[1]; W. Schmidt[1]; 1. Oregon State Univ, USA

11:00 AM

(EMA-S11-003-2016) Giant Energy Density and Improved Discharge Efficiency of Solution-Processed Polymer Nanocomposites for Dielectric Energy Storage (Invited)

Y. Shen*[1]; 1. Tsinghua University, China

11:30 AM

(EMA-S11-004-2016) High Temperature Dielectrics: an assessment of temperature-stable relaxors (Invited)

A. Zeb[1]; M. Ward[1]; D. Hall[2]; D. C. Sinclair[2]; I. MacLaren[3]; S. U. Jan[1]; S. J. Milne*[1]; 1. University of Leeds, United Kingdom; 2. University of Sheffield, United Kingdom; 3. University of Glasgow, United Kingdom

12:00 PM

(EMA-S11-005-2016) Optimising core-shell microstructures using finite element modelling (Invited)

J. S. Dean*[1]; P. Y. Foeller[1]; I. M. Reaney[1]; D. C. Sinclair[1]; 1. University of Sheffield, United Kingdom

Student Speaking Competition Presentations I

Room: Coral A

Session Chairs: Jon Ihlefeld, Sandia National Laboratories; Brian Donovan, University of Virginia

12:45 PM

Introduction

12:50 PM

(EMA-SSC-001-2016) Probing Ionic Transport Mechanisms in Y-doped Barium Zirconate

J. Ding*[2]; E. Strelcov[2]; G. Veith[2]; C. Bridges[2]; J. Balachandran[2]; P. Ganesh[2]; S. Kalinin[2]; N. Bassiri-Gharb[1]; R. Unocic[2]; 1. Georgia Institute of Technology, USA; 2. Oak Ridge National Lab, USA

1:05 PM

(EMA-SSC-002-2016) Direct observation of local chemistry and B-site cation displacements in the relaxor ferroelectric PMN-PT

M. J. Cabral*[1]; X. Sang[1]; E. C. Dickey[1]; J. LeBeau[1]; 1. North Carolina State University, USA

1:20 PM

(EMA-SSC-003-2016) Structure of the Equilibrated Ni(111)-YSZ(111) Solid-Solid Interface

H. Nahor*[1]; W. D. Kaplan[1]; 1. Technion - Israel Institute of Technology, Israel

1:35 PM

(EMA-SSC-004-2016) Effect of Top Electrode Material on Radiation-Induced Degradation of Ferroelectric Thin Films

S. Brewer*[1]; M. Paul[3]; K. Fisher[4]; J. Guerrier[2]; J. L. Jones[2]; R. Rudy[5]; R. G. Polcawich[5]; E. Glaser[6]; C. Cress[6]; N. Bassiri-Gharb[1]; 1. Georgia Institute of Technology, USA; 2. North Carolina State University, USA; 3. Woodward Academy, USA; 4. Riverwood International Charter School, USA; 5. US Army Research Laboratory, USA; 6. Naval Research Laboratory, USA

S1. Multiferroic Materials and Multilayer Ferroic Heterostructures: Properties and Applications

Theory, Modeling, Materials Design I

Room: Coral A

Session Chairs: Burc Misirlioglu, Sabanci University; Daniel Shreiber, US Army Research Laboratory

2:00 PM

(EMA-S1-006-2016) Improper magnetic ferroelectricity of purely electronic nature in cycloidal spiral $CaMn_7O_{12}$ (Invited)

A. M. Rappe*[1]; J. Lim[1]; D. Saldana-Greco[1]; 1. University of Pennsylvania, USA

2:30 PM

(EMA-S1-007-2016) Emergence of ferroelectricity in nanoscale antiferroelectrics (Invited)

B. Mani[1]; S. Lisenkov[1]; I. Ponomareva*[1]; 1. University of South Florida, USA

3:00 PM

(EMA-S1-008-2016) Tailoring ferroelectricity for energy efficient field effect transistors (Invited)

B. Misirlioglu*[1]; P. Alpay[2]; 1. Sabanci University, Turkey; 2. University of Connecticut, USA

3:30 PM

Break

4:00 PM

(EMA-S1-009-2016) Designing Novel Functionalities in Dielectric and Ferroelectric Materials - Compositionally-Graded Thin-Film Heterostructures (Invited)

L. W. Martin*[1]; 1. University of California, Berkeley, USA

4:30 PM

(EMA-S1-010-2016) Miscibility Gap Closure, Interface, Morphology, and Phase Microstructureof 3D Li_xFePO_4 Nanoparticles from Surface Wetting and Coherency Strain (Invited)

M. Welland[1]; D. Karpeyev[2]; D. O'Connor[3]; O. Heinonen*[1]; 1. Argonne National Laboratory, USA; 2. University of Chicago, USA; 3. National Institute of Standards and Technology, USA

5:00 PM

(EMA-S1-011-2016) Cation Substituted Y- Phase Hexagonal Ferrite Materials with Improved High-frequency Permeability Values for Magnetodielctric Antenna Applications

M. D. Hill*[1]; S. Polisetty[1]; 1. Trans-Tech Inc., USA

5:15 PM

(EMA-S1-012-2016) Structural and Magnetic Properties of Nickel Zinc Ferrite Thick Films via Tape Casting

T. Kittel*[1]; G. Naderi[1]; J. Schwartz[1]; 1. North Carolina State University, USA

S2. Functional Materials: Synthesis Science, Properties, and Integration

Functional Materials : Advanced Synthesis and Structure-Property Relationships

Room: Mediterranean A

Session Chairs: Elizabeth Paisley, Sandia National Laboratories; Daniel Potrepka, U.S. Army Research Laboratory

2:00 PM

(EMA-S2-009-2016) Sputtering of complex oxides with *in situ* Reflection High-Energy Electron Diffraction (Invited)

J. P. Podkaminer*[1]; J. Patzner[1]; D. Lee[1]; B. Davidson[2]; C. Eom[1]; 1. University of Wisconsin-Madison, USA; 2. Temple University, USA

2:30 PM

(EMA-S2-010-2016) Thin Film growth of Entropy-Stabilized Oxides using Pulsed Laser Deposition

C. M. Rost*[1]; G. Ryu[2]; J. Maria[1]; 1. North Carolina State University, USA; 2. Changwon National University, The Republic of Korea

2:45 PM

(EMA-S2-011-2016) Epitaxial stabilization of metastable phases during atomic layer deposition and post-deposition annealing

J. E. Spanier*[1]; 1. Drexel University, USA

3:00 PM

(EMA-S2-012-2016) Selective Area Deposition of Oxide Thin Films on Gallium Nitride Surfaces (Invited)

M. D. Losego*[1]; E. A. Paisley[2]; D. Yin[1]; H. Craft[3]; R. Collazo[3]; Z. Sitar[3]; J. Maria[3]; 1. Georgia Institute of Technology, USA; 2. Sandia National Laboratories, USA; 3. North Carolina State University, USA

3:30 PM

Breal

4:00 PM

(EMA-S2-013-2016) First-principles guidance to polymorph selective epitaxial growth of MO_2 dioxides: informing epitaxial growth of metastable polymorphs (Invited)

P. Salvador*[1]; Z. Xu[1]; J. Wittkamper[1]; G. Rohrer[1]; J. R. Kitchin[1]; 1. Carnegie Mellon University, USA

4:30 PM

(EMA-S2-014-2016) In-situ Synchrotron X-ray and Density Functional Theory Studies on the Growth of $LaGaO_3$/ $SrTiO_3$ (001) Epitaxial Thin Films

P. Zapol*[1]; J. A. Eastman[1]; M. Highland[1]; A. Ruth[2]; D. Fong[1]; G. Ju[1]; P. Baldo[1]; C. Thompson[4]; H. Zhou[3]; P. Fuoss[1]; 1. Argonne Nat Lab, USA; 2. University of Notre Dame, USA; 3. Argonne National Lab, USA; 4. Northern Illinois University, USA

4:45 PM

(EMA-S2-015-2016) Effects of phase and texture on the thermal conductivity of chemical solution deposited strontium niobate thin films

K. E. Meyer*[1]; B. F. Donovan[1]; J. Gaskins[1]; J. Ihlefeld[2]; P. E. Hopkins[1]; 1. University of Virginia, USA; 2. Sandia National Laboratories, USA

5:00 PM

(EMA-S2-016-2016) Ferroelectric Switching Dynamics as a Function of Film Strain

L. Ye*[1]; R. Cordier[1]; V. Garcia[2]; M. Bibes[2]; R. Ramesh[3]; S. Salahuddin[3]; B. Huey[1]; 1. University of Connecticut, USA; 2. Unité Mixte de Physique CNRS/Thales, France; 3. University of California, Berkeley, USA

5:15 PM

(EMA-S2-017-2016) Intrinsic Electrocaloric Behavior of Perovskite Oxides

H. Khassaf*[1]; P. Alpay[1]; Z. Kutnjak[2]; 1. University of Connecticut, USA; 2. Jozef Stefan Institute, Slovenia

S3. Use of thermal energy for electrical power generation and refrigeration: Fundamental science, materials development and devices

Materials and Films

Room: Mediterranean B/C

Session Chair: Edward Gorzkowski, Naval Research Lab

2:00 PM

(EMA-S3-007-2016) Advanced Materials for Efficient Thermoelectric Power Generation (Invited)

J. Fleurial*[1]; S. Bux[1]; S. Firdosy[1]; T. Caillat[1]; 1. Jet Propulsion Laboratory, USA

2:30 PM

(EMA-S3-008-2016) Thermoelectric characterization of sputtered Ca-Mg-Si films

M. Uehara*[1]; M. Kurokawa[1]; K. Akiyama[2]; T. Shimizu[1]; M. Matsushima[1]; H. Uchida[3]; Y. Kimura[1]; H. Funakubo[1]; 1. Tokyo Institute of Technology, Japan; 2. Kanagawa Industrial Technology Center, Japan; 3. Sophia University, Japan

2:45 PM

(EMA-S3-009-2016) Crystalline coherence length and phonon-defect scattering effects on the thermal conductivity of MgO thin films

K. E. Meyer*[1]; R. Cheaito[1]; E. A. Paisley[2]; C. T. Shelton[3]; J. Maria[3]; J. Ihlefeld[2]; P. E. Hopkins[1]; 1. University of Virginia, USA; 2. Sandia National Laboratories, USA; 3. North Carolina State University, USA

3:00 PM

(EMA-S3-010-2016) The effect of WSi2 content on the microstructure of Si-Ge thermoelectrics

E. Farghadany*[1]; J. Mackey[1]; F. Dynys[2]; A. Sehirlioglu[1]; 1. Case Western Reserve University, USA; 2. NASA Glenn Research Center, USA

3:15 PM

(EMA-S3-011-2016) Thermal Conductivity of Amorphous Silicon Thin Films: Effects of Size and Elastic Modulus

J. L. Braun*[1]; M. Elahi[2]; J. Gaskins[1]; T. E. Beechem[3]; Z. C. Leseman[2]; H. Fujiwara[5]; S. King[4]; P. E. Hopkins[1]; 1. University of Virginia, USA; 2. University of New Mexico, USA; 3. Sandia National Laboratories, USA; 4. Intel Corporation, USA; 5. Gifu University, Japan

3:30 PM

Break

Materials II

Room: Mediterranean B/C

Session Chair: Edward Gorzkowski, Naval Research Lab

4:00 PM

(EMA-S3-012-2016) Thermoelectric Materials, Efficiency, and Power (Invited)

Z. Ren*[1]; 1. University of Houston, USA

4:30 PM

(EMA-S3-013-2016) Filled $Nd_zFe_xCo_{4-x}Sb_{12-y}Ge_y$ skutterudites: processing and thermoelectric properties

J. Mackey*[1]; A. Sehirlioglu[1]; F. Dynys[2]; 1. Case Western Reserve University, USA; 2. NASA Glenn Research Center, USA

4:45 PM

(EMA-S3-014-2016) Phonon and electron transports on the twin boundary in $CaTiO_3$

S. Funahashi*[1]; T. Nakamura[2]; A. Ando[2]; C. Randall[1]; 1. Pennsylvania State University, USA; 2. Murata Mfg. Co., Ltd., Japan

5:00 PM

(EMA-S3-015-2016) Microstructure and thermoelectric properties of $Sr(Ti_{0.8}Nb_{0.2})O_3$ with addition of SrO and CaO

M. Jeric[1]; M. Ceh*[1]; 1. Jozef Stefan Institute, Slovenia

5:15 PM

(EMA-S3-017-2016) Quasiparticle band structures and thermoelectric transport properties of p-type SnSe

G. Shi*[1]; E. Kioupakis[1]; 1. University of Michigan, USA

5:30 PM

(EMA-S3-018-2016) Evaporation of PbTe and GeTe based thermoelectric materials

Y. Sadia*[1]; T. Ohaion-Raz[1]; O. Ben-Yehuda[1]; Y. Gelbstein[1]; 1. Ben-Gurion University of the Negev, Israel

5:45 PM

(EMA-S3-019-2016) Filled and Unfilled Strontium Barium Niobate (SBN) Bronzes for Thermoelectric Applications

J. H. Chan*[1]; J. A. Bock[1]; S. Trolier-McKinstry[1]; C. Randall[1]; 1. Pennsylvania State University, USA

S5. Multifunctional Nanocomposites

Multifunctional Nanocomposites II

Room: Coral B

Session Chair: Scott Chambers, Pacific Northwest National Laboratory

2:00 PM

(EMA-S5-006-2016) Control of domains and control through domains in ferroelectric superlattices (Invited)

B. Bein[1]; M. Yusuf[1]; H. Hsing[1]; S. Callori[1]; J. Sinsheimer[1]; P. V. Chinta[2]; B. Nielsen[1]; R. Headrick[2]; X. Du[1]; M. Dawber*[1]; 1. Stony Brook University, USA; 2. University of Vermont, USA

2:30 PM

(EMA-S5-007-2016) Interface-induced Polarization in $SrTiO_3$-$LaCrO_3$ Superlattices

R. B. Comes*[1]; S. Spurgeon[1]; P. Sushko[1]; S. Heald[2]; D. Kepaptsoglou[3]; P. Ong[1]; L. Jones[4]; T. Kaspar[1]; M. Engelhard[1]; M. Bowden[1]; Q. Ramasse[3]; S. Chambers[1]; 1. Pacific Northwest National Lab, USA; 2. Argonne National Lab, USA; 3. STFC Daresbury, United Kingdom; 4. University of Oxford, United Kingdom

2:45 PM

(EMA-S5-008-2016) Understanding polarization asymmetry in $PbTiO_3$ based superlattice thin films

H. Hsing*[1]; S. Divilov[1]; M. Yusuf[1]; J. Bonini[2]; J. Bennett[2]; P. Chandra[2]; K. M. Rabe[2]; X. Du[1]; M. Fernandez Serra[1]; M. Dawber[1]; 1. Stony Brook University, USA; 2. Rutgers University, USA

3:00 PM

(EMA-S5-009-2016) Characterization of acceptor-doped BaTiO3 for capacitor and its insulation degradation behavior using charge-based DLTS method (Invited)

T. Okamoto*[1]; J. Long[2]; J. Stitt[2]; R. Wilke[2]; K. Suzuki[1]; H. Kondo[1]; N. Tanaka[1]; A. Ando[1]; C. Randall[2]; 1. Murata Mfg. Co., Ltd., Japan; 2. Pennsylvania State University, USA

3:30 PM

Break

4:00 PM

(EMA-S5-010-2016) Probing the Reaction Pathway in $(La_{0.8}Sr_{0.2})_{0.95}MnO_{3+\delta}$ Using Libraries of Thin Film Microelectrodes (Invited)

S. M. Haile*[1]; R. Usiskin[2]; S. Maruyama[3]; C. Kucharczyk[2]; I. Takeuchi[3]; 1. Northwestern University, USA; 2. California Institute of Technology, USA; 3. University of Maryland, USA

4:30 PM

(EMA-S5-011-2016) Cationic ordering and its effect on the physical properties of functional oxides (Invited)

S. Choi*[1]; 1. Korea Institute of Materials Science, The Republic of Korea

5:00 PM

(EMA-S5-012-2016) Gas Sensing Properties of Epitaxial LaBaCo2O5.5+δ Thin Films

S. Ren*[1]; M. Liu[1]; 1. Xi'an Jiaotong University, China

S7. Processing and microstructure of functional ceramics: Sintering, grain growth and their impact on the materials properties

Defects, Space Charge and Non-Stoichiometry in Sintering and Grain growth

Room: Caribbean B

Session Chairs: Wolfgang Rheinheimer, Karlsruhe Institute of Technology; Michael Hoffmann, Karlsruhe Institute of Technology

2:00 PM

(EMA-S7-007-2016) Conventional solid state synthesis of $BiFeO_3$-$Bi_{0.5}K_{0.5}TiO_3$ solid solution - effects of cation non-stoichiometry and compositional inhomogeneity (Invited)

T. Grande*[1]; 1. Norwegian University of Science and Technology, Norway

2:30 PM

(EMA-S7-008-2016) The effects of non-stoichiometry and ceramic processing on the electrical properties of $Na_{1/2}Bi_{1/2}TiO_3$ (Invited)

D. C. Sinclair*[1]; L. Li[1]; M. Li[1]; H. Zhang[1]; Y. Wu[1]; F. Yang[1]; I. M. Reaney[1]; 1. University of Sheffield, United Kingdom

3:00 PM

(EMA-S7-009-2016) Impedance Spectroscopy as a Tool to Detect Detailed Grain Boundary Properties in Single Phase and Heterogeneous Materials (Invited)

R. A. Gerhardt*[1]; 1. Georgia Institute of Technology, USA

3:30 PM

Break

4:00 PM

(EMA-S7-010-2016) Correlation of microstructure and microwave properties of $(Ba,Sr)TiO_3$ ceramics (Invited)

J. R. Binder*[1]; C. Kohler[1]; A. Friederich[1]; A. Wiens[2]; M. Nikfalazar[2]; H. Maune[2]; R. Jakoby[2]; 1. Karlsruhe Institute of Technology, Germany; 2. Technical University Darmstadt, Germany

4:30 PM

(EMA-S7-011-2016) Conventional and spark plasma sintering of $Na_{1/2}Bi_{1/2}Cu_3Ti_4O_{12}$ giant dielectric ceramics

M. M. Ahmad*[1]; 1. King Faisal University, Saudi Arabia

4:45 PM

(EMA-S7-012-2016) Microstructures and dielectric properties of layered perovskite $K(Sr,Ba)_2Nb_3O_{10}$ ceramics

W. Lee*[1]; S. Kweon[1]; M. Im[1]; S. Nahm[1]; 1. Korea University, The Republic of Korea

5:00 PM

(EMA-S7-013-2016) Piezoresponse in the nano-range for $Ba_{0.9}Ca_{0.1}Zr_{0.1}Ti_{0.9}O_3$ obtained by modified Pechini method

G. M. Herrera*[1]; A. Reyes-Rojas[1]; A. Reyes-Montero[2]; M. Villafuerte-Castrejon[2]; A. Hurtado[1]; O. Solis[1]; R. Ochoa[1]; F. Paraguay-Delgado[1]; L. Fuentes-Cobas[1]; 1. CIMAV, Mexico; 2. UNAM, Mexico

S9. Recent Developments in Superconducting Materials and Applications

New Superconductor 2 - Characterization of Structural, Magnetic, and Superconducting Properties

Room: Pacific

Session Chairs: Athena Sefat, Oak Ridge National Laboratory; Jacilynn Brant, Air Force Research Lab

2:00 PM

(EMA-S9-006-2016) Interplay between density wave order and superconductivity in $Na_2Ti_2Pn_2O$ (Pn=Sb, As) and $Ba_2Ti_2Fe_2As_4O$: an optical spectroscopy study (Invited)

N. Wang*[1]; 1. International Center for Quantum Materials, School of Physics, Peking University, China

2:30 PM

(EMA-S9-007-2016) Recent Findings in Thallium-based Materials of Tl-1223, Tl-2223, and Tl-122 (Invited)

A. Sefat*[1]; 1. Oak Ridge National Laboratory, USA

3:00 PM

(EMA-S9-008-2016) Solid-State Synthesis, Structural Analysis and Physical Property Characterization Toward New Superconducting Materials (Invited)

J. Brant*[1]; D. Vier[2]; C. Ebbing[1]; T. Bullard[1]; T. J. Haugan[1]; 1. Air Force Research Lab, USA; 2. University of California, San Diego, USA

3:30 PM

Break

4:00 PM

(EMA-S9-009-2016) High-pressure and high-temperature synthesis of superconducting materials and related materials (Invited)

K. Yamaura*[1]; 1. National Institute for Materials Science, Japan

4:30 PM

(EMA-S9-010-2016) Pressure-induced metal-semiconductor transition in $ThCr_2Si_2$-type $BaCr_{2-x}Co_xAs_2$

G. Wang*[1]; 1. Institute of Physics, Chinese Academy of Sciences, China

4:45 PM

(EMA-S9-011-2016) Why are Fe-based superconductors so creepy? (Invited)

L. Civale*[1]; 1. Los Alamos National Lab, USA

5:15 PM

(EMA-S9-012-2016) Interplay between magnetism, structure, and superconductivity in Mo3Sb7 (Invited)

J. Yan*[1]; M. McGuire[1]; A. May[1]; D. Mandrus[1]; D. Parker[1]; Y. Feng[3]; J. Cheng[2]; B. Sales[1]; 1. Oak Ridge National Lab, USA; 2. Institute of Physics, China; 3. Argonne National Lab, USA

5:45 PM

(EMA-S9-013-2016) Superconductivity in a ferromagnetic semiconductor

E. Anton*[1]; S. Granville[1]; A. Engel[2]; S. Chong[1]; M. Governale[1]; U. Zülicke[1]; A. Moghaddam[3]; J. Trodahl[1]; F. Natali[1]; S. Vezian[4]; B. Ruck[1]; 1. Victoria University of Wellington, New Zealand; 2. University of Zürich, Switzerland; 3. Institute for Advanced Studies in Basic, The Islamic Republic of Iran; 4. Centre National de la Recherche Scientifique, France

S11. Advanced electronic Materials: Processing, structures, properties and applications

Characterization of Electronic Materials I

Room: Indian

Session Chair: Jacob Jones, North Carolina State University

2:00 PM

(EMA-S11-006-2016) Raman spectroscopy of electronic devices (Invited)

M. Deluca*[1]; 1. Materials Center Leoben Forschung GmbH, Austria

2:30 PM

(EMA-S11-007-2016) Impedance Analysis of Fe-doped $SrTiO_3$ and $BaTiO_3$ during Degradation and Recovery

J. Carter*[1]; T. J. Bayer[1]; C. Randall[1]; 1. Pennsylvania State University, USA

2:45 PM

(EMA-S11-008-2016) Investigating the chemistry at oxide/oxide and oxide/nitride interfaces via scanning transmission electron microscopy

E. D. Grimley*[1]; X. Sang[1]; E. Sachet[1]; C. T. Shelton[1]; C. Rost[1]; J. Maria[1]; J. LeBeau[1]; 1. North Carolina State University, USA

3:00 PM

(EMA-S11-009-2016) Dimensions of cathode, bulk, and anode region during degradation and recovery in Fe-doped STO single crystals

T. J. Bayer*[1]; J. Carter[1]; C. Randall[1]; 1. Pennsylvania State University, USA

3:15 PM

(EMA-S11-010-2016) Direct observation of local chemistry and B-site cation displacements in the relaxor ferroelectric PMN-PT

M. J. Cabral*[1]; X. Sang[1]; E. C. Dickey[1]; J. LeBeau[1]; 1. North Carolina State University, USA

3:30 PM

Break

Characterization of Electronic Materials II

Room: Indian

Session Chair: Marco Deluca, Materials Center Leoben Forschung GmbH

4:00 PM

(EMA-S11-011-2016) Towards functionality in fluorites: nonequilibrium structures in thin films and bulk ceramics (Invited)

J. L. Jones*[1]; C. Fancher[1]; D. Hou[1]; S. Jones[1]; C. Chung[1]; B. Johnson[1]; 1. North Carolina State University, USA

4:30 PM

(EMA-S11-012-2016) Microdomain dynamics in single-crystal $BaTiO_3$ during paraelectric- ferroelectric phase transition measured with time-of-flight neutron scattering

A. Pramanick*[1]; X. Wang[2]; C. Hoffmann[2]; S. Diallo[2]; M. Jorgensen[3]; X. Wang[1]; 1. City University of Hong Kong, Hong Kong; 2. Oak Ridge National Lab, USA; 3. Aarhus University, Denmark

4:45 PM

(EMA-S11-013-2016) Plastic Strain Induced Dislocations and Conductivity Modification in Strontium Titanate

E. A. Patterson*[1]; E. Coskun[1]; T. Frömling[1]; K. G. Webber[2]; W. Donner[1]; J. Rödel[1]; 1. Technical University Darmstadt, Germany; 2. Friedrich-Alexander-University Erlangen-Neurnberg, Germany

5:00 PM

(EMA-S11-014-2016) Investigation of Resistance Degradation and Dielectric Breakdown of Fe-doped $SrTiO_3$ Single Crystal

A. Moballegh*[1]; T. J. Bayer[2]; C. Randall[2]; E. C. Dickey[1]; 1. NC State University, USA; 2. Pennsylvania State University, USA

5:15 PM

(EMA-S11-015-2016) Characterization, mechanical and thermochemical properties of perovskites studied by thermal analysis and calorimetry

K. Lilova*[1]; 1. Setaram Inc., USA

Posters

Poster Session

Room: Atlantic/Arctic

5:30 PM

(EMA-S1-P001-2016) Interface-Engineered BaTiO3-Based Heterostructures for Room Temperature Tunable Microwave Elements

M. Liu*[1]; C. Ma[1]; C. Chen[2]; 1. Xi'an Jiaotong University, China; 2. University of Texas at San Antonio, USA

(EMA-S2-P002-2016) On the origin of electrical fatigue in the giant piezo-strain response of the lead-free piezoelectric Na0.5Bi0.5TiO3-BaTiO3-K0.5Na0.5NbO3

D. K. Khatua*[1]; 1. INDIAN INSTITUTE OF SCIENCE, India

(EMA-S2-P003-2016) Nanostructured oxide composites for high-performance gas sensors

P. Feng[1]; S. Feng-Chen[1]; A. Aldalbahi[2]; E. Li*[1]; M. Rivera[1]; 1. Physics Department, UPR-RP, USA; 2. Department of Chemistry, Collage of Science, King Saud University, Saudi Arabia

(EMA-S2-P004-2016) Organic-Inorganic Hybrid Dielectrics for Film Capacitors

B. D. Piercy*[1]; C. Liu[1]; M. D. Losego[1]; 1. Georgia Institute of Technology, USA

(EMA-S2-P005-2016) The Study of Radiation Tolerance in Ferroelectric Microelectromechanical Switches via *in-situ* X-ray Diffraction

J. Guerrier*[1]; S. Brewer[2]; M. Paul[2]; K. Fisher[2]; R. Rudy[3]; R. G. Polcawich[3]; E. Glaser[4]; C. Cress[4]; N. Bassiri-Gharb[2]; J. L. Jones[1]; 1. North Carolina State University, USA; 2. Georgia Institute of Technology, USA; 3. US Army Research Laboratory, USA; 4. Naval Research Laboratory, USA

(EMA-S3-P006-2016) High Temperature Coatings for Thermosolar Applications

J. Hormadaly*[1]; 1. Ben-Gurion University of the Negev, Israel

(EMA-S3-P007-2016) Size effect in the thermopower of metallic thin-film stripes and its application in temperature sensing at micro/nano-scales
X. Huo*[1]; G. Li[1]; S. Xu[1]; 1. Peking University, China

(EMA-S4-P008-2016) Electrical Properties of Perovskite-Related Cobaltites/Ferrites Mixed Conductors
M. Tange*[1]; A. Mineshige[1]; T. Yazawa[1]; 1. University of Hyogo, Japan

(EMA-S4-P009-2016) $Li_{10}GeP_2S_{12}$-type Superionic Conductors in the Li_4MS_4–Li_3PS_4 System (M = Si, Ge, Sn): Synthesis and Structure–property Relationships
S. Hori*[1]; K. Suzuki[1]; M. Hirayama[1]; R. Kanno[1]; 1. Interdisciplinary Graduate School of Science and Engineering, Tokyo Institute of Technology, Japan

(EMA-S4-P010-2016) Preparation of oxygen-excess-type ionic conducting thin film for fuel cell application
A. Saito*[1]; A. Mineshige[1]; H. Yoshioka[2]; R. Mori[3]; T. Yazawa[1]; 1. University of Hyogo, Japan; 2. Hyogo Prefectural Institute of Technology, Japan; 3. Fuji-Pigment. Co. Ltd., Japan

(EMA-S4-P011-2016) Chemical solution deposition of highly c-axis oriented apatite-type lanthanum silicate thin films
S. Hori*[1]; Y. Takatani[1]; H. Kadoura[1]; T. Uyama[1]; S. Fujita[1]; T. Tani[1]; 1. Toyota Central Research & Development Labs., Inc., Japan

(EMA-S5-P012-2016) Strain and Interface Effects in a Novel Bismuth-Based Self-Assembled Supercell Structure
L. Li*[1]; W. Zhang[1]; M. Fan[1]; J. Huang[1]; J. Jian[1]; A. Chen[2]; H. Wang[1]; 1. Texas A&M University, USA; 2. Los Alamos National Lab, USA

(EMA-S5-P013-2016) Surface- and Strain-Tuning of the Optical Dielectric Function in Epitaxial $CaMnO_3$
D. Imbrenda*[1]; D. Yang[2]; H. Wang[2]; A. R. Akbashev[1]; B. A. Davidson[2]; X. Wu[2]; X. Xi[2]; J. E. Spanier[1]; 1. Drexel University, USA; 2. Temple University, USA

(EMA-S5-P014-2016) Damage Sensing of CNT-Polypropylene (PP) Composites by Electrical Resistance Measurement for Automobile Applications
J. Park*[1]; D. Kwon[1]; L. K. DeVries[2]; 1. Gyeongsang Natl Univ, The Republic of Korea; 2. The University of Utah, USA

(EMA-S6-P015-2016) Controlling Spin Ordering in Rare-Earth Perovskite Vanadates
N. Wagner*[1]; J. Rondinelli[1]; 1. Northwestern University, USA

(EMA-S6-P016-2016) Displacement Radiation Effects in Ferroelectric $BaTiO_3$: A Molecular Dynamics Study
Y. Ma*[1]; 1. University of Wisconsin-Eau Claire, USA

(EMA-S6-P017-2016) Effects of doping on the magnetic ordering in $EuTiO_3$
Z. Gui*[1]; A. Janotti[1]; 1. University of Delaware, USA

(EMA-S7-P018-2016) Development of radio transparent ceramic materials
R. V. Kryvobok*[1]; G. Lisachuk[1]; A. Zakharov[1]; E. Fedorenko[1]; M. Prytkina[1]; 1. National Technical University "Kharkiv Polytechnic Institute", Ukraine

(EMA-S7-P019-2016) Densification and Nanostructural Features of Al_2O_3 Ceramics Prepared with Nanoscale Powders by Microwave-assisted Sintering
N. Cho*[1]; H. Yun[1]; D. Jeong[1]; 1. Inha University, The Republic of Korea

(EMA-S8-P020-2016) $BaTiO_3$ doped ceramics fractal sources dielectric properties
V. Mitic*[1]; L. Kocic[1]; V. Paunovic[1]; 1. Faculty of Electronic Engineering, Serbia

(EMA-S8-P021-2016) Structural Characterization of Organic-Inorganic Hybrid Materials Formed via Vapor-Phase Infiltration of Polymers
C. Leng*[1]; D. Henry[1]; M. D. Losego[1]; 1. Georgia Institute of Technology, USA

(EMA-S8-P022-2016) Understanding solid state dewetting of gold on indium tin oxide
J. A. Lai*[1]; H. Zhou[2]; N. Valanoor[1]; J. L. Jones[2]; 1. University of New South Wales, Australia; 2. North Carolina State University, USA

(EMA-S9-P023-2016) Optimizing Flux Pinning of $YBa_2Cu_3O_{7-\delta}$ Superconductor with $BaHfO_3$+Y_2O_3 Mixed Phase Additions
M. P. Sebastian*[1]; T. Bullard[2]; C. Ebbing[3]; M. Sullivan[3]; J. Huang[4]; H. Wang[4]; J. Wu[5]; T. J. Haugan[1]; 1. Air Force Research Laboratory, USA; 2. UES, USA; 3. UDRI, USA; 4. Texas A&M University, USA; 5. University of Kansas, USA

(EMA-S9-P024-2016) Searching for Signatures of Superconductivity in Rare Earth Oxides
J. Brant*[1]; J. Burke[1]; C. Ebbing[1]; D. Vier[2]; T. Bullard[1]; T. J. Haugan[1]; 1. Air Force Research Lab, USA; 2. University of California, San Diego, USA

(EMA-S9-P025-2016) Searching for superconductivity in doped carbon allotropes
N. Gheorghiu*[1]; B. Pierce[2]; C. Ebbing[3]; T. Bullard[1]; J. Brant[4]; D. Vier[5]; T. J. Haugan[2]; 1. UES, Inc., USA; 2. AFRL/WPAFB, USA; 3. University of Dayton Research Institute, USA; 4. National Academies of Sciences, USA; 5. University of California San Diego, USA

(EMA-S9-P026-2016) Impact of cryogenic and superconducting components for hybrid-electric aircraft propulsion
T. J. Haugan*[1]; G. Panasyuk[2]; 1. Air Force Research Lab, USA; 2. UES, Inc., USA

(EMA-S11-P027-2016) Low Temperature Co-fired High Power Multilayer Piezoelectric Transformers
A. E. Gurdal*[1]; S. Tuncdemir[2]; K. Uchino[1]; C. Randall[1]; 1. Pennsylvania State University, USA; 2. Solid State Ceramics, Inc., USA

(EMA-S11-P028-2016) Electric-field-induced structural changes at the local scale in dielectrics and ferroelectrics
T. Usher*[1]; D. Hou[1]; N. Prasertpalichatr[2]; I. Levin[3]; J. E. Daniels[4]; D. Cann[2]; J. L. Jones[1]; 1. North Carolina State University, USA; 2. Oregon State University, USA; 3. National Institute of Standards and Technology, USA; 4. UNSW Australia, Australia

(EMA-S11-P029-2016) Correlating effects of point defect concentrations on thermal conductivity and coercive field of LiTaO3 single crystals
J. Ivy*[1]; K. Meyer[2]; P. E. Hopkins[2]; G. L. Brennecka[1]; 1. Colorado School of Mines, USA; 2. University of Virginia, USA

(EMA-S11-P030-2016) The effect of 0.5 mol% B_2O_3 addition on the grain growth in ZnO- 0.5 mol% V_2O_5 doped ceramics
G. Hardal[1]; B. Yuksel Price*[1]; 1. Istanbul University Engineering Faculty, Turkey

(EMA-S11-P031-2016) $(Bi_{0.500}Na_{0.500})_{0.920}Ba_{0.065}La_{0.010}TiO_3$: an antiferroelectric lead-free ceramic system
Y. Méndez González[2]; A. Peláiz Barranco[2]; A. Pentón Madrigal[2]; J. de los Santos Guerra*[1]; 1. Federal University of Uberlandia, Brazil; 2. Universidad de La Habana, Cuba

(EMA-S11-P032-2016) Structural analysis of two-, three- and four-layered Aurivillius' ferroelectric ceramics
A. Peláiz Barranco[2]; Y. González Abreu[2]; J. de los Santos Guerra*[1]; Y. Gagou[3]; P. Saint-Grégoire[4]; 1. Federal University of Uberlandia, Brazil; 2. Universidad de La Habana, Cuba; 3. University of Picardie, France; 4. University of Nimes, France

(EMA-S11-P033-2016) Lead-free ferroelectric $Bi_{1/2}Na_{1/2}TiO_3$ targets and thin films
E. Anton*[1]; S. Sambale[1]; T. Müller[1]; T. Sperk[1]; 1. Victoria University of Wellington, New Zealand

(EMA-S11-P034-2016) Effects of the Degree of Crosslinking on Flammability and Reliability of Metal-polymer Composite Films
S. Jeon*[1]; Y. Yun[1]; S. Park[1]; 1. ChangSung Co., Ltd., The Republic of Korea

(EMA-S11-P035-2016) Analysis of the phase transition in rare earth modified PZT ferroelectric ceramics
J. de los Santos Guerra*[1]; S. Hessel[1]; A. Carvalho da Silva[2]; I. Cruvinel dos Reis[2]; R. Guo[3]; A. S. Bhalla[3]; 1. Federal University of Uberlandia, Brazil; 2. Universidade Estadual Paulista, Brazil; 3. The University of Texas at San Antonio, USA

(EMA-S11-P036-2016) Temperature-induced local and mesoscale structural changes of $BaTiO_3$–$Bi(Zn_{0.5}Ti_{0.5})O_3$
D. Hou*[1]; T. Usher[1]; N. Raengthon[2]; N. Triamnak[2]; D. Cann[2]; J. L. Jones[1]; 1. North Carolina State University, USA; 2. Oregon State University, USA

(EMA-S11-P037-2016) Preparation of Nano-sized TiO_2 Electroded Dye Sensitized Solar Cell with Red and Green Chilli-derived Natural Dye Extracts
Y. M. Maung*[1]; 1. Mandalay University, Myanmar

(EMA-S11-P038-2016) Fabrication and Characterization of ZnO Nanowires with Chlorophyll-based Grass Dye Extract for Dye-sensitized Solar Cell Application
T. T. Win*[1]; 1. Mandalay University of Distance Education, Myanmar

(EMA-S11-P039-2016) EMI noise suppression material for the band of 3 ~ 6GHz
S. Kim*[1]; Y. Yun[1]; S. Park[1]; 1. Changsung Corporation, The Republic of Korea

(EMA-S11-P040-2016) Electrical and microstructural properties of $Ni_{0.5}Co_{0.5}Cu_{0.15}Mn_{1.85}O_4$ NTC thermistors by doping 0.1 mol B_2O_3 without calcination
G. Hardal[1]; B. Yuksel Price*[1]; 1. ISTANBUL UNIVERSITY ENGINEERING FACULTY, Turkey

(EMA-S11-P041-2016) Temperature Stable Dielectrics Based on $BaTiO_3$-$Bi(Zn_{1/2}Ti_{1/2})O_3$-$BiScO_3$-$NaNbO_3$
C. S. McCue*[1]; 1. Oregon State University, USA

(EMA-S11-P042-2016) Dielectric analyses and conduction mechanisms in $Bi_{4-x}La_xTi_3O_{12}$ based Aurivillius type ferroelectric ceramics
I. Cruvinel dos Reis*[1]; A. Carvalho da Silva[1]; A. S. Bhalla[2]; R. Guo[2]; J. de los Santos Guerra[3]; 1. Universidade Estadual Paulista, Brazil; 2. The University of Texas at San Antonio, USA; 3. Federal University of Uberlandia, Brazil

(EMA-S11-P043-2016) A critical strain failure criterion of a silver nanowire electrode for highly flexible devices
D. Kim[1]; S. Kim[1]; J. Ahn[1]; S. Kim*[1]; 1. Korea Institute of Science and Technology, The Republic of Korea

(EMA-S11-P044-2016) Unusual Near-field Electromagnetic Absorption Attenuation in Transparent Flexible Graphene
S. Kim*[1]; J. Kang[2]; Y. Kim[3]; J. Choi[4]; B. Hong[3]; 1. Korea Institute of Science and Technology, The Republic of Korea; 2. Northwestern University, USA; 3. Seoul National University, The Republic of Korea; 4. Sungkyunkwan University, The Republic of Korea

(EMA-S11-P045-2016) Electronic and Chemical Characterization of Barium Titanate Interfaces
D. Long*[1]; 1. North Carolina State University, USA

(EMA-S11-P046-2016) Study of $Ge_2Sb_2Te_5$ properties for opto-electronic applications
G. Rodriguez Hernandez*[1]; P. Hosseini[1]; H. Bhaskaran[1]; 1. University of Oxford, United Kingdom

(EMA-S11-P047-2016) Effect of the Fe and Mn Doping on The Piezoelectric Properties of 94NBT-6BT Single Crystal
A. Dogan*[1]; M. Gurbuz[2]; 1. Anadolu University, Turkey; 2. Ondokuz Mayis University, Turkey

(EMA-S11-P048-2016) Effect of glass doping on the Initial permeability of microwave sintered MgCuZn Ferrites
W. Madhuri*[1]; S. K.V.[3]; S. Srigiri[2]; 1. VIT University, Vellore, India; 2. University of New Orleans, USA; 3. Sri Krishnadevaya University, India

(EMA-S11-P049-2016) Optimization of the Morphology of VOC Sensors Based on Polymer-metal Nanocomposites
N. Zerihun*[1]; 1. Addis Ababa Institute of Technology, Ethiopia

Basic Science Division Tutorial

Room: Coral A

7:45 PM - 9:45 PM

Structure and Kinetics of Interfaces in Ceramics
Gregory Rohrer, Carnegie Mellon University, USA; Shen Dillon, University of Illinois, USA

Thursday, January 21, 2016

Plenary Session

Plenary II

Room: Indian

8:30 AM

Introduction

8:40 AM

(EMA-PL-002-2016) The Materials Genome Initiative: NIST, Data, and Open Science
J. A. Warren*[1]; 1. National Institute of Standards and Technology, USA

9:30 AM

Break

S1. Multiferroic Materials and Multilayer Ferroic Heterostructures: Properties and Applications

Theory, Modeling, Materials Design II

Room: Coral A

Session Chairs: Pamir Alpay, University of Connecticut; Tulsi Patel, University of Connecticut

10:00 AM

(EMA-S1-013-2016) Functional superlattices from first principles (Invited)
K. M. Rabe*[1]; 1. Rutgers University, USA

10:30 AM

(EMA-S1-014-2016) Are Ferroelectric Multilayers Capacitors in Series?
F. Sun[1]; T. Kesim[1]; Y. Espinal*[1]; P. Alpay[1]; 1. University of Connecticut, USA

10:45 AM

(EMA-S1-015-2016) Giant Enhancement in the Ferroelectric Field Effect Using a Polarization Gradient
Z. Gu*[1]; M. Islam[2]; J. E. Spanier[1]; 1. Drexel University, USA; 2. State University of New York @ Oswego, USA

11:00 AM

(EMA-S1-016-2016) Extraordinary transmission of terahertz pulses through subwavelength aperture array: The role of thin $Ba_{0.6}Sr_{0.4}TiO_3$ film (Invited)
D. Shreiber*[1]; M. P. Ivill[1]; S. A. Ponomarenko[2]; J. Reeves[3]; M. Cole[1]; 1. US Army Research Laboratory, USA; 2. Dalhousie University, Canada; 3. Menlo Systems, USA

11:30 AM

(EMA-S1-017-2016) Polarization nanodomains in ferroelectric/dielectric superlattice nanostructures (Invited)
P. G. Evans*[1]; Q. Zhang[1]; J. Park[1]; Y. Ahn[1]; M. Dawber[2]; R. Harder[3]; M. Holt[3]; 1. University of Wisconsin, USA; 2. Stony Brook University, USA; 3. Argonne National Lab, USA

12:00 PM

(EMA-S1-018-2016) Probing the interfacial phases of correlated oxides controlled by ferroelectric polarization
T. Meyer*[1]; A. Herklotz[1]; S. Lee[1]; L. Jiang[1]; V. Lauter[1]; M. Fitzsimmons[1]; T. Ward[1]; H. Lee[1]; 1. Oak Ridge National Laboratory, USA

12:15 PM

(EMA-S1-019-2016) Electric–field tunable filters on strain–engineered oxides
N. D. Orloff*[1]; X. Lu[1]; H. Nair[2]; N. Dawly[2]; D. Schlom[2]; J. Booth[2]; 1. NIST, USA; 2. Cornell University, USA

S2. Functional Materials: Synthesis Science, Properties, and Integration

Functional Materials: Integration, Measurement, and Property Enhancement in Piezoelectric Thin Films and Ceramics

Room: Mediterranean A

Session Chair: Mark Losego, Georgia Institute of Technology

10:00 AM

(EMA-S2-018-2016) Optimization of IrO_2 as a top electrode for PZT devices
M. Rivas*[1]; D. M. Potrepka[2]; B. Huey[1]; R. G. Polcawich[2]; 1. University of Connecticut, USA; 2. US Army Research Laboratory, USA

10:15 AM

(EMA-S2-019-2016) Optimization of IrO_2 as a bottom electrode for PZT devices
D. M. Potrepka*[1]; M. Rivas[2]; G. R. Fox[3]; R. G. Polcawich[1]; 1. U.S. Army Research Laboratory, USA; 2. University of Connecticut, USA; 3. Fox Materials Consulting, LLC, USA

10:30 AM

(EMA-S2-020-2016) PiezoMEMS with Integrated Electronics
S. Trolier-McKinstry*[1]; 1. Pennsylvania State University, USA

10:45 AM

(EMA-S2-021-2016) Effect of Mechanical Constraint on Ferroelectric/Ferroelastic Domain Reorientation in {111} Textured Tetragonal Lead Zirconate Titanate Films
G. Esteves*[1]; M. Wallace[2]; R. Johnson-Wilke[3]; C. Fancher[1]; R. Wilke[3]; S. Trolier-McKinstry[2]; J. L. Jones[1]; 1. North Carolina State University, USA; 2. The Pennsylvania State University, USA; 3. Sandia National Laboratory, USA

11:00 AM

(EMA-S2-022-2016) Misfit strain phase diagrams and piezoelectric properties of (001) PMN-PT epitaxial thin films
N. Khakpash*[1]; H. Khassaf[1]; G. Rossetti[1]; P. Alpay[1]; 1. University of Connecticut, USA

11:15 AM

(EMA-S2-023-2016) Analog Memory Storage using a Ferroelectric Capacitor
J. T. Evans*[1]; 1. Radiant Technologies, Inc., USA

11:30 AM

(EMA-S2-024-2016) Simultaneous Electrical and Piezoelectric Characterization of PiezoMEMS Structures via PUND Plus Laser Doppler Vibrometry
R. G. Polcawich*[1]; R. Rudy[1]; M. Rivas[1]; G. R. Fox[2]; 1. US Army Research Laboratory, USA; 2. Fox Materials Consulting, USA

11:45 AM

(EMA-S2-025-2016) Negative Pressure and Property Enhancements in Free Standing Particles
J. Wang[2]; L. McGilly[1]; X. Wei[1]; T. Sluka[1]; N. Setter*[1]; 1. EPFL, Switzerland; 2. Tsinghua University, China

12:00 PM

(EMA-S2-026-2016) Control of properties by modification of phase distribution and microstructure in high temperature piezoelectrics
B. Kowalski*[1]; A. Sehirlioglu[1]; 1. Case Western Reserve University, USA

12:15 PM

(EMA-S2-027-2016) Perovskite-type materials for energy converters
A. Weidenkaff*[1]; W. Xie[1]; M. Widenmeyer[1]; X. Xiao[1]; 1. Universität Stuttgart, Germany

S5. Multifunctional Nanocomposites

Multifunctional Nanocomposites III

Room: Coral B

Session Chair: Aiping Chen, Los Alamos National Lab

10:00 AM

(EMA-S5-013-2016) Multifunctional Mesocrystal systems for Energy Applications (Invited)
Y. Chu*[1]; 1. National Chiao Tung University, Taiwan

10:30 AM

(EMA-S5-014-2016) Exchange Coupling and Magnetotransport Properties in Multifunctional Heteroepitaxial Oxide Nanocomposites
W. Zhang*[1]; M. Fan[1]; L. Li[1]; P. Lu[2]; A. Chen[3]; Q. Jia[3]; J. MacManus-Driscoll[4]; H. Wang[1]; 1. Texas A&M University, USA; 2. Sandia National Laboratories, USA; 3. Los Alamos National Lab, USA; 4. University of Cambridge, United Kingdom

10:45 AM

(EMA-S5-015-2016) Synthesis and Characterization of Epitaxial Nanocomposite Films: Effect of Interface on the Functionalities (Invited)
A. Chen[1]; S. Lee[3]; W. Zhang[2]; H. Wang[2]; J. Zhu[1]; J. MacManus-Driscoll[3]; M. Fitzsimmons[1]; Q. X. Jia*[1]; 1. Los Alamos National Laboratory, USA; 2. Texas A&M University, USA; 3. Univ. of Cambridge, United Kingdom

11:15 AM

(EMA-S5-016-2016) In-situ synchrotron X-ray studies of the synthesis and electrical behavior of In_2O_3-CeO_2 epitaxial nanocomposite thin films
J. A. Eastman*[1]; M. Highland[1]; B. Veal[1]; D. Fong[1]; G. Ju[1]; C. Thompson[2]; P. Zapol[1]; P. Fuoss[1]; H. Zhou[1]; P. Baldo[1]; 1. Argonne National Lab, USA; 2. Northern Illinois University, USA

11:30 AM

(EMA-S5-017-2016) Memory Devices based on Self-Assembled Materials and Processes (Invited)
J. Lee*[1]; 1. Pohang University of Science and Technology(POSTECH), The Republic of Korea

12:00 PM

(EMA-S5-018-2016) Dielectric Nanocomposites for Energy Storage Applications (Invited)
H. Wang*[1]; 1. Xi'an Jiaotong University, China

S7. Processing and microstructure of functional ceramics: Sintering, grain growth and their impact on the materials properties

Sintering Techniques: Conventional Sintering and Field Assisted Sintering

Room: Caribbean B

Session Chairs: Wolfgang Rheinheimer, Karlsruhe Institute of Technology; Michael Hoffmann, Karlsruhe Institute of Technology

10:00 AM

(EMA-S7-014-2016) Grain Boundary formation and grain growth in the presence of externally applied electric fields (Invited)
K. van Benthem*[1]; 1. University of California, Davis, USA

10:30 AM

(EMA-S7-015-2016) Microstructure and Variable Chemistry of Flash Sintered $K_{0.5}Na_{0.5}NbO_3$ Ceramics (Invited)
G. Corapcioglu[1]; M. A. Gulgun*[1]; S. Sturm[3]; R. Raj[2]; 1. Sabanci University, Turkey; 2. Univesity of Colorado at Boulder, USA; 3. Jozef Stefan Institute, Slovenia

11:00 AM

(EMA-S7-016-2016) How to understand sintering of sodium potassium niobate ceramics? (Invited)
B. Malic*[1]; J. Koruza[2]; J. Hreščak[1]; J. Bernard[3]; G. Drazic[4]; A. Bencan[1]; 1. Jozef Stefan Institute, Slovenia; 2. Technical University Darmstadt, Germany; 3. Civil Engineering Institute, Slovenia; 4. National Institute of Chemistry, Slovenia

11:30 AM

(EMA-S7-017-2016) Additive Manufacturing of Aerosol Deposited AZO Conductive Patterns
N. S. Bell*[1]; A. W. Cook[1]; H. J. Brown-Shaklee[1]; 1. Sandia National Laboratories, USA

11:45 AM

(EMA-S7-018-2016) Thermal Diffusivity/Conductivity Measurements of Zirconia during Sintering
E. Post*[1]; 1. NETZSCH Geraetebau GmbH, Germany

12:00 PM

(EMA-S7-019-2016) Increasing oxidation resistance of Ni metal in order to cofire BME capacitors in higher partial pressure of oxygen
D. Sohrabi Baba Heidary*[1]; C. Randall[1]; 1. Penn State, USA

12:15 PM

(EMA-S7-020-2016) Fabrication of electroporcelain composites from local raw materials in Ghana
A. S. Yaya*[1]; 1. University of Ghana, Ghana

S8. Interface Structure, Orientation, and Composition: Influence on Properties and Kinetics

Interface Properties

Room: Mediterranean B/C

Session Chair: Rosario Gerhardt, Georgia Institute of Technology

10:00 AM

(EMA-S8-001-2016) Characterization of Interfaces and Structure via Electrical Measurements (Invited)

R. A. Gerhardt*[1]; 1. Georgia Institute of Technology, USA

10:30 AM

(EMA-S8-002-2016) The role of pores in ferroelectric ceramics materials intergranular impedance

V. Mitic*[1]; V. Paunovic[1]; L. Kocic[1]; 1. Faculty of Electronic Engineering, Serbia

10:45 AM

(EMA-S8-003-2016) Agglomeration of Au/Ni Bilayer Films During Thermal Annealing

X. Cen[1]; X. Zhang[1]; K. van Benthem*[1]; 1. University of California, Davis, USA

11:00 AM

(EMA-S8-004-2016) Nanostructured Metal-Ceramic Composites Made by Internal Reduction (Invited)

I. Reimanis*[1]; A. Morrissey[1]; J. O'Brien[2]; 1. Colorado School of Mines, USA; 2. Off Grid Research, USA

11:30 AM

(EMA-S8-005-2016) Elucidating intermixing in LAO/STO heterointerfaces via SIMS

R. Akrobetu*[1]; A. Sehirlioglu[1]; 1. Case Western Reserve University, USA

11:45 AM

(EMA-S8-006-2016) Thin film deposition using rarefied gas jet

D. Pradhan*[1]; 1. Indian Institute of Science, India

S9. Recent Developments in Superconducting Materials and Applications

Issues related to the Fabrication of Low-cost and High-performance Second Generation Coated Conductors

Room: Pacific

Session Chairs: Judy Wu, University of Kansas; Haiyan Wang, Texas A&M University

10:00 AM

(EMA-S9-014-2016) Doubling in-field J_c in HTS coated conductors by a roll-to-roll ion irradiation process (Invited)

Q. Li*[1]; 1. Brookhaven National Laboratory, USA

10:30 AM

(EMA-S9-015-2016) Comparison of the Flux Pinning Mechanisms of $YBa_2Cu_3O_{7-\delta}$ Superconductor with $BaHfO_3 + Y_2O_3$, $BaSnO_3 + Y_2O_3$, and $BaZrO_3 + Y_2O_3$ Mixed Phase Additions (Invited)

M. P. Sebastian*[1]; C. Ebbing[2]; T. Bullard[3]; G. Panasyuk[3]; M. Sullivan[2]; C. F. Tsai[4]; W. Zhang[4]; J. Huang[4]; H. Wang[4]; J. Wu[5]; T. J. Haugan[1]; 1. Air Force Research Laboratory, USA; 2. UDRI, USA; 3. UES, USA; 4. Texas A&M University, USA; 5. University of Kansas, USA

11:00 AM

(EMA-S9-016-2016) Controlling the dimension and orientation of secondary phase nanostructures in $YBa_2Cu_3O_7$ nanocomposite films for high-field applications (Invited)

J. Wu*[1]; J. Shi[1]; J. Baca[1]; R. Emergo[1]; M. Sebastian[2]; T. J. Haugan[2]; 1. University of Kansas, USA; 2. US Air Force Research labortory, USA

11:30 AM

(EMA-S9-017-2016) Progress in MOCVD Technology for Fabrication of High Performance Coated Conductors (Invited)

G. Majkic*[1]; 1. University of Houston, USA

12:00 PM

(EMA-S9-018-2016) Effects of surface morphology and interlayer on jointing (RE)$Ba_2Cu_3O_{7-x}$ Coated Conductors via electric field assisted proces

M. Li*[1]; C. Jensen[1]; J. Schwartz[1]; 1. North Carolina State University, USA

S11. Advanced electronic Materials: Processing, structures, properties and applications

Processing and Characterization (domain) of Electronic Materials

Room: Indian

Session Chairs: Xiaoli Tan, Iowa State Univ; Tadasu Hosokura, Murata Manufacturing Co., Ltd.

10:00 AM

(EMA-S11-016-2016) Properties of orientation and crystallization controlled $BaTiO_3$, $SrTiO_3$ thin films fabricated by chemical solution deposition (Invited)

T. Hosokura*[1]; A. Ando[1]; T. Konoike[1]; 1. Murata Manufacturing Co., Ltd., Japan

10:30 AM

(EMA-S11-017-2016) Nanofragmentation of ferroelectric domains in lead-free ceramics during polarization fatigue

H. Guo[1]; X. Liu[1]; J. Rödel[2]; X. Tan*[1]; 1. Iowa State Univ, USA; 2. Technische Universität Darmstadt, Germany

10:45 AM

(EMA-S11-018-2016) EBSD Study of Yttrium Iron Garnet Coatings Produced via Aerosol Deposition

E. Gorzkowski*[1]; S. D. Johnson[1]; A. Levinson[1]; 1. Naval Research Lab, USA

11:00 AM

(EMA-S11-019-2016) Magnetic and Structural Properties of Doped Barium Hexaferrite Films Formed by Aerosol Deposition

S. D. Johnson*[1]; C. Gonzalez[2]; Z. Robinson[4]; D. Ellsworth[3]; M. Wu[3]; 1. Naval Research Laboratory, USA; 2. California State University Long Beach, USA; 3. Colorado State University, USA; 4. SUNY Brockport, USA

11:15 AM

(EMA-S11-020-2016) Effects of Domain and Grain Boundaries in Piezoelectric Ceramics and Single Crystals on Elastic Constants Evaluated by Sound Velocities

T. Ogawa*[1]; T. Ikagaya[1]; 1. Shizuoka Institute of Science and Technology, Japan

11:30 AM

(EMA-S11-021-2016) Quantifying the Extent of 180° Domain Switching using *in situ* X-Ray Diffraction

C. Fancher*[1]; S. Brewer[2]; C. Chung[1]; S. Röhrig[3]; G. Esteves[1]; M. Deluca[3]; N. Bassiri-Gharb[2]; J. L. Jones[1]; 1. North Carolina State University, USA; 2. Georgia Institute of Technology, USA; 3. MATERIALS CENTER LEOBEN, Austria

11:45 AM

(EMA-S11-022-2016) Controlled illumination-induced creation of charged domain walls at room temperature in $BaTiO_3$

P. Bednyakov[1]; T. Sluka*[1]; A. Tagantsev[1]; D. Damjanovic[1]; N. Setter[1]; 1. EPFL - Swiss Federal Institute of Technology Lausanne, Switzerland

12:00 PM

(EMA-S11-023-2016) Conductive Domain Walls in Polycrystalline $BiFeO_3$: Local Structure and Dynamics

T. Rojac*[1]; A. Bencan[1]; H. Ursic[1]; G. Drazic[2]; N. Sakamoto[4]; B. Jancar[1]; M. Makarovic[1]; J. Walker[1]; B. Malic[1]; D. Damjanovic[3]; 1. Jozef Stefan Institute, Slovenia; 2. National Institute of Chemistry, Slovenia; 3. Swiss Federal Institute of Technology, Switzerland; 4. Shizuoka University, Japan

Student Speaking Competition Presentations II

Room: Coral A

Session Chair: Christina Rost, North Carolina State University

12:45 PM

(EMA-SSC-005-2016) Intentional defects in 2-D birnessite MnO_2 to improve supercapacitor performance

P. Gao*[1]; P. C. Metz[1]; T. Hey[1]; S. Misture[1]; 1. Alfred University, USA

1:00 PM

(EMA-SSC-006-2016) Thermal Conductivity of Amorphous Silicon Thin Films: Effects of Size and Elastic Modulus

J. L. Braun*[1]; M. Elahi[2]; J. Gaskins[1]; T. E. Beechem[3]; Z. C. Leseman[2]; H. Fujiwara[5]; S. King[4]; P. E. Hopkins[1]; 1. University of Virginia, USA; 2. University of New Mexico, USA; 3. Sandia National Laboratories, USA; 4. Intel Corporation, USA; 5. Gifu University, Japan

1:15 PM

(EMA-SSC-007-2016) Positive effect of an internal depolarization field in ultrathin epitaxial ferroelectric films

G. liu*[1]; J. Chen[1]; C. Lichtensteiger[2]; J. Triscone[2]; P. Aguado-Puente[3]; J. Junquera[4]; N. Valanoor[1]; 1. University of New South Wales, Australia; 2. University of Geneva, Switzerland; 3. CIC Nanogune, Spain; 4. Universidad de Cantabria, Spain

1:30 PM

(EMA-SSC-008-2016) Doping control in epitaxial thin films via reactive RF co-sputtering

K. Kelley*[1]; E. Sachet[1]; H. Kham[1]; S. Franzen[1]; J. Maria[1]; 1. North Carolina State University, USA

S1. Multiferroic Materials and Multilayer Ferroic Heterostructures: Properties and Applications

Synthesis, Characterization, and Applications

Room: Coral A

Session Chairs: Hamidreza Khassaf, University of Connecticut; Yomery Espinal, University of Connecticut

2:00 PM

(EMA-S1-020-2016) Polycrystalline Superlattice-Like PZT Thin Film (Invited)

S. Brewer[1]; H. Khassaf[2]; P. Alpay[2]; N. Bassiri-Gharb*[1]; 1. Georgia Institute of Technology, USA; 2. University of Connecticut, USA

2:30 PM

(EMA-S1-021-2016) *In situ* Characterization of the Epitaxialization of $BiFeO_3$ Films via Atomic Layer Deposition (Invited)

J. E. Spanier*[1]; 1. Drexel University, USA

3:00 PM

(EMA-S1-022-2016) Magnetoelectric Investigations of a Single-Phase Multiferroic Material Possessing the Aurivillius Structure (Invited)

L. Keeney*[1]; A. Faraz[1]; T. Maity[1]; M. Schmidt[1]; A. Amann[2]; N. Deepak[3]; N. Petkov[1]; S. Roy[1]; M. Pemble[1]; R. Whatmore[4]; 1. Tyndall National Institute, University College Cork, Ireland; 2. University College Cork, Ireland; 3. University of Liverpool, United Kingdom; 4. Imperial College London, United Kingdom

3:30 PM

Break

4:00 PM

(EMA-S1-023-2016) Ferroelectric Domain Switching Dynamics in Multiferroics Based on Frames-per-Second PFM Imaging (Invited)

J. Steffes[1]; Z. Thatcher[1]; A. Carter[1]; J. Heron[2]; R. Ramesh[3]; P. Ashby[4]; B. D. Huey*[1]; 1. University of Connecticut, USA; 2. Cornell University, USA; 3. University of California Berkeley, USA; 4. Lawrence Berkeley National Laboratory, USA

4:30 PM

(EMA-S1-024-2016) Perovskite oxide thin films with high room temperature mobilities (Invited)

T. Schumann*[1]; S. Raghavan[1]; J. Zhang[1]; H. Kim[1]; S. Stemmer[1]; 1. University of California, Santa Barbara, USA

5:00 PM

(EMA-S1-025-2016) Metallo-Organic Solution Deposition of Ferroelectric Films onto Additively Manufactured Inconel 718

T. Patel*[1]; H. Khassaf[1]; N. Bassiri-Gharb[2]; P. Alpay[1]; R. Hebert[1]; 1. University of Connecticut, USA; 2. Georgia Institute of Technology, USA

5:15 PM

(EMA-S1-026-2016) Switchable/Tunable FBAR Resonators and Filters with Ba1-xSrxTO3 Thin Films (Invited)

T. S. Kalkur*[1]; 1. University of Colorado Colorado Springs, USA

S4. Ion-conducting Ceramics

Processing and Microstructure Effects on Ion Conduction I

Room: Caribbean B

Session Chair: Fanglin (Frank) Chen, University of South Carolina

2:00 PM

(EMA-S4-001-2016) The Role of Ionic Transport in Nuclear Waste Immobilization and Membrane Separations (Invited)

K. Brinkman*[1]; 1. Clemson University, USA

2:30 PM

(EMA-S4-002-2016) Preparation of Proton Conductor for Pure Hydrogen Separation from Coke Oven Gas

H. Konishi*[1]; H. Ono[1]; 1. Osaka University, Japan

2:45 PM

(EMA-S4-003-2016) Electrical Properties of Lanthanum Silicate-Based Oxygen-Excess-Type Ionic Conductors

A. Mineshige*[1]; T. Nishimoto[1]; A. Heguri[1]; H. Hayakawa[1]; T. Yazawa[1]; 1. University of Hyogo, Japan

3:00 PM

(EMA-S4-004-2016) High performance solid oxide electrolysis cells with hierarchically porous Ni-YSZ support electrode

L. Lei*[1]; Y. Chen[2]; T. Liu[3]; Y. Wang[3]; F. Chen[1]; 1. University of South Carolina, USA; 2. Georgia Institute of Technology, USA; 3. Wuhan University, China

3:15 PM

(EMA-S4-005-2016) "Eel-ectrifying" Membranes: Toward the development of biomimetic, ion-based energy storage

E. Spoerke*[1]; L. Small[1]; A. Martinez[1]; D. Wheeler[1]; V. Vandelinder[1]; G. Bachand[1]; S. Rempe[1]; 1. Sandia National Laboratories, USA

3:30 PM

Break

Processing and Microstructure Effects on Ion Conduction II

Room: Caribbean B

Session Chair: Erik Spoerke, Sandia National Laboratories

4:00 PM

(EMA-S4-006-2016) Grain-boundary resistance in yttrium-doped barium zirconate: influence of fabrication process (Invited)

S. Ricote*[1]; D. Clark[2]; N. Sullivan[1]; W. Coors[2]; 1. Colorado School of Mines, USA; 2. CoorsTek, USA

4:30 PM

(EMA-S4-007-2016) Probing Ionic Transport Mechanisms in Y-doped Barium Zirconate

J. Ding*[2]; E. Strelcov[2]; G. Veith[2]; C. Bridges[2]; J. Balachandran[2]; P. Ganesh[2]; S. Kalinin[2]; N. Bassiri-Gharb[1]; R. Unocic[2]; 1. Georgia Institute of Technology, USA; 2. Oak Ridge National Lab, USA

4:45 PM

(EMA-S4-008-2016) Sodium ion conductivity and scaling effects in NASICON thin films prepared via chemical solution deposition

J. Ihlefeld*[1]; W. Meier[1]; E. Gurniak[1]; M. Blea-Kirby[1]; M. Rodriguez[1]; B. McKenzie[1]; A. McDaniel[1]; 1. Sandia National Laboratories, USA

S5. Multifunctional Nanocomposites

Multifunctional Nanocomposites IV

Room: Coral B

Session Chair: Junwoo Son, Pohang University of Science and Technology(POSTECH)

2:00 PM

(EMA-S5-019-2016) Metal to insulator transition in ultrathin complex-oxide heterostructures (Invited)

A. Janotti*[1]; 1. University of Delaware, USA

2:30 PM

(EMA-S5-020-2016) Thickness and Strain Effect on the Magnetic Properties of Epitaxial $Nd_{0.5}Sr_{0.5}CoO_3$ Thin Films

S. Cheng*[1]; M. Liu[1]; G. Hu[1]; L. Lu[1]; S. Mi[2]; C. Jia[1]; 1. Xi'an Jiaotong University, China; 2. Xi'an Jiaotong University, China

2:45 PM

(EMA-S5-021-2016) Dynamic Hydrogenation of Hexagonal WO_3 Epitaxial Thin Films with Open Tunnels

J. Park*[1]; J. Son[1]; 1. POSTECH, The Republic of Korea

3:00 PM

(EMA-S5-022-2016) Reversible phase transition of hydrogen sponge in multi-valent VO_2 epitaxial thin film

H. Yoon*[1]; M. Choi[2]; T. Lim[2]; H. Kwon[1]; K. Ihm[3]; J. Kim[1]; S. Choi[2]; J. Son[1]; 1. Pohang University of Science and Technology, The Republic of Korea; 2. Korea Institute of Materials Science, The Republic of Korea; 3. Pohang Accelerator Laboratory, The Republic of Korea

3:15 PM

(EMA-S5-023-2016) Wafer-scale growth of VO_2 thin films using a combinatorial approach

H. Zhang*[1]; R. Engel-Herbert[1]; 1. Pennsylvania State University, USA

3:30 PM

Break

4:00 PM

(EMA-S5-024-2016) Many-body effects and band structure of the transparent oxide semiconductors In_2O_3 and SnO_2 (Invited)

M. Feneberg*[1]; 1. Otto-von-Guericke University Magdeburg, Germany, Germany

4:30 PM

(EMA-S5-025-2016) Dielectric Screening and Optical Absorption in In_2O_3 and Ga_2O_3 from First Principles

J. Varley[2]; A. Schleife*[1]; 1. University of Illinois at Urbana-Champaign, USA; 2. Lawrence Livermore National Laboratory, USA

4:45 PM

(EMA-S5-026-2016) Semiconducting oxides - From material design to basic devices (Invited)

H. von Wenckstern*[1]; 1. Universität Leipzig, Germany

5:15 PM

(EMA-S5-027-2016) Semiconducting Ga_2O_3 layers grown by metal organic vapor phase epitaxy (Invited)

M. Baldini*[1]; M. Albrecht[1]; K. Irmscher[1]; R. Schewski[1]; G. Wagner[1]; 1. Leibniz Institute for Crystal Growth, Germany

S6. Computational Design of Electronic Materials

Materials by Design: Electronic Materials I

Room: Mediterranean A

Session Chair: Mina Yoon, Oak Ridge National Laboratory

2:00 PM

(EMA-S6-001-2016) Relaxor behavior and electrocaloric effect of Na1/2Bi1/2TiO3: Insights from computer simulations (Invited)

K. Albe*[1]; 1. Technical University Darmstadt, Germany

2:30 PM

(EMA-S6-002-2016) High thermoelectric figure of merit as a counterindicated property of matter: Transport theory as a guide for resolving this conundrum (Invited)

D. J. Singh*[1]; 1. University of Missouri, Columbia, USA

3:00 PM

(EMA-S6-003-2016) First principle prediction of semiconducting/ metallic phase transitions in Transition Metal Dichalcogenides: Coupled Electron and Strain effects

B. Ouyang*[1]; J. Song[1]; 1. McGill Univesity, Canada

3:15 PM

(EMA-S6-004-2016) Identification of metastable ultrasmall titanium oxide clusters using a hybrid optimization algorithm

E. Inclan*[1]; D. Geohegan[2]; M. Yoon[2]; 1. Georgia Institute of Technology, USA; 2. Oak Ridge National Lab, USA

3:30 PM

Break

Materials by Design/Interface driven Functional Materials

Room: Mediterranean A

Session Chair: Ghanshyam Pilania, Los Alamos National Lab

4:00 PM

(EMA-S6-005-2016) Information-driven approach to materials discovery and design (Invited)

T. Lookman*[1]; 1. Los Alamos National Lab, USA

4:30 PM

(EMA-S6-006-2016) Band-gap and Band-edge Engineering of Multicomponent Garnet Scintillators (Invited)

C. Stanek*[1]; S. Yadav[1]; B. Uberuaga[1]; C. Jiang[2]; M. Nikl[3]; 1. Los Alamos National Laboratory, USA; 2. Thermo-Calc Software, USA; 3. Institute of Physics, Academy of Sciences of the Czech Republic, Czech Republic

5:00 PM

(EMA-S6-007-2016) First-Principles Predication of Two-Dimensional Electrides

W. Ming*[1]; M. Yoon[1]; 1. Oak Ridge National Laboratory, USA

5:15 PM

(EMA-S6-008-2016) Designing quantum spin defects in ceramic materials for scalable solid-state quantum technologies (Invited)

H. Seo*[1]; 1. The University of Chicago, USA

S8. Interface Structure, Orientation, and Composition: Influence on Properties and Kinetics

Interface Structure and Properties

Room: Mediterranean B/C

Session Chair: David McComb, The Ohio State University

2:00 PM

(EMA-S8-007-2016) Metal- Dielectric Interfaces: Temporal Evolution Under Applied Bias (Invited)

E. C. Dickey*[1]; A. Moballegh[1]; L. Chen[2]; J. Wang[2]; H. Huang[2]; 1. North Carolina State University, USA; 2. Pennsylvania State University, USA

2:30 PM

(EMA-S8-008-2016) Impact of space charge on grain growth in perovskite ceramics: growth stagnation, solute drag and intrinsic defects (Invited)

W. Rheinheimer*[1]; F. Lemke[1]; M. J. Hoffmann[1]; 1. Karlsruhe Institute of Technology, Germany

3:00 PM

(EMA-S8-009-2016) Characterization of grain boundary disconnections in general grain boundaries in $SrTiO_3$

H. Sternlicht*[1]; W. Rheinheimer[2]; M. J. Hoffmann[2]; W. D. Kaplan[1]; 1. Technion, Israel; 2. Institute of Applied Materials, Karlsruhe Institute of Technology, Germany

3:15 PM

(EMA-S8-010-2016) Surface and interface composition in LAO/STO hetero-interface

H. Zaid[2]; M. Berger[2]; D. Jalabert[3]; M. Walls[4]; R. Akrobetu[1]; N. Goble[1]; X. Gao[1]; W. Lambrecht[1]; A. Sehirlioglu*[1]; 1. Case Western Reserve University, USA; 2. Mines ParisTech, Centre des Matériaux, France; 3. Univ. Grenoble Alpes, France; 4. CEA, France

3:30 PM

Break

4:00 PM

(EMA-S8-011-2016) Characterizing ordering phenomena at the atomic scale through high-resolution electron microscopy and simulation (Invited)

B. D. Esser[1]; R. E. Williams[1]; D. W. McComb*[1]; 1. The Ohio State University, USA

4:30 PM

(EMA-S8-012-2016) Effect of grain boundary energy and mobility anisotropy on the coarsening kinetics of highly twinned microstructure (Invited)

M. Tang*[1]; 1. Rice University, USA

5:00 PM

(EMA-S8-013-2016) Dominance of Interface Chemistry over the Bulk Properties in Determining the Electronic Structure of Epitaxial Metal/Perovskite Oxide Heterojunctions

P. Sushko*[1]; Y. Du[1]; M. Gu[1]; T. Droubay[1]; S. Hepplestone[2]; H. Yang[3]; C. Wang[1]; N. Browning[1]; S. Chambers[1]; 1. Pacific Northwest National Lab, USA; 2. University College London, United Kingdom; 3. University of Oxford, United Kingdom

5:15 PM

(EMA-S8-014-2016) Structure of the Equilibrated Ni(111)-YSZ(111) Solid-Solid Interface

H. Nahor*[1]; W. D. Kaplan[1]; 1. Technion - Israel Institute of Technology, Israel

5:30 PM

(EMA-S8-015-2016) Effect of Top Electrode Material on Radiation-Induced Degradation of Ferroelectric Thin Films

S. Brewer*[1]; M. Paul[2]; K. Fisher[3]; J. Guerrier[4]; J. L. Jones[4]; R. Rudy[6]; R. G. Polcawich[6]; E. Glaser[5]; C. Cress[5]; N. Bassiri-Gharb[1]; 1. Georgia Institute of Technology, USA; 2. Woodward Academy, USA; 3. Riverwood International Charter School, USA; 4. North Carolina State University, USA; 5. Naval Research Laboratory, USA; 6. US Army Research Laboratory, USA

5:45 PM

(EMA-S8-016-2016) Energetics of All Metal Oxide Junctions

K. Rietwyk*[1]; D. Keller[1]; H. Barad[1]; A. Ginsburg[1]; K. Majhi[1]; A. Anderson[1]; A. Zaban[1]; 1. Bar-Ilan University, Israel

S9. Recent Developments in Superconducting Materials and Applications

Electronic Structure and Superconductivity Mechanism

Room: Pacific

Session Chairs: Xingjiang Zhou, National Lab for Superconductivity; Gang Wang, Institute of Physics, Chinese Academy of Sciences

2:00 PM

(EMA-S9-019-2016) Searching Genes of Unconventional High Temperature Superconductors (Invited)

J. Hu*[1]; 1. Institute of Physics, CAS, China

2:30 PM

(EMA-S9-020-2016) New approaches for enhancing T_c (Invited)

M. Osofsky*[1]; J. Prestigiacomo[1]; C. Krowne[1]; R. Soulen[2]; H. Kim[1]; E. Clements[1]; G. Woods[3]; H. Sikanth[3]; I. Takeuchi[4]; V. Smolyaninova[5]; B. Yost[5]; K. Zansder[5]; T. Gresock[5]; S. Saha[4]; R. Greene[4]; I. Smolyaninov[6]; 1. Naval Research Laboratory, USA; 2. Retired, USA; 3. University of South Florida, USA; 4. University of Maryland, USA; 5. Towson University, USA; 6. University of MAryland, USA

3:00 PM

(EMA-S9-021-2016) Observation of strong electron pairing on bands without Fermi surfaces in $LiFe_{1-x}Co_xAs$ (Invited)

T. Qian*[1]; 1. Institute of Physics, Chinese Academy of Sciences, China

3:30 PM

Break

4:00 PM

(EMA-S9-022-2016) Quantitative Determination of the Pairing Interactions in High Temperature Superconductors (Invited)

X. Zhou*[1]; 1. National Lab for Superconductivity, China

4:30 PM

(EMA-S9-023-2016) Weyl semi-metals and Weyl superconductors (Invited)

X. Dai*[1]; 1. Institute of Physics, Chinese academy of sciences, China

5:00 PM

(EMA-S9-024-2016) Electron-pair state in crystal: a missing piece in solid-state theory (Invited)

G. Hai*[1]; 1. University of Sao Paulo, Brazil

5:30 PM

(EMA-S9-025-2016) A BCS-like model for heavy fermion and cuprate superconductivity (Invited)

Y. Yang*[1]; 1. Institute of Physics, Chinese Academy of Sciences, China

S11. Advanced electronic Materials: Processing, structures, properties and applications

Advanced Electronic Materials: Piezoelectric I

Room: Indian

Session Chairs: Dragan Damjanovic, Swiss Federal Institute of Technology in Lausanne - EPFL; Andrew Bell, University of Leeds

2:00 PM

(EMA-S11-024-2016) 3-Atom Model Parameters in Lead-free and Lead-based Piezoelectric Materials (Invited)

A. J. Bell*[1]; 1. University of Leeds, United Kingdom

2:30 PM

(EMA-S11-025-2016) Emergence of electro-mechanical coupling in complex materials (Invited)

D. Damjanovic*[1]; 1. Swiss Federal Institute of Technology in Lausanne - EPFL, Switzerland

3:00 PM

(EMA-S11-026-2016) Extraordinary High T_c PZT-based Relaxed Single Crystal Thin Films

K. Wasa*[1]; 1. Yokohama City University, Japan

3:15 PM

(EMA-S11-027-2016) Potential of gehlenite single crystals for piezoelectric sensor applications

H. Takeda*[1]; K. Takizawa[1]; K. Yoshida[1]; T. Hoshina[1]; T. Tsurumi[1]; 1. Tokyo Institute of Technology, Japan

3:30 PM

Break

Advanced Electronic Materials: Piezoelectric II

Room: Indian

Session Chairs: Zuo-Guang Ye, Simon Fraser University; Clive Randall, Penn State University

4:00 PM

(EMA-S11-028-2016) Piezoelectric and Dielectric Multilayer Components (Invited)

C. Randall*[1]; 1. Penn State University, USA

4:30 PM

(EMA-S11-029-2016) Rediscovering PZT through Single Crystal Studies (Invited)

Z. Ye*[1]; 1. Simon Fraser University, Canada

5:00 PM

(EMA-S11-030-2016) Ubiquitous Magneto-Mechano-Electric (MME) Generators for wireless sensor network driving (Invited)

J. Ryu*[1]; D. Jeong[2]; S. Choi[1]; W. Yoon[1]; J. Choi[1]; J. Kim[1]; B. Hahn[1]; C. Ahn[1]; D. Park[1]; 1. Korea Institute of Materials Science, The Republic of Korea; 2. Inha University, The Republic of Korea

5:30 PM

(EMA-S11-031-2016) Sol-gel grown PMN-PT films for tunable bulk acoustic wave resonators

M. Spreitzer*[1]; S. Kune[1]; D. Suvorov[1]; 1. Jozef Stefan Institute, Slovenia

Friday, January 22, 2016

Plenary Session

Plenary III

Room: Indian

8:30 AM

Introduction

8:40 AM

(EMA-PL-003-2016) Power Semiconductors

T. Detzel*[1]; 1. Infineon Technologies Austria AG, Austria

9:30 AM

Break

S4. Ion-conducting Ceramics

Ion Conductors for Energy Storage

Room: Caribbean B

Session Chair: Kyle Brinkman, Clemson University

10:00 AM

(EMA-S4-009-2016) Solid State Batteries for Automotive Applications (Invited)

V. Anandan*[1]; A. Drews[1]; 1. Ford Motor Company, USA

10:30 AM

(EMA-S4-010-2016) A facile method for the synthesis of the $Li_{0.3}La_{0.57}TiO_3$ solid state electrolyte (Invited)

G. Cao*[1]; 1. University of Washington, USA

11:00 AM

(EMA-S4-011-2016) Defect Driven Titania Anode for Secondary Sodium and Lithium Batteries

K. A. Smith*[1]; H. Xiong[1]; J. Wharry[1]; D. P. Butt[1]; 1. Boise State University, USA

11:15 AM

(EMA-S4-013-2016) Conductivity, Mechanical Properties, and Stability of $Li_7La_3Zr_2O_{12}$ Solid State Electrolytes (Invited)

C. R. Becker*[1]; J. B. Wolfenstine[1]; J. L. Allen[1]; J. Sakamoto[2]; 1. US Army Research Laboratory, USA; 2. University of Michigan, USA

11:45 AM

(EMA-S4-014-2016) Understanding the ionic conductivity enhancement in lithium conducting garnets

M. M. Ahmad*[1]; 1. King Faisal University, Saudi Arabia

S5. Multifunctional Nanocomposites

Multifunctional Nanocomposites V

Room: Coral B

Session Chair: Aiping Chen, Los Alamos National Lab

10:00 AM

(EMA-S5-028-2016) Impurity and defect effects on phonon transport in complex oxides: Impact on thermal conductivity and tehrmal boundary conductance (Invited)

P. E. Hopkins*[1]; 1. University of Virginia, USA

10:30 AM

(EMA-S5-029-2016) The Transport Properties of Dislocations in the Perovskite-Oxide $SrTiO_3$ (Invited)

R. A. De Souza*[1]; 1. RWTH Aachen University, Germany

11:00 AM

(EMA-S5-030-2016) Electronic Transport in Oxygen Vacancy Doped Epitaxial $BaSnO_3$: Doping, Mobility, and the Insulator-Metal Transition (Invited)

K. Ganguly[1]; J. Walter[1]; P. Ambwani[1]; P. Xu[1]; A. Prakash[1]; J. Jeong[1]; A. Mkhoyan[1]; B. Yang[1]; A. Goldman[1]; B. Jalan[1]; C. Leighton*[1]; 1. University of Minnesota, USA

11:30 AM

(EMA-S5-031-2016) Nanoscale heat transport in complex oxide thin films and superlattices (Invited)

J. Ravichandran*[1]; 1. University of Southern California, USA

12:00 PM

(EMA-S5-032-2016) TaOx thin films for resistance switching memory applications

F. Kurnia[2]; D. Kim[1]; B. Lee[1]; C. Liu*[1]; 1. Hankuk University of Foreign Studies, The Republic of Korea; 2. The University of New South Wales, Australia

S6. Computational Design of Electronic Materials

Materials by Design: Electronic Materials II

Room: Mediterranean A

Session Chair: Wolfgang Windl, Ohio State University

10:00 AM

(EMA-S6-009-2016) Correlating structure and function for nanoparticle electrocatalysts (Invited)

G. Henkelman*[1]; 1. University of Texas at Austin, USA

10:30 AM

(EMA-S6-010-2016) Theoretical Investigation of Silicon-based Materials with Exceptional Optoelectronic Properties (Invited)

B. Huang*[1]; 1. Beijing Computational Science Research Center, China

11:00 AM

(EMA-S6-011-2016) Predictive bandgap engineering in 2H transition metal dichalcogenides through inherent interface coupling

B. Ouyang*[1]; J. Song[1]; 1. McGill Univesity, Canada

11:15 AM

(EMA-S6-012-2016) Uncovering the physics and chemistry of complex oxide surfaces (Invited)

R. Mishra*[1]; 1. Washington University in St. Louis, USA

11:45 AM

(EMA-S6-013-2016) Electronic and Magnetic Properties of Transition-Metal Oxide Nanocomposites: A Tight-Binding Modeling at Mesoscale (Invited)

Y. Tai[1]; J. Zhu*[1]; 1. Los Alamos National Laboratory, USA

12:15 PM

(EMA-S6-014-2016) Creating Two-Dimensional Electron Gas in Nonpolar/Nonpolar Oxide Interface via Polarization Discontinuity: First-Principles Analysis of CaZrO3/SrTiO3 Heterostructure

K. Yang*[1]; S. Nazir[1]; J. Cheng[1]; 1. University of California San Diego, USA

S9. Recent Developments in Superconducting Materials and Applications

Applications and related Material issues including Wire Properties

Room: Pacific

Session Chairs: Timothy Haugan, Air Force Research Lab; Charles Rong, U.S. Army Research Laboratory

10:00 AM

(EMA-S9-026-2016) Advanced Superconducting High-T_c Magnetic Applications (Invited)

F. N. Werfel*[1]; U. Floegel-Delor[1]; 1. Adelwitz Technologiezentrum GmbH (ATZ), Germany

10:30 AM

(EMA-S9-027-2016) The HTS Coated Conductor Roebel cable on route to first applications (Invited)

W. Goldacker*[1]; 1. Karlsruhe Institute of Technology, Germany

11:00 AM

(EMA-S9-028-2016) Persistent Critical Current Characteristics with Closed Superconducting Loops Made Out of RE123 Coated Conductors (Invited)

C. Rong*[1]; J. D. Miller[2]; G. A. Levin[3]; P. N. Barnes[1]; 1. U.S. Army Research Laboratory, USA; 2. Naval Surface Warfare Center Carderock Division, USA; 3. Florida Institute of Technology, USA

11:30 AM

(EMA-S9-029-2016) Fatigue Properties of IBAD-MOCVD REBa2Cu3O7-x

S. Rogers*[1]; J. Schwartz[1]; 1. North Carolina State University, USA

11:45 AM

(EMA-S9-030-2016) Electric Aircraft and Future Need for Cryogenic/Superconducting Components and Drivetrains (Invited)

T. J. Haugan*[1]; G. Panasyuk[2]; 1. Air Force Research Lab, USA; 2. UES Inc., USA

12:15 PM

(EMA-S9-031-2016) AC Loss in High-Temperature Superconducting (HTS) Tapes in a Stator Environment Measured by the Calorimetric Method

N. Gheorghiu*[1]; J. P. Murphy[2]; M. D. Sumption[3]; M. Majoros[3]; E. W. Collings[3]; T. J. Haugan[4]; 1. UES, Inc., USA; 2. University of Dayton Research Institute, USA; 3. Ohio State University, USA; 4. AFRL/WPAFB, USA

12:30 PM

(EMA-S9-032-2016) Superconducting Joint between (RE) $Ba_2Cu_3O_{7-x}$ Coated Conductors via Electric Field Sintering

C. Jensen*[1]; M. Li[1]; J. Schwartz[1]; 1. North Carolina State University, USA

S10. Emerging functionalities in layered-oxide and related materials

Synthesis and Characterization

Room: Mediterranean B/C

Session Chair: Serge Nakhmanson, University of Connecticut

10:00 AM

(EMA-S10-001-2016) Mixed-metal fluorocarbonates as Deep UV NLO Materials: Synthesis, Characterization, and Properties (Invited)

T. Tran*[1]; S. Halasyamani[1]; J. He[2]; J. Rondinelli[2]; 1. University of Houston, USA; 2. Northwestern University, USA

10:30 AM

(EMA-S10-002-2016) From Layers to Scrolls – Layer Construction and Peapod Formation through the Manipulation of Niobium Oxides (Invited)

J. B. Wiley*[1]; 1. University of New Orleans, USA

11:00 AM

(EMA-S10-003-2016) 2-D to 3-D: Assembly of oxide nanosheets into 3-D monoliths

T. A. Gubb*[1]; T. Hey[1]; S. Misture[1]; 1. Alfred University, USA

11:15 AM

(EMA-S10-004-2016) X-ray total scattering analysis of MnO_2 nanosheet assemblies

P. C. Metz*[1]; P. Gao[1]; T. Hey[1]; S. Misture[1]; 1. Alfred University, USA

11:30 AM

(EMA-S10-005-2016) Materials By Design: Superconducting Polymorphs Through Kinetic Control of Solid-state Chemistry (Invited)

J. R. Neilson*[1]; 1. Colorado State University, USA

12:00 PM

(EMA-S10-006-2016) Local epitaxial growth of layered oxides on isostructural polycrystals using combinatorial substrate epitaxy (Invited)

P. Salvador*[1]; G. Rohrer[1]; W. Prellier[2]; 1. Carnegie Mellon University, USA; 2. ENSICAEN, Universite de Basse-Normandie, France

S11. Advanced electronic Materials: Processing, structures, properties and applications

Advanced Electronic Materials: Dielectrics II

Room: Indian

Session Chairs: Ian Reaney, University of Sheffield; Xiang Ming Chen, Zhejiang University

10:00 AM

(EMA-S11-032-2016) A Crystal-Chemical Framework for Relaxor versus Normal Ferroelectric Behavior in Tetragonal Tungsten Bronzes (Invited)

I. M. Reaney*[1]; 1. University of Sheffield, United Kingdom

10:30 AM

(EMA-S11-033-2016) Ferroelectric transition, low-temperature dielectric relaxations and their structural origins of $Ba_5RTi_3Nb_7O_{30}$ (R=La, Nd and Sm) tungsten bronze ceramics (Invited)

X. Chen*[1]; X. Zhu[1]; M. Mao[1]; K. Li[1]; X. Liu[1]; 1. Zhejiang University, China

11:00 AM

(EMA-S11-034-2016) Phase Formation and Microstructure Development of (1-x)$BaTiO_3$ - x$Bi(Zn_{0.5}Ti_{0.5})O_3$

M. A. Kuzara*[1]; A. Mattern[1]; D. Hook[2]; G. Tutuncu[3]; G. Brennecka[1]; 1. Colorado School of Mines, USA; 2. CoorsTek Technical Ceramics, USA; 3. Brookhaven National Laboratory, USA

11:15 AM

(EMA-S11-035-2016) Functionally graded tunable multilayer capacitors

H. Song*[1]; D. Maurya[1]; S. Priya[1]; 1. Virginia Tech., USA

11:30 AM

(EMA-S11-036-2016) Electrical Heterogeneity and Anomalous Conductivity Behaviour in Reduced Titanates. (Invited)

D. C. Sinclair*[1]; M. Ferrarelli[1]; Z. Lu[1]; J. Dean[1]; I. M. Reaney[1]; 1. University of Sheffield, United Kingdom

12:00 PM

(EMA-S11-037-2016) Transport properties of $BaTiO_3$-$Bi(Zn_{1/2}Ti_{1/2})O_3$ ceramics (Invited)

N. Kumar*[1]; D. Cann[1]; E. A. Patterson[2]; T. Frömling[2]; E. Gorzkowski[3]; 1. Oregon State University, USA; 2. Technische Universität Darmstadt, Germany; 3. Naval Research Laboratory, USA

Advanced Electronic Materials: Electrocaloric, Thermoelectric and Devices

Room: Coral A

Session Chairs: Zdravko Kutnjak, Jozef Stefan Institute; Guangzu Zhang, Huazhong University of Science and Technology

10:00 AM

(EMA-S11-038-2016) Relaxor Ferroelectric Ceramics as a Working Body for an Electrocaloric Cooling Device (Invited)

Z. Kutnjak*[1]; U. Plaznik[2]; A. Kitanovski[2]; H. Ursic[1]; M. Vrabelj[1]; B. Malic[1]; B. Rozic[1]; 1. Jozef stefan Institute, Slovenia; 2. University of Ljubljana, Slovenia

10:30 AM

WITHDRAWN

11:00 AM

(EMA-S11-040-2016) Giant Electrocaloric Effect in Polymer Nanocomposites with Nanostructured Ceramic Fillers (Invited)

G. Zhang*[1]; Q. Li[2]; S. Jiang[1]; Y. Zeng[1]; Q. Wang[2]; 1. Huazhong University of Science and Technology, China; 2. Pennsylvania State University, USA

11:30 AM

(EMA-S11-041-2016) Thermal Impact of Point Defect Migration and Buildup at TiO_2-Electrode Boundaries

B. F. Donovan*[1]; D. Long[2]; A. Moballegh[2]; E. C. Dickey[2]; P. E. Hopkins[1]; 1. University of Virginia, USA; 2. North Carolina State University, USA

11:45 AM

(EMA-S11-042-2016) Fabrication and Characterization of PLZT Films for Advanced Power Inverters in Electric Drive Vehicles

B. Balachandran*[1]; B. Ma[1]; T. H. Lee[1]; S. E. Dorris[1]; 1. Argonne National Laboratory, USA

12:00 PM

(EMA-S11-043-2016) Temperature Sensing at the Micro and Nano Scales

X. Huo*[1]; G. Li[1]; S. Xu[1]; 1. Peking University, China

12:15 PM

(EMA-S11-044-2016) Syntheses of large-scale, high-quality 2D wide-band-gap semiconductor nanosheets for high-performance deep ultraviolet photo detectors

P. Feng*[1]; E. Li[1]; M. Rivera[1]; O. Resto[1]; A. Aldalbahi[2]; 1. UPR, USA; 2. Department of Chemistry, Collage of Science, King Saud University, Saudi Arabia

S4. Ion-conducting Ceramics

Oxygen Conducting Ceramics and Films

Room: Caribbean B

Session Chair: Collin Becker, US Army Research Laboratory

1:30 PM

(EMA-S4-015-2016) Magnetic and High Temperature Phase Transformations of Ca-doped Lanthanum Ferrites (Invited)

D. P. Butt*[1]; 1. Boise State University, USA

2:00 PM

(EMA-S4-016-2016) Strain control of oxygen stoichiometry and ionic conduction in epitaxial perovskites (Invited)

H. Lee*[1]; 1. Oak Ridge National Laboratory, USA

2:30 PM

(EMA-S4-017-2016) Strain-Induced Control of Nano-Structuring and Fast Oxide Ion Transport in Thin $SrCrO_{3-x}$ Films

P. Sushko*[1]; Y. Du[1]; H. Zhang[1]; R. Colby[1]; M. Bowden[1]; S. Chambers[1]; 1. Pacific Northwest National Lab, USA

2:45 PM

(EMA-S4-018-2016) Control of oxygen sublattice stability by strain in Ruddlesden-Popper films

T. Meyer*[1]; J. Petrie[1]; L. Jiang[1]; J. Lee[1]; M. Yoon[1]; J. Freeland[2]; T. Egami[1]; H. Lee[1]; 1. Oak Ridge National Laboratory, USA; 2. Argonne National Lab, USA

S5. Multifunctional Nanocomposites

Multifunctional Nanocomposites VI

Room: Coral B

Session Chair: Aiping Chen, Los Alamos National Lab

1:30 PM

(EMA-S5-033-2016) Mesoscale Interfacial Dynamics in Magnetoelectric Nanocomposites (Invited)

D. Viehland*[1]; J. Li[1]; Z. Wang[1]; 1. Virginia Tech, USA

2:00 PM

(EMA-S5-034-2016) Giant magneto-resistance in epitaxial $ZnO:La_{0.7}Sr_{0.3}MnO_3$ nanocomposites

W. Pan*[1]; J. Ihlefeld[1]; P. Lu[1]; S. R. Lee[1]; 1. Sandia National Laboratories, USA

2:15 PM

(EMA-S5-035-2016) Energy-efficient magnetization reversal in multiferroic nanostructures (Invited)

J. Hu*[1]; T. Yang[1]; J. Wang[1]; C. Nan[2]; L. Chen[1]; 1. Pennsylvania State University, USA; 2. Tsinghua University, China

2:45 PM

(EMA-S5-036-2016) Towards Magnetocaloric Response Over A Broad Temperature via Ferromagnetic Bilayers

D. Xue*[1]; A. Chen[1]; Q. Jia[1]; T. Lookman[1]; 1. Los Alamos National Lab, USA

3:00 PM

(EMA-S5-037-2016) UV photoluminescence and cathodoluminescence from Gd^{3+} in $YAlO_3$ thin films

Y. Shimizu*[1]; K. Ueda[1]; H. Takashima[2]; Y. Inaguma[3]; 1. Kyushu Institute of Technology, Japan; 2. National Institute of Advanced Industrial Science and Technology (AIST), Japan; 3. Gakushuin University, Japan

3:15 PM

Break

3:45 PM

(EMA-S5-038-2016) Spatially-resolved mapping of enhanced oxygen ion conduction in Sm-doped CeO_2-$SrTiO_3$ vertical nanocomposite films (Invited)

S. Yang*[1]; S. Lee[2]; J. Jian[3]; W. Zhang[3]; P. Lu[4]; Q. Jia[5]; H. Wang[3]; T. Noh[6]; S. Kalinin[1]; J. MacManus-Driscoll[2]; 1. Oak Ridge National Laboratory, USA; 2. University of Cambridge, United Kingdom; 3. Texas A&M University, USA; 4. Sandia National Laboratories, USA; 5. Los Alamos National Laboratory, USA; 6. Seoul National University, The Republic of Korea

4:15 PM

(EMA-S5-039-2016) Enhanced performance of triboelectric nanogenerator by compositing high dielectric nanoparticles into sponge PDMS film

J. Chen*[1]; H. Guo[1]; C. Hu[1]; 1. Chongqing University, China

4:30 PM

(EMA-S5-040-2016) CuO Nanostructures Synthesised by Chemical Bath Deposition (CBD) on Seed Layers Deposited by SILAR and CSP Methods

C. M. Muiva*[1]; K. Maabong[2]; C. Moditswe[1]; 1. Botswana International University of Science and Technology, Botswana; 2. University of Botswana, Botswana

S6. Computational Design of Electronic Materials

Low Dimensional Systems

Room: Mediterranean A

Session Chair: Emmanouil Kioupakis

1:30 PM

(EMA-S6-015-2016) Computational Discovery of Novel 2D Materials for Optoelectronic and Spintronic Applications (Invited)

R. G. Hennig*[1]; 1. University of Florida, USA

2:00 PM

(EMA-S6-016-2016) Interfaces between one-atom-thick materials and metals:
Indications to the interpretation of scanning tunneling spectroscopy (Invited)

C. Park*[1]; B. G. Sumpter[1]; M. Yoon[1]; 1. Oak Ridge National Laboratory, USA

2:30 PM

(EMA-S6-017-2016) Indiene 2D Monolayer: Theoretical Study of a New Nanoelectronic Material

S. K. Gupta*[1]; D. Singh[3]; I. Lukacevic[2]; Y. Sonvane[3]; 1. St. Xavier's College, Ahmedabad, India; 2. University J. J. Strossmayer,, Croatia; 3. S.V. National Institute of Technology,, India

2:45 PM

(EMA-S6-018-2016) Vibrational Mode Lifetimes: New Insights (Invited)

M. Daw*[1]; 1. Clemson University, USA

3:15 PM

(EMA-S6-019-2016) Anisotropic spin transport and strong visible-light absorbance in few-layer SnSe and GeSe

G. Shi*[1]; E. Kioupakis[1]; 1. University of Michigan, USA

3:30 PM

Break

High-throughput/Multiscaling Calculations

Room: Mediterranean A

Session Chairs: Richard Hennig, University of Florida; Andre Schleife, University of Illinois at Urbana-Champaign

4:00 PM

(EMA-S6-020-2016) First-principles Simulations of Electronic Excitations and Ultrafast Real-time Dynamics in Semiconducting Oxides (Invited)

A. Schleife*[1]; 1. University of Illinois at Urbana-Champaign, USA

4:30 PM

(EMA-S6-021-2016) Pyroelectric and Electrocaloric Properties of Ferroelectric Ceramics: A Mesoscopic Modeling Perspective (Invited)

P. Alpay*[1]; 1. University of Connecticut, USA

5:00 PM

(EMA-S6-022-2016) First-principles High-throughput Screening for Doped-ZnO

K. Yim*[1]; J. Lee[1]; H. Nahm[2]; S. Han[1]; 1. Seoul National University, The Republic of Korea; 2. Institute for Basic Science, The Republic of Korea

5:15 PM

(EMA-S6-023-2016) First Principles screening of Transparent Conducting Oxides Using aMoBT

A. Faghaninia*[1]; M. T. Sullivan[1]; D. I. Becker-Ricketts[1]; C. S. Lo[1]; 1. Washington University in St. Louis, USA

5:30 PM

(EMA-S6-024-2016) Enhancing magnetoelectric coupling in multiferroics via temperature mediated mechanism (Invited)

C. Chang[1]; B. Mani[1]; S. Lisenkov[1]; I. Ponomareva*[1]; 1. University of South Florida, USA

S10. Emerging functionalities in layered-oxide and related materials

Properties and Theory/Simulation

Room: Mediterranean B/C

Session Chairs: Edward Gorzkowski, Naval Research Lab; Bharat Jalan, University of Minnesota

1:30 PM

(EMA-S10-007-2016) High temperature dielectric properties of c-axis oriented bismuth layer-structured dielectric films prepared on Si and Glass substrates using nanosheets buffer layer (Invited)

H. Funakubo*[1]; J. Kimura[1]; I. Takuwa[1]; M. Matsushima[1]; T. Shimizu[1]; H. Uchida[2]; T. Shibata[3]; M. Osada[3]; T. Sasaki[3]; 1. Tokyo Institute of Technology, Japan; 2. Sophia University, Japan; 3. National Institute for Material Center, Japan

2:00 PM

(EMA-S10-008-2016) Octahedral tilting in layered perovskites – Factors that lead to polar space groups (Invited)

P. Woodward*[1]; A. Sharits[1]; 1. Ohio State University, USA

2:30 PM

(EMA-S10-009-2016) Intentional defects in 2-D birnessite MnO_2 to improve supercapacitor performance

P. Gao*[1]; P. C. Metz[1]; T. Hey[1]; S. Misture[1]; 1. Alfred University, USA

2:45 PM

(EMA-S10-010-2016) Engineering the Properties of Perovskite-Based Sn Oxide Transparent Conductors (Invited)

D. J. Singh*[1]; 1. University of Missouri, Columbia, USA

3:15 PM

Break

3:45 PM

(EMA-S10-011-2016) The Aurivillius phases as potential multiferroics: a view from first principles (Invited)

C. Ederer*[1]; 1. ETH Zurich, Switzerland

4:15 PM

(EMA-S10-012-2016) Electrocaloric effects in layered oxides with easy polarization rotation

J. Mangeri[1]; K. Pitike[1]; P. Alpay[1]; S. Nakhmanson*[1]; 1. University of Connecticut, USA

4:30 PM

(EMA-S10-013-2016) The origins of Goldstone-like polar distortions in perovskite-oxide multilayers

K. Pitike[1]; L. Louis[1]; S. Nakhmanson*[1]; 1. University of Connecticut, USA

S11. Advanced electronic Materials: Processing, structures, properties and applications

Advanced Electronic Materials: Lead- free Piezoelectrics

Room: Indian

Session Chairs: Jing-Feng Li, Tsinghua University; Hijime Nagata, Tokyo University of Science

1:30 PM

(EMA-S11-045-2016) $CaZrO_3$-Modified (K,Na)NbO_3-Based Lead-Free Piezoceramics with Enhanced Thermal Stability and Fatigue Resistance (Invited)

J. Li*[1]; K. Wang[1]; F. Yao[1]; 1. Tsinghua University, China

2:00 PM

(EMA-S11-046-2016) High power piezoelectric characteristics of ($Bi_{1/2}Na_{1/2}$)TiO_3-based solid solutiona system and their demonstration for ultrasonic aaplications (Invited)

H. Nagata*[1]; 1. Tokyo University of Science, Japan

2:30 PM

(EMA-S11-047-2016) Potassium-Sodium Niobate (KNN)–Based Piezo-/Ferroelectric Single Crystals

Z. Ye*[1]; J. Y. Wong[1]; N. Zhang[1]; 1. Simon Fraser University, Canada

2:45 PM

(EMA-S11-048-2016) Field-induced structural diversity at the morphotropic phase boundary in ($Na_{1-x}K_x)_{0.5}Bi_{0.5}TiO_3$ perovskite solid solution

D. Suvorov*[1]; 1. Jozef Stefan Institute, Slovenia

3:00 PM

(EMA-S11-049-2016) A first-principles study of phase transition order in $Ba_xSr_{1-x}TiO_3$ solid solution

S. Binomran*[1]; I. Kornev[2]; L. Bellaiche[3]; 1. King Saud University, Saudi Arabia; 2. Laboratoire SPMS, UMR 8580 du CNRS, Ecole Centrale Paris, France; 3. University of Arkansas, USA

3:15 PM

Break

Advanced Electronic Materials for Energy Storage

Room: Indian

Session Chairs: Rudeger (Derek) Wilke, Sandia National Laboratories; Eugene Furman

3:45 PM

(EMA-S11-050-2016) Fringing Field Effect on Ultrathin Glass Dielectrics (Invited)

J. Gao[2]; D. Kwon[2]; E. Furman*[2]; M. Lanagan[2]; B. Akkopru Akgun[2]; B. Balachandran[1]; S. Garner[3]; 1. Argonne National Laboratory, USA; 2. Pennsylvania State University, USA; 3. Corning Incorporated, USA

4:15 PM

(EMA-S11-051-2016) Multi-layer Glass Capacitors with High Dielectric Energy Density

R. H. Wilke*[1]; H. J. Brown-Shaklee[1]; R. Johnson[1]; 1. Sandia National Laboratories, USA

4:30 PM

(EMA-S11-052-2016) Nanoscale Mapping of Current Transport Pathways

Y. Kutes[1]; J. Luria[1]; A. Moore[3]; E. Stach[4]; N. Padture[2]; B. D. Huey*[1]; 1. University of Connecticut, USA; 2. Brown University, USA; 3. Colorado State University, USA; 4. Brookhaven National Laboratory, USA

4:45 PM

(EMA-S11-053-2016) Visible Light Absorption in Semiconducting Ferroelectric Perovskites Designed for Photovoltaic Applications

L. Wu*[1]; A. R. Akbashev[2]; D. Imbrenda[2]; J. E. Spanier[1]; P. K. Davies[1]; 1. University of Pennsylvania, USA; 2. Drexel University, USA

5:00 PM

(EMA-S11-054-2016) Energy storage materials with nano-encapsulated inclusions of a low-melting metal

A. Abraham*[1]; E. Dreizin[1]; M. Schoenitz[1]; 1. New Jersey Institute of Technology, USA

Failure - The Greatest Teacher

Room: Indian

5:45 PM - 6:45 PM

The EMA Sideshow: Freak data points, scientific distractions, and other random musings

D. Cann*, Oregon State University, USA

Wednesday, January 20, 2016

Plenary Session

Plenary I

Room: Indian

8:40 AM

(EMA-PL-001-2016) Thin-Film Alchemy: Using Strain and Dimensionality to Unleash the Hidden Properties of Oxides

D. Schlom*[1]; 1. Cornell University, USA

Guided by theory, unparalleled properties—those of hidden ground states—are being unleashed by exploiting large strains in concert with the ability to precisely control dimensionality in epitaxial oxide heterostructures. For example, materials that are not ferroelectric or ferromagnetic in their unstrained state can be transmuted into ferroelectrics, ferromagnets, or materials that are both at the same time. Similarly, new tunable dielectrics with unparalleled performance have been created. Our studies reveal details about the microscopic growth mechanism of these phases, which are relevant to preparing multicomponent oxide heterostructures with atomic precision. A new era for multicomponent oxide materials for electronic applications is upon us: oxides by design.

S1. Multiferroic Materials and Multilayer Ferroic Heterostructures: Properties and Applications

Synthesis, Processing, and Properties

Room: Coral A

Session Chair: Nazanin Bassiri-Gharb, Georgia Institute of Technology

10:00 AM

(EMA-S1-001-2016) Piezoelectrics on Magnetic Metal Foil (Invited)

S. Trolier-McKinstry*[1]; 1. Pennsylvania State University, USA

The development of self-powered wireless microelectromechanical (MEMS) sensors hinges on the ability to harvest adequate energy from the environment. Here, higher power levels were approached by better coupling mechanical energy into the harvester, using improved piezoelectric layers on flexible metal foils, and efficiently extracting energy through the use of low voltage rectifiers. Strongly {001} oriented PZT could be deposited by chemical solution deposition or RF magnetron sputtering and *ex situ* annealing on (100) oriented $LaNiO_3$ / HfO_2 / Ni foils. The comparatively high thermal expansion coefficient of the Ni facilitates development of a strong out-of-plane polarization. A compliant bimorph beam enabled power to be harvested more efficiently by utilizing a parabolic mode shape for the vibrating structure. Devices were designed with resonant frequencies from 5 – 10 Hz. At an acceleration of 0.05G, a ~6.2 Hz device with a working area of 5.2 cm^2 (including the proof mass) produced an RMS power of 50 microW. The magnetic foil also offers the possibility of magnetically plucking the devices for non-resonant harvesters.

10:30 AM

(EMA-S1-002-2016) Strain-tuning in multiferroics (Invited)

B. Dkhil*[1]; 1. CentraleSupélec-CNRS, France

Strain is a powerful tool for tuning physical properties like polar and/or magnetic orders in multiferroics. This parameter can be generated using various paths including external hydrostatic pressure, biaxial and uniaxial stresses. In case of the model multiferroic $BiFeO_3$ (BFO), the structure which is closely linked to its ferroelectric and magnetic properties shows pressure instabilities [1]. We took advantage of this strain sensitivity to study how coherent acoustic phonons can be generated by a ultrafast pulsed laser, in somehow as kind of "uniaxial pressure" [2]. We also used biaxial stresses through various substrates to tune the whole properties of BFO showing how misfit strain can 1) affect BFO phases allowing original mixed-phase state [3]; 2) tune the critical temperatures of antiferromagnetic and ferroelectric transitions [4]; 3) modify the ferroelectric, dielectric and piezoelectric properties [5]; and 4) control the magnetic properties and spin arrangements [6]. Finally, we will also show results in hybrid or artificial multiferroics in which the so-called magnetoelectric coupling can be mediated at the interface through strain. Here, we showed how the magnetic (AntiFerroMagnetic and FerroMagnetic) states of a FeRh film can be controlled through strain by applying an electric field on an underlying $BaTiO_3$ ferroelectric substrate [7,8]. In this talk, I will illustrate these remarkable features by stressing the key role of the strain.

11:00 AM

(EMA-S1-003-2016) Functionally graded ferroelectric and multiferroic thin film heterostructures (Invited)

D. Maurya*[1]; S. Priya[1]; 1. Virginia Tech, USA

In this presentation, we report the modulated electrical response in functionally graded ferroelectric and multiferroic thin film heterostructures. Multilayer thin film graded structures were synthesized on platinized silicon substrate with varying thickness and composition of ferroelectric/ferromagnetic layers. The functionally graded architecture exhibited translated hysteresis loops on electric field and polarization axes depending upon the direction of an applied electrical bias. These multilayer functionally graded architectures also exhibited diode-like characteristics in current –voltage plots. This modulated electrical response could be further manipulated by applying the external magnetic field. The modulated electrical behavior in these functionally graded thin film architectures can be attributed to the presence of internal bias due to the functional grading across the interface. These systems exhibited a memristor-like current-voltage behavior. The presence of internal bias assisted separation of photo generated charges giving rise to photocurrent in these devices. These results provide an opportunity to design new circuit components for the next generation of multifunctional microelectronic device architectures.

11:30 AM

(EMA-S1-004-2016) The Nature of Magnetoelectric Coupling in the Room Temperature Multiferroic Pb(Zr,Ti)O3-Pb(Fe,Ta)O3 (Invited)

M. Gregg*[1]; D. Evans[1]; J. F. Scott[2]; M. Alexe[3]; A. Schilling[1]; 1. Queen's University Belfast, United Kingdom; 2. University of St Andrews, United Kingdom; 3. University of Warwick, United Kingdom

The last decade has seen an explosion of research activity in multiferroic materials. This has partly been driven by fundamental interest, but partly also by the exciting prospect of new forms of functional devices. Envisioned device performance often requires distinct room temperature coupling between the magnetic moment and the electrical polarization. However, despite concerted effort, very few single-phase materials have been discovered in which strongly coupled behavior has been categorically and unequivocally established at room temperature. One candidate system is the Pb(Zr,Ti)O3–Pb(Fe,Ta)O3 (PZTFT) solid solution, where promising initial observations have been made, but demand more systematic examination. This talk will describe the way in which the ferroelectric behavior of single crystal PZTFT lamellae changes with applied magnetic field. Significant switching of domains using magnetic fields was observed; in addition, strong hysteretic magnetocapacitance effects were noted. A Landau free energy approach demonstrated that *P*2*M*2 coupling behavior was generally evident, but that for magnetic fields applied perpendicular to the lamella surface (those responsible for ferroelectric switching), asymmetric

coupling terms (such as *PM*) were more important. The study reaffirms our initial suspicion that PZTFT is genuinely a room temperature magnetoelectric multiferroic.

12:00 PM

(EMA-S1-005-2016) Pathways to low energy control of magnetism using multiferroics (Invited)

J. T. Heron*[1]; 1. University of Michigan, USA

Modern magnetic memory technology is faced with issues of scalability and energy consumption as the required electrical current causes significant heating and stray magnetic fields. An ideal solution to this problem would be a magnetic device that can be controlled with an electric field in a capacitor structure as the electric field is well-confined and minimal energy is dissipated. Multiferroic materials and ferroic multilayer heterostructures open pathways towards the electric field control of magnetism and low-energy consumption magnetic devices that ultimately depend on the mechanisms of the magnetoelectric coupling. I will discuss the local magnetoelectric switching of an anisotropically strained $BiFeO_3$ film in response to an electric field. The switching requires the ferroelectric order to switch, can be multistage, and is confined by the mechanical and electrical boundary conditions set by the substrate and the domain structure of the film matrix. These factors may need attention for future application considerations. A heterostructure of $BiFeO_3$ and a ferromagnetic metal – $Co_{0.90}Fe_{0.10}$ – is used to probe the magnetic structure of the multiferroic and the predicted multistage magnetoelectric switching which is capable of reversing the ferromagnetic moment of the exchange coupled ferromagnet and can be integrated into a magnetic memory element.

S2. Functional Materials: Synthesis Science, Properties, and Integration

Functional Materials: Oxide Semiconductor Synthesis, Integration, and Properties

Room: Mediterranean A

Session Chair: Jon-Paul Maria, North Carolina State University

10:00 AM

(EMA-S2-001-2016) PEALD ZnO Thin Film Transistors for Electroceramic Device Integration (Invited)

T. Jackson*[1]; 1. Penn State University, USA

In many applications electroceramic devices benefit from combination with semiconductor devices. Direct integration of semiconductor devices with electroceramics, for example piezoelectric or ferroelectric materials, can enable new applications. ZnO thin film transistors (TFTs) deposited by plasma enhanced atomic layer deposition (PEALD) have important advantages for integration with electroceramic devices. Low processing temperature (typically < 200 °C) allows ZnO TFTs to be added at the end of processing, often with no changes in the electroceramic devices. High performance (mobility >20 cm^2/Vs) and good TFT stability allow many options for switches and circuits integrated with electroceramic actuators or sensors. Atomic layer deposition allows good device yield even on imperfect substrates and device layers. Low processing temperature also allows device fabrication on thin flexible polymeric substrates and enables additional application possibilities. This talk will describe the integration ZnO TFTs with PZT actuators and other electroceramic devices.

10:30 AM

(EMA-S2-002-2016) VO_2 Thin Film for Smart Nano Biosensor

D. Kim*[1]; B. Kim[1]; S. Han[1]; C. Kang[1]; S. Nahm[1]; 1. Korea University, The Republic of Korea

In general, the vanadium dioxide (VO_2) ceramics exhibit the dramatic change of resistance due to the metal-insulator transition triggered by thermal energy. Therefore, the VO_2 has been studied for the application to the various thermal sensors. In this work, we propose a new type of the VO_2-based thermal biosensor, which use a thermal reaction between the biomarker and receptor. To synthesize a thermal biosensor, a VO_2 thin film was deposited on the sapphire substrate by using an RF sputtering. Finally, a mixture of nafion and glucose oxidase was uniformly coated on the VO_2 thin film to make the buffer layer and bio-receptor. The structural and electrical properties of the VO_2 film and the VO_2 thermal bio-sensor were investigated by X-ray refraction (XRD), scanning electron microscope (SEM) and four-probe station with a temperature controller. The VO_2 thin film was well formed on the sapphire substrate with a high resistance change of four orders of magnitude. Moreover, the VO_2 thermal bio-sensor also maintained the high resistance change. Therefore, the VO_2 thin film is a promising material for a new thermal biosensor with high performance.

10:45 AM

(EMA-S2-003-2016) Step-free GaN substrates for oxide heteroepitaxy

C. T. Shelton*[1]; I. Bryan[1]; E. A. Paisley[2]; E. Sachet[1]; N. Lavrik[3]; M. Biegalski[3]; J. LeBeau[1]; R. Collazo[1]; Z. Sitar[1]; J. Maria[1]; 1. NCSU, USA; 2. Sandia National Laboratories, USA; 3. Oak Ridge National Lab, USA

Until recently, heteroepitaxially integrating polar oxides with wide-bandgap semiconductors like GaN has been problematic. The large discontinuity in chemistry, bonding and crystal structure across the oxide-nitride interface introduces a great number of extended defects. Mitigating these defects requires a two-pronged approach wherein: 1) the faceting tendency of (111) cubic oxides on GaN is suppressed and 2) misoriented grains in the oxide due to the stepped nature of the substrate are removed. Surfactant assisted PVD can overcome some of these challenges by promoting smooth 2D layer-by-layer growth. But even smooth rocksalt films contain disclination defects where in-plane rotation domains meet. We will elucidate the epitaxial nature of the two in-plane rotation domains and share our efforts to remove them by engineering the substrate using confined-area epitaxy (CAE). CAE regrowth of GaN on native substrates allows for preparation of single-terrace flat GaN and, combined with lattice matched smooth MgCaO, near perfect oxide heteroepitaxy. Collectively, these techniques offer a path to high-quality 'semiconductor-grade' interfaces between heterogeneous systems.

11:00 AM

(EMA-S2-004-2016) Gate oxide band offset dependence on nitride surface chemistry for GaN power electronics

E. A. Paisley*[1]; C. T. Shelton[2]; M. Brumbach[1]; M. D. Losego[3]; C. Rost[2]; S. Atcitty[1]; J. Maria[2]; J. Ihlefeld[1]; 1. Sandia National Laboratories, USA; 2. North Carolina State University, USA; 3. Georgia Institute of Technology, USA

Gate oxides for GaN- HEMT devices may enable normally off device performance with simultaneous gate leakage suppression, given sufficient oxide/nitride band offsets. However, literature values for band offsets to GaN can span 1 eV for the same oxide/nitride material sets. One challenge to this interface is a dependence of Ga:N surface stoichiometry and oxygen surface coverage on GaN growth procedure. These surface chemistry inconsistencies may alter the GaN surface electronic structure by modifying the polarization screening charges. We will discuss nitride surface chemistry influence on reported band offsets and will show measured band offsets for the MgO | GaN case study for films prepared with identical nitride surface cleaning and MgO growth. These films possess

valence band offsets spanning 1.26 to 1.7 eV ± 0.05 eV. Results will be discussed in the context of the influence of Ga:N surface ratio. For completeness, we will also show a comparison study of valence band offsets of Al_2O_3|GaN interfaces, grown by ALD. Interface state densities, D_{it}, for MgO | GaN (~ 3 x 10^{11} $eV^{-1}cm^{-2}$) and Al_2O_3 | GaN will be also discussed. Sandia National Laboratories is a multiprogram laboratory operated by Sandia Corporation, a wholly owned subsidiary of Lockheed Martin Company, for the United States Department of Energy's National Nuclear Security Administration under contract DE-AC04-94AL85000.

11:15 AM

(EMA-S2-005-2016) Physical properties of doped $BaSnO_3$ semiconductors with high electrical mobility and optical transparency at room temperature (Invited)

K. Kim*[1]; 1. Seoul National University, The Republic of Korea

Transparent electronic materials are increasingly demanded for a variety of optoelectronic and display applications, ranging from passive conductive windows to active thin film transistors. $BaSnO_3$ is a semiconducting oxide with a large band gap of more than 3.1 eV. Recently, we have discovered that $BaSnO_3$ doped with a few percent of La exhibits unusually high electrical mobility of 320 $cm^2(Vs)^{-1}$ at room temperature and superior thermal stability at high temperatures. Following that work, we report here various physical properties of (Ba,La)SnO_3 and Ba(Sn,Sb)O_3 single crystals and epitaxial films including temperature-dependent transport and phonon properties, optical properties and first-principles calculations. We find that almost doping-independent mobility of 200-300 $cm^2(Vs)^{-1}$ is realized in the single crystals in a broad doping range from 1.0'10^{19} to 4.0'10^{20} cm^{-3}. Moreover, the conductivity of ~10^4 $W^{-1}cm^{-1}$ reached at the latter carrier density is comparable to the highest value previously reported in the transparent oxides. We attribute the high mobility to several physical features of (Ba,La)SnO_3: a small effective mass coming from the ideal Sn-O-Sn bonding in a cubic perovskite network, small disorder effects due to the doping away from the SnO_6 octahedra, and reduced carrier scattering due to the high dielectric constant.

11:45 AM

(EMA-S2-006-2016) High Mobility Conductive Oxides for Optoelectronic Components in the mid-IR

E. Sachet*[1]; K. Kelley[1]; C. T. Shelton[1]; S. Franzen[1]; J. Maria[1]; 1. North Carolina State University, USA

The development of high mobility conductive oxides such as CdO:Dy enabled a variety of novel optoelectronic structures that operate in the mid-IR. As a prototypical Drude metal, CdO's dielectric properties are directly dependent on the free carrier concentration. This implies that the materials transition energy from dielectric to metallic can be tuned over a wide energy range, from the far-IR (8-12 μm) up to near IR energies (2 μm). This unprecedented tunability is augmented by extremely high electron mobilities (~500 $cm^2V^{-1}s^{-1}$), which minimize optical losses throughput the entire tuning space. Here we present experimental data that demonstrates this tunability, as well as an experimental overview of novel applications for conductive oxides. -) CdO is used for plasmonically assisted chemical sensing in the mid-IR, by matching a surface plasmon's energy with absorption bands of analytes. -) High mobility, low-doped CdO can be used as tunable IR transparent window at mid-IR energies, with competitive conductivities (>4.0E+03 1/Ω cm) and >90% transparency. -) Parallel plate capacitors comprised of thin CdO films allow for active tuning of CdOs dielectric function, enabling active optical components that operate at mid-IR wavelengths. The examples presented in this talk offer an exciting outlook into an emerging field of applications for conductive metal oxides.

12:00 PM

(EMA-S2-007-2016) Doping control in epitaxial thin films via reactive RF co-sputtering

K. Kelley*[1]; E. Sachet[1]; H. Kham[1]; S. Franzen[1]; J. Maria[1]; 1. North Carolina State University, USA

In recent years, conductive oxides have been increasingly investigated in the context of plasmonics. The interest in plasmonic technologies surrounds many emergent optoelectronic applications, such as plasmon lasers, transistors, sensors, and information storage. While plasmonic materials for UV-VIS and near infrared wavelengths have been found, the mid-infrared range remains a challenge to address. Recent developments show Dy-doped CdO (CdO:Dy) grown via molecular beam epitaxy (MBE) can achieve electron mobilities (~500 $cm^2V^{-1}s^{-1}$) and carrier densities (10^{20} cm^{-3}) that satisfy the criteria for mid-infrared spectrum plasmonics, and overcome the losses seen in conventional plasmonic materials, such as noble metals. Highly accurate doping using MBE was the key to investigate the structure property relations in CdO:Dy. However MBEs limited throughput and high cost present a barrier towards larger scale application of this material. In this work, we present a deposition technique for controllably doped CdO grown via reactive RF co-sputtering. Epitaxial films grown by this method depict electrical and optical properties comparable to MBE grown materials and thus offer a more accessible route towards ubiquitous IR plasmonic technologies based on CdO. Efforts thus far have produced co-sputtered CdO:Dy on Al_2O_3 with carrier densities of 10^{20} cm^{-3} and mobilities in excess of 300 $cm^2V^{-1}s^{-1}$.

12:15 PM

(EMA-S2-008-2016) A Study on The Transparent and Flexible EMI Shielding Film Manufactured by Impringting Method

H. Choi*[1]; G. Lee[1]; 1. Changsung Corporation, The Republic of Korea

There are growing concerns and needs on the transparent and flexible shielding film for controlling the EMI (Electro-Magnetic Interference) problems in various electronic industries. Specially, as smart devices and wearable devices have a tendancy to become highly functionalized, flexible and transparent, some high performance materials like EMI shielding films should be used inevitably. There have been various kinds of transparent EMI shielding films, ordinary metal etching type, carbon based printing type, ITO (Indium Tin Oxide) based type and so on. We studied another type of transparent electroconductive film based on the impringting process. Line width and depth (same as thickness) as well as line spacing can be controlled the transparency and EMI shielding effectiveness which is proportional with electroconductivity of the film. And we also designed intaglio imprinting pattern to enhance flexibility of the transparent film, because flexibility will be a critical factor to be used as a candidate material for future wearable devices. We evaluated the flexibility with a specially designed bendable tester.

S3. Use of thermal energy for electrical power generation and refrigeration: Fundamental science, materials development and devices

Conversion of Thermal Energy

Room: Mediterranean B/C
Session Chair: Jon Mackey, University of Akron

10:00 AM

(EMA-S3-001-2016) Novel thermoelectric optimization methods (Invited)

Y. Gelbstein*[1]; 1. Ben-Gurion University of the Negev, Israel

In the recent years, demands for energy efficiency have motivated many researchers globe-wide to seek for innovative methods capable of enhancement the efficiency of heat to electricity thermoelectric

(TE) energy conversion. Many of these methods incorporated sub-micron features, which are very effective in phonon scattering, for reduction of the lattice contribution to the thermal conductivity, k_l, without adversely affecting the other involved electronic properties. Although such an approach resulted in increased TE efficiencies, stabilizing the nano-centers while preventing coarsening under practical operation conditions, combined with an additional electronic optimization, is still required. The presentation will cover a combination of several novel methods approaching toward a higher technology readiness level (TRL) of TE devices. These methods include: Phase separation into the sub-micron scale with an enhanced thermodynamic stability. Co-doping of known thermoelectric compounds, while one doping element introduces vacancies which are occupied by another doping element, for optimizing the electronic TE properties. Functionally graded materials (FGM) generation, with an optimal *ZT* envelope over a wide temperature range. Besides of the listed above approaches for optimizing the TE compositions, the presentation will cover some of the procedures required for development of practical TE devices.

10:30 AM

(EMA-S3-002-2016) Thermoelectric modules for Efficient Power Generation (Invited)

N. Pryds*[1]; 1. Technical University of Denmark, Denmark

Improvement in the conversion efficiency of a thermoelectric module can be achieved by controlling the thermal transport of the thermoelectric materials. The ability to control and tune the thermal properties of materials is the primary goal to improve device efficiency and improve electric energy generation. One of the major obstacles for achieving even higher conversion efficiency of modules today is the inherent electrical and thermal resistance at contacts, both internally in segmented legs and externally at e.g. electrical contacts. In this talk, experimental and modelling results of high-performance segmented and non-segmented thermoelectric modules will be presented. The physics underlying the interplay between the interfacial imperfections and the thermal transport across these interfaces and their influence on a working thermoelectric module will also be discussed.

11:00 AM

(EMA-S3-016-2016) Experimental Investigation of the Ferroelectric Proximity Effect in Bilayer PZT Heterostructures via Thermal Transport Measurements

B. M. Foley*[1]; D. Scrymgeour[2]; E. A. Paisley[2]; J. Michael[2]; B. McKenzie[2]; M. Wallace[3]; D. Medlin[2]; S. Trolier-McKinstry[3]; J. Ihlefeld[2]; P. Hopkins[1]; 1. University of Virginia, USA; 2. Sandia National Laboratories, USA; 3. Pennsylvania State University, USA

Techniques such as piezoresponse force microscopy (PFM) and channeling-contrast scanning electron microscopy (CC-SEM) have been used to confirm the complex domain nucleation/rearrangement occurring at the top surface of the bilayer PZT system while under applied fields. However, it has been suggested that an even richer array of domain interactions may be occurring at the heterointerface between the 30/70 tetragonal PZT top layer and the 70/30 rhombohedral PZT bottom layer due to the "ferroelectric proximity effect". While plan-view imaging of domain interactions under applied bias using PFM has been well established, performing *in-situ* imaging of the film cross-section is much more challenging and is primarily performed via transmission electron microscopy (TEM) by only a few groups. As an alternative, we employ thermal transport measurements as a means to probe the domain interactions at the bilayer PZT heterointerface. Using time-domain thermoreflectance (TDTR), we are able to probe this buried interface and explore the complex domain interactions based on the changes in thermal transport properties due to phonon scattering at domain boundaries. Observations of these domain interactions are made as a function of both applied electric field, as well as sample temperature near/above the Curie temperature of the rhombohedral bottom layer.

11:15 AM

(EMA-S3-004-2016) DRREAM: Drastically Reduced Use of Rare Earths in Applications of Magnetocalorics (Invited)

K. G. Sandeman*[1]; 1. Brooklyn College of The City University of New York, USA

The aim of DRREAM, an EC-FP7-funded collaborative research project, was to reduce the use of rare earths (REs) in the life cycle of a future magnetic cooling device. We forecast that the most significant reduction in the required volume of RE-containing permanent magnet will come from the use of refrigerants with enhanced magnetocaloric effects and from the improved heat transfer properties of optimally-produced regenerator parts. Efforts in these directions, and in the minimisation of wastage in the production of regenerator parts, will be described. Parallel research on potential thermomagnetic power generation materials will also be outlined. The research leading to these results has received funding from the European Union Seventh Framework Programme (FP7/2007-2013) under grant agreement n° 310748.

11:45 AM

(EMA-S3-005-2016) Strategies for enhancing caloric responses using ferroelectric oxides

B. Dkhil*[1]; 1. CentraleSupélec-CNRS, France

The search for alternative solid-state refrigeration materials to hazardous gases in conventional and cryogenic cooling devices is a very active field of condensed matter. The use of phase transitions is efficient to achieve giant caloric effects in ferroic materials in which magnetization, polarization, strain and/or volume can be strongly tuned under a moderate external stimulus. Here, we explored various phenomena existing in ferroelectrics to reveal their potentialities as solid state coolers. By using Landau-based phenomenological calculations, we studied the elasto- and electro-caloric properties of the ecofriendly $BaTiO_3$ in details including bulk and thin film form, the role of the external uniaxial stress, electric field, substrate, film thickness and electrodes. We show that ferroelectrics are natural multicaloric materials in which both giant elasto- and electro-caloric responses can be achieved near room temperature and that the 2^{nd}-order nature of transitions can be beneficial. We also investigated how multiphase points composition can be used to enhance electrocaloric effects. Moreover, in addition to conventional electrocaloric effect, we show that negative effect can be also generated efficiently and thus used as a supplemental tool for designing enhanced caloric responses. As a conclusion, our findings clearly demonstrate promising perspectives for ferroelectrics in solid-state refrigeration.

12:00 PM

(EMA-S3-006-2016) Multicaloric ferroelectrics (Invited)

X. Moya*[1]; 1. University of Cambridge, United Kingdom

Thermal changes in ferroelectrics can be driven using electric fields and hydrostatic pressures. The resulting electrocaloric and barocaloric effects are large near ferroelectric phase transitions, and have been proposed for environmentally friendly cooling applications. I will describe the fundamentals of these caloric effects from a historical perspective and present recent advances on multicaloric ferroelectric materials.

S5. Multifunctional Nanocomposites

Multifunctional Nanocomposites I

Room: Coral B

Session Chair: Roman Engel-Herbert, The Pennsylvania State University

10:00 AM

(EMA-S5-001-2016) Magnetism and Nanoscale Structural and Compositional Irregularities in MBE-grown La_2MnNiO_6 on $SrTiO_3$(001) (Invited)

S. Chambers*[1]; 1. Pacific Northwest National Laboratory, USA

Double perovskites ($A_2BB'O_6$) are a fascinating class of oxides with considerable potential for applications requiring simultaneous ferromagnetic and semiconducting properties. In the ideal structure, - B - O - B' - O - bonding facilitates superexchange between B and B'. If this interaction results in parallel spin alignment on B and B', the ferromagnetic moment per formula unit can be quite large. We have investigated MBE-grown La_2MnNiO_6 in considerable detail and have found that despite the fact that Mn and Ni are present as 4+ (d^3: $t_{2g}^3e_g^0$) and 2+ (d^8: $t_{2g}^6e_g^2$) respectively, and exhibit suitable XMCD signatures, the volume-averaged moment per formula unit is considerably less than 5 Bohr magnetons. Our electron energy loss spectroscopy (STEM-EELS) and atom probe tomography (APT) results to date reveal that there is considerable disorder in the B-site sublattice for as-deposited films, despite excellent volume-averaged stoichiometry. While air annealing results in substantial ordering, the moment remains low due to the nucleation of epitaxially ordered NiO inclusions with needle-like shapes revealed only by APT. First principles modeling suggests that even though the double perovskite is quite stable if nucleated in excess O, the presence of O vacancies facilitates structural disorder. In this talk, we will present our latest results on this fascinating material.

10:30 AM

(EMA-S5-002-2016) Templated Self-assembly of Multiferroic Oxide Nanocomposites (Invited)

C. Ross*[1]; 1. Massachusetts Institute of Technology, USA

Multiferroic oxides with two different coexisting order parameters, such as ferromagnetism and ferroelectricity, possess a range of useful phenomena such as voltage-controlled magnetism which can enable memory or logic devices. Two-phase multiferroics can be made by coupling a ferrimagnetic spinel (e.g. $CoFe_2O_4$) with a ferroelectric perovskite (e.g. $BiFeO_3$) in a self-assembled nanocomposite, in which pillars of spinel grow inside a perovskite matrix with well-defined vertical interfaces. However, the random positions of the pillars limit their utility. We will show how substrate patterning can direct the nucleation to form well ordered structures, using either focussed ion beam or block copolymer lithography to pattern small pits in the surface of the $SrTiO_3$ substrate to provide pillar nucleation sites. Nanocomposites can be integrated onto Si using an 8 nm $SrTiO_3$ buffer layer, and composites with modulated pillar widths or compositions can be grown. Nanocomposites are made with pillar composition of $Co_{1-x}Ni_xFe_2O_4$ in which the increase in x lowers the magnetoelastic anisotropy while maintaining the magnetostatic coupling between pillars. For x=0.8 the magnetostatic interactions are strong enough to produce an ac-demagnetized state consisting of alternating up and down magnetized pillars. These materials provide a playground for the investigation of nanoscale magnetic, ferroelectric and multiferroic phenomena.

11:00 AM

(EMA-S5-003-2016) First Principles Design of High T_c Superconductors (Invited)

T. Birol*[1]; 1. Rutgers University, USA

Efforts for designing new materials using first principles theory have gained momentum in the recent years with increased computational power and better computational tools. New materials have been successfully predicted and experimentally observed to have novel functionalities, such as ferroelectricity, multiferroicity, or (conventional) superconductivity. A holy grail of condensed matter physics is to predict a room temperature superconductor. While the unknowns in the mechanisms of high T_c superconductivity render such an endeavour a daunting task, information about various structural correlates have been accumulated and can be used to guide the search. In this talk, I will talk about some ideas to use this information to design new high T_c superconductors or increase the T_c. After discussing our recent work on $Hg(CaS)_2CuO_2$, a possible copper oxsulfide compound, I will mention some strategies to tune the crystal structure of iron pnictides to boost T_c.

11:30 AM

(EMA-S5-004-2016) Electron Pairing Without Superconductivity (Invited)

J. Levy*[1]; 1. University of Pittsburgh, USA

Strontium titanate ($SrTiO_3$) is the first and best known superconducting semiconductor. It exhibits an extremely low carrier density threshold for superconductivity, and possesses a phase diagram similar to that of high-temperature superconductors—two factors that suggest an unconventional pairing mechanism. Despite sustained interest for 50 years, direct experimental insight into the nature of electron pairing in $SrTiO_3$ has remained elusive. Here we perform transport experiments with nanowire-based single-electron transistors at the interface between $SrTiO_3$ and a thin layer of lanthanum aluminate, $LaAlO_3$. Electrostatic gating reveals a series of two-electron conductance resonances that bifurcate above a critical pairing field B_p of about 1–4 tesla, an order of magnitude larger than the superconducting critical magnetic field. For magnetic fields below B_p, these resonances are insensitive to the applied magnetic field; for fields in excess of B_p, the resonances exhibit a linear Zeeman-like energy splitting. Electron pairing is stable at temperatures as high as 900 millikelvin, well above the superconducting transition temperature.These experiments demonstrate the existence of a robust electronic phase in which electrons pair without forming a superconducting state. Key experimental signatures are captured by an attractivbe-U Hubbard model that describes real-space electron pairing as a precursor to superconductivity.

12:00 PM

(EMA-S5-005-2016) Detangling Extrinsic and Intrinsic Hysteresis for Detecting Dynamic Switch of Electric Dipoles using Graphene Field-Effect Transistors

C. Ma*[1]; Y. Gong[2]; R. Lu[2]; E. Brown[3]; B. Ma[4]; J. Li[3]; J. Wu[2]; 1. Xi\'an Jiaotong University, China; 2. University of Kansas, USA; 3. Kansas Sate University, USA; 4. Argonne National Laboratory, USA

A transition in source-drain current vs. back gate voltage (I_D–V_{BG}) characteristics from extrinsic polar molecule dominant hysteresis to anti-hysteresis induced by an oxygen deficient surface layer that is intrinsic to the ferroelectric films has been observed on graphene field-effect transistors on $Pb_{0.92}La_{0.08}Zr_{0.52}Ti_{0.48}O_3$ gates (GFET/PLZT-Gate) during a vacuum annealing process developed to systematically remove the polar molecules adsorbed on the GFET channel surface. This allows detangle of the extrinsic and intrinsic hysteresis on GFET/PLZT-gate devices and detection of the dynamic switch of electric dipoles using GFETs, taking advantage of their high gating efficiency on ferroelectric gate. A model of the charge trapping and pinning mechanism is proposed to explain the transition. In response to pulsed V_{BG} trains of positive, negative, and

alternating polarities, respectively, the source-drain current I_D variation is instantaneous with the response amplitude. A detection sensitivity of around 212 dipole/μm^2 has been demonstrated at room temperature, suggesting the GFET/ferroelectric-gate devices provide a promising high-sensitivity scheme for uncooled detection of electrical dipole dynamic switch.

S7. Processing and microstructure of functional ceramics: Sintering, grain growth and their impact on the materials properties

Grain Growth and Abnormal Grain Growth

Room: Caribbean B

Session Chair: Wolfgang Rheinheimer, Karlsruhe Institute of Technology

10:00 AM

(EMA-S7-001-2016) Adsorption, Fields and Grain Boundary Mobility (Invited)

W. D. Kaplan*[1]; 1. Technion - Israel Institute of Technology, Israel

The role of dopants in processing ceramics has been an important issue for many years, especially given the contradicting reports of retarded or accelerated grain growth by key dopants and impurities. New analysis of grain boundary (GB) mobility of alumina as a function of dopant concentration has shown that some segregating dopants increase the GB mobility, i.e. the opposite of solute-drag. The segregating dopants are associated with 2-D structural and compositional transitions at the GBs, and possible changes in the mechanism of GB migration. This presentation will review recent GB mobility measurements and the concept of 2-D GB transitions and their potential role on the mechanism of GB motion. A comparison will be made with recent measurements of the remarkable increase of GB mobility due to the application of external electrical fields.

10:30 AM

(EMA-S7-002-2016) Grain Boundary Character Distributions in Perovskite Ceramics (Invited)

G. Rohrer*[1]; S. Ratanaphan[2]; 1. Carnegie Mellon University, USA; 2. King Mongkut's University of Technology Thonburi, Thailand

Grain boundary character distributions (GBCDs) in polycrystals evolving by normal grain growth are controlled by the grain boundary energy anisotropy. It was recently discovered that grain boundary energy distributions (GBED) in isostructural materials, a class of materials that share the same crystal structure, are directly related to one another. This suggests that GBCDs in isostructural materials might also be related in a similar way. To test this hypothesis, electron backscatter diffraction (EBSD) was used to map grain orientations in SrTiO3 and BaTiO3 ceramics. The GBCDs were determined from the stereological interpretation of EBSD maps. It was found that the GBCDs of perovskite ceramics are statistically correlated, as are those of body-centered cubic and face centered cubic metals. The observations are compared to measured grain boundary energies.

11:00 AM

(EMA-S7-003-2016) Triggering abnormal grain growth by pressure assisted sintering in $BaLa_4Ti_4O_{15}$ (Invited)

A. M. Senos*[1]; M. Fernandes[1]; N. Selvaraj[1]; J. Abrantes[2]; P. Vilarinho[1]; 1. University of Aveiro/ CICECO, Portugal; 2. UIDM, ESTG, Instituto Politecnico de Viana do Castelo, Portugal

This talk is about the role of stresses on the movement of grain boundaries (GBs) for grain growth in ceramics. We have been investigating this topic in titanates, namely in $BaLa_4Ti_4O_{15}$ (BLT), a very important material for microwave applications, and reported for the first time that stresses created during the constrained sintering of thick films affect the GB mobility, enhancing anisotropic grain growth and altering electrical properties. To investigate the effect of applied compressive stresses in 3D ceramics, hot isostatic pressing with 65 MPa, hot pressing with 60 MPa and conventional sintering, without any external pressure, for comparison, were used to design microstructures of BLT with different grain size distributions, having all the samples the same thermal history. The grain size distributions were separated into two populations, normal (NGs) and abnormal grains (AGs), and it was achieved that the main effect of external pressure was on triggering AG growth, increasing both the number and size of AGs and leading to a more anisotropic grain growth (more elongated and oriented grains), whereas not a significant change was found for the NGs population. Complementarily, it is also shown that the structure of grains and GBs of pressure assisted samples is quite different of that of free sintered specimens, showing a larger density of crystal imperfections and thicker GB disorder regions.

11:30 AM

(EMA-S7-004-2016) The Influence of Impurities on the Microstructural Evolution of Alumina

R. Moshe*[1]; W. D. Kaplan[1]; 1. Technion - Israel Institute of Technology, Israel

The main goal of the present research is to study the influence of impurities, at concentrations below the solubility limit, on the evolving microstructure of alumina. The microstructure of a sintered body strongly depends on the composition of the powder used for the sintering process, where dopants and impurities are known to affect sintering rates and grain growth. In this study, the impurity content was varied by doping alumina with different amounts of CaO, below the solubility limit. The amount of cation in the alumina was determined by conducting fully standardized wavelength dispersive spectroscopy (WDS) and the change in grain boundary mobility as a function of the amount of dopant was characterized using scanning electron microscopy. Unlike segregating dopants which reduce grain boundary mobility by solute-drag, CaO increases the rate of grain growth. Possible mechanisms by which CaO increases grain boundary mobility will be discussed.

11:45 AM

(EMA-S7-005-2016) 3D Microstructure Evolution in Strontium Titanate with Non-destructive Imaging

A. Trenkle*[1]; M. Syha[1]; W. Rheinheimer[1]; M. Echlin[3]; W. Lenthe[3]; W. Ludwig[2]; D. Weygand[1]; P. Gumbsch[1]; 1. Karlsruhe Institute of Technology, Germany; 2. European Synchrotron Radiation Facility, France; 3. University of California - Santa Barbara, USA

Strontium titanate is known for its anisotropic interface properties, which influence microstructural evolution during grain growth. Non-destructive imaging methods in three-dimensions (3d) are necessary to observe grain growth in bulk material. X-ray diffraction contrast tomography (DCT) was used to characterize a polycrystalline strontium titanate sample of two coarsening stages in terms of shape and orientation of each grain in 3d. The resulting reconstructions were additionally validated by femtosecond laser ablation based serial sectioning via the TriBeam system. The evolution of single grains was analyzed by means of morphology, topology and crystallography. Relatively large grains tend to become more cuboidal with a reduced volume change rate. A general preference of low-energy oriented faces was also observed.

12:00 PM

(EMA-S7-006-2016) Influence of an electric field on grain growth and sintering in strontium titanate

W. Rheinheimer*[1]; M. J. Hoffmann[1]; 1. Karlsruhe Institute of Technology, Germany

Within the last years considerable efforts were done in investigating electric field assisted sintering (flash sintering). But since the experiments are very hard to control, the present study focuses on grain growth under electric field for strontium titanate. The impact of an electric field on grain growth in strontium titanate is investigated between 1350°C and 1550°C for fields of up to 50 V/mm. To prevent joule heating by a current flowing through the material, insulating Al_2O_3 plates separate the electrodes from the samples. The seeded polycrystal technique is used. The growth direction of the single crystalline seeds is perpendicular to the electric field; hence electrostatic forces do not influence the growth. Below 1425°C the influence of the electric field is weak. Above 1425°C the field results in an increase of the grain boundary mobility at the negative electrode. It is shown that abnormal grain growth can be triggered by the electric field. These experimental findings lead to a model based on a shift of charged defects. The enhancement of the grain boundary mobility on the negative electrode is explained by an accumulation of oxygen vacancies. This accumulation induces a reduction of the material. A reduction of strontium titanate by atmosphere also results in an increase of the grain boundary mobility, which accords well with the observed behavior under electric field.

S9. Recent Developments in Superconducting Materials and Applications

New Superconductor 1- New Superconducting Materials and Phenomena

Room: Pacific

Session Chairs: Gang Wang, Institute of Physics, Chinese Academy of Sciences; Claudia Cantoni, Oak Ridge National Laboratory

10:00 AM

(EMA-S9-001-2016) Growth of Stanene and single-layer FeSe on $SrTiO_3$ with a superconducting T_c above 100 K (Invited)

J. Jia*[1]; 1. Shanghai Jiao Tong University, China

Stanene is composed of tin atoms arranged in a single layer honeycomb structure. Stanene and its derivatives were proposed to be a 2D topological insulator (TI) with a very large band gap and support enhanced thermoelectric performance, topological superconductivity and the near-room- temperature quantum anomalous Hall (QAH) effect. In the first part of my talk, I will report a successful fabrication of 2D stanene by MBE. The atomic and electronic structures were determined by STM and ARPES in combination with first-principles calculations. In the second part, I will talk about a direct transport measurement of high T_c superconductivity in the FeSe/STO system. By *in situ* 4-point probe technique that can be conducted at an arbitrary position of the single-layer FeSe films on STO, we detected superconductivity transition at a temperature above 100 K.

10:30 AM

(EMA-S9-002-2016) 2D interfacial superconductivity by local manipulation of atoms and electron spins (Invited)

C. Cantoni*[1]; 1. Oak Ridge National Laboratory, USA

Lately 2D superconductor systems have been the object of a great interest because their electron density can be easily manipulated, and competing mechanisms (e.g., spin order) are different than in 3D, giving rise to new and tunable electronic phenomena. For applications, 2D superconducting devices with high switching speed and lossless interconnects are regarded as possible answer to the critical integration density of the current semiconductor technology. Here I will discuss two different examples of novel 2D superconducting systems originating at the interface of insulating oxides. One of these systems, the interface between $SrTiO_3$ and $CaCuO_2$ can reach a T_c of 50 K and offers valuable insight in the physics of cuprate superconductors. The other, the $LaAlO_3/EuTiO_3/SrTiO_3$ interface shows interplay of magnetic interactions, superconductivity, and spin-orbit coupling in the same q2DES, pointing to the emergence of novel quantum phases in low dimensional materials . Research supported by the U.S. Department of Energy, Office of Science, Basic Energy Sciences, Materials Sciences and Engineering Division.

11:00 AM

(EMA-S9-003-2016) Two-Dimensional Oxide Topological Insulator With Iron-Pnictide Superconductor LiFeAs Structure (Invited)

H. Weng*[1]; 1. Institute of Physics, Chinese Academy of Sciences, China

By using first-principles calculations, we propose that ZrSiO can be looked as a three-dimensional (3D) oxide weak topological insulator (TI) and its single layer is a long-sought-after 2D oxide TI with a band gap around 30 meV. The experimental achievements in growing oxides with atomic precision ensure that the single layer ZrSiO can be readily synthesized. This will lead to novel devices based on TIs, the so called "topotronic" devices, operating under room-temperature and stable in air. Thus, a new field of "topotronics" will arise. Another intriguing thing is this oxide 2D TI has the similar crystal structure as the well-known iron-pnictide superconductor LiFeAs. This brings great promise in realizing the combination of superconductor and TI, paving the way to various extraordinary quantum phenomena, such as topological superconductor and Majorana modes. We further find that there are many other isostructural compounds hosting the similar electronic structure and forming a WHM-family with W being Zr, Hf or La, H being group IV or group V element, and M being group VI one.

11:30 AM

(EMA-S9-004-2016) Artificially engineered superlattices of pnictide superconductor (Invited)

C. Eom*[1]; 1. University of Wisconsin-Madison, USA

Artificial layered pnictide superlattices offer unique opportunity towards tailoring superconducting properties and understanding the mechanisms of superconductivity by creating model structures which do not exist in nature. For high field applications, very high critical current density (J_c) and irreversibility field (H_{irr}) are indispensable along all crystal directions. On the other hand the development of superconducting devices such as tunnel junctions requires multilayered heterostructures. We have domonstrated that artificially engineered undoped Ba-122 / Co-doped Ba-122 compositionally modulated superlattices produce *ab*-aligned nanoparticle arrays by layering and self-assembled *c*-axis aligned defects that combine to produce very large J_c and H_{irr} enhancements over a wide angular range. We also demonstrate a structurally modulated $SrTiO_3$ (STO) / Co-doped Ba-122 superlattice with atomically sharp interfaces. Success in superlattice fabrication involving pnictides will serve to spur progress in heterostructured systems exhibiting novel interfacial phenomena and device applications. This work has been done in collaboration with S. Lee, J.H. Kang, C. Tarantini, P. Gao, J. Jiang, J. D. Weiss, F. Kametani, Y. Zhang, X. Q. Pan, E. E. Hellstrom, and D. C. Larbalestier. The work at the University of Wisconsin was supported by funding from the DOE Office of Basic Energy Sciences under award number DE-FG02-06ER46327.

12:00 PM

(EMA-S9-005-2016) Growth of iron chalcogenide thin films on various substrates and pinning enhancement by incorporated nanolayers

J. Huang*[1]; L. Chen[1]; J. Jian[1]; L. Li[1]; H. Wang[1]; 1. Texas A&M University, USA

Iron-based superconductors have attracted great research interests from both the intriguing fundamental superconducting mechanism aspects and their potential applications in high fields owing to their high critical field H_{c2} and low field anisotropy. However, one critical factor limiting the commercial applications of superconducting coated conductors is the significant manufacturing costs involved in the processing of the complex layered buffers and the subsequent epitaxial growth of superconducting coated conductors. Here we demonstrate a much simplified superconducting coated conductor design for $FeSe_xTe_{1-x}$ on glass and metallic substrates without bi-axial texturing buffers, and the films show obvious superconducting properties. Furthermore, nanolayers (including non-magnetic CeO_2 and magnetic $(CeO_2)_{0.9}(CoFe_2O_4)_{0.1}$ nanocomposite) are incorporated into $FeSe_{0.1}Te_{0.9}$ films for pinning enhancement, the results show that these nanolayers can provide effective pinning centers for iron-chalcogenide films.

S11. Advanced electronic Materials: Processing, structures, properties and applications

Advanced Electronic Materials: Dielectrics I

Room: Indian

Session Chairs: David Cann, Oregon State Univ; Takaaki Tsurumi, Tokyo Institute of Technology

10:00 AM

(EMA-S11-001-2016) Concept of Solid State Ionic Capacitor for Future MLCCs (Invited)

T. Tsurumi*[1]; R. Ishikawa[1]; T. Hoshina[1]; H. Takeda[1]; Y. Sakabe[1]; 1. Tokyo Institute of Technology, Japan

We will propose a new concept of solid ionic capacitors where ionic motions in solids are used to generate interfacial polarization. The solid ionic capacitor will be a candidate of energy storage capacitors and future MLCCs with high capacitance density. Development of a new energy storage device that can replace lithium ion batteries is one of the most important subjects for stopping global warming. Capacitors have an advantage over batteries with respect to the endurance for charge - discharge recycling. The capacitance density of MLCC has been increased one million times by reducing thickness of dielectric layer down to 1 micron in 40 years. However, very serious problem that restricts the capacitance density of MLCC has come up in these 5 years. The problem is known as the size effect barium titanate where dielectric constant of barium titanate somehow decreases with the size of grains sin ceramics. Some experimental results on energy storage property and dielectric response of solid ionic capacitors will be presented.

10:30 AM

(EMA-S11-002-2016) Non-Stoichiometry in Bismuth Perovskites (Invited)

D. Cann*[1]; N. Prasertpalichatr[1]; N. Kumar[1]; W. Schmidt[1]; 1. Oregon State Univ, USA

The defect chemistry is of paramount importance for many applications because, ultimately, point defects often have a profound influence on phenomena such as piezoelectric fatigue, reliability, breakdown, and leakage current. Perovskite materials with Bi^{3+} on the A-site have been the focus of great technical interest, and while there has been progress in improving the materials properties of these new materials the underlying defect chemistry has remained relatively unexplored. This presentation will highlight research on two Bi-perovskite systems where non-stoichiometry has a significant impact on performance. First, the influence of A-site stoichiometry in the Pb-free piezoelectric material $(Bi_{0.5}Na_{0.5})TiO_3$-$BaTiO_3$ will be discussed. Variations in the Na/Bi ratio can lead to hardening behavior with an increase in mechanical Q, or low resistivities (ρ~1000 Ω-cm) along with impedance spectra that indicates ionic conduction. Next, the impact of non-stoichiometry in BZT-BT dielectric ceramics will be discussed. While pure BT exhibits extrinsic p-type conduction, it is reported that BT-BZT ceramics exhibit intrinsic n-type conduction using atmosphere dependent conductivity measurements. This suggests the possibility of unintended donor doping, which may also be linked to the improvement in resistivity in BT-BZT ceramics as compared to pure BT. Overall, these results show that the defect chemistry of Bi-perovskites has a profound impact.

11:00 AM

(EMA-S11-003-2016) Giant Energy Density and Improved Discharge Efficiency of Solution-Processed Polymer Nanocomposites for Dielectric Energy Storage (Invited)

Y. Shen*[1]; 1. Tsinghua University, China

Dielectric materials with high dielectric permittivity, high breakdown strength, low dielectric loss, and hence high electric energy density are of critical importance in a number of the modern electronics and electrical power systems. A main bottleneck limiting the energy density of nanocomposites is the adverse coupling of dielectric permittivity and breakdown strength. In this talk, we present and demonstrate a totally new approach towards concurrent enhancement of dielectric permittivity and high breakdown strength. TiO_2 nanofibers embedded with $BaTiO_3$ nanoparticles (TiO_2@$BaTiO_3$ nanofibers) are prepared via electrospinning and then fused with PVDF-HFP into polymer nanocomposite films. Inside the TiO_2@$BaTiO_3$ nanofibers, **atomic scale engineering of the hierarchical interfaces between TiO_2 and $BaTiO_3$ gives rise to much increased dielectric permittivity** while the large aspect ratio and partial orientation of TiO_2@$BaTiO_3$ nanofibers render the nanocomposites with improved breakdown strength. These favorable features combined result in **an ultrahigh energy density of ~ 31.2 J/cm^3** with a dielectric breakdown strength at 800 kV/mm, which is enhanced by **>80% over that for the pristine PVDF-HFP** and is **1675% greater than the energy density of biaxially oriented polypropylenes (BOPP), the bench mark polymer dielectrics of current use.**

11:30 AM

(EMA-S11-004-2016) High Temperature Dielectrics: an assessment of temperature-stable relaxors (Invited)

A. Zeb[1]; M. Ward[1]; D. Hall[2]; D. C. Sinclair[2]; I. MacLaren[3]; S. U. Jan[1]; S. J. Milne*[1]; 1. University of Leeds, United Kingdom; 2. University of Sheffield, United Kingdom; 3. University of Glasgow, United Kingdom

The search for new dielectric ceramics with high charge storage density and operating temperatures higher than commercial X7R-X9R materials is motivated by emerging applications in power electronics and control and sensing electronic systems for deployment in harsh environments. The demand is for robust components with stable performance to >>200°C. Dielectric ceramics in the system (1-x)(Ba,Ca)TiO_3-x$Bi(Mg_{0.5}Ti_{0.5})O_3$ [BCT-BMT] show promise in this regard. With increasing BMT content, a change in relative permittivity-temperature response occurs, from that of a normal relaxor with broad ε_r(T) peak, to a temperature-stable response with a wide ε_r(T) plateau. Optimum compositions contain ~ 50 mol% BMT, for which ε_{rmid} ~ 1000 ± 15 % across the temperature range ≤ 100 °C to 400/500 °C, with low dielectric loss tangent and high electrical resistivity. Compositional modifications to BCT-BMT, along with demonstrations of novel solid solution systems which achieve the standard specification of X-R type stability in ε_r from -55 to ≥ 300°C, and high to moderate values of

ε_{rmid} will also be presented. Structural reasons for the development of temperature-stable properties in selected materials will be discussed with reference to results of electrochemical impedance spectroscopy and (scanning) transmission electron microscopy.

12:00 PM

(EMA-S11-005-2016) Optimising core-shell microstructures using finite element modelling (Invited)

J. S. Dean*[1]; P. Y. Foeller[1]; I. M. Reaney[1]; D. C. Sinclair[1]; 1. University of Sheffield, United Kingdom

The volume fraction of core-shell regions of doped $BaTiO_3$ is crucial in obtaining the temperature coefficient of capacitances (TCCs) required for X7 and X8R multi-layer capacitors (MLCCs). Previous studies optimise the materials and microstructure needed to improve performance by combining experimental techniques such as transmission and scanning electron microscopy with fixed-frequency dielectric and impedance spectroscopy measurements. Given the sensitivity of the electrical properties of $BaTiO_3$ to low levels of dopants and contaminants, the ratio required will vary for different dopants, dopant couples and processing conditions. This procedure requires a large amount of time, effort and cost to identify the correct ratio for each system. Using an in-house developed finite element package (ElCer) solving Maxwell's equations in space and time, we present a new methodology to find the optimised ratio. This does not rely on models based on the brick-work layer or effective medium theory and can simulate the electrical response of realistic microstructures including features such as multiple grain shapes and sizes, grain boundaries, core-shell, contacts, and pores. By combining this method with experimental data, we predict the optimised volume ratio of core-shell for doped $BaTiO_3$ for improved TCC. Other features are also discussed such as roughness and porosity, highlighting the significance these play on TCC.

Student Speaking Competition Presentations I

Room: Coral A

Session Chairs: Jon Ihlefeld, Sandia National Laboratories; Brian Donovan, University of Virginia

12:50 PM

(EMA-SSC-001-2016) Probing Ionic Transport Mechanisms in Y-doped Barium Zirconate

J. Ding*[2]; E. Strelcov[2]; G. Veith[2]; C. Bridges[2]; J. Balachandran[2]; P. Ganesh[2]; S. Kalinin[2]; N. Bassiri-Gharb[1]; R. Unocic[2]; 1. Georgia Institute of Technology, USA; 2. Oak Ridge National Lab, USA

Barium zirconate (BZO) has been widely studied as electrolyte in proton-conducting solid oxide fuel cells (PT-SOFCs), due to its high proton conductivity and excellent chemical stability at intermediate temperatures (500-700 °C). Previous work has concentrated on the conduction mechanisms and ionic transport in BZO; however, the role of defects, such as yttrium dopant and oxygen vacancies, on the proton transport, especially on the nanoscale and atomic scale, is still under debate. Here, we explore the ionic dynamics in pure and yttrium doped BZO (Y-BZO) films using energy discovery platforms, a synergy of nanofabricated device and in-situ characterization methods under controllable external stimuli. Through time resolved Kelvin probe force microscopy (tr-KPFM), the local potential in both the space and time domains is obtained, enabling analysis of local proton transport dynamics on the 10-2 to 102 s scale as a function of temperature and Y concentration. The activation energy increases with increasing dopant concentration, which is explained by the lattice distortion effect from the dopant clustering via density functional theory. Simulation of ion transport through finite element method allows for creation of a physical model consistent with observed phenomena, and establishing of the dynamic characteristics of the process, including proton mobility and diffusivity.

1:05 PM

(EMA-SSC-002-2016) Direct observation of local chemistry and B-site cation displacements in the relaxor ferroelectric PMN-PT

M. J. Cabral*[1]; X. Sang[1]; E. C. Dickey[1]; J. LeBeau[1]; 1. North Carolina State University, USA

Using aberration-corrected scanning transmission electron microscopy (AC-STEM) combined with advanced imaging methods, we directly observe atom column specific, picometer scale displacements in solid solutions of the relaxor $Pb(Mg_{1/3}Nb_{2/3})O_3$-$PbTiO_3$ (PMN-PT). These complex, thermodynamically frustrated materials possess local inhomogeneities due to cation composition at the B-site which give rise to local strain and polarization on the nanometer scale resulting in "polar nanoregions". While prior experiments have utilized x-ray and neutron diffuse scattering in order to understand the behavior of "polar nanoregions", they provide a statistical average over a large sampling volume and, to date, do not provide correlations with local chemistry. With the development of revolving STEM (RevSTEM) we are now able to remove sample drift from STEM images, enabling picometer scale resolution. In this talk we will present an investigation of atomic level displacements in PMN-PT where the A-site contains Pb and the B-site contains Mg, Nb, or Ti. These displacements can be related to the charge variation of the various B-site cations. Further, we will relate these displacements to local chemistry in the structure with the application of atomic resolution energy dispersive x-ray spectroscopy (EDS).

1:20 PM

(EMA-SSC-003-2016) Structure of the Equilibrated Ni(111)-YSZ(111) Solid-Solid Interface

H. Nahor*[1]; W. D. Kaplan[1]; 1. Technion - Israel Institute of Technology, Israel

The stability of metal films on oxide surfaces is important for the performance of devices such as solid oxide fuel cells (SOFCs) and thermal barrier coatings (TBCs). Ni-YSZ serves as an anode material in SOFCs. During SOFC operation, the metal-ceramic interface is subjected to high temperatures and a reducing atmosphere, which can lead to coarsening of the Ni nanoparticles, which decreases the number of three-phase boundaries. The three-phase boundaries (Ni/YSZ/fuel-gas) are essential for catalytic activity which controls the electrical properties. A better understanding of the equilibrated Ni-YSZ interfacial structure and energy can lead to improved adhesion and long-term stability of SOFCs. In this work, solid-state dewetting of continuous Ni films deposited on the (111) surface of yttrium stabilized zirconia (YSZ) was used to produce equilibrated Ni particles, and the solid-solid interface structure was determined using aberration corrected transmission electron microscopy (TEM). The ~150nm thick Ni films were annealed at 1350°C (0.94 T_m) in Ar+H_2 (99.9999%) at a partial pressure of oxygen of 10^{-20} atm for 6 hours. TEM of equilibrated particles was conducted to analyze the structure at the interface, and revealed that despite the 31% lattice mismatch between Ni and YSZ, the interface is semi-coherent and a two dimensional network of misfit dislocations was identified.

1:35 PM

(EMA-SSC-004-2016) Effect of Top Electrode Material on Radiation-Induced Degradation of Ferroelectric Thin Films

S. Brewer*[1]; M. Paul[3]; K. Fisher[4]; J. Guerrier[2]; J. L. Jones[2]; R. Rudy[5]; R. G. Polcawich[5]; E. Glaser[6]; C. Cress[6]; N. Bassiri-Gharb[1]; 1. Georgia Institute of Technology, USA; 2. North Carolina State University, USA; 3. Woodward Academy, USA; 4. Riverwood International Charter School, USA; 5. US Army Research Laboratory, USA; 6. Naval Research Laboratory, USA

The large dielectric, piezoelectric and pyroelectric response of ferroelectric thin films has drawn a substantial interest over recent years for use in millimeter-scale robotics, in which the ferroelectric material fulfills multiple functionalities such as sensing, actuation, energy harvesting, mechanical logic, etc. Of specific interest are applications in dangerous or difficult-to-reach locations such as

nuclear power plants and aerospace. This work addresses the mechanisms of radiation interaction with ferroelectric $Pb[Zr_{0.52}Ti_{0.48}]O_3$ thin films deposited on platinized silicon wafers, with IrO_2 or Pt top electrodes. All samples were irradiated with 2.5 Mrad (Si), using a ^{60}Co gamma radiation and the dielectric and electromechanical response were characterized before and after irradiation. Samples with IrO_2 electrodes generally showed less degradation of dielectric properties compared to samples with Pt electrodes. Pinching in polarization-electric field hysteresis loops and formation of secondary peaks in C-V curves were observed only in samples with metallic top electrodes. The electromechanical response of the samples was substantially more stable for the oxide electrodes than samples with Pt top electrode. The quantitative results will be discussed in terms of ion-blocking or ion-conducting electrode materials and possible approaches for "self-healing," radiation-hard devices.

S1. Multiferroic Materials and Multilayer Ferroic Heterostructures: Properties and Applications

Theory, Modeling, Materials Design I

Room: Coral A

Session Chairs: Burc Misirlioglu, Sabanci University; Daniel Shreiber, US Army Research Laboratory

2:00 PM

(EMA-S1-006-2016) Improper magnetic ferroelectricity of purely electronic nature in cycloidal spiral $CaMn_7O_{12}$ (Invited)

A. M. Rappe*[1]; J. Lim[1]; D. Saldana-Greco[1]; 1. University of Pennsylvania, USA

In improper magnetic ferroelectrics (FEs), polarization (*P*) is induced by noncentrosymmetric spiral magnetism. These materials have received much attention due to strong magnetoelectric effect and technologically relevant applications as spin-driven electronics. In charge-ordered quadruple perovskite system $CaMn_7O_{12}$, cycloidal magnetic order breaks inversion symmetry, generating a very large magnetically coupled FE *P* experimentally measured to be 2870 $\mu C/m^2$. We use first-principles calculations to study the microscopic origin of the *P*. When the ions are held fixed in the inversion symmetry geometry, the Berry's phase computed pure electronic *P* is significant, determined by Mn spin canting and *p-d* orbital mixing. The existing mechanisms of FE in $CaMn_7O_{12}$ have not provided a unified explanation for both the nonionic nature of the *P* and its direction perpendicular to the spin rotation plane. We employ the generalized spin-current model with octahedral rotation as a variable to resolve these issues. Furthermore, we provide an orbital-resolved understading of the spin-dependent local charge density redistribution and nonuniform orbital ordering. Ultimately, our results suggest that persistent electronic *P* activated solely by helical spin order in inversion-symmetric ionic crystal lattices could realize ultrafast magnetoelectric effect in a single FE-magnetic domain.

2:30 PM

(EMA-S1-007-2016) Emergence of ferroelectricity in nanoscale antiferroelectrics (Invited)

B. Mani[1]; S. Lisenkov[1]; I. Ponomareva*[1]; 1. University of South Florida, USA

Ferroelectrics and antiferroelectrics appear to have just the opposite behavior upon scaling down. Below a critical thickness of just a few nanometers the ferroelectric phase breaks into nanodomains that mimic electric properties of antiferroelectrics very closely. On the other hand, antiferroelectric thin films were found to transition from the antiferroelectric behavior to a ferroelectric one under certain growth conditions. At present the origin of such transition is controversial. We use first-principles simulations to reveal an overlooked surface effect that could be responsible for the emergence of ferroelectricity in nanoscale antiferroelectrics. The intrinsic surface effect stabilizes the ferroelectric phase by removing energetically costly short-range interactions between "head-to-tail" dipoles. We will present computational data on the size-driven onset of ferroelectricity in a variety of nanostructures made of antiferroelectric $PbZrO_3$ and discuss the role of size and electrical boundary conditions on the nanoscale phases in this material. The work is supported by the US Department of Energy, Office of Basic Energy Sciences, Division of Materials Sciences and Engineering under Grant No. DE-SC0005245.

3:00 PM

(EMA-S1-008-2016) Tailoring ferroelectricity for energy efficient field effect transistors (Invited)

B. Misirlioglu*[1]; P. Alpay[2]; 1. Sabanci University, Turkey; 2. University of Connecticut, USA

Ferroelectric Field Effect Transistors (FeFETs) entered the agenda of the semiconductor device groups following the first papers in mid 1990s. Other than controlling the dielectric response of the ferroelectric to obtain transistor action in a channel, presence of remnant polarization is also an attractive property for solid-state non-volatile memories. Termination of the ferroelectric polarization at the ferroelectric-semiconductor interface leads to additional band bending in both the semiconductor and the ferroelectric and can be tailored for effective control of carriers at the interface in FETs. In this study, we present theoretical results on the effect of semiconductor electrodes on the functional response of ferroelectric layers and superlattices. Stability limit of the polar phase is explored, revealing the importance of the boundary conditions on device functionality and possible integration efforts of well-known ferroelectrics. Electrical domains can be tailored, contrary to the desire to utilize a switchable single domain state, for power efficient binary logic FETs.This is followed by comments on the limit of use of such layers for the much desired "non-volatile memory" function of the gate such as tailoring the thickness effect of the ferroelectric to minimize domain density keeping in mind some recent results in ferroelectric-paraelectric superlattice structures.

4:00 PM

(EMA-S1-009-2016) Designing Novel Functionalities in Dielectric and Ferroelectric Materials - Compositionally-Graded Thin-Film Heterostructures (Invited)

L. W. Martin*[1]; 1. University of California, Berkeley, USA

We focus on recent advances in understanding of how strain can be controlled to elicit new types of responses in ferroelectrics beyond what can be achieved with traditional lattice mismatch effects. In particualr, we focus on deterministic production of large strain gradients ($>10^{-5}$ m^{-1}) via compositional grading. We highlight work on compositionally-graded $PbZr_{1-x}Ti_xO_3$ and $Ba_{1-x}Sr_xTiO_3$ where careful control of lattice mismatch and chemistry combine to produce large strain gradients, exotic properties, and new approaches to independently control traditionally coupled properties. We will report on the evolution of the crystal and domain structure as a function of the end-members of the compositional gradient, thickness of the film, and substrate. Advanced band-excitation piezoresponse force microscopy, switching spectroscopy, and non-linearity studies have also been applied. Such studies reveal unexpected crystal and domain structures and exotic low- and high-field responses including nearly temperature-independent dielectric permittivity from 25-500°C, labile ferroelastic domain walls, and much more. The presentation will highlight the role new types of epitaxy strain in driving the development of understanding of complex materials with numerous applications.

4:30 PM

(EMA-S1-010-2016) Miscibility Gap Closure, Interface, Morphology, and Phase Microstructureof 3D Li_xFePO_4 Nanoparticles from Surface Wetting and Coherency Strain (Invited)

M. Welland[1]; D. Karpeyev[2]; D. O'Connor[3]; O. Heinonen*[1]; 1. Argonne National Laboratory, USA; 2. University of Chicago, USA; 3. National Institute of Standards and Technology, USA

Li_xFePO_4 is used as an electrode material. However, electrodes made from bulk Li_xFePO_4 suffer from phase separation into lithiated and de-lithiated phases, which leads to slow charge and discharge rates. On the other hand, nanoparticles have been shown to have fast charge and discharge rates. It has been proposed previously that the miscibility gap that causes phase separation in bulk systems in suppressed in nanoparticles. Here, we present results of a study of the mesoscopic effects which modify phase-segregation in Li_xFePO_4 nanoparticles using a multiphysics phase-field model. We simulate 3D spherical particles of radii from 3 nm to 40 nm and examine the equilibrium microstructure and voltage profiles as a they depend on size and overall lithiation. The model includes anisotropic, concentration-dependent elastic moduli, misfit strain, and facet dependent surface wetting within a Cahn-Hilliard formulation. We find that the miscibility gap vanishes for particles of radius approximately 5 nm, and the solubility limits change with overall particle lithiation. Surface wetting stabilizes minority phases by aligning them with energetically beneficial facets. The equilibrium voltage profile is modified by these effects in magnitude, and the length and slope of the voltage plateau during two-phase coexistence.

5:00 PM

(EMA-S1-011-2016) Cation Substituted Y- Phase Hexagonal Ferrite Materials with Improved High-frequency Permeability Values for Magnetodielctric Antenna Applications

M. D. Hill*[1]; S. Polisetty[1]; 1. Trans-Tech Inc., USA

Magnetodielectric antennas have the advantage over conventional dielectric antennas in that they show improved efficiencies and greater bandwidths. Unfortunately, these materials are limited to applications below 500 MHz due to a lack of available low-loss ferrite materials with a permeability values greater than 2 at frequencies near 1 GHz. Ba2Co2Fe12O22 and Sr2Co2Fe12O22 (Y-Phase Hexagonal Ferrites) exhibit resonant frequencies well above 1 GHz but are limited for antenna applications due to their modest magnetic permeability values. However, by select cation substitutions, permeability values > 6 may be obtained with acceptable magnetic losses in the 500 MHz- 1 GHz range. The effect of single and coupled substitutions has been explored, with several materials optimized for applications in the 700 MHz - 1 GHz range.

5:15 PM

(EMA-S1-012-2016) Structural and Magnetic Properties of Nickel Zinc Ferrite Thick Films via Tape Casting

T. Kittel*[1]; G. Naderi[1]; J. Schwartz[1]; 1. North Carolina State University, USA

Nickel zinc ferrite ($Ni_{0.5}Zn_{0.5}Fe_2O_4$ (NZF)) is an interesting material for high-frequency signal and power electronic applications due to its high electrical resistivity, low coercivity, and high magnetization saturation. Here, we present a method for creating NZF thick films utilizing a tape casting system. The slurry, composed of NZF powder, plasticizer, binder, and dispersant, allows for the creation of flexible green tape. In this study, different processing conditions are examined including sintering temperature, heating rate, and total sintering time. Scanning electron microscopy is used to study the changes in density, thickness, microstructure, and grain size with processing conditions. Densification is quantified using image analysis for porosity area fraction. Variations in crystallographic texture are studied using X-Ray Diffraction. Magnetization behavior is characterized using vibrating superconducting quantum interference device magnetometer. Relationships between magnetization behavior, microstructure, and processing conditions were found. For instance, results show that varying sintering time causes microstructural changes, in particular variations in crystallographic texture and density, while increased sintering temperature yields increased saturation magnetization. Approaches to creating thicker films via stacking of tape cast films is also explored.

S2. Functional Materials: Synthesis Science, Properties, and Integration

Functional Materials : Advanced Synthesis and Structure-Property Relationships

Room: Mediterranean A
Session Chairs: Elizabeth Paisley, Sandia National Laboratories; Daniel Potrepka, U.S. Army Research Laboratory

2:00 PM

(EMA-S2-009-2016) Sputtering of complex oxides with *in situ* Reflection High-Energy Electron Diffraction (Invited)

J. P. Podkaminer*[1]; J. Patzner[1]; D. Lee[1]; B. Davidson[2]; C. Eom[1]; 1. University of Wisconsin-Madison, USA; 2. Temple University, USA

As novel phenomena at materials interfaces draws increasing attention, it is vital to gain atomic control of material growth to further understand and engineer their properties. Currently, Reflection High-Energy Electron Diffraction (RHEED) is the most commonly used *in situ* diagnostic tool for both molecular beam epitaxy and pulsed laser deposition growth techniques, where it is used to observe layer-by-layer growth and control it at the unit cell level. Sputtering is a common, inexpensive, and industrially viable growth technique for many complex oxide materials but lacks the powerful *in situ* analysis techniques used by pulsed laser deposition and molecular beam epitaxy. Here we demonstrate the integration of RHEED into the sputtering environment as an *in situ* tool during the growth of oxide materials. We will present on the challenges associated with performing RHEED analysis during sputter deposition and provide a practical and effective approach for mitigating these challenges. Experimentally we observe strong RHEED specular spot oscillations during oxide growth for many tens of unit cells, demonstrating the possibility for precise layer-by-layer control of complex oxides during sputter deposition. We apply our approach to the growth of several novel epitaxial heterostructures to demonstrate precise unit cell and interface control.

2:30 PM

(EMA-S2-010-2016) Thin Film growth of Entropy-Stabilized Oxides using Pulsed Laser Deposition

C. M. Rost*[1]; G. Ryu[2]; J. Maria[1]; 1. North Carolina State University, USA; 2. Changwon National University, Korea (the Democratic People's Republic of)

We continue investigations of entropy stabilized oxides (ESOs); a novel class of multicomponent material characterized by high configurational disorder of the systemic cation species while exhibiting an unusual degree of structural perfection. Currently, we have catalogued seven unique compositions. The simplest is of rock-salt structure, containing equal amounts of Mg, Co, Cu, Ni and Zn randomly distributed among the cation sublattice, and oxygen on the anion sublattice. Five additional compositions resemble spinel and one system resembles a LiCoO2–like structure. While the bulk ceramics are synthesized through solid state sintering above 875°C in air, thin films are grown via pulsed laser deposition (PLD) with a controllable variability between polycrystalline and epitaxial structures. PLD also provides sufficient energy to overcome kinetic barriers due to temperature limitations of bulk synthesis, making additional ESOs accessible; including, but not limited to, those compositions that do not form a solid solution under normal synthesis conditions up to 1600°C and compositions with more than

five different cation species. In this talk, additional compositions- those only stable in thin film form- are presented, and we discuss the structure morphology of these films in terms of growth parameters. Collectively, ESOs pave the way for novel materials development and structure-property relationships.

2:45 PM

(EMA-S2-011-2016) Epitaxial stabilization of metastable phases during atomic layer deposition and post-deposition annealing

J. E. Spanier*[1]; 1. Drexel University, USA

We report on the substrate-dependent structural phase evolution of pure and Fe-doped bismuth oxide (Bi-O and Bi-Fe-O) thin films grown by atomic layer deposition (ALD). *In situ* X-ray diffraction was used to map the evolution of phase composition and orientational growth of the oxides during the gradual crystallization of the films from the amorphous state on single-crystalline substrates. The formation of (001)-oriented $Bi_2O_{2.3}$ was observed at temperatures as low as 300ºC on $SrTiO_3$(001), with a gradual transformation into a thermodynamically stable Bi_2O_3. A similar crystallization of Fe-doped Bi_2O_3 on $ZrO_2(Y_2O_3)$(111) leads to the formation of (111)-oriented δ-Bi_2O_3 above 400ºC instead of the sillenite phase. We thus demonstrate that epitaxial stabilization of the metastable phases can take place during ALD of oxides as well as post-deposition annealing. *In situ* crystallization of the amorphous Bi-Fe-O films revealed the evolution of oxide phases in the film with the sillenite composition. These results are important for the design of annealing procedures to obtain phase-pure epitaxial $BiFeO_3$ thin films from the amorphous stoichiometric Bi-Fe-O grown by ALD. Work supported by ONR under N00014-15-11-2170 and in part by the NSF under DMR 1124696.

3:00 PM

(EMA-S2-012-2016) Selective Area Deposition of Oxide Thin Films on Gallium Nitride Surfaces (Invited)

M. D. Losego*[1]; E. A. Paisley[2]; D. Yin[1]; H. Craft[3]; R. Collazo[3]; Z. Sitar[3]; J. Maria[3]; 1. Georgia Institute of Technology, USA; 2. Sandia National Laboratories, USA; 3. North Carolina State University, USA

Lateral patterning of thin films is an essential step in the fabrication of microelectronic devices. Traditional lithographic patterning of lateral device structures is time consuming and expensive and can lower material quality and pattern registry. Deposition processes that lead to self-directed lateral patterning during film growth are highly sought to lower costs and improve device performance. Selective deposition of III-V semiconductors via chemical vapor deposition approaches are well known and employed regularly in the microelectronics industry. Here we discuss a new form of selective deposition for laterally patterned oxide thin films on gallium nitride (GaN) surfaces. Chlorination of the GaN surface via wet chemical processing is found effective to disrupt Mg adsorption and selectively prevent molecular beam epitaxy (MBE) growth of MgO films. MgO films grown on neighboring, non-chlorinated surfaces are epitaxial with a (111) MgO || (0001) GaN crystallographic relationship. Better than 3 μm lateral resolution for the selective area growth of MgO on GaN is demonstrated. The surface chemistry of this selective deposition process has been explored with XPS. Potential mechanisms will be discussed in the context of finding a more generalized route to selective growth of oxide films on GaN surfaces.

4:00 PM

(EMA-S2-013-2016) First-principles guidance to polymorph selective epitaxial growth of MO_2 dioxides: informing epitaxial growth of metastable polymorphs (Invited)

P. Salvador*[1]; Z. Xu[1]; J. Wittkamper[1]; G. Rohrer[1]; J. R. Kitchin[1]; 1. Carnegie Mellon University, USA

Functional properties of dioxide MO_2 polymorphs are strongly dependent on the *M* cation and the crystal structure. Epitaxial stabilization can be used to direct the synthesis of specific polymorphs, including new and metastable materials. We have used combinatorial substrate epitaxy (*CSE*)- depositing films on polished surfaces of polycrystals and determining the local epitaxy using electron back-scatter diffraction- to understand the preferred epitaxy and polymorph formation of TiO_2, SnO_2, and RuO_2. This high-throughput method is used to direct first principles computations (density functional theory) to understand epitaxial growth of (1) anatase and rutile TiO_2 on *AE*TiO_3 perovskite surfaces (*AE* = Ca, Sr, and Ba) and (2) columbite (α-PbO_2) and rutile TiO_2, SnO_2, and RuO_2 on columbite-structured substrates. DFT is used to calculate either (1) total energies of thin epitaxial layers or (2) the relevant energy terms included in continuum models: epitaxial interface energies, surface energies, and substrate-induced strain energies of the film. The strengths and weaknesses of using standard DFT to inform synthesis of new materials will be discussed, as will the relevance of the two approaches. Finally, the combination of high-throughput epitaxy and computational predictions of phase stabilities will be discussed for predictive synthesis.

4:30 PM

(EMA-S2-014-2016) In-situ Synchrotron X-ray and Density Functional Theory Studies on the Growth of $LaGaO_3$/ $SrTiO_3$ (001) Epitaxial Thin Films

P. Zapol*[1]; J. A. Eastman[1]; M. Highland[1]; A. Ruth[2]; D. Fong[1]; G. Ju[1]; P. Baldo[1]; C. Thompson[4]; H. Zhou[3]; P. Fuoss[1]; 1. Argonne Nat Lab, USA; 2. University of Notre Dame, USA; 3. Argonne National Lab, USA; 4. Northern Illinois University, USA

The $LaGaO_3$ / $SrTiO_3$ (001) heterostructure contains polar interfaces and exhibits 2D electron gas behavior, but it has been much less studied than the similar $LaAlO_3$ / $SrTiO_3$ (001) system. Here we aim to understand the effects of polarity and interfacial charge on $LaGaO_3$ growth behavior. Periodic DFT calculations of the films with different thicknesses and layer sequence are performed to elucidate structure and properties of the films as a function of their thickness and termination. In particular, energetics of layer switching was examined. Understanding of growth behavior requires the ability to synthesize materials with sub-monolayer control while characterizing their structure at the atomic level in real time. Films are grown using a magnetron sputter deposition system built for in-situ synchrotron X-ray studies at Sector 12-ID-D of the Advanced Photon Source. The $LaGaO_3$ films were deposited one half-unit cell of thickness at a time using two separate cation sources on TiO_2-terminated $SrTiO_3$ (001) to enable precise control of their composition and termination. Layer structural arrangements were examined depending on the sequence of the deposited La and Ga species and synthesis parameters. We will compare the experimental results with those from the calculations. Calculated electronic properties are also discussed.

4:45 PM

(EMA-S2-015-2016) Effects of phase and texture on the thermal conductivity of chemical solution deposited strontium niobate thin films

K. E. Meyer*[1]; B. F. Donovan[1]; J. Gaskins[1]; J. Ihlefeld[2]; P. E. Hopkins[1]; 1. University of Virginia, USA; 2. Sandia National Laboratories, USA

We have measured the cross-plane thermal conductivity of strontium niobate thin films via time-domain thermoreflectance. Thin films were deposited onto (0001)-oriented sapphire substrates via chemical solution deposition. By varying crystallization temperature and oxygen atmosphere, we vary both phase and texture across the film series. Crystallization in oxygen at 1000°C yielded phase pure, highly (010)-oriented $Sr_2Nb_2O_7$ films, whereas crystallizing at 900°C in a low oxygen atmosphere formed a randomly oriented, polycrystalline perovskite $SrNbO_{3-\delta}$. We observe a reduction in thermal conductivity in the layered $Sr_2Nb_2O_7$ films as compared to the polycrystalline $SrNbO_{3-\delta}$; this suggests a more dominant phonon scattering mechanism due to the weak interlayer bonding along the *b*-axis in the $Sr_2Nb_2O_7$ structure. This shows that atomic-scale

impurities in lattices of naturally layered crystals can increase the thermal conductivity, contrary to the typically observed reduction in phonon transport in isotropic crystals due to phonon-defect scattering.

5:00 PM

(EMA-S2-016-2016) Ferroelectric Switching Dynamics as a Function of Film Strain

L. Ye*[1]; R. Cordier[1]; V. Garcia[2]; M. Bibes[2]; R. Ramesh[3]; S. Salahuddin[3]; B. Huey[1]; 1. University of Connecticut, USA; 2. Unité Mixte de Physique CNRS/Thales, France; 3. University of California, Berkeley, USA

Ferroelectrics are essential materials in a wide range of applications. Domain configurations and switching dynamics have drawn particular attention due to their correlations to switching speed, switching energy, and domain stability. This work, employing Out-of-Plane (OP) and In-Plane (IP) Piezoresponse Force Microscopy (PFM), reveals switching kinetics of domain walls in PZT and $BiFeO_3$ ferroelectric thin films for a variety of distinct strain conditions. In particular, domain configurations for $BiFeO_3$ films with varying film thickness from 20 nm to 4.6 nm are considered for a single substrate. Due to lattice mismatch the film thickness couples to strain, which is directly shown here to influence the balance between rhombohedral and tetragonal phases during switching. Furthermore, the dynamics of domain polarization are investigated for micro and nano scale islands of PZT. These geometrically strain-relieved structures allow direct investigations of the influence of strain on switching dynamics including nucleation and growth statistics. Such studies are crucial towards optimizing the performance of future ferroelectric and multiferroic devices.

5:15 PM

(EMA-S2-017-2016) Intrinsic Electrocaloric Behavior of Perovskite Oxides

H. Khassaf*[1]; P. Alpay[1]; Z. Kutnjak[2]; 1. University of Connecticut, USA; 2. Jozef Stefan Institute, Slovenia

The electrothermal properties of the perovskite oxides (1− x)•P-b($Mg_{l/3}Nb_{2/3}$)O_3− x• $PbTiO_3$ (PMN–xPT), $BaTiO_3$ (BT), and $PbTiO_3$ (PT) are computed near the temperatures of their ferroelectric phase transitions and over a wide range of temperature. The computations are performed using a nonlinear phenomenological thermodynamic model considering the cjange of applied electric field and temperature. PMN−0.1PT and PMN−0.35PT possess higher adiabatic temperature change compare to their counterparts BT and PT for relatively low temperature of T=25, 150, and 275 °C. At higher temperature of 400 °C, PMN−PT has higher adiabatic temperature change at ΔE=400 kV/cm where as for ΔE=50 kV/cm, PT delivers the highest magnitude. Our calculations suggest that for relatively low working temperatures, electrocaloric behavior of PMN−PT is dominant over its barium and lead based counterparts.

S3. Use of thermal energy for electrical power generation and refrigeration: Fundamental science, materials development and devices

Materials and Films

Room: Mediterranean B/C

Session Chair: Edward Gorzkowski, Naval Research Lab

2:00 PM

(EMA-S3-007-2016) Advanced Materials for Efficient Thermoelectric Power Generation (Invited)

J. Fleurial*[1]; S. Bux[1]; S. Firdosy[1]; T. Caillat[1]; 1. Jet Propulsion Laboratory, USA

Thermoelectric power sources have consistently demonstrated their extraordinary reliability and longevity for deep space missions as well as terrestrial applications where unattended operation in remote locations is required. They are static systems, tolerant of extreme environments, with a high degree of redundancy, no electromagnetic interferences, with well documented "graceful degradation" characteristics and a high level of scalability. The development of new, more efficient materials and devices is the key to improving existing space power technology and expanding into efficient, cost-effective systems using high grade heat sources, generated through fossil fuel combustion or as a waste exhaust stream. We present an overview of NASA-funded collaborative research efforts to identify advanced bulk thermoelectric materials, capable of quadrupling current state-of-practice average ZT values over the available operating temperature range of 1275 K to 475 K, through the exploration of structurally complex compounds allowing for a wide range of chemical tuning and the possibility of forming stable nano- and micro-scale composites. Device-level experimental performance validation accomplished to date and plans for infusing the new technology into future thermoelectric power systems are discussed.

2:30 PM

(EMA-S3-008-2016) Thermoelectric characterization of sputtered Ca-Mg-Si films

M. Uehara*[1]; M. Kurokawa[1]; K. Akiyama[2]; T. Shimizu[1]; M. Matsushima[1]; H. Uchida[3]; Y. Kimura[1]; H. Funakubo[1]; 1. Tokyo Institute of Technology, Japan; 2. Kanagawa Indudtrial Technology Center, Japan; 3. Sophia University, Japan

For the mobile applications of thermoelectric power generator, such as automobile, thermoelectric materials consisting of non-toxic, lightweight, and abundant elements are highly required. We focused on materials in Ca-Mg-Si system as a candidate for *p*-type materials that are combined with *n*-type Mg_2Si. However, reports on thermoelectric properties in this ternary system have been limited. In the present study, we addressed fabrication of sputtered Ca-Mg-Si films with various compositions and systematically measurement of their electrical conductivity and the Seebeck coefficient. The compositions of films were controlled by the deposition temperature at 260-500 °C as well as the area ratio of the Ca and Si chips mounted on the Mg disk that was used as a sputtering target. Films consisting of the single phases of $CaSi_2$, CaSi and Ca_5Si_3 were obtained in Ca-Si binary system. Among these compounds, Ca_5Si_3 films showed better *p*-type conduction. On the other hand, crystalline phase was hardly detected for the films with Ca/(Ca+Mg)=0.3 - 0.7 except CaMgSi phase at Ca/(Ca+Mg)= 0.5 under the fixed Si/(Ca+Mg+Si)= 0.3 - 0.4. These films also show the *p*-type conduction. Moreover, amorphous phase with Ca/(Ca+Mg)=0.5 and Si/(Ca+Mg+Si)=0.5 showed the largest power factor with the Seebeck coefficient of +100 μV/K at 673K.

2:45 PM

(EMA-S3-009-2016) Crystalline coherence length and phonon-defect scattering effects on the thermal conductivity of MgO thin films

K. E. Meyer*[1]; R. Cheaito[1]; E. A. Paisley[2]; C. T. Shelton[3]; J. Maria[3]; J. Ihlefeld[2]; P. E. Hopkins[1]; 1. University of Virginia, USA; 2. Sandia National Laboratories, USA; 3. North Carolina State University, USA

We examine the dependence of thermal conductivity on crystal coherence length in MgO thin films. Sputter deposited films were prepared on (100) silicon and then annealed to vary the crystalline coherence, as characterized using x-ray diffraction line broadening. We find that the measured thermal conductivity of the MgO films varies proportionally with crystal coherence length. This crystalline coherence length is dictated by the microstructural length scales associated with crystalline defects, such as small angle tilt boundaries and dislocations, and our results demonstrate the role that phonon-defect scattering has on thermal conductivity of thin films. Furthermore, through comparisons to various analytical models for phonon conduction, we show that traditional semi-classical approaches to predicting phonon-defect scattering and resulting

thermal conductivity fail to properly account for varying crystalline coherence length effects that are driven by defects.

3:00 PM

(EMA-S3-010-2016) The effect of WSi2 content on the microstructure of Si-Ge thermoelectrics

E. Farghadany*[1]; J. Mackey[1]; F. Dynys[2]; A. Sehirlioglu[1]; 1. Case Western Reserve University, USA; 2. NASA Glenn Research Center, USA

Radioisotope Thermoelectric Generators have been used by NASA to power space probes mainly due to their reliability despite their low efficiency. Si/Ge alloys have been historically the material of choice. Introduction of silicides into Si/Ge is expected to increase the conversion efficiency. However, the properties depend on precipitate size and distribution. An n-type Si/Ge alloy with WSi2 precipitates of 5 and 0.8 vol% has been studied. Samples were processed via mechano-chemical alloying and Spark Plasma Sintering. Si/Ge ratio and dopant (P) concentration was kept at 80/20 and 2%, respectively. STEM and transmission kikuchi diffraction was employed. Sample with high silicide content showed a finer grain size distribution with the average grain size of 100 nm that increases to 1 μm with decreasing silicide content. Consistently the former sample contains precipitates of smaller size with a more homogenous distribution. Disorientation mapping showed that the silicide particles as small as 50 nm were still polycrystalline. Using EDS, elemental distribution was studied. P was found both in the precipitate and the matrix, with a higher concentration in silicide; critical to maximizing the power factor since the nominal P concentration is used to control electrical conductivity and assumed to all go into the matrix. The study includes the effects of oxygen present and its integration to the microstructure.

3:15 PM

(EMA-S3-011-2016) Thermal Conductivity of Amorphous Silicon Thin Films: Effects of Size and Elastic Modulus

J. L. Braun*[1]; M. Elahi[2]; J. Gaskins[1]; T. E. Beechem[3]; Z. C. Leseman[2]; H. Fujiwara[5]; S. King[4]; P. E. Hopkins[1]; 1. University of Virginia, USA; 2. University of New Mexico, USA; 3. Sandia National Laboratories, USA; 4. Intel Corporation, USA; 5. Gifu University, Japan

We investigate thickness-limited size effects on the thermal conductivity of amorphous silicon thin films ranging from 3 – 1636 nm grown via sputter deposition. While exhibiting a constant value up to ~100 nm, the thermal conductivity increases with film thickness thereafter. This trend is in stark contrast with previous thermal conductivity measurements of amorphous systems, which have shown thickness-independent thermal conductivities. The thickness dependence we demonstrate is ascribed to boundary scattering of long wavelength vibrations and an interplay between the energy transfer associated with propagating modes (propagons) and non-propagating modes (diffusons). A crossover from propagon to diffuson modes is deduced to occur at a frequency of ~1.8 THz via simple analytical arguments. We extend this study to an amorphous silicon system with various levels of hydrogenation. Fixing the sample thickness to 200 nm, we measure the thermal conductivity of a-Si:H films having different elatic moduli (measured with nanoindentation) to demonstrate that thermal conductivity increases with increasing elastic modulus. In both cases, the minimum thermal conductivity model fails to capture the trend observed.

Materials II

Room: Mediterranean B/C
Session Chair: Edward Gorzkowski, Naval Research Lab

4:00 PM

(EMA-S3-012-2016) Thermoelectric Materials, Efficiency, and Power (Invited)

Z. Ren*[1]; 1. University of Houston, USA

The past decade has witnessed significant advances in the field of thermoelectric materials thanks to extensive research along new pathways to enhance properties, in particular nanostructuring bulk materials to largely reduce the thermal conductivity, which has resulted in high peak thermoelectric figure of merit (ZT). Achieving high peak ZT has been the goal of the thermoelectric community. Is high peak ZT good enough? Does a high peak ZT necessary translated into a high efficiency? How about the engineering $(ZT)_{eng}$? In this talk, I will demonstrate how a high peak ZT cannot warrantee a high efficiency, and how the $(ZT)_{eng}$ should be seen as the most relevant parameter. I will also demonstrate how a high conversion efficiency does not warrantee high output power, but the high engineering power factor $(PF)_{eng}$ does, and this is what matters most for thermoelectric power generators. Finally I will also discuss how the reduction of thermal conductivity is not without limitation when practical devices are to be built due to the limited mechanical properties of the thermoelectric materials, contacts, and boding materials.

4:30 PM

(EMA-S3-013-2016) Filled $Nd_zFe_xCo_{4-x}Sb_{12-y}Ge_y$ skutterudites: processing and thermoelectric properties

J. Mackey*[1]; A. Sehirlioglu[1]; F. Dynys[2]; 1. Case Western Reserve University, USA; 2. NASA Glenn Research Center, USA

Skutterudites have proven to be a useful thermoelectric system as a result of their enhanced figure of merit (ZT>1), cheap material cost, favorable mechanical properties, and good thermal stability. The majority of skutterudite interest in recent years has been focused on binary skutterudites like $CoSb_3$. Binary skutterudites are often double and triple filled, with a range of elements from the lanthanide series, in order to reduce the lattice component of thermal conductivity. Ternary and quaternary skutterudites, such as $Co_4Ge_6Se_6$ or $Ni_4Sb_8Sn_4$, provide additional paths to tune the electronic structure. The thermal conductivity can further be improved in these complex skutterudites by the introduction of fillers. The $Nd_zFe_xCo_{4-x}Sb_{12-y}Ge_y$ system has been investigated as a p-type thermoelectric material, and is stable up to 600°C. The influence of Fe and Ge content, along with filler Nd, was investigated on thermoelectric transport properties. In addition to the chemical influence on properties, some processing details of the system will also be addressed.

4:45 PM

(EMA-S3-014-2016) Phonon and electron transports on the twin boundary in $CaTiO_3$

S. Funahashi*[1]; T. Nakamura[2]; A. Ando[2]; C. Randall[1]; 1. Pennsylvania State University, USA; 2. Murata Mfg. Co., Ltd., Japan

Recently, unique research about thermal technology has been reported, for example phonon transport on the nano-scale interface, multicalorics and thermoelectric. The reason why these technologies are so important is that there are a lot of waste heat energies and many industries are trying to reduce it. We also suggested here a multilayer type thermoelectric device for energy harvesting. This device uses La-doped $SrTiO_3$ as a thermoelectric material, and has the same layered structure used in multilayer ceramic capacitors can be ready for mass producing. It has a higher density, mass productivity and reliability than other thermoelectric generators. This device is useful for energy harvesting applications, but higher conversion efficiency will be required to extend the market. Another thermoelectric oxide material should be developed for the device of next generation. Now our group is interested in $CaTiO_3$ because it

has lower thermal conductivity than $SrTiO_3$. $CaTiO_3$ is known as a dielectric material and has twin structures, but $SrTiO_3$ doesn't have it at room temperature. The domain structures in these materials will be shown. Then phonon and electron transports on the nano-scale interface will be discussed. We are assuming that the interface between two domains helps to reduce thermal conductivity, but it doesn't limit electron transport. The details will be reported in this paper.

5:00 PM

(EMA-S3-015-2016) Microstructure and thermoelectric properties of $Sr(Ti_{0.8}Nb_{0.2})O_3$ with addition of SrO and CaO

M. Jeric[1]; M. Ceh*[1]; 1. Jozef Stefan Institute, Slovenia

Microstructure and thermoelectric properties of $Sr(Ti_{0.8}Nb_{0.2})O_3$ (STN) with addition of SrO and CaO were investigated. Both alkaline oxides were added to STN in the form of carbonates. The mixtures were sintered under different sintering regimes. The microstructural analysis of samples revealed that the addition of SrO and CaO into STN results in the formation of Ruddlesden-Popper-type (RP) planar faults with the rock salt-type structure that form either random 3D networks along {001} STN crystallographic planes and/or more or less ordered polytypoidic sequences with general formula (Sr,Ca)O.n(Sr(Ti,Nb)O_3). Atom-resolved transmission electron microscopy showed that chemical composition of the observed planar faults systematically varied with the amount of added CaO. The thermoelectric measurements showed that thermal conductivities of SrO and CaO-doped STN were app. twice lower as compared to undoped STN. This was associated with the phonon-scattering effect at a single and/or polytypoidic sequences within the STN. Consequently, the figure of merit (ZT) for CaO-doped STN was improved by a factor of two. On the other hand, the ZT for SrO-doped STN was lower due to reduced electrical conductivity. It was concluded that the inclusion of CaO RP planar faults into the STN may well be a promising method to improve the ZT in this thermoelectric material.

5:15 PM

(EMA-S3-017-2016) Quasiparticle band structures and thermoelectric transport properties of p-type SnSe

G. Shi*[1]; E. Kioupakis[1]; 1. University of Michigan, USA

SnSe has been attracting lots of attention as a thermoelectric material since it was recently reported to have figure-of-merit values as high as 2.6 in single-crystal samples. In this work, we used density functional and many-body perturbation theory to calculate the quasiparticle band structures and electronic transport parameters of p-type SnSe both for the low-temperature Pnma and high-temperature Cmcm phases. The calculated band gap of Pnma phase (0.829 eV) has good agreement with experiment. We found multiple local band extrema that lie close in energy to the band edges and need to be considered when calculating the thermoelectric transport properties. We calculated the electronic transport coefficients as a function of doping concentration and temperature for single-crystal and polycrystalline materials to understand previous experimental measurements. The electronic transport properties show a significant degree of anisotropy between the perpendicular direction and the two in-plane directions, and are also strongly affected by bipolar effects at high temperatures and low carrier concentrations. Our results predict that SnSe would show optimal thermoelectric performance at high temperature when doped in the 10^19-10^20 cm^3 range.

5:30 PM

(EMA-S3-018-2016) Evaporation of PbTe and GeTe based thermoelectric materials

Y. Sadia*[1]; T. Ohaion-Raz[1]; O. Ben-Yehuda[1]; Y. Gelbstein[1]; 1. Ben-Gurion University of the Negev, Israel

Thermoelectric materials have seen a large increase in interest in the few past years, with the increase of the thermoelectric figure of merit from ZT=1 to ZT=1.5. However there has been no major change in the production of actual devices. One of the main reasons for the long delay between material production and its use in industry is the "Valley of Death" associated with long term testing of various properties of the materials. In this study a simple evaporation model was proposed to test the evaporation of various materials using a simple TGA analysis to extrapolate long term evaporation. The model was tested using *n*-type PbTe and *p*-type $Pb_{0.5}Sn_{0.5}Te$, TAGS-85, and $Ge_{0.87}Pb_{0.13}Te$ doped with 3%Bi_2Te_3. Results showed that for a 10 year operation with less then 10% loss in contact area, a temperature of about 420°C is the highest allowed for TAGS-85, and $Ge_{0.87}Pb_{0.13}Te$ doped with 3%Bi_2Te_3 and a temperature of about 520°C is the highest allowed for PbTe and $Pb_{0.5}Sn_{0.5}Te$. The materials where also analyzed by XRD and SEM to determine the mode of evaporation and the reasons for degradation in the alloys. Through the analysis it is clear why the GeTe type alloys behave in very similar manners and why the PbTe and $Pb_{0.5}Sn_{0.5}Te$ also behave in very similar manners.

5:45 PM

(EMA-S3-019-2016) Filled and Unfilled Strontium Barium Niobate (SBN) Bronzes for Thermoelectric Applications

J. H. Chan*[1]; J. A. Bock[1]; S. Trolier-McKinstry[1]; C. Randall[1]; 1. Pennsylvania State University, USA

An understanding of the mechanism responsible for high electrical conductivities in SBN would be useful in optimizing this material for thermoelectrics. SBN ceramics were fabricated by conventional solid-state sintering. Commercial oxide powders were reacted at 1300°C and then vibration milled to reduce the particle sizes. X-Ray diffraction showed that filled bronzes achieved solid solution up to 80:20 (Sr:Ba). Scanning electron micrographs revealed that grain sizes did not significantly affect electrical conductivities. Compositional mapping in the transmission electron microscope showed that the ceramics were homogeneous and had no secondary phases along grain boundaries. Hall measurements illustrated that the carrier density (/cm^3) between filled and unfilled bronzes annealed at ~10^{-14} atm P_{O2} were $1.55x10^{19}$+/-$1.44x10^{17}$ and $1.13x10^{21}$+/-$3.66x10^{19}$, respectively. The oxygen loss data assessed by thermogravimetric analysis was used to independently estimate the carrier concentrations. The study can conclude the following: oxygen activity is controlling the conductivity, not cation occupation; there is a fundamental difference in how the 5-site and 6-site chemistries are compensated at a particular annealing condition which affects their conductivity. The carrier concentration in heavily reduced samples ~10^{-16} atm P_{O2} is higher than the typical optimum of 10^{19} carriers/cm^3.

S5. Multifunctional Nanocomposites

Multifunctional Nanocomposites II

Room: Coral B

Session Chair: Scott Chambers, Pacific Northwest National Laboratory

2:00 PM

(EMA-S5-006-2016) Control of domains and control through domains in ferroelectric superlattices (Invited)

B. Bein[1]; M. Yusuf[1]; H. Hsing[1]; S. Callori[1]; J. Sinsheimer[1]; P. V. Chinta[2]; B. Nielsen[1]; R. Headrick[2]; X. Du[1]; M. Dawber*[1]; 1. Stony Brook University, USA; 2. University of Vermont, USA

In finely layered ferroelectric superlattices, the polarization domain configuration is determined by a complex interplay of strain, electrostatics and other local distortions of the crystal lattice. One emphasis in this talk will be on the development of polarization and domain structure during the growth of our artificially layered structures, which we have studied using in-situ synchrotron x-ray diffraction. We developed a new technique allowing for scan times substantially faster than the growth of a single layer of material, which enable continuous monitoring of multiple structural parameters as the film grows. We used this technique to continuously monitor ferroelectric domain spacing, surface termination, lattice parameters (and thereby polarization) and bilayer thickness during the growth of $BaTiO_3/SrTiO_3$ superlattices by off-axis RF magnetron sputtering, and investigated the effect of electrostatic boundary conditions and superlattice composition on all of these parameters. Another focus is on how to use ferroelectric polarization to control the charge transport properties of graphene. We have developed a procedure to acheive a clean interface between a ferroelectric superlattice surface and graphene and here report on nanoscale manipulation of polarization domains, and hence the local charge transport properties of the graphene, by scanning probe microscopy methods.

2:30 PM

(EMA-S5-007-2016) Interface-induced Polarization in $SrTiO_3$-$LaCrO_3$ Superlattices

R. B. Comes*[1]; S. Spurgeon[1]; P. Sushko[1]; S. Heald[2]; D. Kepaptsoglou[3]; P. Ong[1]; L. Jones[4]; T. Kaspar[1]; M. Engelhard[1]; M. Bowden[1]; Q. Ramasse[3]; S. Chambers[1]; 1. Pacific Northwest National Lab, USA; 2. Argonne National Lab, USA; 3. STFC Daresbury, United Kingdom; 4. University of Oxford, United Kingdom

Ferroelectric oxide superlattices combining ferroelectric and non-ferroelectric materials are intriguing for the polarization that is induced in the non-ferroelectric phase. When a ferroelectric is combined with a non-polar material like $SrTiO_3$ (STO), the STO layer may become ferroelectric. However, there has been no demonstration of a superlattice where two non-ferroelectric materials combine to produce bulk ferroelectricity. We present work studying STO-$LaCrO_3$ (LCO) superlattices and show that by controlling interfacial termination between layers we can induce ferroelectricity. Density functional theory (DFT) predicts that by alternating terminations between positively charged TiO_2-LaO and negative CrO_2-SrO interfaces ferroelectricity will be induced in both materials. Using molecular beam epitaxy, we have synthesized superlattices with such alternating interfaces. A built-in electric field is observed using x-ray photoelectron spectroscopy. X-ray absorption spectroscopy shows that the Ti cations are displaced off-center along the growth direction, consistent with ferroelectric polarization. Scanning transmission electron microscopy is used to calculate the polarization field within the superlattice. We also explore the role of defects using characterization and DFT and find that the polarization is not defect-dependent. These results open the door for interfacial engineering of ferroelectricity in superlattices.

2:45 PM

(EMA-S5-008-2016) Understanding polarization asymmetry in $PbTiO_3$ based superlattice thin films

H. Hsing*[1]; S. Divilov[1]; M. Yusuf[1]; J. Bonini[2]; J. Bennett[2]; P. Chandra[2]; K. M. Rabe[2]; X. Du[1]; M. Fernandez Serra[1]; M. Dawber[1]; 1. Stony Brook University, USA; 2. Rutgers University, USA

In ferroelectric superlattices, polarization asymmetry, where one polarization state is preferred over another, is frequently observed. While this asymmetry may be generated by strain or composition gradients, it may also be influenced by extrinsic effects such as asymmetric electrodes or the inhomogeneous distribution of oxygen vacancies. In this work, we comprehensively studied the origin of polarization asymmetry for ferroelectric $PbTiO_3$ based superlattice films. We prepared several compositions of $PbTiO_3/SrTiO_3$ (PTO/STO) superlattice thin films through RF magnetron off-axis sputtering. Samples were prepared either in the symmetric $SrRuO_3$-PTO/STO-$SrRuO_3$ configuration or asymmetric Pd-PTO/STO-$SrRuO_3$ configuration, and electrical characterization to determine the built-in field was performed. We also carried out repetitive electrical cycling on the samples to study the effect of migration of oxygen vacancies and measured the capacitance-voltage characteristic of our samples at different temperatures. Finally, we compare PTO/STO superlattices with $PbTiO_3/SrRuO_3$ (PTO/SRO) superlattices, which have an additional intrinsic compositional asymmetry due to variation of both A and B cations. By combining our experimental results with theoretical modelling we aim to identify the magnitude and scaling behavior of all the potential sources of polarization asymmetry.

3:00 PM

(EMA-S5-009-2016) Characterization of acceptor-doped BaTiO3 for capacitor and its insulation degradation behavior using charge-based DLTS method (Invited)

T. Okamoto*[1]; J. Long[2]; J. Stitt[2]; R. Wilke[2]; K. Suzuki[1]; H. Kondo[1]; N. Tanaka[1]; A. Ando[1]; C. Randall[2]; 1. Murata Mfg. Co., Ltd., Japan; 2. Pennsylvania State University, USA

Doping multilayer capacitors based on BaTiO3 is a key to engineering their performance for both temperature dependent properties and reliability. There have been studies on time dependent failure on the viewpoint how/where it progresses, such as using KFM/TEM, but little is known on transient changes to dopant defects under high bias prior to time dependent breakdown processes. To investigate them more completely, we are considering deep level transient spectroscopy (DLTS). This is a widely used process for characterizing trap levels in depletion layers in semiconductors, but could possibly be used in BaTiO3 based dielectrics. We perform DLTS and directly analyze the relaxation behaviors of induced electric charges by pulse waves. Our charge-based DLTS has successfully detected several trap levels and their properties were estimated qualitatively. Charge-based DLTS is shown as the promising method to electrically characterize them for BaTiO3 based dielectrics for capacitors and their insulation degradation behavior.

4:00 PM

(EMA-S5-010-2016) Probing the Reaction Pathway in $(La_{0.8}Sr_{0.2})_{0.95}MnO_{3+\delta}$ Using Libraries of Thin Film Microelectrodes (Invited)

S. M. Haile*[1]; R. Usiskin[2]; S. Maruyama[3]; C. Kucharczyk[2]; I. Takeuchi[3]; 1. Northwestern University, USA; 2. California Institute of Technology, USA; 3. University of Maryland, USA

Lanthanum strontium manganite (LSM) is the canonical cathode material for solid oxide fuel cells, yet fundamental questions concerning the electrochemical reaction pathway at the oxygen|LSM|electrolyte interface remain. To address the many open questions, here libraries of $(La_{0.8}Sr_{0.2})_{0.95}MnO_{3+\delta}$ thin film microelectrodes with systematically varied thickness or growth temperature were prepared by pulsed laser deposition, and a novel robotic instrument was used

to characterize these libraries in automated fashion by impedance spectroscopy. The measured impedance spectra are found to be described well by an electrochemical model based on a generalized transmission model for a mixed conducting oxide, and all trends are consistent with a reaction pathway involving oxygen reduction over the LSM surface followed by diffusion through the film and into the electrolyte substrate. The surface activity is found to be correlated with the number of exposed grain boundary sites, which decreases with either increasing film thickness (at constant growth temperature) or increasing film growth temperature (at constant thickness). These findings suggest that exposed grain boundaries in LSM films are more active than exposed grains towards the rate-limiting surface process, and that oxygen ion diffusion through nanocrystalline LSM films is faster than many prior studies have concluded.

4:30 PM

(EMA-S5-011-2016) Cationic ordering and its effect on the physical properties of functional oxides (Invited)

S. Choi*[1]; 1. Korea Institute of Materials Science, The Republic of Korea

Among all of the thermodynamic variables, the point defects in the functional, such as cation vacancies, anti-site defects, and hydrogen impurities, are known to critically affect the physical properties of the minerals including electrical conduction, ionic diffusion, and deformation behavior. Determination of the cation partitioning between the two different octahedral interstitial sites in the unit cell has been a particularly important issue for understanding crystallographic stability under specific circumstances. Most of the analytical investigations on the antisite exchange were largely based on powder diffraction methods, which only show the overall simple distribution of metal cations between the two sites through the refinement of obtained spectra. In this regard, direct atomic-level observation of the anti-site defects is essential to precisely probe the local distribution of the defects in the crystal lattice, especially when the degree of the exchange is quite low. By utilizing aberration-corrected STEM, antisite defects were successfully visualized in olivine-structured oxides, such as $LiFePO_4$ and $LiMnPO_4$, as well as double perovskites oxides, such as Sr_2FeReO_6 and Sr_2CrReO_6. Based on the atomic scale imaging and first principles calculations, we can understand the correlation between cationic ordering and their physical properties in the functional oxides.

5:00 PM

(EMA-S5-012-2016) Gas Sensing Properties of Epitaxial LaBaCo2O5.5+δ Thin Films

S. Ren*[1]; M. Liu[1]; 1. Xi'an Jiaotong University, China

Chemical reactivity and stability of highly epitaxial mixed-conductive LaBaCo2O5.5+δ (LBCO) thin films on (001) LaAlO3 (LAO) single-crystalline substrates, fabricated by using pulsed laser deposition system, were systematically investigated. Microstructure studies from x-ray diffraction indicate that the films are *c*-axis oriented with the interface relationship of [100]LBCO//[100]LAO and (001) LBCO//(001)LAO. LBCO thin films can detect the ethanol vapor concentration as low as 10ppm and the response of LBCO thin film to various ethanol vapor concentrations is very reliable and reproducible with the switch between air and ethanol vapor. Moreover, the fast response of the LBCO thin film, as the *p*-type gas sensor, is better than some *n*-type oxide semiconductor thin films and comparable with some nanorods and nanowires. These findings indicate that the LBCO thin films have great potential for the development of gas sensors in reducing/oxidizing environments.

S7. Processing and microstructure of functional ceramics: Sintering, grain growth and their impact on the materials properties

Defects, Space Charge and Non-Stoichiometry in Sintering and Grain growth

Room: Caribbean B

Session Chairs: Wolfgang Rheinheimer, Karlsruhe Institute of Technology; Michael Hoffmann, Karlsruhe Institute of Technology

2:00 PM

(EMA-S7-007-2016) Conventional solid state synthesis of $BiFeO_3$-$Bi_{0.5}K_{0.5}TiO_3$ solid solution - effects of cation non-stoichiometry and compositional inhomogeneity (Invited)

T. Grande*[1]; 1. Norwegian University of Science and Technology, Norway

$BiFeO_3$ (BFO) and $Bi_{0.5}K_{0.5}TiO_3$ (BKT) are two lead-free candidate compounds in current research to find alternatives to the state of the art $Pb(Zr,Ti)O_3$ electroceramics. Rhombohedral BFO possesses large polarization and crystallographic strain and a high Currie temperature (830°C), which makes the material interesting for high temperature applications. BKT has a tetragonal symmetry and also a relatively high Currie temperature. The particular crystal symmetry of these two compounds opens up for a morphotropic phase boundary (MPB) in BFO-BKT solid solutions, which have motivated several recent studies of this system. $B_{i2}O_3$ and K_2CO_3 are used as precursors in solid state synthesis of BFO-BKT, compounds which possess low melting point and are volatile at elevated temperatures. Transient liquid formed due to melting of precursors strongly influence the phase purity and homogeneity of the material. Loss of volatile oxide during high temperature processing will results in point defects, which will strongly influence on the electrical performance. Conventional solids state synthesis of BFO-BKT solid solutions is discussed with particular focus on cation non-stoichiometry and composition homogeneity. Finally, we address the influence of point defects on the ferroelectric and ferroelastic properties.

2:30 PM

(EMA-S7-008-2016) The effects of non-stoichiometry and ceramic processing on the electrical properties of $Na_{1/2}Bi_{1/2}TiO_3$ (Invited)

D. C. Sinclair*[1]; L. Li[1]; M. Li[1]; H. Zhang[1]; Y. Wu[1]; F. Yang[1]; I. M. Reaney[1]; 1. University of Sheffield, United Kingdom

The electrical properties of the ferroelectric perovskite $Na_{1/2}Bi_{1/2}TiO_3$ are very sensitive to low levels of A-site non-stoichiometry and can transform it from a Pb-free piezoelectric (electronic) insulator into a fast-ion (oxide) conductor. Here we explore the ternary phase diagram Na_2O-Bi_2O_3-TiO_2 in the vicinity of '$Na_{1/2}Bi_{1/2}TiO_3$' to establish the level of non-stoichiometry in this phase to fully evaluate its influence on the ceramic microstructure and electrical properties. We also report the influence of different processing routes (eg traditional solid state synthesis versus sol-gel processing), the volatility of the A-site species, and chemical doping via donor/acceptor dopants on the physical and electrical microstructure of the ceramics. This is achieved using a combination of X-ray Diffraction, Analytical Scanning and Transmission Electron microscopy, Impedance Spectroscopy, Polarisation-Electric field hysteresis loops and oxide-ion transport number measurements. Finally, we discuss the defect chemistry of $Na_{1/2}Bi_{1/2}TiO_3$ is relation to other $ATiO_3$ perovskites (where A = Ba,Sr, Pb).

3:00 PM

(EMA-S7-009-2016) Impedance Spectroscopy as a Tool to Detect Detailed Grain Boundary Properties in Single Phase and Heterogeneous Materials (Invited)

R. A. Gerhardt*[1]; 1. Georgia Institute of Technology, USA

Impedance spectroscopy, an alternating current technique is ideal for detecting the presence of more than one current path in materials and devices. A substantial amount of work since the 1980s has shown that even single phase materials will show a different response along the grain boundaries under certain conditions. The expectation is that measuring the electrical properties will give rise to the appearance of more than one semicircle in the complex impedance plane. This is often explained by assigning a parallel RC circuit to the grains and another to the grain boundaries. However, there are many cases where such a simple model does not fit the measured response due to the presence of porosity, inadvertent impurities or the formation of percolating paths that can provide other conducting paths. This is because the simplest version of such a model assumes that no current flow occurs along the parallel paths. In this talk, it will be demonstrated that there are many more details that can be obtained by comparing the impedance response of the same materials made by different sintering methods, or by changing the grain size or by combining two distinct phases that do not intermingle and can thus be assigned clearly separated conducting paths. Experimental results will be supplemented by simulation modeling.

4:00 PM

(EMA-S7-010-2016) Correlation of microstructure and microwave properties of (Ba,Sr)TiO_3 ceramics (Invited)

J. R. Binder*[1]; C. Kohler[1]; A. Friederich[1]; A. Wiens[2]; M. Nikfalazar[2]; H. Maune[2]; R. Jakoby[2]; 1. Karlsruhe Institute of Technology, Germany; 2. Technical University Darmstadt, Germany

Barium strontium titanate (BST) is a promising material for applications in tunable microwave devices such as phase shifters or tunable matching networks. The advantages of the ferroelectric materials compared to other technologies are the very fast tuning speed, the low DC power consumption due to negligible leakage currents and the high linearity of the devices. The performance of the microwave devices depends on the design of the varactors and the material properties. The RF properties of BST can be influenced by doping elements as well as by tailoring the microstructure. The correlation of the microstructure and the microwave properties of BST ceramics were investigated by varying the particle size of the used powders and the sintering conditions. From these results we can summarize that the larger the ratio between the grain sizes and the sizes of sintering necks, the higher is the improvement of the tunability. Further investigations deal with the powder processing to achieve a larger range of grain sizes and different porosities. Whereas the influence of grain size on the tunability was remarkable again, the dependency of porosity was not noticeable. Based on this knowledge different tunable ferroelectric-dielectric composites were realized and their microstructure and microwave properties were investigated.

4:30 PM

(EMA-S7-011-2016) Conventional and spark plasma sintering of $Na_{1/2}Bi_{1/2}Cu_3Ti_4O_{12}$ giant dielectric ceramics

M. M. Ahmad*[1]; 1. King Faisal University, Saudi Arabia

Materials with high values of the dielectric constant are technologically important in high energy density storage and microelectronics applications. Giant dielectric constant (GDC) > 10000 was discovered in the perovskite family of $ACu_3Ti_4O_{12}$ materials. The observed GDC is due to internal barrier layer capacitance (IBLC) effects that originate from the electrical heterogeneity of the materials. Here, we present our results on the room temperature mechanosynthesis of $Na_{1/2}Bi_{1/2}Cu_3Ti_4O_{12}$ followed by conventional (CS) and spark plasma sintering (SPS) at different temperatures. The mechanosynthesized powder has a particle size < 50 nm. CS at 1000 °C for 10 h led to coarse grained ceramics with GDC of 1.4 x 10^4. Further increase of the sintering time to 20 h increases the dielectric constant to 2.4 x 10^4. SPS at 800 – 900 °C produced fine grained ceramics with grain size of 250 – 450 nm. The SPS-900 ceramics have GDC of 3 x 10^4 at RT, which is higher than the conventionally sintered ceramics. The transport properties of the investigated ceramics are studied by impedance spectroscopy, where the grain and grain boundaries contributions could be separated. Where the bulk conductivity of the CS and SPS ceramics are in the same range of ~ 10^{-2} S/cm at RT, we notice that the conductivity of the grain boundaries of the SPS ceramics is much higher than that of the CS ceramics.

4:45 PM

(EMA-S7-012-2016) Microstructures and dielectric properties of layered perovskite $K(Sr,Ba)_2Nb_3O_{10}$ ceramics

W. Lee*[1]; S. Kweon[1]; M. Im[1]; S. Nahm[1]; 1. Korea University, The Republic of Korea

$KSr_2Nb_3O_{10}$ (KSN) is one of the Dion-Jacobson (D-J) layered perovskites which are useful for the application of ultra-thin films. They can be easily exfoliated layer-by-layer to form nano-sized sheets. Recently, these exfoliated nano-sheets have been widely investigated for the application to the nanoelectronics, such as multilayer thin film capacitor, gate insulator and memory devices. However there is no systematically investigation on the relationship between microstructure and dielectric properties of KSN bulk ceramics. By the way, higher molecular dipole moment and thus better dielectric properties are expected as the size of Ba^{2+} is bigger than Sr^{2+}. In this study, the KSN with different Ba^{2+} substitution content of 0~25% for Sr^{2+} was sintered using the conventional solid state reaction. Moreover, effects of the addition of Ba^{2+} on the microstructure and dielectric response were investigated. In addition, the sintering mechanism of the KSN ceramics with different Ba^{2+} substitution content for Sr^{2+} was also presented in this work.

5:00 PM

(EMA-S7-013-2016) Piezoresponse in the nano-range for $Ba_{0.9}Ca_{0.1}Zr_{0.1}Ti_{0.9}O_3$ obtained by modified Pechini method

G. M. Herrera*[1]; A. Reyes-Rojas[1]; A. Reyes-Montero[2]; M. Villafuerte-Castrejon[2]; A. Hurtado[1]; O. Solis[1]; R. Ochoa[1]; F. Paraguay-Delgado[1]; L. Fuentes-Cobas[1]; 1. CIMAV, Mexico; 2. UNAM, Mexico

$Ba_{0.9}Ca_{0.1}Zr_{0.1}Ti_{0.9}O_3$ (BCZT) compound was prepared by the modified Pechini method at 700 ºC during 1 h. The stabilization of tetragonal crystal phase for the BCZT at nanoscale was confirmed by differential scanning calorimeter analysis (DSC) followed by the Rietveld refinements of X-ray powder diffraction (XRD). Raman and Fourier transform infrared (FTIR) spectroscopy were carried out to confirm the tetragonality and the complete decomposition of organic groups into BCZT phase. In comparison, the XRD for the sample sintered at 1275 ºC during 5h revealed the coexistence of tetragonal and rhombohedra crystal phases. The crystallite size distribution determined by transmission electron microscopy (TEM) and carried out on the sample heated at 700 ºC is center around 30 nm. The optical band gap for BCZT nanocrystalline powder was obtained using Kubelka Munk function and was found to be around 3.13 eV. The microstructure monitored by scanning electron microscopy reveals the presence of mesocrystals in the samples sintered from the possible organization of nanosized particles. The comparison of the roughness and the piezo-response by the atomic force microscopy and piezo-response force microscope was performed on the samples in the nanoscale and micro range. The d_{33} coefficients obtained for 30 nm and 12 microns sized crystallites were 8 pmV^{-1} and 107 pmV^{-1} respectively.

S9. Recent Developments in Superconducting Materials and Applications

New Superconductor 2 - Characterization of Structural, Magnetic, and Superconducting Properties

Room: Pacific

Session Chairs: Athena Sefat, Oak Ridge National Laboratory; Jacilynn Brant, Air Force Research Lab

2:00 PM

(EMA-S9-006-2016) Interplay between density wave order and superconductivity in $Na_2Ti_2Pn_2O$ (Pn=Sb, As) and $Ba_2Ti_2Fe_2As_4O$: an optical spectroscopy study (Invited)

N. Wang*[1]; 1. International Center for Quantum Materials, School of Physics, Peking University, China

Two-dimensional (2D) titanium oxypnictide compounds containing octahedral layers Ti_2Pn_2O (Pn = As, Sb) show intriguing competing phenomenon between density wave (DW) order and superconductivity. We present optical spectroscopy study on single crystals of $Na_2Ti_2Pn_2O$ (Pn=Sb, As), the sister compounds of superconducting titanium oxypnictide $BaTi_2Sb_2O$, and $Ba_2Ti_2Fe_2As_4O$, a compound arising from the intergrowth of $BaFe_2As_2$ and $BaTi_2As_2O$ and showing a coexistence of superconductivity and DW orders. The study reveals weak correlation effect in titanium oxypnictides and significant spectral weight change across the DW transitions. Most of the Drude spectral weigh was removed by the formation of DW energy gap. The ratio of the DW energy gap over the transition temperature, $2\Delta/k_BT_{DW}$, is considerably larger than the mean-field value of BCS weak-coupling theory. For the compound of $Ba_2Ti_2Fe_2As_4O$, further spectral change associated with the superconducting condensate was identified. The analysis indicates a dirty limit superconductivity, being similar to $BaFe_{1.85}Co_{0.15}As_2$. The low frequency optical conductivity could be well modeled within the Mattis-Bardeen approach with two isotropic energy gaps. Work done with Y. Huang, H. P. Wang, Y. G. Shi, T. Dong, R. Y. Chen, Y. L. Sun and G. H. Cao.

2:30 PM

(EMA-S9-007-2016) Recent Findings in Thallium-based Materials of Tl-1223, Tl-2223, and Tl-122 (Invited)

A. Sefat*[1]; 1. Oak Ridge National Laboratory, USA

Although toxic, cuprates containing the Tl heavy element and Tl-O interlayers are found to give highest superconducting transition temperatures in $TlBa_2Ca_2Cu_3O_{9-\delta}$ and $Tl_2Ba_2Ca_2Cu_3O_{10+\delta}$. In iron-based superconductors, T_c values of up to ~ 30 K was shown to be possible in Tl-containing selenides with $A_xFe_{2-y}Se_2$ (A = Tl, Tl/K, Tl/Rb) composition. In this talk, I will review a few of *our most recent findings* on some of these thallium-based materials. Here is my proposed talk: (1) Present an account of the bulk preparation of Tl-1223 at ambient pressure (T_c =106 K), and the improved superconducting features under thermal-annealing conditions (T_c =125 K); (2) Review on the effect of addition of Li_2O on the ease of phase formation and improved superconducting properties (shielding, J_c) of Tl-2223. (3) Give result of Tl-doped $BaFe_2As_2$ (Tl-122) and the demonstration of competition between magneto-elastic coupling and charge addition. *This work was supported by the U.S. Department of Energy (DOE), Office of Science, Basic Energy Sciences, Materials Science and Engineering Division.*

3:00 PM

(EMA-S9-008-2016) Solid-State Synthesis, Structural Analysis and Physical Property Characterization Toward New Superconducting Materials (Invited)

J. Brant*[1]; D. Vier[2]; C. Ebbing[1]; T. Bullard[1]; T. J. Haugan[1]; 1. Air Force Research Lab, USA; 2. University of California, San Diego, USA

A quest for new materials with the potential for high-temperature superconductivity was guided by the structural features and compositions of recognized superconductors in a variety of material families. Specifically, new materials with layered structures have been targeted via high-temperature solid-state synthesis. The structures and phase-purity of the polycrystalline products were analyzed via Rietveld refinement using X-ray powder diffraction (XRPD) data. Magnetic Field Modulated Microwave Spectroscopy (MFMMS), which can selectively detect superconducting transitions with high sensitivity, was used in conjunction with zero field cooled (ZFC) and field-cooled (FC) vibrating sample magnetometry (VSM) to search for indications of superconductivity. High resolution synchrotron X-ray powder diffraction (SXRPD) complements MFMMS in the analysis of complex polycrystalline product mixtures, and the resulting information has further guided synthetic efforts.

4:00 PM

(EMA-S9-009-2016) High-pressure and high-temperature synthesis of superconducting materials and related materials (Invited)

K. Yamaura*[1]; 1. National Institute for Materials Science, Japan

In general, high-pressure and high-temperature synthesis is effective to expand the range of chemical composition of the superconductor beyond the limit set by the regular solid-state method. Besides, it is effective for developing correlated materials as well. Indeed, expanded chemical compositions occasionally provided opportunities to improve the superconducting properties and correlated electrons properties. Our high-pressure facilities (belt-type and multi-anvil-type) cover the synthesis condition up to 6 GPa/1800 C for few hours. In the condition, we were successful to control the doping level of non-magnetic impurity of Zn of Fe-based superconductor as well as to grow crystals of several correlated spin-orbit materials. In this talk, an overview will be presented about our progress of studies of Zn-doped Fe-based superconductors and perovskite-based osmium oxides.

4:30 PM

(EMA-S9-010-2016) Pressure-induced metal-semiconductor transition in $ThCr_2Si_2$-type $BaCr_{2-x}Co_xAs_2$

G. Wang*[1]; 1. Institute of Physics, Chinese Academy of Sciences, China

$ThCr_2Si_2$-type structure is simple but the physical properties of corresponding compounds are very rich, such as superconductivity, ferromagnetic quantum critical transition and so on. The layered feature makes them easier to tune the band structures and properties by structural manipulation, carrier injection and application of pressure. Here I present the investigation of crystal structure, physical properties and electronic structure of new $ThCr_2Si_2$-type compound $BaCr_{2-x}Co_xAs_2$. The temperature-dependent resistivity for $BaCr_{2-x}Co_xAs_2$ crystal at ambient pressure exhibits metallic behavior. Under hydrostatic pressures up to 8 GPa, a metal-semiconductor transition is observed. This unexpected behavior is assumed to be related to the charge transfer between the transition metal atoms within the T_2X_2 layer.

4:45 PM

(EMA-S9-011-2016) Why are Fe-based superconductors so creepy? (Invited)

L. Civale*[1]; 1. Los Alamos National Lab, USA

Fe-based superconductors have several characteristics, such as relatively high transition temperatures (T_c), very large upper critical

fields (H_{c2}) and low anisotropy (g), which make them attractive for applications, potentially competing with $NbSn_3$ and MgB_2. However, one surprising detrimental characteristic is that they exhibit flux creep rates (S) as large as, or larger than, those found in oxide high temperature superconductors (HTS). This very fast vortex dynamics appears to be inconsistent with the estimate of the influence of the thermal fluctuations as quantified by the Ginzburg number (Gi), which measures the ratio of the thermal energy to the condensation energy in an elemental superconducting volume. In particular, compounds of the AFe_2As_2 family ("122") have $Gi \sim 10^{-5}$ to 10^{-4}, so they could be expected to have S in between low T_c materials (where typically $Gi \sim 10^{-8}$) and HTS such as $YBa_2Cu_3O_7$ ($Gi \sim 10^{-2}$), as indeed occurs in other superconductors that have intermediate fluctuations such as MgB_2 ($Gi \sim 10^{-6}$ to 10^{-4}). We have found the solution to this puzzle: the fast creep rates in 122 compounds are due to non-optimized pinning landscapes. Initial evidence comes from our previous studies showing that the introduction of additional disorder by irradiation decreases creep significantly in 122 single crystals, although still remaining well above the ideal limit.

5:15 PM

(EMA-S9-012-2016) Interplay between magnetism, structure, and superconductivity in Mo3Sb7 (Invited)

J. Yan*[1]; M. McGuire[1]; A. May[1]; D. Mandrus[1]; D. Parker[1]; Y. Feng[3]; J. Cheng[2]; B. Sales[1]; 1. Oak Ridge National Lab, USA; 2. Institute of Physics, China; 3. Argonne National Lab, USA

Despite a relatively low superconducting transition temperature T_c = 2.08 K, the Zintl compound Mo_3Sb_7 has attracted much interest due to the possible involvement of magnetism in superconducting pairing, and promising thermoelectric performance with proper doping. Mo_3Sb_7 crystallizes in Ir_3Ge_7-type cubic structure with space group Im3m at room temperature. A structure transition from cubic to tetragonal (I4/mmm) was observed at T_{str} = 53 K and this symmetry lowering is accompanied by the opening of a 120 K spin gap. Mo_3Sb_7 thus provides an interesting platform to study the interplay between a structural anomaly, magnetism, and superconductivity. In this talk, I will present the intrinsic physical properties of Mo_3Sb_7 and how chemical doping and hydrostatic pressure disturb the complex interplay between structure, magnetism, and superconductivity. The role of magnetism will be discussed based on thermal conductivity change across Tc and the pressure/doping dependence of Tc and Tstr. Work at ORNL was supported by the US Department of Energy, Office of Science, Basic Energy Sciences, Materials Sciences and Engineering Division.

5:45 PM

(EMA-S9-013-2016) Superconductivity in a ferromagnetic semiconductor

E. Anton*[1]; S. Granville[1]; A. Engel[2]; S. Chong[1]; M. Governale[1]; U. Zülicke[1]; A. Moghaddam[3]; J. Trodahl[1]; F. Natali[1]; S. Vezian[4]; B. Ruck[1]; 1. Victoria University of Wellington, New Zealand; 2. University of Zürich, Switzerland; 3. Institute for Advanced Studies in Basic, The Islamic Republic of Iran; 4. Centre National de la Recherche Scientifique, France

We recently discovered superconductivity in SmN, an intrinsic ferromagnetic semiconductor. Whereas superconductivity has been found in ferromagnetic materials and semiconductors separately, the coexistence of all three phases in one material is unprecedented and a major step towards identifying materials merging superconductivity and spintronics. SmN previously revealed unusual properties. Even though it is ferromagnetic with a large spin magnetic moment, its net magnetic moment is nearly zero. The reason is that the orbital contribution to the magnetic moment is not quenched, and in SmN the spin and orbital moments cancel nearly perfectly. Nevertheless, the strong coupling between the spins ensures ferromagnetic order. The ferromagnetic Curie temperature of SmN is 27 K, superconductivity sets in at about 1.5 K, deep in the ferromagnetic phase. We have also made superlattices of SmN and a strong ferromagnetic material, GdN. The superconductivity is not only stable in the vicinity of a strong ferromagnet, but T_c is even enhanced, pointing towards stable coexistence of the two phases. Experimental evidence of the superconductivity both by vanishing resistivity and the Meissner effect will be presented.

S11. Advanced electronic Materials: Processing, structures, properties and applications

Characterization of Electronic Materials I

Room: Indian

Session Chair: Jacob Jones, North Carolina State University

2:00 PM

(EMA-S11-006-2016) Raman spectroscopy of electronic devices (Invited)

M. Deluca*[1]; 1. Materials Center Leoben Forschung GmbH, Austria

Research on functional oxide, ceramic and semiconductor materials for electronics is driven by the need of designing a specific *property* important for the end *application* of the device. Often the key to new or enhanced properties is the role of the local (nanoscopic) material structure, which has to be fully understood in order to tailor the desired performance and its stability with respect to temperature, mechanical stress and environmental conditions. This involves a profound knowledge of the relationship between local material structure and chemistry, and must rely on characterization methods giving information on phase arrangements, chemical bonding and residual stress on a relevant length scale. In this talk, the use of Raman spectroscopy for the characterization of these material classes will be presented. Due to its sensitivity to the short-range structure, this technique is especially effective if used together with dielectric, piezoelectric measurements or X-ray diffraction, methods that generally give a macroscopic picture of the structure and properties of the material. Several examples of the application of the Raman technique to the study of the ferroelectric-relaxor crossover in Ba-based compositions, of the ferroelectric domain texture in dependence of external thermal and mechanical loadings, and of residual stress in metal-silicon interfaces will be discussed.

2:30 PM

(EMA-S11-007-2016) Impedance Analysis of Fe-doped $SrTiO_3$ and $BaTiO_3$ during Degradation and Recovery

J. Carter*[1]; T. J. Bayer[1]; C. Randall[1]; 1. Pennsylvania State University, USA

Nonlinear dielectric materials are very attractive for use in capacitors that must operate in high power, temperature, and frequency applications due to intrinsic polarization mechanisms. It is extremely important to understand the effects of temperature and voltage on the electrical properties of these materials. Single crystals of strontium titanate and barium titanate were chosen as the dielectric material to eliminate the effects of grains and grain boundaries. Impedance data was measured before, during, and after DC bias. The time resolved degradation and recovery data are then compared and equivalent circuit analysis is used to compliment this study. Comparisons are also drawn between impedance data and thermally stimulated depolarization current measurements.

2:45 PM

(EMA-S11-008-2016) Investigating the chemistry at oxide/oxide and oxide/nitride interfaces via scanning transmission electron microscopy

E. D. Grimley*[1]; X. Sang[1]; E. Sachet[1]; C. T. Shelton[1]; C. Rost[1]; J. Maria[1]; J. LeBeau[1]; 1. North Carolina State University, USA

The advent of the aberration corrector redefined the field of scanning transmission electron microscopy (STEM) and has aided the technique in becoming indispensable for quantifying chemistry at

the atomic scale, yet the deleterious impact of imperfect scan systems and of thermal drift have continued to limit the information obtainable from STEM images. The recently developed Revolving-STEM (RevSTEM) technique eliminates drift by acquiring an image series from which drift can be measured and removed, allowing frame averaging of undistorted images. The resulting STEM images possess dramatically improved signal to noise ratio, accuracy, and precision of features. We will present results from the CdO/MgO interface where significant lattice mismatch results in a regular array of misfit dislocations. Using RevSTEM, we are able to measure both the lattice strain surrounding the dislocation cores and the relaxation of the strain as the CdO/MgO planes realign. We will additionally present results from hetero-interface studies of rocksalt oxides grown on GaN. These results will demonstrate the ability of RevSTEM to glean knowledge of the rich chemistry occurring at defects and at interfaces between similar and dissimilar materials.

3:00 PM

(EMA-S11-009-2016) Dimensions of cathode, bulk, and anode region during degradation and recovery in Fe-doped STO single crystals

T. J. Bayer*[1]; J. Carter[1]; C. Randall[1]; 1. Pennsylvania State University, USA

Nonlinear dielectrics are the most promising candidate to develop capacitors with improved stability. As an important reference to obtain a more fundamental understanding of resistance degradation, strontium titanate is often used. Analysis of simulation, leakage, and impedance data revealed the formation of regions with lower resistivity at both electrodes. While simulations are time resolved, experimental data is only given after degradation. Here, we will present impedance data recorded during and immediately after degradation for different points in time. In the mixed ionic conductor STO, the ionic contribution mainly leads to time-dependent formation and disappearance of low resistive cathode and anode regions. Analysis of modulus data shows that each region is characterized by its discrete RC element arranged in series. Fitting the impedance data with an appropriate equivalent circuit allows for the determination of the capacitance of each region and the calculation of their actual dimensions as a function of time. Thus tracking the reduction in cathode and anode regions during the recovery process becomes possible. The insights gained by this method will be discussed and used to reassess the published data meaning that the measured data of degraded STO needs to be put in context with the corresponding recovery state of the sample.

3:15 PM

(EMA-S11-010-2016) Direct observation of local chemistry and B-site cation displacements in the relaxor ferroelectric PMN-PT

M. J. Cabral*[1]; X. Sang[1]; E. C. Dickey[1]; J. LeBeau[1]; 1. North Carolina State University, USA

Using aberration-corrected scanning transmission electron microscopy (AC-STEM) combined with advanced imaging methods, we directly observe atom column specific, picometer scale displacements in solid solutions of the relaxor $Pb(Mg_{1/3}Nb_{2/3})O_3$-$PbTiO_3$ (PMN-PT). These complex, thermodynamically frustrated materials possess local inhomogeneities due to cation composition at the B-site which give rise to local strain and polarization on the nanometer scale resulting in "polar nanoregions". While prior experiments have utilized x-ray and neutron diffuse scattering in order to understand the behavior of "polar nanoregions", they provide a statistical average over a large sampling volume and, to date, do not provide correlations with local chemistry. With the development of revolving STEM (RevSTEM) we are now able to remove sample drift from STEM images, enabling picometer scale resolution. In this talk we will present an investigation of atomic level displacements in PMN-PT where the A-site contains Pb and the B-site contains Mg, Nb, or Ti. These displacements can be related to the charge variation of the various B-site cations. Further, we will relate these displacements to local chemistry in the structure with the application of atomic resolution energy dispersive x-ray spectroscopy (EDS).

Characterization of Electronic Materials II

Room: Indian

Session Chair: Marco Deluca, Materials Center Leoben Forschung GmbH

4:00 PM

(EMA-S11-011-2016) Towards functionality in fluorites: nonequilibrium structures in thin films and bulk ceramics (Invited)

J. L. Jones*[1]; C. Fancher[1]; D. Hou[1]; S. Jones[1]; C. Chung[1]; B. Johnson[1]; 1. North Carolina State University, USA

In 2011, HfO2-based thin film capacitors were shown to exhibit ferroelectric behavior when crystallized with certain elements (e.g., Si, Y, Zr, and Gd). The ferroelectric behavior is only observed when the materials are processed in specific conditions, for example, unique stress states induced by special annealing procedures. A non-centrosymmetric and polar space group is suspected in the films, though no rigorous crystallographic analyses of the materials has been published. In this work, we synthesized doped HfO2 ceramics and powders in order to study the structures and phase stability using X-ray powder diffraction and structure inversion methods (i.e., the Rietveld method). Our results demonstrate that dopants (Si, Gd, Y, and Zr) substitute for Hf and, in some cases, can create non-equilibrium structures. The phase evolution of Si-doped HfO2 non-equilibrium structure was determined as a function of calcination temperature. The HfSiO4 secondary phase is ultimately precipitated with increased temperature. In addition, X-ray diffraction patterns were measured on Si, Gd, Y, and Zr doped HfO2 under high pressures up to 30 GPa. The observed pressure-induced sequence confirmed the structures predicted by a computational model published by other investigators. Overall, the results point towards paths to polar phases and ferroelectricity in HfO2-based materials.

4:30 PM

(EMA-S11-012-2016) Microdomain dynamics in single-crystal $BaTiO_3$ during paraelectric- ferroelectric phase transition measured with time-of-flight neutron scattering

A. Pramanick*[1]; X. Wang[2]; C. Hoffmann[2]; S. Diallo[2]; M. Jorgensen[3]; X. Wang[1]; 1. City University of Hong Kong, Hong Kong; 2. Oak Ridge National Lab, USA; 3. Aarhus University, Denmark

Microscopic polar clusters can play an important role in the phase transition of ferroelectric perovskite oxides such as $BaTiO_3$, which exhibit large electrocaloric properties, although their topological and dynamical characteristics are yet to be clarified. Here, we report sharp changes in neutron Bragg peaks from a $BaTiO_3$ single crystal during cooling/heating through the phase transition temperature T_C. The Bragg peaks in both the paraelectric and ferroelectric phases remain elongated, which indicated the presence of microdomains that have correlated <111>-type polarization vectors within the {110}-type crystallographic planes. No significant increase in the average size of the microdomains (~10 nm) near T_C could be observed from diffraction measurements, which is also consistent with small changes in the relaxation times for Ti ions measured with Quasi-elastic-neutron-scattering (QENS). The current observations do not indicate that the paraelectric-ferroelectric phase transition in $BaTiO_3$ is primarily caused by an increase in the size of the microscopic polar clusters or critical slowing down of Ti ionic motion. The sharp and strong increases in widths and intensities of Bragg peaks during cooling through T_C is explained as a result of microstrains that are developed at microdomain interfaces.

4:45 PM

(EMA-S11-013-2016) Plastic Strain Induced Dislocations and Conductivity Modification in Strontium Titanate

E. A. Patterson*[1]; E. Coskun[1]; T. Frömling[1]; K. G. Webber[2]; W. Donner[1]; J. Rödel[1]; 1. Technical University Darmstadt, Germany; 2. Friedrich-Alexander-University Erlangen-Neurnberg, Germany

The possibility of inducing dislocations via plastic deformation of alkali halides at room temperature is well established. There are, however, only few oxide ceramics known which are plastically deformable at low temperatures. Strontium titanate in single crystal form is the most prominent example and has recently been shown to deform plastically over a large temperature range. Due to the induced dislocations the material obtains unique electrical properties.In this work, plastic deformation of (001) oriented single crystal strontium titanate was achieved via application of uniaxial compressive loads at different temperatures (up to 450°C) and for different total plastic strain values (up to 2%). Dislocation densities were quantified with rocking curve measurements and the macroscopic change in electrical conductivity of the single crystal was investigated with impedance spectroscopy. Different sample annealing conditions and increasing electric fields were applied to samples prior to impedance spectroscopy to investigate additional changes in conductivity. The results are discussed with respect to future opportunities to control dislocation networks to intentionally modify their electrical properties.

5:00 PM

(EMA-S11-014-2016) Investigation of Resistance Degradation and Dielectric Breakdown of Fe-doped $SrTiO_3$ Single Crystal

A. Moballegh*[1]; T. J. Bayer[2]; C. Randall[2]; E. C. Dickey[1]; 1. NC State University, USA; 2. Pennsylvania State University, USA

Recently, there has been a strong motivation to fundamentally investigate resistance degradation and electrical breakdown of non-linear dielectrics. In this work, we aim to understand ionic defect electromigration in bulk and at the electrode interface as a function of degradation time and temperature. To understand the resistance degradation mechanism, Fe-doped $SrTiO_3$ single crystal with well-established initial defect chemistry is utilized as a model system. In $SrTiO_3$, the drift/diffusion of oxygen vacancies leads to accumulation of the point defects at the cathode interface where the Pt electrode blocks mass transport across the interface. Consequently, inhomogeneity in electrical and chemical potentials impacts on local polarization, thermal, and electrical transports that lead to resistance degradation and dielectric breakdown. The variation in the local microstructure and microchemistry are characterized in multiple length scale. Cathodoluminescence (CL) spectroscopy is utilized to measure local non-stoichiometry in sub-micrometer length scale, capable of giving information related to exact type of defect varies during the defect transport. To get more insight in atomic length scale, transmission electron microscope (TEM) and electron energy loss spectroscopy (EELS) are used to provide local stoichiometry and chemistry at dielectric/electrode interfaces.

5:15 PM

(EMA-S11-015-2016) Characterization, mechanical and thermochemical properties of perovskites studied by thermal analysis and calorimetry

K. Lilova*[1]; 1. Setaram Inc., USA

Perovskites are a diverse group of ferroelectric, piezoelectric, catalytic, magnetic materials with various applications in commercial devices as sensors, actuators, memories, high energy batteries, hydrogen storage. The thermomechanical analysis (TMA) and dilatometry are the preferred techniques to study the densification behavior (e.g. barium cerate). The thermodynamic stability and the phase transformation of lead free tantalates can be investigated using high temperature calorimetry. Combining this technique with water adsorption calorimetry allows to obtain directly the surface energetics of nanosized perovskites (e.g. dielectric titanates). A complete study of the perovskites thermodynamics can be done by combining heat capacity, DSC and high temperature calorimetric data thus obtaining the formation enthalpies, entropies and Gibbs free energies (e.g. $CaCu_3Ti_4O_{12}$) The oxygen vacancies in perovskites has a significant effect on their electronic and magnetic properties. The oxygen nonstoichiometry vs. the partial oxygen pressure can be measured by TG-DSC combined with a gas mixing system. Using a manometric system to investigate the properties of compounds with perovskite structure (NaMgH3) with an application in high capacity energy materials can provide crucial information regarding the isothermal kinetic and temperature dependent sorption properties.

Posters

Poster Session

Room: Atlantic/Arctic

(EMA-S1-P001-2016) Interface-Engineered BaTiO3-Based Heterostructures for Room Temperature Tunable Microwave Elements

M. Liu*[1]; C. Ma[1]; C. Chen[2]; 1. Xi'an Jiaotong University, China; 2. University of Texas at San Antonio, USA

Environment friendly ferroelectric Lead-free $Ba_{0.5}Sr_{0.5}TiO_3$, $Ba_{0.6}Sr_{0.4}TiO_3$, $Ba(Zr_{0.2}Ti_{0.8})O_3$ single-layer thin films and $BaTiO_3$// $SrTiO_3$ heterostructures were fabricated by the pulsed laser deposition technique. Microstructure studies with X-ray diffraction and transmission electron microscopy reveal that the films studied have good epitaxial quality along with an atomic sharp interface at the substrate. The films have excellent tunable dielectric properties and in some cases Mn doping can significantly improve further these properties. The interface engineering of $BaTiO_3$//$SrTiO_3$ heterostructures show very low dielectric loss tangent of 0.02 at 18GHz. The excellent tunable microwave response of our thin film suggests that the deposition approach taken for obtaining the $BaTiO_3$-based composition thin films, is useful in developing the room temperature tunable microwave devices and several ferroelectric based applications.

(EMA-S2-P002-2016) On the origin of electrical fatigue in the giant piezo-strain response of the lead-free piezoelectric Na0.5Bi0.5TiO3-BaTiO3-K0.5Na0.5NbO3

D. K. Khatua*[1]; 1. INDIAN INSTITUTE OF SCIENCE, India

Na0.5Bi0.5TiO3 based lead free piezoelectrics have drawn significant attention for its high piezo response behaviour. The modified system (0.94-x)Na0.5Bi0.5TiO3-0.06BaTiO3-xK0.5Na0.5NbO3 (NBT-BT-KNN) is known to exhibit giant piezoelectric strain. We have carried out a systematic study of the structural, dielectric and piezoelectric behavior of this giant piezo-strain exhibiting lead-free system as a function of composition ($0.0 \leq x \leq 0.025$), electric field and temperature. Analysis of the neutron powder diffraction data revealed that the structure in the zero field state consists of a long period modulation of the type Ö2 x Ö2 x 16 of the cubic unit cell, arising due to competing/collaborative antiferrodistortive modes. A composition x = 0.01 was identified to exhibit very large strain of 0.3 % at a moderate field of 4 kV/mm. We have also identified the structural origin of the electrical fatigue in the giant piezoresponse of this system. A detailed analysis revealed that the cause of fatigue is incomplete recovery of the long period modulated phase after having subjected the system to a field-induced critical transformation to the rhombohedral (R3c) phase. A correlation between depolarization temperature, electric fatigue and the critical field for field induced transformation is also indicated.

(EMA-S2-P003-2016) Nanostructured oxide composites for high-performance gas sensors

P. Feng[1]; S. Feng-Chen[1]; A. Aldalbahi[2]; E. Li*[1]; M. Rivera[1]; 1. Physics Department, UPR-RP, USA; 2. Department of Chemistry, Collage of Science, King Saud University, Saudi Arabia

We report the results on synthesis of various oxide composite nanowires for development of high-performance gas sensors. The morphologic surface, crystallographic structures, chemical compositions of the obtained nanowires have been investigated using scanning electron microscopy (SEM), x-ray diffraction (XRD), and Raman scattering, respectively. The operating temperature has a great influence on the properties of the sensor. Quick recovery time down to few seconds has been observed, but there is no obvious improvement in response time. Differing from the response (by an increase of its resistance) to the methane gas, the fabricated sensor responded to hydrogen gas by decreasing of its resistance. Response and recovery time to the hydrogen gas are less than 5 s operated at 20 ppm, and 1.5 minutes at 2 ppm. The general interpretation for the gas sensing mechanism is based on the interaction between the negatively charged oxygen adsorbed on the surface of composite and the targeted gas. Since there is a large amount of metal component mixed with the oxide semiconductor in the present case, if the sensor is exposed to the targeted gas, these gas molecules will not only react with the negatively charged oxygen adsorbed on the tungsten oxide surface but also react with the metal component. The change in the sensitivity is attributed to a synergistic or competitive effect.

(EMA-S2-P004-2016) Organic-Inorganic Hybrid Dielectrics for Film Capacitors

B. D. Piercy*[1]; C. Liu[1]; M. D. Losego[1]; 1. Georgia Institute of Technology, USA

Vapor phase infiltration (VPI) is an emerging technique to economically produce hybrid organic-inorganic materials. In VPI, polymer films are exposed to volatile organometallics, which diffuse into the film to form hybrid organic-inorganic materials. VPI of polymeric films is expected to introduce new mechanisms of charge storage in dielectric applications while maintaining low DC leakage and low dielectric loss. In this presentation, a systematic study on PET and PMMA dielectric films modified with titanium tetrachloride precursors will be discussed. Changes in dielectric constant and dielectric loss will be compared for different amounts of inorganic loading.

(EMA-S2-P005-2016) The Study of Radiation Tolerance in Ferroelectric Microelectromechanical Switches via *in-situ* X-ray Diffraction

J. Guerrier*[1]; S. Brewer[2]; M. Paul[2]; K. Fisher[2]; R. Rudy[3]; R. G. Polcawich[3]; E. Glaser[4]; C. Cress[4]; N. Bassiri-Gharb[2]; J. L. Jones[1]; 1. North Carolina State University, USA; 2. Georgia Institute of Technology, USA; 3. US Army Research Laboratory, USA; 4. Naval Research Laboratory, USA

Ferroelectrics are an increasingly important class of electromechanical materials that enable coupling between electrical signals and mechanical displacement. They are being used in the development of micro- and nano-scale electromechanical devices, energy harvesting systems, and non-volatile memories. Uniquely, mechanical logic relays using ferroelectric materials for the actuator have been demonstrated as an alternative to complementary metal-oxide semiconductor devices [Proie et al]. Using ferroelectric materials, the logic switches can operate with lower static and dynamic power consumption and offer potential alternative lower power circuit architectures. In the present work, the effects of Gamma radiation on ferroelectric $Pb[Zr_{0.30}Ti_{0.70}]O_3$ thin films deposited on platinized silicon wafers, with IrO_2 or Pt top electrodes, were characterized using polarization-electric field loops and *in-situ* XRD with applied electric field. Half of the samples were irradiated at the Naval Research Laboratory to 10 Mrad (Si) using their ^{60}Co Gamma radiation pool. The data shows that there were negligible differences in the electromechanical phenomena between non-irradiated and irradiated samples, suggesting that the ferroelectric materials are radiation tolerant.

(EMA-S3-P006-2016) High Temperature Coatings for Thermosolar Applications

J. Hormadaly*[1]; 1. Ben-Gurion University of the Negev, Israel

Compositions based on black pigments (RuO_2, Co_3O_4, black spinels), glass, ceramic additives and fugitive organic constitutes were studied. Composition in a paste or paint consistency were applied to stainless steel substrate and heat treated in the temperature range 700-800°C in air atmosphere. Fired compositions have very good adhesion to the stainless steel substrates and retain black color. Performance of the experimental compositions was compared with a commercial product Pyromark ® 2500.

(EMA-S3-P007-2016) Size effect in the thermopower of metallic thin-film stripes and its application in temperature sensing at micro/nano-scales

X. Huo*[1]; G. Li[1]; S. Xu[1]; 1. Peking University, China

For low-dimensional materials, size effect of a physical property is usually expected to occur when one (or more) of the dimension sizes decreases to that comparable to or smaller than one of the intrinsic characteristic lengths, e.g., the mean free path. We have observed an unexpected thermoelectric size effect, showing the absolute Seebeck coefficient of metallic thin-film stripes decreases with width in the range of 3-100μm, which is 100–1000 times larger than the intrinsic mean free path of the material. This was repeatedly observed in more than 10 different metals, including Ni, Cr, Ti, Pd, Pt, W, etc. Based on this effect, we have developed dual-beam temperature sensors made from a single metallic thin film. By using arrays of the sensors, we have obtained 2D maps of local temperatures in a small area. We have developed multiplexier circuits to record signals from 10x10 arrays and obtained nearly real-time 2D temperature maps. We have fabricated thermal sensors with a total width under 1μm and a resolution of 0.1-0.5K. We also fabricated them on ultrathin flexible Parylene-C substrates with a thickness of 1–10μm for measuring temperatures of curved surfaces. With the merits of simple structure and flexible choice of materials, the novel single-layered sensors may find practical applications in MEMS, lab-on-a-chip and flexible electronic devices.

(EMA-S4-P008-2016) Electrical Properties of Perovskite-Related Cobaltites/Ferrites Mixed Conductors

M. Tange*[1]; A. Mineshige[1]; T. Yazawa[1]; 1. University of Hyogo, Japan

Lanthanum silicate (LSO) has been considered as promising electrolytes for intermediate temperature SOFCs. However, it is necessary to enhance power density by reducing large polarization resistance of cathode at intermediate temperature range. In the present study, electrical properties of Ruddlesden-Popper (RP)-type cathode materials, $(La,Sr)_2(Co,Fe)O_4$ and its cathodic properties in the LSO-based cell were investigated. Specimens of $(La_{2-x}Sr_x)(Co_{0.5}Fe_{0.5})O_{4-d}$ were synthesized via solid-state reaction route. Phase relation and crystal structure were studied by using powder X-ray diffraction, and oxygen nonstoichiometry was determined by iodometric titration. Electrical conductivity was measured with a DC four probe method. A single phase RP obtained in the composition range $1.0 \leqq x \leqq 1.5$, showed *p*-type electronic conductivity under higher $P(O_2)$ region, and the electrical conductivity increased with increasing x up to $x = 1.3$. This is because the negative charge due to Sr-doping was compensated mainly by the change in valency of B site cations. On the other hand, electrical conductivity decreased with x at $1.3 < x$, indicating that the charge compensation was mainly done by the oxygen vacancy formation. The RP-type cathode printed on the LSO electrolyte showed a lower area specific resistance, which was one order of magnitude lower than that for a conventional perovskite-type oxide cathode.

(EMA-S4-P009-2016) $Li_{10}GeP_2S_{12}$-type Superionic Conductors in the Li_4MS_4–Li_3PS_4 System (M = Si, Ge, Sn): Synthesis and Structure–property Relationships

S. Hori*[1]; K. Suzuki[1]; M. Hirayama[1]; R. Kanno[1]; 1. Interdisciplinary Graduate School of Science and Engineering, Tokyo Institute of Technology, Japan

A novel superionic conductor, $Li_{10}GeP_2S_{12}$ (LGPS), shows an extremely high conductivity of 1.2×10^{-2} Scm^{-1} at room temperature and promising application as a solid electrolyte in all-solid-state batteries. To understand conduction mechanisms and improve ionic conductivity, we synthesized solid solutions and introduced element substitution for LGPS-type phases in the pseudo binary system Li_4MS_4–Li_3PS_4 (M = Si, Ge, and Sn). The powdered samples synthesized with the formula [$(1-k)$ Li_4MS_4 + k Li_3PS_4] were characterized by thermal analysis, structural analysis using diffraction data, and conductivity measurements. A phase diagram was constructed for the Li_4GeS_4–Li_3PS_4 system, which provided information on the synthesis conditions of Si- and Sn- based phases. The solid solution range changed depending on the cation M (Ge: $0.50 \le k \le 0.67$; Si: $0.525 \le k \le 0.60$; Sn: $0.67 \le k \le 0.75$). These compositional variations affect the lithium distribution, conduction pathway, and maximum ionic conductivity (Ge: 1.4×10^{-2} Scm^{-1}; Si: 6.7×10^{-3} Scm^{-1}; Sn: 5.0×10^{-3} Scm^{-1}). Although composition variation of the cations was not considered in previous theoretical studies, we experimentally clarified that controlling the compositions and configurations of the cations are practically important for the phase formation and ionic conduction properties of LGPS-type phases.

(EMA-S4-P010-2016) Preparation of oxygen-excess-type ionic conducting thin film for fuel cell application

A. Saito*[1]; A. Mineshige[1]; H. Yoshioka[2]; R. Mori[3]; T. Yazawa[1]; 1. University of Hyogo, Japan; 2. Hyogo Prefectural Institute of Technology, Japan; 3. Fuji-Pigment. Co. Ltd., Japan

Reduction of the operating temperature of solid oxide fuel cells (SOFCs) is required. Oxygen-excess-type lanthanum silicate (LSO) is a promising electrolyte material of intermediate-temperature SOFCs because of high ion conductivity and low activation energy for conduction. In this study, Mg-doped LSO, $La_{9.8}(Si_{5.7}Mg_{0.3})O_{26.4}$ (MDLS) electrolytes were coated on Ni-MDLS substrates (anode supports), and their electrical properties and fuel cell performances were evaluated. Ni-MDLS substrates were prepared from the mixture of 60 wt.% NiO and 40 wt.% MDLS. MDLS films were applied on top of the Ni-MDLS substrates by spin coating using nano-sized printable paste. The sintered half cells were then coated with $(La_{0.6}Sr_{0.4})(Co_{1-y}Fe_y)O_{3-d}$ cathode. AC impedance measurements were conducted under open circuit voltage (OCV) conditions using oxygen/diluted hydrogen gases. The OCV of the cell was about 1.1 V, indicating that LSO is a pure ionic conductor, and gas-tight electrolyte was obtained. The ohmic and polarized resistances of the cell at 873 K were 3.2 and 3.1 Ω cm^2, respectively. Both were able to be reduced with optimizing preparation conditions of MDLS, anode and cathode materials. As a result, the cell performance was largely improved, and the cell showed the power density of 401 and 30 mW cm^{-2} at 1073 and 873 K, respectively.

(EMA-S4-P011-2016) Chemical solution deposition of highly c-axis oriented apatite-type lanthanum silicate thin films

S. Hori*[1]; Y. Takatani[1]; H. Kadoura[1]; T. Uyama[1]; S. Fujita[1]; T. Tani[1]; 1. Toyota Central Research & Development Labs., Inc., Japan

Apatite-type lanthanum silicate (LSO) is an oxide ion conductor applicable to the intermediate-temperature (ca. 500°C) solid oxide fuel cells. LSO has a hexagonal crystal structure and exhibits anisotropic ionic conductivity with an order of magnitude greater value in the *c*-axis direction than that in the *a*-axis direction. Although *c*-axis oriented LSO layer must be prepared for achieving the high conductivity, such attempts especially for thin films have had only limited success. In this study, we demonstrate the chemical solution deposition of highly *c*-axis oriented LSO thin films on Si substrates through simple spin-coating and post-annealing methods. The prepared LSO films were a few hundred nanometer thick and composed of vertically-aligned columnar grains with a width of 50 – 200 nm. A 50 nm thick SiO_2 interlayer was formed between LSO and Si substrate during the post-annealing. Transmission electron microscopy revealed that each columnar grain maintained a same crystallographic orientation from its bottom to top of the column, which indicates a grain boundary-free structure in the thickness direction. XRD pole figure measurement shows a random in-plane orientation for the LSO thin films. This result implies that the oriented structure would be formed through self-orientation.

(EMA-S5-P012-2016) Strain and Interface Effects in a Novel Bismuth-Based Self-Assembled Supercell Structure

L. Li*[1]; W. Zhang[1]; M. Fan[1]; J. Huang[1]; J. Jian[1]; A. Chen[2]; H. Wang[1]; 1. Texas A&M University, USA; 2. Los Alamos National Lab, USA

A novel bismuth-based self-assembled supercell structure, i.e., $Bi_3Fe_2Mn_2O_x$ supercell (BFMO322 SC), with desirable room-temperature multiferroism, has been fabricated on $LaAlO_3$ (LAO). Interestingly, the novel BFMO322 SC can also be obtained on CeO_2 buffered LAO or $SrTiO_3$ (STO). However, the effect of different CeO_2 thicknesses to the growth and property of the new BFMO322 SC structure has never been studied. By controlling the CeO_2 thickness, the effect of strain and interface to the structure and magnetic property of BFMO322 SC was investigated in this study. From the thickness dependence study, it is shown that a thin CeO_2 buffer layer is essential and sufficient enough to trigger the formation of the novel BFMO322 SC structure. Our results have demonstrated that strain and interface could be utilized to generate novel thin film structures and to tune the functionalities of the thin films.

(EMA-S5-P013-2016) Surface- and Strain-Tuning of the Optical Dielectric Function in Epitaxial $CaMnO_3$

D. Imbrenda*[1]; D. Yang[2]; H. Wang[2]; A. R. Akbashev[1]; B. A. Davidson[2]; X. Wu[2]; X. Xi[2]; J. E. Spanier[1]; 1. Drexel University, USA; 2. Temple University, USA

We present on an anomalously strong thickness dependence of the optical complex dielectric function in epitaxial $CaMnO_3$(001) thin films on $SrTiO_3$(001), $LaAlO_3$(001), and $SrLaAlO_4$(001). A doubling of peak imaginary part of the dielectric permittivity and large spectral shifts for a given magnitude of absorption are observed. On the basis of the experimental data and first-principles density functional theory simulations, the evolution of the complex dielectric function with thickness has several regimes. In the thinnest, strain-coherent films, the response is characterized by a significant contribution from the free surface that exceeds that for the strain. However, at intermediate and larger thicknesses approaching the bulk-like film, strain coherence and partial strain relaxation persist and influence the complex dielectric function. Work supported by AFOSR under FA9550-13-1-0124.

(EMA-S5-P014-2016) Damage Sensing of CNT-Polypropylene (PP) Composites by Electrical Resistance Measurement for Automobile Applications

J. Park*[1]; D. Kwon[1]; L. K. DeVries[2]; 1. Gyeongsang Natl Univ, The Republic of Korea; 2. The University of Utah, USA

Carbon nanotubes (CNT)-polypropylene (PP) composites were compounded for automobile applications to disperse the filler uniformly and then prepared using twin screw extruder. Mechanical and interfacial properties of CNT-PP composites were investigated and compared with neat PP. Measurements in changes in electrical resistance were used to monitor clearly the internal damage during bending and fatigue loading. The effects of low CNT concentrations on mechanical and interfacial properties of PP were investigated using tensile, impact and microdroplet pull-out tests. Mechanical properties increases were attributed to the good reinforcing effects of the CNT filler, whereas dispersion degree could contribute to micro-damage sensing performance significantly.

(EMA-S6-P015-2016) Controlling Spin Ordering in Rare-Earth Perovskite Vanadates

N. Wagner*[1]; J. Rondinelli[1]; 1. Northwestern University, USA

We investigate the role and influence of local structure distortions on the antiferromagnetic spin ordering temperatures for large A-site radii RVO_3 perovskites (R=Yb-La) using a combination of data analytics (DA) and density functional theory (DFT). First, mode crystallography is used to parameterize the structural phase space. Next, we identify the important local structural features that correlate strongly with the Néel temperatures using Pearson correlation coefficients and principal component analysis. From this data, we then formulate a regression model using gradient boosted decision trees (GBDT) that returns the relative importance of each feature in predicting the Néel temperature. Our analysis indicates that the amplitude of the subtle Jahn-Teller active mode, which leads to variations in the V-O bond lengths and angles, could be used as an effective structural control parameter to modify the spin ordering temperature. We then validate these data-driven structure-property relationship in artificial vanadate structures using Néel temperatures based on both our GBDT model and a model Hamiltonian using DFT energies. This combined DA-DFT approach allows us to gauge the accuracy of existing models for the critical ordering temperatures in vanadates and opens possible strategies to deterministically design materials with targeted magnetic ordering temperatures.

(EMA-S6-P016-2016) Displacement Radiation Effects in Ferroelectric $BaTiO_3$: A Molecular Dynamics Study

Y. Ma*[1]; 1. University of Wisconsin-Eau Claire, USA

Displacement radiation effect can create a large number of defects in materials that may have a significant impact on the performance of materials and devices. For ferroelectrics, these defects will not only lead to polarization loss but also result in other serious problems such as ferroelectric fatigue and imprint failure. To obtain an atomistic understanding of the radiation effects in ferroelectric materials, the displacement radiation cascades in $BaTiO_3$ were simulated using molecular dynamics simulations with a modifed shell model. Primary knock-on atoms with different energies were introduced to the system and the resulting defects distribution and associated polarization loss were analyzed. Compressive strain was then introduced and it was found that the number of defects created decreases with increasing strain. Furthermore, polarization reversal was simulated to investigate the effect of radiation on the coercive field. Finally, the impact of the displacement radiation on the domain structure was studied.

(EMA-S6-P017-2016) Effects of doping on the magnetic ordering in $EuTiO_3$

Z. Gui*[1]; A. Janotti[1]; 1. University of Delaware, USA

Eu-based perovskites have attracted considerable attention due to the strong spin-lattice coupling, that can potentially lead to robust multiferroicity. One particular member is $EuTiO_3$ (ETO), which is a complex oxide that displays a large magneto-electric effect, and undergoes a series of structural and magnetic phase transitions when subjected to pressure or epitaxial strain. ETO adopts a cubic structure and is paramagnetic at high temperatures, while at very low temperatures it transforms to an antiferrodistortive tetragonal structure with a G-type antiferromagnetic (AFM) ordering. Several approaches have been presented to tune the magnetic ordering from the G-type antiferromagnetism to the F-type ferromagnetism, often relying on external pressure or epitaxial strain. Doping at the europium sites or creating oxygen vacancies have also been proposed to lead to ferromagnetism. However, the fundamental mechanism by which excess from impurities or defects lead to ferromagnetic ordering is unclear. In this study, we explore the effects of doping on the magnetic ordering in $EuTiO_3$ through first-principles calculations. We show how itinerant carriers in the Ti-d-derived conduction-band states interact with the lower-lying europium f states, inducing an alignment of the large moments on the europium ions. The effects of doping on different types of magnetic ordering are considered, and possible ways of doping are discussed.

(EMA-S7-P018-2016) Development of radio transparent ceramic materials

R. V. Kryvobok*[1]; G. Lisachuk[1]; A. Zakharov[1]; E. Fedorenko[1]; M. Prytkina[1]; 1. National Technical University "Kharkiv Polytechnic Institute", Ukraine

In recent times, scientists attention is paid to the synthesis of glass-ceramic and ceramic radio transparent materials based on celsian and slavsonite, which are characterized by ε ≤ 6-8, tgδ ≤ 1-50 • 10-4, have high melting temperature (1650 and 1760 ° C) low coefficient of thermal expansion ≤ 3,8 • 10-6 K-1 and high mechanical strength (E = 110 ÷ 115 GPa). With the purpose to expand the composition of radio transparent ceramic materials with low dielectric and high mechanical properties, the experiment was conducted with using of the simplex-lattice planning (Sheffs plans)). The area of technological compositions in ternary system SrO-Al2O3-SiO2 with the content of the components SrO - 25-45 wt. %, SiO2 - 30-50 wt. %, Al2O3 - 25-35 wt. % was selected for studying. Preparation of the samples was performed by the following technology. Raw ingredients was milled in a porcelain mill to the residue 4 - 6% on sieve 10,000 Holes. / Cm2. Pressing of the samples was performed on a hydraulic press P-125 at the specific pressure of 20 MPa. Pressed samples were dried in the oven at 110 ° C for 1 hour. Firing of samples was conducted in a laboratory oven at a temperature range of 1250-1450 ° C. On the basis of the research, new compositions of radio transparent ceramic materials, which are characterized by reduced values of dielectric permittivity (ε) - 5-9 and dielectric loss tangent (tg δ) - 60-110 • 10-4 were set.

(EMA-S7-P019-2016) Densification and Nanostructural Features of Al_2O_3 Ceramics Prepared with Nanoscale Powders by Microwave-assisted Sintering

N. Cho*[1]; H. Yun[1]; D. Jeong[1]; 1. Inha University, The Republic of Korea

Al_2O_3 can be used for various engineering applications owing to its unique and useful physical features. Since the nanotechnology was introduced a few decades ago, much efforts has been made to fabricate nano-grained Al_2O_3 ceramics for various applications. In this study, densification and nanostructural features of Al_2O_3 ceramics prepared with nanoscale powders by microwave-assisted sintering (MWS) were investigated. To investigate the effects of initial powder size on the densification, Al_2O_3 powders with an average size of a few hundred nm were prepared and sintered by MWS and conventional sintering (CS). A MWS furnace equipped with a microwave generator (frequence: 2.45 GHz, power: 4 kW) was used. The structural features of the initial nanoscale powders and ceramics were examined by X-ray diffraction and transmission electron microscopy. The activation energy of the sintering processes was estimated to appreciate the kinetic behaviors of densification. The MWS of nanoscale powders yielded a relative density (RD) of over 90% when sintered at temperatures down to ~1200°C, whereas the same RD was achieved over ~1500°C by CS. In addition, nano-grained Al_2O_3 ceramics with RD of >90% can be obtained by MWS method. It was found that the response of nanoscale powders to microwave turns out to be more significant as the initial powder size decreases.

(EMA-S8-P020-2016) $BaTiO_3$ doped ceramics fractal sources dielectric properties

V. Mitic*[1]; L. Kocic[1]; V. Paunovic[1]; 1. Faculty of Electronic Engineering, Serbia

The rare earth doped $BaTiO_3$-ceramics is investigated regarding their microstructural and dielectric characteristics influenced by the triple fractality "source". Doped BaTiO3 were prepared using conventional solid state reaction and sintering at 1320 °C. Additive materials ensure the upper grain limit size to be 2-10 mm. Dielectric measurements were carried out as a function of temperature up to 180°C. The low doped samples (0.01wt%) sintered at 1320°C, display the high value of dielectric permittivity (e_r = 2300), at room

temperature. A nearly flat permittivity-response was obtained in specimens with higher (1.0 wt%) additive content. The Curie temperature of doped samples is ranged from 124 to 129°C. The Curie constant decreases with increase of dopant concentration and the lowest values were measured from samples doped with 0.01 wt% of aditive. New aspect here is fractal correction, introduced as slight variation of temperature T entered from outside, due to three fractal factors being responsible for complex geometry of both morphologic and dynamic nature. These are a_S (induced by the grain surface fractality), a_P (fractality of pores) and a_M (moving particle fractal nature). This correction naturally has impact on the Curie-Weiss low, which is stressed in this paper.

(EMA-S8-P021-2016) Structural Characterization of Organic-Inorganic Hybrid Materials Formed via Vapor-Phase Infiltration of Polymers

C. Leng*[1]; D. Henry[1]; M. D. Losego[1]; 1. Georgia Institute of Technology, USA

Organic-inorganic hybrid materials are of interest for realizing novel synergistic properties derived from each component. Here, we examine a relatively new approach to hybrid material formation via the infusion of polymeric materials with gas-phase organometallic precursors. For this presentation, we will specifically examine the chemical and structural changes that occur when poly(methyl methacrylate) (PMMA) films are infused with Al- and Ti-containing organometallic precursors. The gas precursors react and chemically bond with the carbonyl groups on PMMA chains, and we find that the PMMA thin films swell when infiltrated. We have developed a diffusion model to better understand the kinetics of this swelling process and to extract diffusion constants for the gas phase constituents. Ultimately, we expect these materials to provide enhanced performance in various applications including as vapor barrier materials in organic electronics and as solvent barrier and structural enhancement materials in polymer separators in Li-ion batteries.

(EMA-S8-P022-2016) Understanding solid state dewetting of gold on indium tin oxide

J. A. Lai*[1]; H. Zhou[2]; N. Valanoor[1]; J. L. Jones[2]; 1. University of New South Wales, Australia; 2. North Carolina State University, USA

Solid-state dewetting of 10-15nm Au thin films on an indium tin oxide (ITO)-glass substrate was investigated. Films were prepared by sputter coating and thermally annealed in a nitrogen atmosphere tube furnace then examined by ex-situ microscopy techniques. Scanning electron microscopy (SEM) and atomic force microscopy (AFM) analyses revealed the formation of holes in the films at grain boundary sites and their subsequent growth and impingement by surface diffusion. The rate of interface area reduction varied as a function of the annealing temperatures (300-600°C) and thickness. The formation of many, separated islands was observed above 400°C and at longer time periods, close to two hours, there was a consistent observed height drop as there was a reaction between the gold and underlying substrate. This effect can be seen by AFM topography and cross-sectional TEM. These results provide a threshold time and temperature for the transition from a continuous to a discontinuous structure on the processing of Au/ITO, and can be significant as it reveals limits on heating times depending on the application, i.e. for metallic contacts, etch masks, plasmonics etc

(EMA-S9-P023-2016) Optimizing Flux Pinning of $YBa_2Cu_3O_{7-\delta}$ Superconductor with $BaHfO_3$+Y_2O_3 Mixed Phase Additions

M. P. Sebastian*[1]; T. Bullard[2]; C. Ebbing[3]; M. Sullivan[3]; J. Huang[4]; H. Wang[4]; J. Wu[5]; T. J. Haugan[1]; 1. Air Force Research Laboratory, USA; 2. UES, USA; 3. UDRI, USA; 4. Texas A&M University, USA; 5. University of Kansas, USA

Adding nanophase defects to $YBa_2Cu_3O_{7-\delta}$ (YBCO) superconductor thin films is well-known to enhance flux pinning; resulting in an increase in current density (J_{ct}). While many previous studies focused on single phase additions, the addition of several phases simultaneously shows promise in improving current density by combining different pinning mechanisms. This paper studies the effect of the addition of insulating, nonreactive phases of barium hafnate (BHO) and yttrium oxide (Y_2O_3) to YBCO thin films. Processing parameters varied the target composition volume percent of BHO from 2 – 6 vol. %, while maintaining 3 vol. % Y_2O_3, and the remaining vol. % YBCO. Pulsed laser deposition produced thin films on La AlO_3 (LAO) and $SrTiO_3$ (STO) substrates at various deposition temperatures. Comparison of strong and weak flux pinning mechanisms, current densities, critical temperatures, and microstructures of the resulting films will be presented.

(EMA-S9-P024-2016) Searching for Signatures of Superconductivity in Rare Earth Oxides

J. Brant*[1]; J. Burke[1]; C. Ebbing[1]; D. Vier[2]; T. Bullard[1]; T. J. Haugan[1]; 1. Air Force Research Lab, USA; 2. University of California, San Diego, USA

A search for new high-temperature superconductors with layered structures was inspired by a general valence pairing approach. RE-M-Ox compounds containing RE2+,3+ and M3+,4+ were synthesized using conventional solid-state reactions in which RE2O3 and M2O3 were pelletized and heated to 1200-1500°C. The structures and phase-purity of the bulk materials were analyzed via Rietveld refinement using X-ray powder diffraction (XRPD) data, while magnetic properties were assessed using zero-field cooled (ZFC) and field-cooled (FC) vibrating sample magnetometry (VSM). The polycrystalline product mixtures were analyzed using Magnetic Field Modulated Microwave Spectroscopy (MFMMS), which can be used to selectively detect superconducting transitions with high sensitivity. High-resolution synchrotron X-ray powder diffraction (SXRPD) complements MFMMS by allowing the identification of low weight fraction phases that may give rise to interesting spectral features. As a result, binary rare earth oxides (e.g., RE-M-O3, RE2-M-O5) with phase-purity were targeted for property analysis.

(EMA-S9-P025-2016) Searching for superconductivity in doped carbon allotropes

N. Gheorghiu*[1]; B. Pierce[2]; C. Ebbing[3]; T. Bullard[1]; J. Brant[4]; D. Vier[5]; T. J. Haugan[2]; 1. UES, Inc., USA; 2. AFRL/WPAFB, USA; 3. University of Dayton Research Institute, USA; 4. National Academies of Sciences, USA; 5. University of California San Diego, USA

Carbon (C) allotropes have excellent physical properties for aerospace applications: 4-5× lighter than most metals, tensile strengths 100× larger than steel, high thermal conductivity, flexibility, wear resistance, and far superior mechanical-stress cycling capability when compared to metals. Transforming these materials into high-temperature superconductor wires could be of strong interest to employ in aerospace applications such as power system devices. Superconductivity can be induced by charge carrier (electron or hole) doping of base materials. We are studying the effect doping has on several C allotropes: amorphous thin films, graphite, carbon nanotubes, C fiber, and diamond-like-carbon films. Ion implantation of P, S, and O elements into the C host was done at a desired depth and calculated necessary dosing to represent a C:dopant ratio percentage. Resistivity measurements for temperatures ranging from 10 K to 300 K, Raman microscopy, SEM imaging, and PPMS characterization were employed. Results are here discussed and conclusions drawn regarding our future work. Acknowledgements: This work was supported by The Air Force Office of Scientific Research (AFOSR) and the Aerospace Systems Directorate.

(EMA-S9-P026-2016) Impact of cryogenic and superconducting components for hybrid-electric aircraft propulsion

T. J. Haugan*[1]; G. Panasyuk[2]; 1. Air Force Research Lab, USA; 2. UES, Inc., USA

Hybrid-electric-vehicle (HEV) or electric-vehicle (EV) propulsion is well understood from the automotive industry, and achieves very significant increases of energy efficiencies of 2-3x from the use of non-combustion technologies and 'smart' energy management including brake regeneration. The possibility of hybrid-electric propulsion for aircraft has increasingly been considered in the last

5 years, and has been successfully implemented in 2 and 4 passenger aircraft. This paper will summarize recent progress in this field, and present how cryogenic electric power systems can positively impact hybrid-electric propulsion and capabilities, for different size and power level aircraft. Cryogenic components to be studied include generators and motors, power transmission cables, power storage devices including Li-batteries and superconducting magnetic energy storage (SMES), power electronics including inverters, and cryogenic technologies. Properties of cryogenic systems and components will be compared to Cu-wire based systems, and the effect of different cooling options may be considered. Acknowledgments: Air Force Office of Scientific Research (AFOSR), and the Aerospace Systems Directorate of The Air Force Research Laboratory (AFRL/RQ).

(EMA-S11-P027-2016) Low Temperature Co-fired High Power Multilayer Piezoelectric Transformers

A. E. Gurdal*[1]; S. Tuncdemir[2]; K. Uchino[1]; C. Randall[1]; 1. Pennsylvania State University, USA; 2. Solid State Ceramics, Inc., USA

New generation electronic devices demand high efficiency in compact volumes. Piezoelectric transformers are capable of fulfilling this requirement due to their solid-state nature compared to their electromagnetic counterparts. Multilayer technology enables lower excitation voltage and higher capacitance, which are essential for good high power performance. A commercially available MnO_2- and Nb_2O_5-doped hard-PZT composition (APC 814) was used as the base material system. Flux materials, 0.2%wt CuO and 1.1%wt ZnO, were added to enable low temperature sintering while maintaining essential material properties. Disk-shape (k_p) ceramics were sintered at 900°C for 2h in ambient conditions and they possessed material properties at satisfactory levels ($Q_{m:}$ 971, $k_{p:}$ 0.42, tan δ: 0.02, and K: 1105). Multilayer square-shape step-down piezoelectric transformers (13×13×0.8:l×w×t mm) were manufactured via traditional tape casting, screen-printing, and lamination methods. Transformers were co-fired with silver/palladium (Ag/Pd:90/10) electrodes at similar conditions to that of bulk ceramics and dense microstructures were observed. Prototyped step-down transformers were able to reach 30 W/cm^3 output power densities with a 30°C temperature rise at loads as low as 10 Ω. The results are promising to further optimize sintering conditions to enable copper co-fired high power multilayer piezoelectric transformers.

(EMA-S11-P028-2016) Electric-field-induced structural changes at the local scale in dielectrics and ferroelectrics

T. Usher*[1]; D. Hou[1]; N. Prasertpalichatr[2]; I. Levin[3]; J. E. Daniels[4]; D. Cann[2]; J. L. Jones[1]; 1. North Carolina State University, USA; 2. Oregon State University, USA; 3. National Institute of Standards and Technology, USA; 4. UNSW Australia, Australia

Electric fields can elicit multiple local-scale structural responses from dielectrics and ferroelectrics. The former can exhibit atomic and ionic polarization, while the latter can additionally exhibit dipolar polarization, piezoelectric lattice strain, and domain reorientation. The extent and interplay of these mechanisms influences the properties. However, there are few experimental techniques that can probe field-induced local structural phenomena. We present results from a recently developed technique in which X-ray total scattering is measured during *in situ* application of electric fields. Pair distribution functions are calculated from the total scattering which allows the observation of electric-field-induced changes in the local structure (atom-atom distances from ≈2 to >50 Å). The behavior of several dielectrics and ferroelectrics including $BaTiO_3$, $Na_{0.5}Bi_{0.5}TiO_3$, $SrTiO_3$, HfO_2, $(1\text{-}x)BaTiO_3\text{–}xNa_{1/2}Bi_{1/2}TiO_3$, and $(1\text{-}x)BaTiO_3\text{–}xBi(Zn_{1/2}Ti_{1/2})O_3$, are compared/contrasted. Ionic polarization is observed in dielectrics while piezoelectric strain is observed in $BaTiO_3$ and similar compositions, demonstrating that various responses can be probed and differentiated with this technique. Relaxor ferroelectric compositions undergo greater changes, due to both ionic and strain effects in addition to other phenomena, e.g., electric-field-induced phase transitions and dipole reorientation.

(EMA-S11-P029-2016) Correlating effects of point defect concentrations on thermal conductivity and coercive field of LiTaO3 single crystals

J. Ivy*[1]; K. Meyer[2]; P. E. Hopkins[2]; G. L. Brennecka[1]; 1. Colorado School of Mines, USA; 2. University of Virginia, USA

It is well known that point defects are important during ferroelectric domain switching, but their precise effects are still so unclear that pinning or scattering sites are typically described in terms of abstract energy landscapes. This study focuses on identifying the scattering effects that point defects in lithium tantalate single crystals have on phononic vibrations as well as electrical properties. Lithium tantalate single crystals are used as a model system due to well-defined and easily confirmed defect concentrations. As-grown congruent lithium tantalate (CLT) has a high percentage of Li+ vacancies, approximately four percent, which can be filled when annealed in a Li rich atmosphere, producing stoichiometric lithium tantalate (SLT) and reducing the coercive field by a factor of ~200. The effects of Li+ vacancy concentration on phonon scattering are revealed via time-domain thermoreflectance measurements of thermal conductivity. Effects on dielectric and hysteretic properties are explored via Rayleigh and Preisach methods. Comparison of spectrally resolved phonon scattering effects with electrical response enables a more quantitative description of both the spatial distribution and energetics of domain pinning, phonon-scattering point defects within a model ferroelectric.

(EMA-S11-P030-2016) The effect of 0.5 mol% B_2O_3 addition on the grain growth in ZnO- 0.5 mol% V_2O_5 doped ceramics

G. Hardal[1]; B. Yuksel Price*[1]; 1. Istanbul University Engineering Faculty, Turkey

In recent years, the effect of small amounts of other metal oxide additions to the microstructural properties of zinc oxide ceramics have been investigated by many researchers. Among these metal oxides, B_2O_3 and V_2O_5 are very important sintering aids due to their low melting point in order to decrease the sintering temperature of ZnO ceramics. For this purpose, the dual effect of B_2O_3 and V_2O_5 additions on the grain growth of ZnO ceramics was investigated. Three compositions were prepared, undoped ZnO (composition code: Z), 0.5 mol% V_2O_5 doped ZnO (composition code: ZV) and 0.5 mol% V_2O_5-0.5 mol% B_2O_3 doped ZnO (composition code: ZVB). These samples were sintered at 900 and 1100 °C for 1 hour. The average grain size of Z was found ≤ 1 µm whereas ZV and ZVB samples were found as 9 and 17 µm when these samples were sintered at 900°C. The anisotropic grain growth in ZnO-V_2O_5 ceramic systems has been reported in previous studies, this was also observed in our study. The addition of B_2O_3 gave rise to more homogenous grain growth in ZVB samples than that of ZV samples.

(EMA-S11-P031-2016) $(Bi_{0.500}Na_{0.500})_{0.920}Ba_{0.065}La_{0.010}TiO_3$: an antiferroelectric lead-free ceramic system

Y. Méndez González[2]; A. Peláiz Barranco[2]; A. Pentón Madrigal[2]; J. de los Santos Guerra*[1]; 1. Federal University of Uberlandia, Brazil; 2. Universidad de La Habana, Cuba

$(Bi_{1/2}Na_{1/2})TiO_3$-$BaTiO_3$ (BNBT) system is a promising lead-free material, which has been extensively studied because of its enhanced piezoelectric properties. BNBT exhibits complex dielectric behaviors, including the transformation from the ferroelectric to the antiferroelectric phase on heating stage. The objective of the present work is to investigate the structural, dielectric and ferroelectric properties of the BNBT ceramic system for the $(Bi_{0.500}Na_{0.500})_{0.920}Ba_{0.065}La_{0.010}TiO_3$ composition. The dielectric behavior showed two phase transitions, one of them exhibiting typical relaxor characteristics. On the other hand, the electric field dependence of the polarization (*P-E*) showed typical antiferroelectric hysteresis loops in a wide frequency and temperature range, from room temperature up to temperatures around the first phase transition. The authors thank CAPES, CNPq and FAPEMIG Brazilian agencies for the financial support and to

the ICTP (Trieste-Italy) for financial support of Latin-American Network of Ferroelectric Materials (NET-43).

(EMA-S11-P032-2016) Structural analysis of two-, three- and four-layered Aurivillius' ferroelectric ceramics

A. Peláiz Barranco[2]; Y. González Abreu[2]; J. de los Santos Guerra*[1]; Y. Gagou[3]; P. Saint-Grégoire[4]; 1. Federal University of Uberlandia, Brazil; 2. Universidad de La Habana, Cuba; 3. University of Picardie, France; 4. University of Nimes, France

Previous reports in ferroelectrics systems from the Aurivillius' family have shown interesting properties with the increase of the perovskite blocks into the crystalline structure. These systems are characterized for having *m* blocks of perovskites ($[A_{m-1}B_mO_{3m+1}]^{2-}$) placed between bismuth layers ($[Bi_2O_2]^{2+}$). For these materials, the polarization direction as well as the structural symmetry change with the number of the perovskite blocks into the structure. The aim of the present work is to study the structural properties of the $Sr_{0.5}Ba_{0.5}Bi_2Nb_2O_9$, $SrBaBi_2TiNb_2O_{12}$ and $Sr_{1.5}Ba_{1.5}Bi_2Ti_2Nb_2O_{15}$ Aurivillius' systems. The structural characterization has been performed by using x-ray diffraction analysis and Raman spectroscopy at room temperature. The structural results are interpreted considering the presence of Sr^{2+}/Ba^{2+} in the *A*- and/or bismuth-sites of the structure. The authors thank CAPES, CNPq and FAPEMIG Brazilian agencies for the financial support and to the ICTP (Trieste-Italy) for financial support of Latin-American Network of Ferroelectric Materials (NET-43).

(EMA-S11-P033-2016) Lead-free ferroelectric $Bi_{1/2}Na_{1/2}TiO_3$ targets and thin films

E. Anton*[1]; S. Sambale[1]; T. Müller[1]; T. Sperk[1]; 1. Victoria University of Wellington, New Zealand

Ferroelectric thin films have important applications for micro-electro mechanical systems (MEMS). However, it remains an urgent task for researchers to develop environmentally friendly and especially lead-free ferroelectric thin films with high performance. Whereas there has been much progress on lead-free bulk ceramics, many open questions remain regarding thin films. The effect of strain induced by the substrate on lead-free ferroelectric thin films remains largely unexplored. This study presents the development of $Bi_{1/2}Na_{1/2}TiO_3$-based thin films with industrially applicable methods. This involves the production of the target by conventional sintering and thin film preparation using rf-magnetron sputtering. The powder preparation is a crucial step towards the successful sintering of the large ceramic targets. The effects of the milling on crack development and density of the final target will be presented. Raman spectroscopy has proven to be a powerful tool to investigate structural changes on a local scale, as needed for the local distortions associated with ferroelectricity in this class of materials. Depolarisation temperatures of lead-free ferroelectrics measured using Raman spectroscopy will be presented.

(EMA-S11-P034-2016) Effects of the Degree of Crosslinking on Flammability and Reliability of Metal-polymer Composite Films

S. Jeon*[1]; Y. Yun[1]; S. Park[1]; 1. ChangSung Co., Ltd., The Republic of Korea

Flammability and reliability of metal-polymer composite films were investigated in terms of the degree of crosslinking. All specimens were fabricated using metal powders, polymer binders, and environmentally friendly, nitrogen based flame retardants. It was found that fire resistance as well as complex magnetic permeabilities can be improved by increasing the degree of crosslinking. Significant decrease in the total flaming combustion time was observed with increasing content of cross-linking agent. A specimen with the addition of 10 phr of cross linking agent met UL 94 flammability compliance requirements for V-0. Temperature-humidity bias (THB) test revealed that an increase in the degree of crosslinking also give rise to mechanical properties under severe conditions. It is well known that brominated compounds and red phosphorus are more effective than nitrogen or inorganic compounds as a flame retardant. This results indicate that the highest level of flammability compliance requirements can be achieved by increasing the degree of crosslinking, without using environmentally hazardous materials such as halogenated substances, red phosphorous, and antimony oxides.

(EMA-S11-P035-2016) Analysis of the phase transition in rare earth modified PZT ferroelectric ceramics

J. de los Santos Guerra*[1]; S. Hessel[1]; A. Carvalho da Silva[2]; I. Cruvinel dos Reis[2]; R. Guo[3]; A. S. Bhalla[3]; 1. Federal University of Uberlandia, Brazil; 2. Universidade Estadual Paulista, Brazil; 3. The University of Texas at San Antonio, USA

Ferroelectric materials have been widely investigated during the last four decades, because of their excellent physical properties, which make them promissory materials for technological applications. In particular, for the lead zirconate titanate (PZT) system desired properties can be easily controlled when modified with several chemical additives, thus providing some relevant characteristics for application in specific electro-electronic devices. The aim of the present work is to investigate the physical properties of rare earth (RE) modified PZT ferroelectric ceramics. The structural, ferroelectric and dielectric properties have been studied in details as a function of the amount of the RE cation. The characteristics of the paraelectric-ferroelectric (PE-FE) phase transition have been carefully analyzed for compositions containing either normal or relaxor ferroelectric behavior. The authors thank CAPES, CNPq and FAPEMIG Brazilian agencies and INAMM/NSF (Grant No. 0884081) for the financial support.

(EMA-S11-P036-2016) Temperature-induced local and mesoscale structural changes of $BaTiO_3$–$Bi(Zn_{0.5}Ti_{0.5})O_3$

D. Hou*[1]; T. Usher[1]; N. Raengthon[2]; N. Triamnak[2]; D. Cann[2]; J. L. Jones[1]; 1. North Carolina State University, USA; 2. Oregon State University, USA

Polycrystalline dielectrics of composition (1-*x*)$BaTiO_3$-*x*$Bi(Zn_{0.5}Ti_{0.5})O_3$ (BT-*x*BZT) exhibit desirable dielectric properties over a broad temperature range. In order to establish the relationship between temperature-induced structural changes and dielectric properties, we introduce an *in situ* characterization method that reveals the long- and short-range structures of BT-*x*BZT as a function of temperature. The method employs atomic pair distribution functions (PDFs), which are determined from X-ray total scattering, to probe structural changes over different length scales during *in situ* heating of BT-*x*BZT. The structures determined from the *in situ* PDFs show tetragonal distortions in BT-*x*BZT at room temperature, and alloying with more BZT decreases the tetragonality. Increasing temperature disrupts the long-range ferroelectric symmetry present in BT-0.08BZT and BT-0.06BZT, while long-range structural changes in BT-0.10BZT and BT-0.20BZT are insensitive to temperature. An analysis of the data at different length scales shows that the tetragonal distortions persists at the local scale (<20 Å) at room temperature in all compositions. Moreover, the length-scale dependent tetragonal distortions are maintained even at temperatures higher than Curie point in BT-0.08BZT and BT-0.06BZT. These results suggest that the local scale tetragonal distortions may be responsible for high dielectric permittivity.

(EMA-S11-P037-2016) Preparation of Nano-sized TiO_2 Electroded Dye Sensitized Solar Cell with Red and Green Chilli-derived Natural Dye Extracts

Y. M. Maung*[1]; 1. Mandalay University, Japan

Nanocrystalline TiO_2 (P-25) was mixed with acetic acid to form TiO_2 sol solution. It was deposited onto ITO/ glass substrate and annealed at 200°C for 1h. In this study, TiO_2 film was served as a photoanode electrode. The graphite (carbon) electrode was used as the counter electrode. Red and green color dyes were obtained from the red and green chilli dye extracts (without seeds and stalks) after piquancy. Photo-electrochemical properties (FF and η_{con}) were determined by I-V characteristic of red dye sensitized TiO_2 film. The incident light to electric energy conversion efficiency with TiO_2 photo-electrode

for green chilli (0.69 %) was found to be smaller than that of TiO_2 photo-electrode with red chilli (1.06 %). Thus, the present investigation suggested that chilli dye-sensitized TiO_2 films emerged as photoconductor as well as a good candidate for harvesting solar light for construction of dye sensitized solar cell.

(EMA-S11-P038-2016) Fabrication and Characterization of ZnO Nanowires with Chlorophyll-based Grass Dye Extract for Dye-sensitized Solar Cell Application

T. T. Win*[1]; 1. Mandalay University of Distance Education, Japan

The structure of ZnO nanoparticles prepared at 500°C was confirmed by X-ray diffraction (XRD) technique. ZnO film was formed onto ITO/glass substrate by spin coating technique. The structure of ZnO nanofilm was also confirmed by XRD. To grow ZnO nanowires, the seed film was subsequently dipped in a mixture of equal molar zinc nitrate hexahydrate and hexamethylenetetramine solution with DIW by chemical bath deposition method (CBD) and annealed at 80 °C.XRD analysis was performed to examine the structural properties of ZnO nanowire. As a result, it was obvious that ZnO nanowire was significantly formed on ZnO seed layer .Field emission scanning electron microscopy (FESEM) was used to study the microstructure and diameter of ZnO nanowires. ZnO nanowires were also observed by UV-Vis spectroscopy. Chlorophyll-based grass dyes were prepared at different extracting temperatures and time intervals. Optical properties of grass dyes were examined by UV-Vis Spectrometer. Output characteristics of ZnO nanowires with different grass extracts were measured. According to the experimental results, ZnO nanowires with grass dyes may be promising, credible and applicable in use for photoelectrode of DSSC architecture.

(EMA-S11-P039-2016) EMI noise suppression material for the band of 3 ~ 6GHz

S. Kim*[1]; Y. Yun[1]; S. Park[1]; 1. Changsung Corporation, The Republic of Korea

High-frequency EMI radiated by electronic devices, noise above 1GHz, is attracting increased scrutiny, reports variety Journal. Revisions to EMI standards have expanded the scope of regulated frequencies into the GHz waveband. To start, regulations on EMI up through 6GHz will be implemented in Europe and Japan in October 2010 for printers and certain other items. In this work, we have examined the effect of alloy composition, crystal structure, milling condition for flake and annealing condition in Fe-based soft magnetic powder/polymer composite sheets available for the frequency range of 1~6 GHz. We made the four type of Fe-based powder, Fe-Al, Fe-Si-, Fe-Si-Cr(1), Fe-Si-Cr(2). All of the Fe-based powders were mechanically milled to flake and annealed 300~600°C. The crystal structure and crystal size of each Fe-based powder was determined by XRD analysis. And the grain size calculated using Scherrer Equation. Magnetic permeabilities of composites sheets were measured using an impedance analyzer(Agilent 4291B). Frequency dependency of magnetic permeability was measured from 45 MHz~6 GHz. As a result Fe-Si-Cr(2) powder showed the best performance for the frequency range of 1~6 GHz. After milling flake size is 40 ~ 60 um and annealing temperature were most excellent permeability properties at 500°C.

(EMA-S11-P040-2016) Electrical and microstructural properties of $Ni_{0.5}Co_{0.5}Cu_{0.15}Mn_{1.85}O_4$ NTC thermistors by doping 0.1 mol B_2O_3 without calcination

G. Hardal[1]; B. Yuksel Price*[1]; 1. ISTANBUL UNIVERSITY ENGINEERING FACULTY, Turkey

The aim of this work is to investigate the effect of B_2O_3 addition as sintering aid to the electrical and microstructural properties of $Ni_{0.5}Co_{0.5}Cu_{0.15}Mn_{1.85}O_4$ thermistors fabricated by the conventional solid-state reaction method without calcination. High purity NiO, Co_3O_4, CuO, Mn_2O_3 and H_3BO_3 (as a source of B_2O_3) powders were weighed and the powder mixtures were ball-milled using ZrO_2 balls as a grinding media with ethyl alcohol in a jar for 6 hrs. The obtained slurries were dried and only $Ni_{0.5}Co_{0.5}Cu_{0.15}Mn_{1.85}O_4$ powders were calcinated at 900°C for 2 hrs. The disc shaped samples were sintered at 1100°C for 5 hrs in air. The bulk density of the sintered samples were calculated from their weights and dimensions. The electrical resistance was measured in a temperature programmable furnace between 25°C and 85°C. The microstructure of samples was observed using scanning electron microscopy. The resistance of samples was logged every 0.1°C and the plots of log ρ versus 1000/T for the samples were generated. The material constant "B" and sensitivity coefficient "α" values were calculated for the NTC thermistors. This study is supported by TÜBITAK (The Scientific and Technical Research Council of Turkey), Project number 3001-114M860. We would like to thank TÜBITAK for its financial support.

(EMA-S11-P041-2016) Temperature Stable Dielectrics Based on $BaTiO_3$-$Bi(Zn_{1/2}Ti_{1/2})O_3$-$BiScO_3$-$NaNbO_3$

C. S. McCue*[1]; 1. Oregon State University, USA

High performance dielectric materials are needed for high power SiC- or GaN-based electronics which combine the best features of high energy density, low dielectric loss and high reliability. To achieve ceramic capacitors with temperature-stable permittivity characteristics, lead-free perovskite ceramic solid solutions were investigated with the aim of achieving a temperature coefficient of relative permittivity near zero. Samples were synthesized from oxide and carbonate precursors and calcined in air at temperatures ranging from 700 to 900°C and sintered in air at temperatures ranging from 1050 to 1150°C. This work involves the synthesis and characterization of compositions based on the compound $BaTiO_3$-$Bi(Zn_{1/2}Ti_{1/2})O_3$ along with additives $BiScO_3$ and $NaNbO_3$. These materials have excellent temperature stable dielectric properties due to a relaxor dielectric mechanism which is derived from cation disorder. Initial results focused on the $BaTiO_3$-$Bi(Zn_{1/2}Ti_{1/2})O_3$-$BiScO_3$-$NaNbO_3$ quaternary system show a minimal temperature dependence with a temperature coefficient of permittivity (TCe) as low as -387 ppm/°C and a transition temperature near 0°C. Future work involves compositional modifications aimed at increasing the relative permittivity which would allow device miniaturization as well characterization of the dielectric properties at high electric fields (E > 100 kV/cm).

(EMA-S11-P042-2016) Dielectric analyses and conduction mechanisms in $Bi_{4-x}La_xTi_3O_{12}$ based Aurivillius type ferroelectric ceramics

I. Cruvinel dos Reis*[1]; A. Carvalho da Silva[1]; A. S. Bhalla[2]; R. Guo[2]; J. de los Santos Guerra[3]; 1. Universidade Estadual Paulista, Brazil; 2. The University of Texas at San Antonio, USA; 3. Federal University of Uberlandia, Brazil

The studies of the dielectric and ferroelectric properties of bismuth layer structured ferroelectrics (BLSF), well known as Aurivillius' family compounds, has received special attention in the last decades because of their potential for practical application. These systems can be represented by the formula $[Bi_2O_2]$ $(A_{m-1}B_mO_{3m+1})$, where m is the number of layers of perovskite (BO_6 octahedron) sandwiched between two plates of $[Bi_2O_2]^{2+}$. It has been found that physical properties can be modulated by modifying either the *A*- or *B*-site with doping elements, such as rare earth ions. In this work, the doping effects on the structural, microstructural and dielectric properties of bismuth layer structured $Bi_4Ti_3O_{12}$ (BIT) ferroelectric ceramics has investigated in details. In particular, the *A*-site cation substitution of Bi^{2+} by La^{3+} has been considered. It has been found that the physical properties of the studied $Bi_{4-x}La_xTi_3O_{12}$ (BLT) system are strongly affected by the doping content. The characteristics of the phase transition have been investigated from the dielectric response, in a wide temperature and frequency range. The authors would like to thank CNPq, CAPES and FAPEG Brazilian agencies and INAMM/NSF (Grant No. 0884081) for the financial support.

(EMA-S11-P043-2016) A critical strain failure criterion of a silver nanowire electrode for highly flexible devices

D. Kim[1]; S. Kim[1]; J. Ahn[1]; S. Kim*[1]; 1. Korea Institute of Science and Technology, The Republic of Korea

With recent increasing demand on flexible displays (FDs) for mobile electronic devices, the development of flexible electrodes has been accelerating from a curved device to wearable and foldable devices. As these FDs are under various stress states, the developers of the FDs have used the threshold radius of curvatures (ROCs) of the FDs as a failure criterion, which have shown a trend towards reduction from 10 mm for the bendable to less than 5~3 mm for the rollable and foldable. In this work, we have reported the in-situ tensile and buckling characteristics of a 5-fold Ag NW providing the threshold ROC as a failure criterion for evaluating the conductive electrodes of FDs under various stress modes. The individual Ag NW in the tensile mode failed with little plastic deformation at the intrinsic yield strain of average 2%, which is corresponding to the threshold ROC of 0.5~5 mm of the transparent electrodes causing a 10% increase of sheet resistance. Under the in-situ compressive loading-unloading, the individual Ag NW exhibits cyclic buckling characteristics without failure up to the threshold ROC of 1.1~2.4 μm, corresponding to the buckling yield strain of 2.7~5.2%. The extended yield strain of the electrodes can provide higher flexibilities for the application of futuristic FDs, in the buckling mode rather than the tensile mode.

(EMA-S11-P044-2016) Unusual Near-field Electromagnetic Absorption Attenuation in Transparent Flexible Graphene

S. Kim*[1]; J. Kang[2]; Y. Kim[3]; J. Choi[4]; B. Hong[3]; 1. Korea Institute of Science and Technology, The Republic of Korea; 2. Northwestern University, USA; 3. Seoul National University, The Republic of Korea; 4. Sungkyunkwan University, The Republic of Korea

Recently, the widespread use of mobile devices and wireless networks has created unintentional electromagnetic fields, which can cause various disturbances in integrated circuits. Here, we report unusual magnetic wave absorption attenuation in ultra-thin, lightweight, flexible, and transparent graphene films grown by chemical vapor deposition in a near-field magnetic field. The experimental and simulated results of the magnetic field transmission loss characteristics exhibit two orders greater shielding attenuation of electromagnetic interference (EMI) normalized to the film thickness than those of conventional EMI shielding or absorbing materials over frequency ranges of 0.1 to 6 GHz, which have not been achieved at an atomic layer thickness, which is much less than skin depth. The unique characteristic of graphene films result in the peculiar properties of excellent conductance and absorbance for electromagnetic radiation, which enable broad range applications, including telecommunications, aerospace, and next-generation transparent, flexible electronics.

(EMA-S11-P045-2016) Electronic and Chemical Characterization of Barium Titanate Interfaces

D. Long*[1]; 1. North Carolina State University, USA

Barium Titanate is an industrially important dielectric which is used heavily in multi-layer ceramic capacitors(MLCCs). Often an elemental metal electrode such as Nickel is used in the MLCCs to reduce the cost of the capacitors. Due to the ease of oxidation of the nickel electrode, the green body MLCC must be fired in a reducing environment to avoid oxidation of the nickel. Here we present the electronic band alignment and chemistry of the barium titanate/nickel and barium titanate/nickel oxide interfaces. The interfaces were investigated using X-Ray Photoelectron Spectroscopy. The schottky barriers which play a critical role in the leakage current, and thus the effectiveness, of the MLCC were studied in situ during the interface formation and were found to be similar to those found in Stronium Titanate. The BTO/NiO interface showed the highest electron barriers ie. lowest fermi level ever reported for STO and BTO interfaces and the deposition of the nickel and nickel oxide did not reduce the substrate. These results will be utilized to study dielectric breakdown in extreme environments of high temperatures and high electric fields.

(EMA-S11-P046-2016) Study of $Ge_2Sb_2Te_5$ properties for opto-electronic applications

G. Rodriguez Hernandez*[1]; P. Hosseini[1]; H. Bhaskaran[1]; 1. University of Oxford, United Kingdom

Phase change material $Ge_2Sb_2Te_5$ (GST) has been recently highlighted as an ideal candidate for the development of novel opto-electronic applications because its optical and electrical properties change when the material switches between the amorphous and crystalline phases. Also because the phase transition is very fast, non-volatile and can be induced by optical or electrical pulses. However, during the phase change, the evolution of the optical and electrical properties follow different trends. Understanding the relationship between the evolution of both properties, is key for the development of opto-electronic applications. In this study we examine the evolution of reflectivity and electrical resistance of GST when the crystallization is induced by either optical or electrical pulses. For this purpose, we designed a crossbar nano-device with transparent electrodes that allows us to have optical and electrical access to a thin film of GST contained between the electrodes. Results indicate that during crystallization, factors like the device thermal profile, applied electric field, and pulse characteristics have an effect on the way the reflectivity and resistance evolve with respect to each other. We suggest that such factors influence the direction of crystallization of the GST in the device, and that accounts for the variations in the evolution of the reflectivity and resistance observed.

(EMA-S11-P047-2016) Effect of the Fe and Mn Doping on The Piezoelectric Properties of 94NBT-6BT Single Crystal

A. Dogan*[1]; M. Gurbuz[2]; 1. Anadolu University, Turkey; 2. Ondokuz Mayis University, Turkey

There is an enormous interest on lead free piezoelectric ceramics because of environmental regulations that may be effective in near future. Therefore, synthesis and characterization of new lead free piezoelectric materials are necessary for various applications. NBT-BT based compositions are one of the important candidates in this field. Especially $94Na_{0.5}Bi_{0.5}TiO_3$-$6BaTiO_3$ (94NBT-6BT) ceramics may be an alternative to lead containing ceramics. In this study, 94NBT-6BT single crystals were grown by flux growth method. X-ray diffraction (XRD), energy dispersive X-ray (EDX) and X-ray fluorescence (XRF) technique were used to characterize crystal structure and chemical composition of grown crystals. Influences of the some dopant such as Li, Fe and Mn on dielectric and leakage current characteristics of the grown single crystals were analyzed by impedance/gain phase analyzer, LCR meter, AIXACT (aixPES/CMA) piezoelectric and ferroelectric analyzer. From the results, Mn doped single crystals showed better dielectric and leakage current properties than other single crystals.

(EMA-S11-P048-2016) Effect of glass doping on the Initial permeability of microwave sintered MgCuZn Ferrites

W. Madhuri*[1]; S. K.V.[3]; S. Srigiri[2]; 1. VIT University, Vellore, India; 2. University of New Orleans, USA; 3. Sri Krishnadevaya University, India

Lately ferrites find applications as multilayer chip inductor (MLCI) cores. During the MLCI fabrication the core has to be sintered with an internal electrode like silver. The sintering temperature of ferrites can be reduced in many ways. In the present study two techniques are simultaneously used for the purpose vice doping of glass and choosing to sinter using microwaves. Undoped and lead borosilicate glass doped MgCuZn ferrites with generic formula $Mg_{0.5}Cu_xZn_{0.5-x}Fe_2O_4$ at x = 0.05-0.3 were synthesized by conventional solid state reaction route and were characterized for structural, surface and magnetic properties. From X-ray diffraction studies it was found that all the undoped and glass doped samples were single phase spinel structure. Glass doped MgCuZn Ferrites samples exhibited

lower permeabilities than that of undoped MgCuZn Ferrites. A flat frequency response was observed in the glass doped $Mg_{0.5}Cu_xZn_{0.5-x}Fe_2O_4$ samples at x = 0.1 and 0.2.

(EMA-S11-P049-2016) Optimization of the Morphology of VOC Sensors Based on Polymer-metal Nanocomposites

N. Zerihun*[1]; 1. Addis Ababa Institute of Technology, Ethiopia

The current work involves fabrication, characterization, evaluation and subsequent optimization of Poly(methyl methacrylate) (PMMA) thin polymer films coated with gold nanoparticle sensors for detecting analytes of Volatile Organic Compounds (VOCs). For VOC sensors based on polymer/metal nanocomposites, the morphology of clusters, i.e. the cluster size and density principally affects the sensing property. And the morphology of clusters is a function of the method of production and process parameters. An optimum polymer film thickness of 100 nm deposited by spin coating gives the highest sensitivity and reversibility. By varying the polymer/metal nanocomposites' synthesis conditions in terms of thermal evaporation and sputtering, the sensing performances of the PMMA-gold nanocomposite sensors were systematically optimized. The morphology of clusters prepared at different synthesis conditions was systematically investigated by high resolution Transmission Electron Microscopy (TEM). Based on the TEM investigation and response signal, an optimum condition for VOC sensor manufacturing lies in nanoampere current region.

Thursday, January 21, 2016

Plenary Session

Plenary II

Room: Indian

8:40 AM

(EMA-PL-002-2016) The Materials Genome Initiative: NIST, Data, and Open Science

J. A. Warren*[1]; 1. National Institute of Standards and Technology, USA

In this talk I will present an overview of the Materials Genome Initiative, covering the current and planned efforts across the Federal government. After an overview where I will provide insight into community-led activities, I will discuss our attempts at NIST to address some of challenges to creating the materials innovation infrastructure that lies at the heart of the Materials Genome Initiative. In particular NIST is now devoting considerable effort, in concert with its partners in industry, academia and government, to develop the tools, standards and techniques for (i) establishing model and data exchange infrastructure (ii) establishing best practices and new methods for ensuring data and model quality and (iii) developing the Big Data analytics to enable "data driven" materials science. To properly address these problems involves a deeper examination of the nature of materials data than is typical. In particular, the essential linkage between models and measurements implies that many of the conceptual challenges with materials data can be most efficiently resolved using methods that address the role of materials models as the core concept of the scientific method. This insight, and associated examinations of the manner in which we collect and disseminate data are the keys to overcoming the impediments to a materials innovation infrastructure.

S1. Multiferroic Materials and Multilayer Ferroic Heterostructures: Properties and Applications

Theory, Modeling, Materials Design II

Room: Coral A

Session Chairs: Pamir Alpay, University of Connecticut; Tulsi Patel, University of Connecticut

10:00 AM

(EMA-S1-013-2016) Functional superlattices from first principles (Invited)

K. M. Rabe*[1]; 1. Rutgers University, USA

Recent dramatic progress in the experimental synthesis and characterization and theoretical analysis of atomic-scale superlattices has revealed the rich physics of these systems. One notable feature is that ultrathin layers of complex-oxide compounds can, in a superlattice, exhibit novel nonbulk structure and functional properties, including metal-insulator transitions, magnetic ordering, ferroelectricity and multiferroicity, and dielectric and piezoelectric enhancement, leading to novel properties for the superlattice as a whole. In addition, distinctive properties of a superlattice system can be generated by the symmetry breaking of the superlattice layering and by atomic and electronic reconstruction at the interfaces. In this talk, I will present recent results for prototypical superlattices obtained from first-principles calculations and construction of first-principles-based models, and discuss progress and challenges in theoretical-experimental integration.

10:30 AM

(EMA-S1-014-2016) Are Ferroelectric Multilayers Capacitors in Series?

F. Sun[1]; T. Kesim[1]; Y. Espinal*[1]; P. Alpay[1]; 1. University of Connecticut, USA

We show that ferroelectric multilayers are not simple capacitors in series (CIS) and treating these as CIS may lead to misinterpretation of experimental results and to erroneous conclusions. Here, we present a theoretical model of ferroelectric bilayers using basic thermodynamics taking into account the appropriate electrical boundary conditions and electrostatic fields. The spontaneous polarization mismatch in ferroelectric/ferroelectric (FE/FE), FE/paraelectric (FE/PE), and FE/dielectric (FE/DE) bilayers results in a non-linear electrostatic coupling which produces significant deviations in the overall dielectric response if it is computed using the simple capacitor-inseries (CIS) model. Our results show that the CIS approach is a good approximation only for DE/DE multilayers and for FE heterostructures if the individual layers are electrostatically screened from each other.

10:45 AM

(EMA-S1-015-2016) Giant Enhancement in the Ferroelectric Field Effect Using a Polarization Gradient

Z. Gu*[1]; M. Islam[2]; J. E. Spanier[1]; 1. Drexel University, USA; 2. State University of New York @ Oswego, USA

Coupling of switchable ferroelectric polarization with the carrier transport in an adjacent semiconductor enables a robust, non-volatile manipulation of the conductance in a host of low-dimensional systems, including the two-dimensional electron liquid that forms at the $LaAlO_3$-$SrTiO_3$ interface. However, strength of the gate-channel coupling is relatively weak, limited in part by the electrostatic potential difference across a ferroelectric gate. Here, through application of phenomenological Landau-Ginzburg-Devonshire theory and self-consistent Poisson-Schrödinger model calculations, we show how compositionally grading of $PbZr_{1-x}Ti_xO_3$ ferroelectric gates enables a more than twenty-five-fold increase in the LAO/STO channel conductance on/off ratios. Incorporation of polarization

gradients in ferroelectric gates can enable breakthrough performance of ferroelectric non-volatile memories.

11:00 AM

(EMA-S1-016-2016) Extraordinary transmission of terahertz pulses through subwavelength aperture array: The role of thin $Ba_{0.6}Sr_{0.4}TiO_3$ film (Invited)

D. Shreiber*[1]; M. P. Ivill[1]; S. A. Ponomarenko[2]; J. Reeves[3]; M. Cole[1]; 1. US Army Research Laboratory, USA; 2. Dalhousie University, Canada; 3. Menlo Systems, USA

The discovery of extraordinary transmission of light through thin metal gratings of subwavelength holes has generated extraordinary interest in surface plasmonics where surface plasmon polaritons (SPP), the hybrid photon-electron surface modes, play a central role. Specifically, the SPP tunneling through the holes and their coupling to outgoing radiating waves on the other side of the metal film generate extraordinary transmission through the sub-wavelength diameter holes. We experimentally discover that the presence, position and continuity of a thin (200 nm) $Ba_{0.6}Sr_{0.4}TiO_3$ (BST) coating with a large dielectric constant strongly influence the magnitude of spectral maxima of terahertz pulses transmitted through a periodic array of subwavelength apertures perforated in a metal foil. The dielectric films were deposited by RF Magnetron sputtering either on the entrance or the exit side of the foil, or else it was absent at all. One sample under investigation contained a continuous thin film whereas the other one was discontinuous. The three cases give rise to quantitatively different transmitted spectra for both samples. We provide a qualitative explanation of the counterintuitive transmission amplification effect due to the presence of thin discontinuous dielectric coating with high dielectric constant.

11:30 AM

(EMA-S1-017-2016) Polarization nanodomains in ferroelectric/dielectric superlattice nanostructures (Invited)

P. G. Evans*[1]; Q. Zhang[1]; J. Park[1]; Y. Ahn[1]; M. Dawber[2]; R. Harder[3]; M. Holt[3]; 1. University of Wisconsin, USA; 2. Stony Brook University, USA; 3. Argonne National Lab, USA

Polarization domain patterns form spontaneously in ferroelectric/dielectric superlattices as a result of the competition of depolarization and domain wall energies. In ferroelectric $PbTiO_3$- dielectric $SrTiO_3$ superlattices, such domain patterns are highly disordered, characterized by a short-coherence length motif. The domain pattern is of scientific interest at both the atomic scale, at which polarization vortex structures have been recently observed, and at longer scales where the dynamics of the domain pattern in applied electric fields are beginning to be explored. We have previously used a series of synchrotron x-ray nanobeam measurements to probe the structural and domain dynamics phenomena associated with $PbTiO_3$-$SrTiO_3$ superlattices in applied electric fields. The results reveal important aspects of the domain dynamics, but highlight the need to develop probes for the microscopic configuration of domains rather than the average parameters of their arrangement. Here we show that x-ray scattering studies conducted using x-rays with a high degree of transverse coherence are sensitive to the exact (rather than average) arrangement of domains, and that such probes can be used to study the response of domain patterns to the mechanical constraint imposed by nanostructures patterned into the superlattice thin film.

12:00 PM

(EMA-S1-018-2016) Probing the interfacial phases of correlated oxides controlled by ferroelectric polarization

T. Meyer*[1]; A. Herklotz[1]; S. Lee[1]; L. Jiang[1]; V. Lauter[1]; M. Fitzsimmons[1]; T. Ward[1]; H. Lee[1]; 1. Oak Ridge National Laboratory, USA

The term 'interface' in oxide heterostructures has become a ubiquitous tool for discovering novel properties and phenomena not observed in bulk materials. In fact, many would claim that controlling and understanding the interface is essential for the advancement and fabrication of new devices. Here, we use polarized neutron reflectivity to explore the detailed magnetic structure of ferromagnetic, $La_{0.8}Sr_{0.2}MnO_3$ (LSMO) and ferroelectric $PbZr_{0.2}Ti_{0.8}O_3$ (PZT) heterostructures. We find that the addition of PZT has the capability to both deplete and accumulate holes at its interface with LSMO depending upon the polarization direction. Specifically, we have determined that the suppressed magnetization common to the manganite-air interface can be enhanced if the polarization in PZT is oriented in a way to accumulate holes. Through these carefully designed heterostructures, we show that field effect doping is an efficient and powerful method to effectively tune the hole concentrations and phase diagrams of a wide range of materials. This work was supported by the U.S. Department of Energy, Office of Science, Basic Energy Sciences, Materials Sciences and Engineering Division.

12:15 PM

(EMA-S1-019-2016) Electric–field tunable filters on strain–engineered oxides

N. D. Orloff*[1]; X. Lu[1]; H. Nair[2]; N. Dawly[2]; D. Schlom[2]; J. Booth[2]; 1. NIST, USA; 2. Cornell University, USA

Demand for mobile data, the implementation of new wireless devices, and an explosion of mobile users has stressed our current telecommunications infrastructure to its limits. Naturally, engineers have pushed existing devices and networks to ever-increasing frequencies and more complicated channel access methods in an effort to address this multifaceted problem. With the march to higher frequencies and evolution of frequency agile components, there is a growing clamor that conventional materials are not up to the challenge. Recent advances in strain-engineered oxides—specifically, the $Sr_{n+1}Ti_nO_{3n+1}$ Ruddlesden-Popper series of phases—showed remarkably low dielectric loss and high tunability at microwave frequencies up to 125 GHz. Here, we develop filters based on a $Sr_7Ti_6O_{19}$ (n = 6) Ruddlesden-Popper thin-film commensurately strained on a (110) $DyScO_3$ substrate. At room temperature, our devices showed a frequency tunability of 5 % with an insertion loss of 4 dB. We then explored how tunability and tuning speed changed for temperatures between 150 K and 300 K. These experiments are our first step to explore how these materials might be used in frequency agile components in next generation wireless systems, potentially allowing a single component to tune the operating frequency between the operating bands of today and the available bands of the near future in less than a microsecond.

S2. Functional Materials: Synthesis Science, Properties, and Integration

Functional Materials: Integration, Measurement, and Property Enhancement in Piezoelectric Thin Films and Ceramics

Room: Mediterranean A

Session Chair: Mark Losego, Georgia Institute of Technology

10:00 AM

(EMA-S2-018-2016) Optimization of IrO_2 as a top electrode for PZT devices

M. Rivas*[1]; D. M. Potrepka[2]; B. Huey[1]; R. G. Polcawich[2]; 1. University of Connecticut, USA; 2. US Army Research Laboratory, USA

Iridium Oxide (IrO_2) is a promising substitute for platinum (Pt) as a top electrode on current lead zirconate titanate (PZT) based piezoelectric microelectromechanical systems (PiezoMEMS) devices due to its thermal stability, reliability performance, and ability to prevent hydrogen diffusion. Preliminary project data shows that changing the oxygen flow during sputter deposition has an impact on IrO_2 sheet resistance and structure. IrO_2 with nominal thickness of 100

nm was deposited onto 500 nm thick PZT films with a Zr/Ti ratio of 52/48. The IrO_2 was deposited using an O_2 flow of 0-80 sccm at 1 kW power, 100 sccm Ar flow, and substrate temperatures (T_s) of 40 °C and 500 °C. X-Ray Diffraction, Four Point Probe, Atomic Force Microscopy, and Scanning Electron Microscopy are used to obtain material orientation, sheet resistance (Rs), surface roughness, and microstructure respectively of the IrO_2 both for pre and post 650 °C anneals in flowing O_2. To analyze the impact of the IrO_2 as a top electrode, the ferroelectric, dielectric, and piezoelectric properties of the PZT films were analyzed using a combination of polarization, capacitance, and displacement measurements, each versus electric field. The deposition process, the impact of the O_2 flow, and T_s on the overall characterization data for IrO_2 films, as well as the resulting comparison between Pt and IrO_2 top electrodes for PZT will be discussed.

10:15 AM

(EMA-S2-019-2016) Optimization of IrO_2 as a bottom electrode for PZT devices

D. M. Potrepka*[1]; M. Rivas[2]; G. R. Fox[3]; R. G. Polcawich[1]; 1. U.S. Army Research Laboratory, USA; 2. University of Connecticut, USA; 3. Fox Materials Consulting, LLC, USA

Iridium Oxide (IrO_2) is a promising substitute for platinum (Pt) as a bottom electrode on current lead zirconate titanate (PZT) based piezoelectric microelectromechanical systems (PiezoMEMS) devices due to its thermal stability, reliability, and ability to prevent hydrogen diffusion. Preliminary project data shows that changing the O_2 flow during sputter deposition impacts IrO_2 sheet resistance (R_s) and crystalline texture. To compare with a documented Pt/TiO_2 electrode, 100 nm IrO_2 was deposited onto 30 nm TiO_2 films using an O_2 flow of 0-80 sccm at 1 kW power, 100 sccm Ar flow, and substrate temperatures (T_s) of 40 °C and 500 °C. X-Ray Diffraction, Four Point Probe, AFM, and SEM are used to obtain Lotgering Factor, Rs, surface roughness, and microstructure respectively of the IrO_2 for pre and post 650 °C anneals in 3 SLM O_2. To analyze IrO_2 as a bottom electrode, 500 nm PZT with a Zr/Ti ratio of 52/48 was deposited via chemical solution deposition. A Pt top electrode was sputter deposited onto the PZT film. Capacitor and cantilever structures were fabricated and the PZT ferroelectric, dielectric, and piezoelectric properties were analyzed using polarization, capacitance, and displacement measurements, each versus electric field. The deposition process, impact of O_2 flow and T_s on the characterization data for IrO_2 films, and comparison between Pt and IrO_2 bottom electrodes for PZT will be discussed.

10:30 AM

(EMA-S2-020-2016) PiezoMEMS with Integrated Electronics

S. Trolier-McKinstry*[1]; 1. Pennsylvania State University, USA

The integration of electronics with piezoMEMS enables a wide variety of applications, including adjustable & reconfigurable surfaces, conformal actuators, self-powered electronics, and replacement of conventional semiconductor chips with a far more energy efficient computation methodology. This, in turn, should boost the functionality of a wide variety of systems, by providing large, readily controlled displacements, increasing the charge collection efficiency for energy scavenging for unattended sensors, and facilitating efficient computation/storage at local nodes in low-power networks. Among the systems being investigated are: - Arrays of low voltage, high energy density actuators for low power electronics, including the mirror segments for X-ray telescopes. - High efficiency, lightweight energy harvesters for self-powered sensing and actuation systems - Flexible hybrid electronics, including ultrasound systems

10:45 AM

(EMA-S2-021-2016) Effect of Mechanical Constraint on Ferroelectric/Ferroelastic Domain Reorientation in {111} Textured Tetragonal Lead Zirconate Titanate Films

G. Esteves*[1]; M. Wallace[2]; R. Johnson-Wilke[3]; C. Fancher[1]; R. Wilke[3]; S. Trolier-McKinstry[2]; J. L. Jones[1]; 1. North Carolina State University, USA; 2. The Pennsylvania State University, USA; 3. Sandia National Laboratory, USA

The piezoelectric properties of $PbZr_xTi_{1-x}O_3$ are a function of the film crystallographic texture. Ferroelectric/ferroelastic domain reorientation was measured in 2.0 µm thick tetragonal {111} textured thin films using synchrotron X-ray diffraction (XRD). Lattice strain from the peak shift in the 111 Bragg reflection, $\%\varepsilon_{111}$, and domain reorientation were quantified as a function of applied electric field amplitude. Domain reorientation was quantified through the intensity exchange between the 112 and 211 Bragg reflections. Results from three different film types are reported: dense films that are clamped to the substrate (as-processed), dense films that are partially released from the substrate, and films with 3 % volume porosity. The highest amount of domain reorientation is observed in grains that are misoriented with respect to the {111} texture. Relative to the clamped films, films that were released from the substrate or had porosity exhibited no significant enhancement in domain reorientation and $\%\varepsilon_{111}$. In contrast, similar experiments on {100} textured and randomly oriented films showed significant enhancement in domain reorientation in released and porous films. Therefore, {111} textured films become less susceptible to mechanical constraint due to a decrease in domain reorientation contribution to the overall film's response.

11:00 AM

(EMA-S2-022-2016) Misfit strain phase diagrams and piezoelectric properties of (001) PMN-PT epitaxial thin films

N. Khakpash*[1]; H. Khassaf[1]; G. Rossetti[1]; P. Alpay[1]; 1. University of Connecticut, USA

Misfit strain-temperature phase diagrams of three compositions of (001) pseudocubic $(1-x)Pb(Mg_{1/3}Nb_{2/3})O_3$-$xPbTiO_3$ (PMN-PT) thin films are computed using a phenomenological model. Two compositions (x = 0.30, 0.42) are located near the morphotropic phase boundary (MPB) of bulk PMN-PT at room temperature and one composition (x = 0.70) is located far from the MPB. The variation of the crystallographic anisotropy of polarization with misfit strain and temperature reveal that it is possible to stabilize an adaptive monoclinic phase having a stability region that is much larger than that predicted for barium strontium titanate (BST) and lead zirconate titanate (PZT) films under equivalent conditions. As a result, compositions far away from the MPB are also predicted to have large piezoelectric coefficients, of the order of hundreds of pm/V, which can be achieved by carefully engineering the magnitudes of in-plane strains.

11:15 AM

(EMA-S2-023-2016) Analog Memory Storage using a Ferroelectric Capacitor

J. T. Evans*[1]; 1. Radiant Technologies, Inc., USA

A functional memory storing analog states in a ferroelectric capacitor is described. A ferroelectric capacitor has an almost infinite number of remanent polarization states it may assume between positive and negative saturation states. Analog memories utilizing ferroelectric remanent polarization have been proposed in the past but analog memory storage and retrieval has proven difficult to implement in real-world capacitors. The typical approach is to use a programming voltage tuned to an intermediate remanent polarization state within the switching regime of the capacitor. This approach is rendered ineffective by the tendency of ferroelectric capacitors to change their coercive voltages between actuations. A more effective approach is to meter charge into the capacitor starting

from a known charge state. Charge transfer circuits will move the assigned charge value independent of the required voltage, eliminating the impact of drifting coercive voltage values. An autonomous memory circuit consisting of a conductive load, the ferroelectric capacitor, and a current controlled switch such as a bipolar transistor or a current mirror FET pair will implement such a charge transfer scheme. The circuit can operate from the microsecond time range to the millisecond time range by adjusting component values. Such a single analog memory bit can operate within a dedicated IC memory circuit or independently as a discrete circuit.

11:30 AM

(EMA-S2-024-2016) Simultaneous Electrical and Piezoelectric Characterization of PiezoMEMS Structures via PUND Plus Laser Doppler Vibrometry

R. G. Polcawich*[1]; R. Rudy[1]; M. Rivas[1]; G. R. Fox[2]; 1. US Army Research Laboratory, USA; 2. Fox Materials Consulting, USA

In the continued advancement of piezoelectric MEMS (PiezoMEMS) technology, one area of interest is conveniently evaluating the piezoelectric quality of the material. Specific to ferroelectric materials, such as lead zirconate titanate (PZT), is evaluating both the ferroelectric and piezoelectric quality of the material. To accomplish this task in a simultaneous measurement, one can leverage the pulse switching measurement (PUND) developed for evaluating ferroelectric random access memory (FeRAM) and combine it with monitoring the out-of-plane displacement of piezoelectric actuators using laser Doppler vibrometry (LDV). For this measurement, a Polytec LDV is used to measure the displacement of the actuator while the electrical output from the pulse switching measurement is captured using an oscilloscope. Through this measurement, the pulse switching characteristics can be evaluated along with the strain induced displacement performance of the actuator. Currently, this technique is being used to evaluate the effects of Pt and IrO_2 electrodes on PZT based thin film actuators, the effect of radiation exposure on PiezoMEMS devices, and evaluating the long term reliability of PiezoMEMS actuators.

11:45 AM

(EMA-S2-025-2016) Negative Pressure and Property Enhancements in Free Standing Particles

J. Wang[2]; L. McGilly[1]; X. Wei[1]; T. Sluka[1]; N. Setter*[1]; 1. EPFL, Switzerland; 2. Tsinghua University, China

Strain engineering is commonly used for property enhancement. E.g., Ge doping results in stretched lattice of Silicon, enhancing electron mobility. Less common is strain engineering in freestanding functional elements. We report on the creation of negative pressure (tension), sustained during years, in freestanding ferroelectric particles. The material shows strongly enhanced properties: Curie temperature, spontaneous polarization, and piezoelectric activity. To obtain negative pressure we do the following: We use materials that undergo solid-solid phase transformation in which the final phase has a higher density than the initial phase, in parallel exploiting conditions during the transformation that prevent the transformed structure from relaxation. Thus we prepared nanowires of the PX phase of $PbTiO_3$ by hydrothermal route; the low-density PX phase was converted to the high-density ferroelectric perovskite phase by heating in air. This conversion requires catalytic oxygen, which diffuses from the surface into the particle. Because the conversion of the outer shell precedes that of the inner part, the inner part cannot relax during the conversion and remains stretched, resulting in highly enhanced properties. The process may work on a large range of materials to potentially produce a variety of nano- and micro-structures with properties enhanced by negative pressure.

12:00 PM

(EMA-S2-026-2016) Control of properties by modification of phase distribution and microstructure in high temperature piezoelectrics

B. Kowalski*[1]; A. Sehirlioglu[1]; 1. Case Western Reserve University, USA

In recent years there has been an increased interest in high temperature piezoelectrics, usually in a morphotropic phase boundary (MPB) region, to provide enhanced dielectric and electromechanical properties, for utilizing the converse effect in terrestrial and aerospace applications. Properties can be manipulated through substitution on the A- and/or B-site cations, controlling grain size, or introduction of secondary phases. Sintering to a similarly high density can be achieved at a range of temperatures for a given material system; however with a variety of properties due to microstructure, compositional heterogeneities, and core-shell structure. The work that will be presented focuses on investigating the effects of processing temperature on the phase distribution in the MPB region, and the related changes in properties. Material systems studied contains $BiScO_3$, $PbTiO_3$, and $Bi(Zn_{0.5}Zr_{0.5})O_3$ with a mixed rhombohedral and tetragonal phase mixture at the MPB region; the ratio of which dictates resultant properties. For example, lowering the sintering temperature from 1100°C to 1000°C increases the rhombohedral content of phase distribution for a given MPB composition; properties improve with d_{33} increasing from 473 pm/V to 570 pm/V and the planar coupling factor (k_p) from 0.39 to 0.42.

12:15 PM

(EMA-S2-027-2016) Perovskite-type materials for energy converters

A. Weidenkaff*[1]; W. Xie[1]; M. Widenmeyer[1]; X. Xiao[1]; 1. Universität Stuttgart, Germany

Perovskite-type oxides, half-Heusler compounds as well as their nanocomposites are prospective candidates for energy conversion processes [1-3]. The relation between sample preparation methods, microstructure, and properties are studied to design high efficiency materials and devices. Their good performance can be explained based on e.g. their suitable band structures, adjusted charge carrier density, effective mass and - mobility, hindered phonon transport, electron filtering potentials, and strongly correlated electronic systems. These properties are tuneable by changing the composition, structure, crystallites size, interfaces and materials combinations with tailor-made scalable synthesis procedures. The resulting improved materials are characterised and tested in diverse energy conversion applications to improve the efficiency and energy density of e.g. photoelectrocatalytic and thermoelectric conversion processes. The goal is to finally utilize the investigated materials to convert solar energy into electricity or fuels.

S5. Multifunctional Nanocomposites

Multifunctional Nanocomposites III

Room: Coral B

Session Chair: Aiping Chen, Los Alamos National Lab

10:00 AM

(EMA-S5-013-2016) Multifunctional Mesocrystal systems for Energy Applications (Invited)

Y. Chu*[1]; 1. National Chiao Tung University, Taiwan

Self-assembled functional mesocrystal systems have fascinated oxide family to next level for decades in addition to conventional heterstructure and superlattice, because it provides degree of freedom to explore condensed matter physics and design coupled multifunctionlities. Recently, of particular interest is the self-assembled perovskite-spinel mesocrystals, covering wide spectrum of promising applications. In this talk, taking care from the fabrication aspect, growth control and mechanisms are discussed thoroughly,

providing researchers a comprehensive bluemap to construct self-assembled functional mesocrystals. Following the fabrication section, the state-of-art design concepts for multifunctionalties are proposed and reviewed by outstanding examples. Summarizing by outlook of this field, we are excitedly expecting this field to rise with significant contributions ranging from scientific value to practical applications in the foreseeable future.

10:30 AM

(EMA-S5-014-2016) Exchange Coupling and Magnetotransport Properties in Multifunctional Heteroepitaxial Oxide Nanocomposites

W. Zhang*[1]; M. Fan[1]; L. Li[1]; P. Lu[2]; A. Chen[3]; Q. Jia[3]; J. MacManus-Driscoll[4]; H. Wang[1]; 1. Texas A&M University, USA; 2. Sandia National Laboratories, USA; 3. Los Alamos National Lab, USA; 4. University of Cambridge, United Kingdom

Multifunctional heteroepitaxial oxide nanocomposite films have emerged as a fascinating paradigm for creating novel states of matter. In vertically aligned nanocomposite (VAN) films, strong correlation between different degrees of freedom and heteroepitaixal vertical interfaces provide another pathway for creating fascinating functionalities. In this talk, we introduce two examples achieved by the ferromagnetic/antiferromagnetic interface coupling in the VAN design. First example is the strong perpendicular exchange bias (PEB) achieved in strained, epitaxial $BiFeO_3$:$La_{0.7}Sr_{0.3}MnO_3$ nanocomposite films. The vertical strain coupling exhibits important effect on the interface structure and the associated PEB effects. Second example is exchange biased magnetotransport in epitaxial NiO:$La_{0.7}Sr_{0.3}MnO_3$ nanocomposite films. The exchange coupling along the vertical interfaces enables a dynamic and reversible switch of the resistivity between two distinct exchange biased states.

10:45 AM

(EMA-S5-015-2016) Synthesis and Characterization of Epitaxial Nanocomposite Films: Effect of Interface on the Functionalities (Invited)

A. Chen[1]; S. Lee[3]; W. Zhang[2]; H. Wang[2]; J. Zhu[1]; J. MacManus-Driscoll[3]; M. Fitzsimmons[1]; Q. X. Jia*[1]; 1. Los Alamos National Laboratory, USA; 2. Texas A&M University, USA; 3. Univ. of Cambridge, United Kingdom

Epitaxial nanocomposite films, in which emerging behavior can be achieved through interfacing different materials at nanoscales, provide a new design paradigm to produce enhanced and/or novel functionalities that cannot be obtained in the individual constituents. In this talk, I will overview our effort to understand, exploit, and control competing interactions of a range of epitaxial nanocomposite metal-oxide films. Using controlled synthesis, advanced probing, and theoretical modeling, we are able to provide a framework to address some key challenges to understand emergent behaviors at oxide interfaces. We will use both superlattices and vertically aligned epitaxial nanocomposites as model systems to illustrate the effect of interfaces on the functionalities (magnetic and ionicproperties) of metal-oxide films.

11:15 AM

(EMA-S5-016-2016) In-situ synchrotron X-ray studies of the synthesis and electrical behavior of In_2O_3-CeO_2 epitaxial nanocomposite thin films

J. A. Eastman*[1]; M. Highland[1]; B. Veal[1]; D. Fong[1]; G. Ju[1]; C. Thompson[2]; P. Zapol[1]; P. Fuoss[1]; H. Zhou[1]; P. Baldo[1]; 1. Argonne National Lab, USA; 2. Northern Illinois University, USA

The growth behavior and electrical properties of In_2O_3 / CeO_2 vertically aligned epitaxial thin film nanocomposites grown on Y_2O_3-stabilized ZrO_2 (YSZ) substrates will be described. Interesting gas sensing and catalytic properties have recently been demonstrated in In_2O_3 / CeO_2 composites, motivating our studies, which focus on understanding the effects of various growth conditions on epitaxial nanocomposite morphology, strain state, and electrical behavior. Films are grown using a magnetron sputter deposition system built for in-situ synchrotron X-ray studies at Sector 12-ID-D of the Advanced Photon Source. By monitoring surface-sensitive locations in reciprocal space during synthesis, the growth rate and growth mode are determined under a range of deposition conditions (e.g., temperature, sputtering power, and composition). Island nucleation and coalescence, as well as phase separation behavior, are characterized by monitoring changes in diffuse X-ray scattering intensity during growth. Computational studies help to explain our observations. Electrical behavior of In_2O_3 / CeO_2 nanocomposite films is measured and compared with the electric field-induced oxygen vacancy doping we recently observed in single phase epitaxial In_2O_3 films grown on YSZ substrates.

11:30 AM

(EMA-S5-017-2016) Memory Devices based on Self-Assembled Materials and Processes (Invited)

J. Lee*[1]; 1. Pohang University of Science and Technology(POSTECH), The Republic of Korea

Device fabrication based on top-down approach will reach its limit due to difficulties in patterning and processes below 10 nm node. The bottom-up approach using self-assembled materials and processes can be a viable candidate for further device scaling, but the fabrication processes are mostly not compatible with current device fabrication. In this presentation, device fabrication strategy for next-generation data-storage devices will be discussed in detail based on self-assembled materials and processes. The emphasis is placed on compatibility with current device fabrication strategies. Ordered array of various materials and systems based on bottom-up nanotechnology can be utilized as the charge storage layer for memory devices and the templates for nanoscale device fabrication. Novel device applications, for example, printed/flexible/transparent electronic devices, will be explored based on the self-assembly processes. Finally, recent research activities related to bio-inspired memory devices will be presented for low-power device applications.

12:00 PM

(EMA-S5-018-2016) Dielectric Nanocomposites for Energy Storage Applications (Invited)

H. Wang*[1]; 1. Xi'an Jiaotong University, China

Dielectric capacitors for energy storage have advantages in fast charge-discharge capability and high power density but their energy densities are at least an order of magnitude lower than that of electrochemical devices, such as batteries and double-layer supercapacitors. Thus the dielectric materials with high energy densities are highly desirable and have been investigated to reduce the size and cost of electric power system. In this presentation, a brief review of the state of arts on the polymer-based nanocomposites for energy storage applications and our recent highlight works that exhibit excellent energy storage properties will be given. With the introduction of ceramic fillers with the studies on filler surface modification, composite structure type tailoring and the interface controlling, the dielectric and energy storage properties of obtained polymer-based nanocomposites have been significantly improved with the optimal combination of high energy density and low dielectric loss. A new kind of advanced material for energy storage capacitors, which has a favorable energy density of 18.8 J cm^{-3} with the breakdown strength of 470 MV m^{-1}, have been achieved by a novel macro-micro structure design of the composite structure as well as the fillers distribution.

S7. Processing and microstructure of functional ceramics: Sintering, grain growth and their impact on the materials properties

Sintering Techniques: Conventional Sintering and Field Assisted Sintering

Room: Caribbean B

Session Chairs: Wolfgang Rheinheimer, Karlsruhe Institute of Technology; Michael Hoffmann, Karlsruhe Institute of Technology

10:00 AM

(EMA-S7-014-2016) Grain Boundary formation and grain growth in the presence of externally applied electric fields (Invited)

K. van Benthem*[1]; 1. University of California, Davis, USA

The application of electric fields can enable the accelerated consolidation of materials during field assisted sintering, such as spark plasma sintering or flash sintering. Although such techniques are already employed for the synthesis of a wide variety of microstructures with unique macroscopic properties, a fundamental understanding of the atomic-scale mechanisms for grain boundary formation and subsequent migration in the presence of electrostatic potentials is mostly absent from the literature. In this presentation we report about our recent in situ transmission electron microscopy studies that were designed to investigate densification and grain growth mechanisms in the absence and presence of electrical fields. Examples for yttrium-stabilized ZrO_2 and $MgAl_2O_4$ spinel will be discussed. This research is supported by the University of California Laboratory Fee Program (12-LR-238313) and the US Army Research Office (program manager: Dr. D. Stepp) under grant W911nf-12-1-0491-0.

10:30 AM

(EMA-S7-015-2016) Microstructure and Variable Chemistry of Flash Sintered $K_{0.5}Na_{0.5}NbO_3$ Ceramics (Invited)

G. Corapcioglu[1]; M. A. Gulgun*[1]; S. Sturm[3]; R. Raj[2]; 1. Sabanci University, Turkey; 2. Univesity of Colorado at Boulder, USA; 3. Jozef Stefan Institute, Slovenia

Sodium Potassium Niobate (KNN) is one of the high temperature candidates among the lead-free piezoelectric ceramics. KNN is the solid solution between ferroelectric $KNbO_3$ and anti-ferroelectric $NaNbO_3$. The hurdles for KNN to replace PZT in most applications are related to the poor sintering ability of KNN due to a narrow range of sintering temperatures, volatilization of alkali elements, and formation of secondary phases. KNN ceramics were fabricated using flash sintering, a method that was initiated at the University of Colorado. By applying electric field to the sample via two electrodes, sample is sintered in a few seconds during the heating process. It was shown that sintering temperature was reduced about 100-150 °C depending on applied field when compared to conventional sintering. Microstructural and chemical investigations of the sample were done by transmission electron microscopy utilizing a STEM equipped with an EDS spectrometer. STEM-EDX analysis showed that there was an inhomogeneous Na and K distribution between and most importantly within grains. This distribution resembles a core shell structure with excess K being in the shell and Na in the core region. Interpretation of the EDX quantification values with the help of the existing phase diagram showed that a selective melting at grain boundaries via joule heating plays an important role for the formation of core-shell like structure.

11:00 AM

(EMA-S7-016-2016) How to understand sintering of sodium potassium niobate ceramics? (Invited)

B. Malic*[1]; J. Koruza[2]; J. Hreščak[1]; J. Bernard[3]; G. Drazic[4]; A. Bencan[1]; 1. Jozef Stefan Institute, Slovenia; 2. Technical University Darmstadt, Germany; 3. Civil Engineering Institute, Slovenia; 4. National Institute of Chemistry, Slovenia

Since the late 1990s much of the research in the field of piezoelectric ceramic materials has been oriented towards environment-friendly, lead-free materials. The potassium sodium niobate $(K_xNa_{1-x})NbO_3$ solid solution with the composition x = 0.5 ($K_{0.5}Na_{0.5}NbO_3$ or KNN) has been considered as one of the promising candidates to replace highly efficient lead-based piezoelectrics. Already in the first reports on KNN in the 1950s and 1960s it has been evident that it is extremely difficult to obtain materials with high density and fine-grained microstructure by conventional sintering. In the contribution we discuss different approaches to obtain dense ceramics with controlled microstructure which include solid state sintering, also studied on $NaNbO_3$ as the model system, sintering in the presence of a liquid phase, and chemical modification.

11:30 AM

(EMA-S7-017-2016) Additive Manufacturing of Aerosol Deposited AZO Conductive Patterns

N. S. Bell*[1]; A. W. Cook[1]; H. J. Brown-Shaklee[1]; 1. Sandia National Laboratories, USA

Conductive Oxides are important components of optoelectronic devices including flat panel displays, organic light emitting devices, and solar cells. On demand production by additive manufacturing leads to needs in forming nanoinks that can be patterned and reacted at low temperatures to generate functional materials. Low temperature reactivity and manufacturing compatible processing are significant challenges which must be overcome to support ceramic component integration on thermally sensitive substrates. An Aluminum doped ZnO nanoparticle ink was formulated using a glycol synthesis route, and printed using direct write aerosol deposition to form films and conductive patterns. Consolidation of these nanoparticle films were studied on glass substrates using conventional thermal methods and contrasting rapid thermal processing approaches. The structural, electronic, and optical properties of the printed materials are characterized for understanding the structure-property relationships of these nanoinks. Comparisons of the Al doping content and the viability of the conductive features are drawn from the results. Sandia National Laboratories is a multi-program laboratory managed and operated by Sandia Corporation, a wholly owned subsidiary of Lockheed Martin Corporation, for the U.S. Department of Energy's National Nuclear Security Administration under contract DE-AC04-94AL85000.

11:45 AM

(EMA-S7-018-2016) Thermal Diffusivity/Conductivity Measurements of Zirconia during Sintering

E. Post*[1]; 1. NETZSCH Geraetebau GmbH, Germany

The laser flash analysis (LFA) technique is a very fast and universal method for the determination of the thermal diffusivity of a broad range of materials. With the knowledge of the temperature dependent specific heat and the density of the specimen the thermal conductivity can be calculated. LFA measurements were performed during isothermal temperature steps, in opposite to dilatometer measurements (thermal expansion data, density change) or specific heat measurements by differential scanning calorimetry (DSC) where usually a linear heating rate is applied. This means, the temperature treatment of the LFA and dilatometer samples is different and the shrinkage (sintering) during the isothermal steps is usually not taken into account for the length correction (sample thickness, density change). In this paper the influence on the TD/TC results were discussed using length change data from dynamic

dilatometer measurements and dilatometer measurements with identical temperature profile than the LFA measurements.

12:00 PM

(EMA-S7-019-2016) Increasing oxidation resistance of Ni metal in order to cofire BME capacitors in higher partial pressure of oxygen

D. Sohrabi Baba Heidary*[1]; C. Randall[1]; 1. Penn State, USA

Oxygen vacancies increase the amount of leakage current and decrease the life time of base metal electrode capacitors. In this study, we explored fast sintering and coating Ni particles in order to increase its oxidation resistance, so we would be able to cofire Ni electrode capacitor in higher partial pressure of oxygen. After testing the effectiveness of various coatings such as ALD (atomic layer deposition) coatings with different thickness, some of them illustrates four orders of magnitude decrease in the resistivity of Ni particles after sintering in 1020 C for 4 minutes in air. The BME capacitors were produced by fast sintering with and without the coating around Ni particles in the different partial pressure of oxygen. It was demonstrated that the coating increase the oxidative resistance of Ni electrode and also it increases the height of Schottky barrier due to the better bonding between the electrode and the dielectric.

12:15 PM

(EMA-S7-020-2016) Fabrication of electroporcelain composites from local raw materials in Ghana

A. S. Yaya*[1]; 1. University of Ghana, Ghana

It makes sense economically for Ghana to address the feasibility of having its own electro-porcelain industry given the sources of raw materials known to be in Ghana. For example, quartz, used as a filler, is found in Akwatia, feldspar, used as a flux, is found in Akyem-Akroso and kaolin, used as a clay, is found in Nkroful, Assin-Fosu and Kumasi. In this research project, electro-porcelain ceramics will be formulated from these deposits and the properties of the resultant fired materials will be explored in relation to their workability, firing temperature, dielectric and mechanical characteristics. A comparison will be made with internationally sourced electro-porcelain ceramics in order to ensure any newly developed electro-porcelain ceramics are able to meet international standards.

S8. Interface Structure, Orientation, and Composition: Influence on Properties and Kinetics

Interface Properties

Room: Mediterranean B/C

Session Chair: Rosario Gerhardt, Georgia Institute of Technology

10:00 AM

(EMA-S8-001-2016) Characterization of Interfaces and Structure via Electrical Measurements (Invited)

R. A. Gerhardt*[1]; 1. Georgia Institute of Technology, USA

The properties of materials depend on their composition, their structure and thermal treatment history. Each material has a wide range of internal and external interfaces. External interfaces can be modified by adsorbed or desorbed species while internal interfaces can be modified by segregation to or away from the boundaries. In all of these cases, the electrical properties of these materials can often be affected by orders of magnitude changes in their resistivity and dielectric properties because of space charge formation, the presence of inadvertent impurities or other factors such as the size of grains or their orientation. In this talk, I will demonstrate that using impedance spectroscopy measurements is an excellent technique for identifying the conditions under which a given material has experienced one or more of these interfacial phenomena. Three examples will be given. One will describe the effect of adsorbed species on the dielectric response of insulating materials and how one can distinguish it from bulk diffusion. Another will show the effect of segregation of a phase into discrete and continuous boundaries surrounding a second phase. The third example will demonstrate the effect of space charge accumulation at the interface between the active material and the current collector. If there is time, the effect of grain size will also be discussed.

10:30 AM

(EMA-S8-002-2016) The role of pores in ferroelectric ceramics materials intergranular impedance

V. Mitic*[1]; V. Paunovic[1]; L. Kocic[1]; 1. Faculty of Electronic Engineering, Serbia

Ceramics grains contacts are essential for understanding complex dielectric properties of electronic ceramics materials. Constitutional parts of these contacts are also pores. The unity of all pores in the ferroelectric ceramics materials forms so called "negative space" having important role in forming intergranular electric phenomena, predominantly the capacity. In the experiments, fractal modeling algorithms are used in reconstruction of microstructure configurations, like shapes of pores or intergranular contacts. The fractality of grains' surfaces implies the fractality of pores' inner walls, that can be successfully represent by Minkowski hull. The fractal modification of the Curie-Weiss law as well as the Heywang model is employed to build the model of intergranular impedance from the pores point of view. The resulting equivalent circuit models provide the more realistic representation of the electronic materials electrical properties. The intergranular contacts distribution fractal model together with its electrical properties characterization is done. Considering the obtained results, the directions of possible ferroelectric ceramics materials properties prognosis are determined according to the correlations synthesis-structure-properties.

10:45 AM

(EMA-S8-003-2016) Agglomeration of Au/Ni Bilayer Films During Thermal Annealing

X. Cen[1]; X. Zhang[1]; K. van Benthem*[1]; 1. University of California, Davis, USA

Annealing of Au/Ni bilayer films deposited onto SiO_2/Si substrates was investigated by electron microscopy techniques to clarify edge retraction and agglomeration of bilayer films consisting of two immiscible metal components. Localized dewetting and long-range edge retraction were both observed under isothermal annealing condition. Morphology and chemical composition of Au and Ni changed significantly across large distances along the direction normal to the retracting edge. The pinch-off perturbation of Au ahead of the receding edge triggered opposite diffusion behavior for two components. Both void formation at film/substrate triple junctions and grain boundary grooving at the top surface of the film initiate and thus facilitate the localized dewetting of bilayer film. While voids were predominantly formed at Ni/SiO_2 interface besides Au/Ni phase boundary, thermal grooving was mostly initiated at Au/Au grain boundaries. The experimental observations suggest that stress within as-deposited metal films combined with unequal self-diffusion coefficient for the metal components control the bilayer dewetting process. This research is supported by a Faculty Early Career award from the US National Science Foundation (DMR-0955638).

11:00 AM

(EMA-S8-004-2016) Nanostructured Metal-Ceramic Composites Made by Internal Reduction (Invited)

I. Reimanis*[1]; A. Morrissey[1]; J. O'Brien[2]; 1. Colorado School of Mines, USA; 2. Off Grid Research, USA

The nucleation and growth of metallic particles within metal-doped oxides exposed to reducing conditions is relevant to the processing

of materials for catalysts, fuel cells, and structural applications. Here, the precipitation of metallic nickel during the internal reduction of nickel-doped yttria stabilized zirconia is studied with electron microscopy and SQUID magnetometry. It is shown that the microstructure evolution proceeds in three distinct stages, each with its own kinetics description, dependent on the porosity and grain size. The transitions between stages depend on electrostatic potentials at the grain boundaries that act upon the relevant transporting species, namely oxygen vacancies, electrons, nickel ions and zirconium vacancies. An understanding of these mechanisms enables the design of specific nanostructures.

11:30 AM

(EMA-S8-005-2016) Elucidating intermixing in LAO/STO heterointerfaces via SIMS

R. Akrobetu*[1]; A. Sehirlioglu[1]; 1. Case Western Reserve University, USA

The observation of a tunable 2D conductivity at the heterointerface of $SrTiO_3$ (STO) and $LaAlO_3$ (LAO) has galvanized immense interest ever since its discovery over a decade ago. Amongst the list of obstacles in understanding this phenomena is the difficulty in elucidating the degree of intermixing at the LAO/STO interface, as well as marking the heterointerface itself. The conventional method for investigation of intermixing relies on electron microscopy which is limited by the respective masses of the atoms present and the small length of the interface that can be examined. LAO/STO epitaxial films were grown via Pulsed Laser Deposition, and the films were subjected to surface and depth analyses via Secondary Ion Mass Spectroscopy (SIMS). The position of the heterointerface was marked by tracking a minor amount Cr atoms present on the surface of the substrate prior to deposition. Intermixing was studied as a function of deposition temperature and film thickness by utilizing fragmented ions containing cations of both the film and the substrate (i.e., $LaSrO_2$) through the use of a proprietary Matlab software and were modeled in 3D with Avizo modeling software. The information gathered through novel implementation of SIMS is useful in obtaining greater statistical information about the interface through characterization of larger areas (i.e., 100x100um) and the results can be related to the film's electrical properties.

11:45 AM

(EMA-S8-006-2016) Thin film deposition using rarefied gas jet

D. Pradhan*[1]; 1. Indian Institute of Science, India

The rarefied gas jet of Aluminium is studied at Mach number Ma = (U_j / \sqrt{kb T_j / m}) in the range 0.01 < Ma < 2, and Knudsen number Kn = (1 / (\sqrt{2} \pi d^2 n_d H) in the range 0.01 < Kn < 15, using two-dimensional (2D) Direct Simulation Monte Carlo (DSMC) simulations, to understand the flow phenomena and deposition mechanisms in a physical vapor deposition (PVD) process. Here, H is the characteristic dimension, U_j and T_j are the jet velocity and temperature, n_d is the number density of the jet, d is the molecular diameter, and kb is the Boltzmann constant. The variation of local flux along the stream-wise direction away from the jet are studied. The qualitative nature of the local flux at high Mach number (Ma = 2) is similar to those in the incompressible limit (Ma = 0.01). These include the initial fast decay, then slow variation, and finally rapid decay near the substrate. However, there are important differences. The amplitudes of the local flux increase as the Mach number increases. There is significant velocity and temperature slip ((Pradhan and Kumaran, JFM-2011); (Kumaran and Pradhan, JFM-2014)) at the solid surfaces of the substrate. An important finding is that the capture width (cross-section of the gas jet deposited on the substrate) is symmetric around the centerline of the substrate, and decreases with increased Mach number (Ma from 0.01 to 2) due to an increase in the momentum of the gas molecules.

S9. Recent Developments in Superconducting Materials and Applications

Issues related to the Fabrication of Low-cost and High-performance Second Generation Coated Conductors

Room: Pacific

Session Chairs: Judy Wu, University of Kansas; Haiyan Wang, Texas A&M University

10:00 AM

(EMA-S9-014-2016) Doubling in-field J_c in HTS coated conductors by a roll-to-roll ion irradiation process (Invited)

Q. Li*[1]; 1. Brookhaven National Laboratory, USA

Although the performance of the cuprate high temperature superconducting (HTS) wires at self-field has been improved to the level required for commercial cable applications, Poor in-field (1- 7T) performance of the production HTS wire limits its use in superconducting rotating machines. Hence, increasing their current capacity in the presence of magnetic fields is critical for superconductors used in generators for wind turbines, hydro power, marine propulsion, and for magnet used in accelerators and medical imaging machines. In this presentation, we will discuss our recent study at BNL's Tandem Van de Graaff facility. We demonstrated a roll-to-roll irradiation process on production $(RE)Ba_2Cu_3O_{7-d}$ (RE = rare earth elements) coated conductor wires 46 mm wide and 80 meters long that resulted in doubling the critical current in the 4 – 50 K operating regime targeted for rotating machine and high field magnet applications. The optimum pinning enhancement in magnetic field above 1T is achieved with 18 MeV Au ions, at a dose of $6x10^{11}$ Au ions/cm^2 for the coated conductors a few micrometers thick, including protective silver layer. [Ref. Martin Rupich, Q. Li et al, "Engineered Pinning Landscapes for Enhanced 2G Coil Wire" EUCAS 2015.] These moderate ion energies are readily accessible with commercial electrostatic generators. *In collaboration with T. Ozaki, M. W. Rupich, and V. Solovyov.

10:30 AM

(EMA-S9-015-2016) Comparison of the Flux Pinning Mechanisms of $YBa_2Cu_3O_{7-\delta}$ Superconductor with $BaHfO_3$ + Y_2O_3, $BaSnO_3$ + Y_2O_3, and $BaZrO_3$ + Y_2O_3 Mixed Phase Additions (Invited)

M. P. Sebastian*[1]; C. Ebbing[2]; T. Bullard[3]; G. Panasyuk[3]; M. Sullivan[2]; C. F. Tsai[4]; W. Zhang[4]; J. Huang[4]; H. Wang[4]; J. Wu[5]; T. J. Haugan[1]; 1. Air Force Research Laboratory, USA; 2. UDRI, USA; 3. UES, USA; 4. Texas A&M University, USA; 5. University of Kansas, USA

Adding nanophase defects to $YBa_2Cu_3O_{7-\delta}$ (YBCO) superconductor thin films is well-known to enhance flux pinning, resulting in an increase in current densities (J_{ct}). Previously, most studies have focused on single-phase additions; however the addition of several phases simultaneously has shown strong improvements by combining different flux pinning mechanisms. This paper compares and contrasts the effect of mixed phase nanoparticle pinning for three optimized systems comprised of insulating, nonreactive phases: $BaSnO_3$ (BSO) and Y_2O_3, $BaZrO_3$ (BZO) and Y_2O_3, and $BaHfO_3$ (BHO) and Y_2O_3. Processing parameters varied the volume percent of BHO, BSO, and BZO in individual YBCO targets, while maintaining the addition of Y_2O_3 constant at three volume percent. The respective YBCO doped films were prepared by pulsed laser deposition on $LaAlO_3$ and $SrTiO_3$ substrates at optimized deposition temperatures. Results comparing the contributions of strong and weak flux pinning, current densities, critical temperatures, and microstructures will be presented.

11:00 AM

(EMA-S9-016-2016) Controlling the dimension and orientation of secondary phase nanostructures in $YBa_2Cu_3O_7$ nanocomposite films for high-field applications (Invited)

J. Wu*[1]; J. Shi[1]; J. Baca[1]; R. Emergo[1]; M. Sebastian[2]; T. J. Haugan[2];
1. University of Kansas, USA; 2. US Air Force Research labortory, USA

A theoretical model based on an analytical solution of the elastic energy of strained lattices is developed to extract the key parameters that determine the diameter and orientations of self-assembled secondary phase nanorods in epitaxial films. The primary mechanism that determines the nanorod diameter is found to be the lattice strain decay inside the nanorods, which depends only on the ratios of elastic constants of nanorod material and is independent of film/nanorod lattice mismatch. The discovered correlation between the nanorod diameter and the elastic properties of the secondary phase oxides explains well a few experimentally observed nanorods including $BaZrO_3$, $BaSnO_3$ and $BaHfO_3$ and has been used as guidance in the quest of smaller nanorods in epitaxial $YBa_2Cu_3O_7$ nanocomposite films for high field applications and the results on a few promising ones will be reported. In addition, we have found that the doping concentration and the matrix strain provide correlated tuning on the orientation of the nanorods and a mixed phase of the c-axis aligned nanorods and the ab-plane aligned planar nanostructures can be obtained using this tunning, leading to a three-dimensional pinning landscape with single impurity doping and much improved Jc in almost all directions of applied magnetic field.

11:30 AM

(EMA-S9-017-2016) Progress in MOCVD Technology for Fabrication of High Performance Coated Conductors (Invited)

G. Majkic*[1]; 1. University of Houston, USA

We present recent progress in metal organic chemical vapor deposition (MOCVD) technology for deposition of thick REBCO films for coated conductors. MOCVD is one of the major deposition technologies used for coated conductors. Common to all deposition techniques is the need to increase production yield via elimination of defects by tighter process control, increase of deposition rate and increase in raw material utilization, in case of MOCVD metalorganic precursors. A novel MOCVD reactor has been developed at the University of Houston with the goal of addressing the mentioned issues. The system features a susceptor-less design utilizing direct ohmic heating of substrate, suspended (no contact) tape in deposition zone, contactless optical temperature monitoring and highly laminar cross-flow vapor path configuration. The recent progress in coated conductors fabricated using the Advanced MOCVD tool will be presented. This work was supported by the Advanced Research Projects Agency-Energy (ARPA-E).

12:00 PM

(EMA-S9-018-2016) Effects of surface morphology and interlayer on jointing (RE)$Ba_2Cu_3O_{7-x}$ Coated Conductors via electric field assisted proces

M. Li*[1]; C. Jensen[1]; J. Schwartz[1]; 1. North Carolina State University, USA

(RE)$Ba_2Cu_3O_{7-x}$ (REBCO) coated conductors (CCs) have been of interest for high energy physics applications due to their high critical current density J_c with relatively low dependence on external magnetic field, and superior mechanical strength. Due to limitations in batch lengths, and the benefits of grading conductors for large magnets, there is a need for superconducting joint that will enable persistent current mode operation. Currently, there is no suitable joining technique that is readily compatible with magnet manufacturing. Here were report on a new technique that uses an electric field to reduce the required temperature to join (RE)BCO CCs. The technique relies strongly on intimate contact between (RE) BCO layers, and thus the joining efficiency is reduced by the rough surfaces caused by the *a*-axis grains. Here, we performed ultrafine polish to (RE)BCO tapes, so that good surface contacts could be realized. Moreover, a thin interlayer of Ag was deposited by e-beam evaporation to further improve the surface quality. We studied the effects of various surface roughness and thickness of Ag interlayer on microstructure, size, strength, and J_c of joints by scanning electron microscopy and low temperature four-point probe measurements.

S11. Advanced electronic Materials: Processing, structures, properties and applications

Processing and Characterization (domain) of Electronic Materials

Room: Indian

Session Chairs: Xiaoli Tan, Iowa State Univ; Tadasu Hosokura, Murata Manufacturing Co., Ltd.

10:00 AM

(EMA-S11-016-2016) Properties of orientation and crystallization controlled $BaTiO_3$, $SrTiO_3$ thin films fabricated by chemical solution deposition (Invited)

T. Hosokura*[1]; A. Ando[1]; T. Konoike[1]; 1. Murata Manufacturing Co., Ltd., Japan

Barium titanate ($BaTiO_3$) thin films are of significant interest as ferroelectric materials for thin-film capacitors. In recent years, there has been increasing interest in enhancing ferroelectric behavior by inducing strain, such as through the synthesis of artificial superlattices of oxide materials, control of substrate thermal expansion coefficients, and control of layer orientation. We synthesized epitaxially grown $SrTiO_3$(100)/$BaTiO_3$(100) artificial superlattices on Pt(100)/MgO(100) substrates by a chemical solution deposition method to improve the substrate's dielectric properties by inducing a mismatch between the $SrTiO_3$ and $BaTiO_3$ layers. Furthermore, we synthesized orientation-controlled (100), (110), and (111) $BaTiO_3$ films on Pt(100)/MgO(100), Pt(110)/MgO(110), and Pt(111)/MgO(111) substrates, respectively, by the chemical solution deposition method as the dielectric constants were assumed to be enhanced by differences in the orientation of the $BaTiO_3$. The electric properties of the fabricated $BaTiO_3$ thin films were evaluated, and dielectric constants of 2000 were found for the synthesized (110)-oriented $BaTiO_3$ film and (111)-oriented $BaTiO_3$ film, with temperature dependence stabilized from 20 °C to 150 °C.

10:30 AM

(EMA-S11-017-2016) Nanofragmentation of ferroelectric domains in lead-free ceramics during polarization fatigue

H. Guo[1]; X. Liu[1]; J. Rödel[2]; X. Tan*[1]; 1. Iowa State Univ, USA; 2. Technische Universität Darmstadt, Germany

The microscopic mechanism for electric fatigue in ferroelectric oxides has remained an open issue for several decades in the condensed matter physics community. Even though numerous models are proposed, a consensus has yet to be reached. Since polarization reversal is realized through ferroelectric domains, their behavior during electric cycling is critical to elucidating the microstructural origin for the deteriorating performance. In this study, electric field *in situ* transmission electron microscopy is employed for the first time to reveal the domain dynamics at the nanoscale through more than 10^3 cycles of bipolar fields. A novel mechanism of domain fragmentation is directly visualized in a polycrystalline $[(Bi_{1/2}Na_{1/2})_{0.95}Ba_{0.05}]_{0.98}La_{0.02}TiO_3$ ceramic. Fragmented domains break the long-range polar order and, together with domain wall pinning, contribute to the reduction of switchable polarization. Complimentary investigations into crystal structure and properties of this material corroborate our microscopic findings. The results

will help to understand electric fatigue in ferroelectrics and eventually lead to manufacturing of fatigue-free electric devices.

10:45 AM

(EMA-S11-018-2016) EBSD Study of Yttrium Iron Garnet Coatings Produced via Aerosol Deposition

E. Gorzkowski*[1]; S. D. Johnson[1]; A. Levinson[1]; 1. Naval Research Lab, USA

Aerosol deposition (AD) is a thick-film deposition process that can produce layers up to several hundred micrometers thick with densities greater than 95% of the bulk. The primary advantage of AD is that the deposition takes place entirely at ambient temperature; thereby enabling film growth in material systems with disparate melting temperatures. The bonding and densification of the film and film/substrate interface are thought to be facilitated by local temperature rise, high pressure, and chemical bonding during deposition, which leads to a dense nano-grained microstructure. In this talk we present results from an Electron Backscatter Diffraction (EBSD) investigation of yttrium iron garnet deposited onto sapphire to illuminate grain size and possible texture development in the film due to the spray process. EBSD results will be augmented with representative characterization from scanning electron microscopy, energy dispersive spectroscopy, and profilometry.

11:00 AM

(EMA-S11-019-2016) Magnetic and Structural Properties of Doped Barium Hexaferrite Films Formed by Aerosol Deposition

S. D. Johnson*[1]; C. Gonzalez[2]; Z. Robinson[4]; D. Ellsworth[3]; M. Wu[3]; 1. Naval Research Laboratory, USA; 2. California State University Long Beach, USA; 3. Colorado State University, USA; 4. SUNY Brockport, USA

Aerosol deposition is a room-temperature thick film deposition technique that produces > 95% dense polycrystalline films several microns in thickness at very high deposition rates of several microns per minute. One distinct advantage of aerosol deposition is the ability to produce films with the same stoichiometry as the powdered precursor material. For this work, we deposited a proprietary doped barium hexaferrite ($BaFe_{12}O_{19}$) film from powder produced by *Temex Ceramics*. This material is designed for microwave absorption near 18 GHz via ferromagnetic resonance and has potential applications in microwave electronics. In addition to comparing the structural and magnetic properties of the as-deposited film, bulk material, and starting powder, this work is the first to report structural and magnetic material properties of this compound. For this purpose, we employed scanning electron microscopy, x-ray photoemission spectroscopy, x-ray diffraction, vibrating sample magnetometry, and broad-band ferromagnetic resonance characterization techniques.

11:15 AM

(EMA-S11-020-2016) Effects of Domain and Grain Boundaries in Piezoelectric Ceramics and Single Crystals on Elastic Constants Evaluated by Sound Velocities

T. Ogawa*[1]; T. Ikagaya[1]; 1. Shizuoka Institute of Science and Technology, Japan

Sound velocities were measured in piezoelectric ceramic disks (dimensions of 14 mm diameter and 0.5-1.5 mm thickness) composed of PZT, lead titanate and lead-free, and relaxor single-crystal plates (21 mm length, 14 mm width and 0.4 mm thickness) of (100) $0.70Pb(Mg_{1/3}Nb_{2/3})TiO_3$-$0.30PbTiO_3$ (PMNT70/30) using an ultrasonic precision thickness gauge (Olympus Model 35DL) with high-frequency (longitudinal wave: 30 MHz and transvers wave: 20 MHz) pulse generation. Directions of DC poling and sound wave propagation are in thickness. Calculating elastic constants by sound velocities, it was possible to evaluate effects of domain and grain boundaries on elastic constants. Piezoelectric ceramics with high coupling factor (k) were realized in small Young's modulus (Y) and rigidity (G), furthermore, large Poisson's ratio (σ) and bulk modulus (K). PMNT70/30 single-crystal plates possessed relatively small σ (0.16) and K (7.8×10^{10} N/m^2) after poling in comparison with the ones of ceramics (σ=0.27-0.43 and K=8.7-13.6$\times10^{10}$ N/m^2). The existence of domain boundaries in single-crystal plates caused increasing Y, G and decreasing σ and K. The existence of grain boundaries in ceramics caused decreasing transvers wave velocity (V_S), as the result, Y and G become smaller and σ and K become larger in comparison with the ones in single-crystal plates.

11:30 AM

(EMA-S11-021-2016) Quantifying the Extent of 180° Domain Switching using *in situ* X-Ray Diffraction

C. Fancher*[1]; S. Brewer[2]; C. Chung[1]; S. Röhrig[3]; G. Esteves[1]; M. Deluca[3]; N. Bassiri-Gharb[2]; J. L. Jones[1]; 1. North Carolina State University, USA; 2. Georgia Institute of Technology, USA; 3. MATERIALS CENTER LEOBEN, Austria

Polarization in ferroelectric materials is induced through several mechanisms (*e.g.* polarization switching and dielectric displacement). Polarization reversal can occur through the motion of planar defects such as domain walls. In ferroelectric materials, two types of domain walls are present (i.e., non-180° and 180°). In recent years *in situ* X-ray diffraction experiments have been invaluable for quantifying non-180° domain wall motion during application of electric fields. In this paper, we present an approach to calculate 180° domain reversal during application of electric fields. We demonstrate this method by determining the contribution of 180° domain switching to polarization in soft lead zirconate titanate (PZT). We show that the application of a strong (2 kV/mm) electric field to a soft PZT induces nearly complete 180° domain reversal (~90%). This result demonstrates that 180° domain reversal is the dominant contribution to polarization. We also apply this method to quantify the contribution of 180° domain switching to the dielectric response of $BaTiO_3$. This results suggests that 180° domain switching accounts for ~60% of the dielectric response.

11:45 AM

(EMA-S11-022-2016) Controlled illumination-induced creation of charged domain walls at room temperature in $BaTiO_3$

P. Bednyakov[1]; T. Sluka*[1]; A. Tagantsev[1]; D. Damjanovic[1]; N. Setter[1]; 1. EPFL - Swiss Federal Institute of Technology Lausanne, Switzerland

Charged Domain Walls (CDWs) in ferroelectrics were predicted to be metallically conducting interfaces that can be created, displaced and erased inside a monolith of nominally insulating materials. Such CDWs are thus promising elements for the envisaged reconfigurable nanoelectronics. Indeed, highly elevated and non-thermally activated conductivity was observed at CDWs in proper, improper and hybrid-improper ferroelectrics. The progress towards CDW exploitation is however hindered by the absence of practical CDW engineering techniques. CDWs were found either locked in as grown patterns in improper ferroelectrics, or were created locally with scanning probe techniques or stochastically with defect assisted compensation in proper ferroelectrics. Here we introduce a simple room temperature bulk method which creates regular patterns of electronically compensated CDWs in crystals of prototypical proper ferroelectric $BaTiO_3$. The method uses superbandgap illumination to generate free carries inside a crystal that is held in a field induced phase. The free carriers simultaneously screen the external electric field which induces a phase transition and compensate appearing CDWs. This method provides a new road to the creation of movable conducting channels in insulating ferroelectrics.

12:00 PM

(EMA-S11-023-2016) Conductive Domain Walls in Polycrystalline $BiFeO_3$: Local Structure and Dynamics

T. Rojac*[1]; A. Bencan[1]; H. Ursic[1]; G. Drazic[2]; N. Sakamoto[4]; B. Jancar[1]; M. Makarovic[1]; J. Walker[1]; B. Malic[1]; D. Damjanovic[3]; 1. Jozef Stefan Institute, Slovenia; 2. National Institute of Chemistry, Slovenia; 3. Swiss Federal Institute of Technology, Switzerland; 4. Shizuoka University, Japan

Enhanced electrical transport at domain walls has been commonly observed in a number of ferroelectrics, including $BiFeO_3$, $LiNbO_3$, $Pb(Zr,Ti)O_3$ and rare-earth manganites. Most of the studies on conductive domain walls have been so far focused on local, nanoscale properties. In this contribution, we will show that these conductive interfaces significantly affect the macroscopic electromechanical properties of polycrystalline $BiFeO_3$ due to the coupling between the local conductivity and the mobility of DWs under applied external (electrical or stress) fields. We will present evidence of spontaneously formed conductive DWs in polycrystalline $BiFeO_3$ using a combination of scanning electron microscopy (SEM), electron backscattered diffraction (EBSD), atomic- and piezoresponse-force microscopy (AFM, PFM), and Cs-probe corrected scanning transmission electron microscopy (STEM) analyses. In particular, STEM analysis will pinpoint a number of atomic-scale features of the DWs in $BiFeO_3$, which are consistent with the observed local conductivity. The local transport properties of domain walls will be linked to the macroscopic behavior by introducing the nonlinear, piezoelectric Maxwell-Wagner effect. This work was supported by the Slovenian Research Agency (P2-0105 and J2-5483).

Student Speaking Competition Presentations II

Room: Coral A

Session Chair: Christina Rost, North Carolina State University

12:45 PM

(EMA-SSC-005-2016) Intentional defects in 2-D birnessite MnO_2 to improve supercapacitor performance

P. Gao*[1]; P. C. Metz[1]; T. Hey[1]; S. Misture[1]; 1. Alfred University, USA

2-D birnessite MnO_2 nanosheets were successfully modified by reduction treatments to double the electrochemical capacitance to values in excess of 300 F/g. The nanosheets were prepared by solid state sintering of the parent K-Mn-oxide, followed by ion-exchange and exfoliation. MnO_2 nanosheet suspensions were flocculated to assemble 3-D porous nanostructures, and finally subjected to reduction treatments to generate surface defects. SEM images demonstrate porous structures assembled from ultra-thin 2-D MnO_2 nanosheets with the birnessite structure that have high surface area. XPS, XANES and high energy X-ray PDF analyses indicated an increase in the Mn^{3+}/Mn^{4+} ratio with partial reduction of MnO_2 nanosheets, where the Mn^{3+} cations shift from the plane of the 2-D nanosheet to the nanosheet surface. This defect geometry is likely to create more active surface sites that can promote sodium ion intercalation. Electrochemical measurements showed that the charge storage capacitance increased from about 150 F/g to over 300 F/g when we intentionally reduced the MnO_2 nanosheets to form out-of-plane Mn ions, and the charge transfer resistance decreased from ~18 Ω to ~3 Ω correspondingly. These experimental results demonstrate that self-assembled 3-D porous MnO_2 nanostructures are of commercial value when engineered to optimize their defect structures.

1:00 PM

(EMA-SSC-006-2016) Thermal Conductivity of Amorphous Silicon Thin Films: Effects of Size and Elastic Modulus

J. L. Braun*[1]; M. Elahi[2]; J. Gaskins[1]; T. E. Beechem[3]; Z. C. Leseman[2]; H. Fujiwara[5]; S. King[4]; P. E. Hopkins[1]; 1. University of Virginia, USA; 2. University of New Mexico, USA; 3. Sandia National Laboratories, USA; 4. Intel Corporation, USA; 5. Gifu University, Japan

We investigate thickness-limited size effects on the thermal conductivity of amorphous silicon thin films ranging from 3 – 1636 nm grown via sputter deposition. While exhibiting a constant value up to ~100 nm, the thermal conductivity increases with film thickness thereafter. This trend is in stark contrast with previous thermal conductivity measurements of amorphous systems, which have shown thickness-independent thermal conductivities. The thickness dependence we demonstrate is ascribed to boundary scattering of long wavelength vibrations and an interplay between the energy transfer associated with propagating modes (propagons) and non-propagating modes (diffusons). A crossover from propagon to diffusion modes is deduced to occur at a frequency of ~1.8 THz via simple analytical arguments. We extend this study to an amorphous silicon system with various levels of hydrogenation. Fixing the sample thickness to 200 nm, we measure the thermal conductivity of a-Si:H films having different elastic moduli (measured with nanoindentation) to demonstrate that thermal conductivity increases with increasing elastic modulus. In both cases, the minimum thermal conductivity model fails to capture the trend observed.

1:15 PM

(EMA-SSC-007-2016) Positive effect of an internal depolarization field in ultrathin epitaxial ferroelectric films

G. liu*[1]; J. Chen[1]; C. Lichtensteiger[2]; J. Triscone[2]; P. Aguado-Puente[3]; J. Junquera[4]; N. Valanoor[1]; 1. University of New South Wales, Australia; 2. University of Geneva, Switzerland; 3. CIC Nanogune, Spain; 4. Universidad de Cantabria, Spain

The effect of purposely introducing a large depolarization field in (001)-oriented, epitaxial $Pb(Zr_{0.2}TiO_{0.8})O_3$ (PZT) ultra-thin films grown on $La_{0.67}Sr_{0.33}MnO_3$ (LSMO) buffered $SrTiO_3$ (STO) substrates is investigated. Inserting between 3 to 10 unit cells of STO between two 3nm thick PZT films significantly influences the out-of-plane (*c*) lattice constant as well as the virgin domain state. Piezoresponse force microscopy images reveal a nanoscale (180°) polydomain structure in these films. In comparison, the "reference" single layer PZT sample (6 nm thick without STO spacer) exhibits an elongated PZT *c*-axis (0.416nm) and is preferentially "down"-polarized with large regions of monodomain contrast. It shows asymmetric switching loops (i.e. imprint) coupled with a sluggish domain switching under external bias. We show that the insertion of STO drives a monodomain to 180° polydomain transition in the as-grown state, which reduces the imprint by 80%. Furthermore, the speed of electrical-field initiated domain switching is shown to have improved by 2 orders of magnitude compared to the reference sample. This demonstrates that it is possible to manipulate the depolarization field in a way that has positive effects on the ferroelectric behavior of ultrathin PZT films.

1:30 PM

(EMA-SSC-008-2016) Doping control in epitaxial thin films via reactive RF co-sputtering

K. Kelley*[1]; E. Sachet[1]; H. Kham[1]; S. Franzen[1]; J. Maria[1]; 1. North Carolina State University, USA

In recent years, conductive oxides have been increasingly investigated in the context of plasmonics. The interest in plasmonic technologies surrounds many emergent optoelectronic applications, such as plasmon lasers, transistors, sensors, and information storage. While plasmonic materials for UV-VIS and near infrared wavelengths have been found, the mid-infrared range remains a challenge to address. Recent developments show Dy-doped CdO

(CdO:Dy) grown via molecular beam epitaxy (MBE) can achieve electron mobilities (~500 $cm^2V^{-1}s^{-1}$) and carrier densities (10^{20} cm^{-3}) that satisfy the criteria for mid-infrared spectrum plasmonics, and overcome the losses seen in conventional plasmonic materials, such as noble metals. Highly accurate doping using MBE was the key to investigate the structure property relations in CdO:Dy. However MBEs limited throughput and high cost present a barrier towards larger scale application of this material. In this work, we present a deposition technique for controllably doped CdO grown via reactive RF co-sputtering. Epitaxial films grown by this method depict electrical and optical properties comparable to MBE grown materials and thus offer a more accessible route towards ubiquitous IR plasmonic technologies based on CdO. Efforts thus far have produced co-sputtered CdO:Dy on Al_2O_3 with carrier densities of 10^{20} cm^{-3} and mobilities in excess of 300 $cm^2V^{-1}s^{-1}$.

S1. Multiferroic Materials and Multilayer Ferroic Heterostructures: Properties and Applications

Synthesis, Characterization, and Applications

Room: Coral A

Session Chairs: Hamidreza Khassaf, University of Connecticut; Yomery Espinal, University of Connecticut

2:00 PM

(EMA-S1-020-2016) Polycrystalline Superlattice-Like PZT Thin Film (Invited)

S. Brewer[1]; H. Khassaf[2]; P. Alpay[2]; N. Bassiri-Gharb*[1]; 1. Georgia Institute of Technology, USA; 2. University of Connecticut, USA

Leveraging the drive for spontaneous Zr/Ti gradient formation during crystallization of chemical solutions processed PZT films, superlattice-like (SL) thin films with compositional gradient through the thickness, and centered at the morphotropic phase boundary were deposited on Pt/Ti/SiO_2/Si substrates. SL films, with stacking periodicity ranging from 15 to 120 nm were obtained. X-Ray Diffraction (XRD) patterns showed pure perovskite phase and preferential (100) orientation. XRD spectra and XPS depth profile chemical analysis are consistent with alternating rhombohedral and tetragonal phases in each deposited layer, leading to up to 20% higher dielectric permittivity and 45% higher piezoelectric response, compared with compositional gradient-free films and traditionally processed films of similar thickness. The local electromechanical response of the films, with unusual amplitude of piezoresponse and an acoustic softening are consistent with presence of polar-glass-like phases polarization rotation and phase switching in the films. Dependence of the dielectric and piezoelectric response of the SL films on the stacking periodicity and the extent of the compositional gradient will be also discussed.

2:30 PM

(EMA-S1-021-2016) *In situ* Characterization of the Epitaxialization of $BiFeO_3$ Films via Atomic Layer Deposition (Invited)

J. E. Spanier*[1]; 1. Drexel University, USA

I will highlight our recent progress in using a low-temperature atomic layer deposition (ALD) and post-growth annealing process to produce high-quality complex oxide films, and in understanding the growth process. We present new results on the epitaxial stabilization of phase-pure ferroelectric model system $BiFeO_3$(001) onto different perovskite and non-perovskite crystals at temperatures as low as 375ºC, hundreds of degrees lower than high-vacuum and high-temperature routes, including *in situ* X-ray diffraction and X-ray photoelectron spectroscopy studies during epitaxialization, ferroelectric and ferromagnetic property characterizations, and related studies involving formation of metastable phases. Obtained in a material that is challenging to obtain in phase-pure film form by any method, single-crystal ALD-grown $BiFeO_3$ films are comparable in atomic structural quality to thin films obtained by high-vacuum, high-temperature methods. We have extended process knowledge to attain lower-temperature formation of crystallographically well-oriented $BiFeO_3$(001) films on SiO_x/Si(100). Work supported by the ONR under N00014-15-11-2170 and in part by the NSF and SRC under DMR 1124696.

3:00 PM

(EMA-S1-022-2016) Magnetoelectric Investigations of a Single-Phase Multiferroic Material Possessing the Aurivillius Structure (Invited)

L. Keeney*[1]; A. Faraz[1]; T. Maity[1]; M. Schmidt[1]; A. Amann[2]; N. Deepak[3]; N. Petkov[1]; S. Roy[1]; M. Pemble[1]; R. Whatmore[4]; 1. Tyndall National Institute, University College Cork, Ireland; 2. University College Cork, Ireland; 3. University of Liverpool, United Kingdom; 4. Imperial College London, United Kingdom

Single-phase multiferroic materials, displaying both ferroelectric (FE) and ferromagnetic (FM) memory states, are much sought-after for application in high-density, low power data storage applications. However, until very recently, there were no materials demonstrating single-phase multiferroic properties at room temperature, due to conflicting electronic structure requirements for ferroelectricity and ferromagnetism. By manipulating a layer-structured material to accommodate both FE and FM cations within the same structure, we synthesised Aurivillius phase $Bi_6Ti_{2.8}Fe_{1.52}Mn_{0.68}$ by a chemical solution deposition (CSD) technique (DOI: 10.1111/jace.12467). This material is a genuine, single-phase multiferroic thin film material demonstrating magnetoelectric coupling at room temperature. Thin films of $Bi_6Ti_xFe_yMn_zO_{18}$ (B6TFMO) grown by liquid injection chemical vapour deposition (LICVD) demonstrate a significantly stronger ferromagnetic signal (Ms of 215 emu/cm^3 compared with 6.05 emu/cm^3 for CSD-grown films) and increased volumes (17% compared with 7% for the CSD-grown films) of the films engage in magnetoelectric coupling. Recent results will be presented showing both reversible and irreversible switching of FE domains by a magnetic field in LICVD grown films and the nature of the magnetoelectric coupling in this fascinating B6TFMO material will be discussed.

4:00 PM

(EMA-S1-023-2016) Ferroelectric Domain Switching Dynamics in Multiferroics Based on Frames-per-Second PFM Imaging (Invited)

J. Steffes[1]; Z. Thatcher[1]; A. Carter[1]; J. Heron[2]; R. Ramesh[3]; P. Ashby[4]; B. D. Huey*[1]; 1. University of Connecticut, USA; 2. Cornell University, USA; 3. University of California Berkeley, USA; 4. Lawrence Berkeley National Laboratory, USA

The dynamics of domain switching in ferroelectrics and multiferroics are crucial to the kinetics, stability, and energy consumption of data storage systems, magneto-electric coupling devices, filters and capacitors, etc. But mapping polarization vectors requires simultaneous in-plane and out-of-plane pfm imaging, which is generally challenging and slow contrary to the objective of directly monitoring domain poling or relaxation. To defeat this limitation, both quasi-pump-probe methods as well multiple-frame-per-second AFM scanning are employed. This yields several new observations for $BiFeO_3$ ferroelectric domains. First, statistics of nucleation, growth, and the number of steps in the switching process at any given location are directly observed. Second, reversible and irreversible domain patterns are investigated and related to structural and polarization defects. Third, domain switching is performed for microscale and nanoscale islands, providing insight into switching dynamics for multiferroics as a function of strain relief. Such direct nanoscale studies are key towards optimizing the design, processing, and performance of multiferroic devices.

4:30 PM

(EMA-S1-024-2016) Perovskite oxide thin films with high room temperature mobilities (Invited)

T. Schumann*[1]; S. Raghavan[1]; J. Zhang[1]; H. Kim[1]; S. Stemmer[1]; 1. University of California, Santa Barbara, USA

High-mobility oxides are of interest for a number of applications, including as transparent conductors. Among those, perovskite rare-earth stannates are of special interest, because they have room temperature electron mobilities unmatched by any other transparent conducting oxide or semiconductor at comparable carrier densities. Bulk crystals of $BaSnO_3$ show electron mobilities of 300 cm^2/Vs at room temperature, while possessing a large band gap (3.1 eV). To further explore their electric properties and to integrate them into devices, high-quality thin films are required. In this talk, we will demonstrate epitaxial $BaSnO_3$ thin films grown by molecular beam epitaxy (MBE). Solid-source high temperature Knudsen cells are used to provide Ba and Sn, while oxygen is provided by an rf-plasma source. La is used as dopant. The impact of the different growth methods and substrates on the structural and electrical quality will be discussed. Structure and morphology are characterized by XRD measurements, AFM and TEM, while the electrical properties are determined by magnetotransport measurements as a function of temperature. In-situ RHEED and XRD measurements confirm smooth, single-phase $BaSnO_3$ films under optimized growth conditions, with room temperature electron mobilities exceeding 100 cm^2/Vs. We will also discuss MBE of high quality stannate heterostructures for high mobility, functional oxide devices.

5:00 PM

(EMA-S1-025-2016) Metallo-Organic Solution Deposition of Ferroelectric Films onto Additively Manufactured Inconel 718

T. Patel*[1]; H. Khassaf[1]; N. Bassiri-Gharb[2]; P. Alpay[1]; R. Hebert[1]; 1. University of Connecticut, USA; 2. Georgia Institute of Technology, USA

Ferroelectric films have many unique dielectric, piezoelectric, and pyroelectric properties. Lead zirconate titanate (PZT) is an industry-standard ferroelectric in sensors and actuators. Considering the recent advances in additive manufacturing (AM) of high-temperature alloys for aerospace applications, an investigation of the feasibility of deposition of PZT directly onto such alloys is of great interest. Here, we have grown 300 nm thick $PbZr_{0.2}Ti_{0.8}O_3$ (PZT 20/80) films on Ni, commercial Inconel 718, and AM Inconel 718 substrates using metallo-organic solution deposition. Deposits were characterized using X-ray diffraction, electron microscopy, profilometry, and piezoresponse force microscopy. Electrical measurements were carried out at room temperature and 1 kHz to determine the spontaneous polarization, dielectric constant and loss, and leakage currents. Our results show that films on all three substrates display ferroelectricity, although the dielectric loss and leakage are substantially higher for PZT 20/80 films on both commercial and AM Inconel substrates. We attribute this to the native oxides that form on the superalloy.

5:15 PM

(EMA-S1-026-2016) Switchable/Tunable FBAR Resonators and Filters with Ba1-xSrxTO3 Thin Films (Invited)

T. S. Kalkur*[1]; 1. University of Colorado Colorado Springs, USA

Thin Film Bulk Acoustic wave Resonators (BAW) based on BST are important for the fabrication of compact resonators and filters for wireless communications. Aluminum nitride is the most common piezoelectric material used for the fabrication of FBAR devices but it has low piezoelectric coefficient. SAW devices were used to fabricate filters, resonators up to frequency 3GHz but BAW based devices are theoretically expected to boost the frequency to 15 GHz to cover the frequency bands of future communication systems. Barium Strontium Titanate thin films are paraelectric at room temperature. They exhibit voltage dependent piezoelectricity and therefore are expected to have wide applications in the fabrication of switchable and tunable filters, resonators and duplexers. We will review different approaches in the design, fabrication and characterization of solidly mounted BST based FBARs and filters for switchable RF modules for future communication systems.

S4. Ion-conducting Ceramics

Processing and Microstructure Effects on Ion Conduction I

Room: Caribbean B

Session Chair: Fanglin (Frank) Chen, University of South Carolina

2:00 PM

(EMA-S4-001-2016) The Role of Ionic Transport in Nuclear Waste Immobilization and Membrane Separations (Invited)

K. Brinkman*[1]; 1. Clemson University, USA

The emergent properties arising from the interactions of phases including interfacial contributions and phase evolution at the mesoscale present new opportunities, as well as challenges, for materials performance and functionality. This presentation will highlight interfacial contributions to system level performance in two diverse fields: i) Mixed Ionic and Electronic Conducting (MIEC) separation membranes and ii) Ceramic waste forms for nuclear waste storage. Mixed ionic-electronic conductors are widely used in devices for energy conversion and storage. Grain boundaries in these materials have nanoscale spatial dimensions, which can generate substantial resistance to ionic transport due to dopant segregation. Here, we report a concept of targeted phase formation in ceramic composites that serves to enhance the grain boundary ionic conductivity. Hollandite oxides similar to materials used as Li battery cathodes are currently under evaluation for the immobilization of Cesium. The phase formation, experimentally determined ionic conductivity, and propensity for elemental release were determined for substituted hollandites containing different levels of Cs. Implications for controlling the ionic transport in diverse applications of ceramic-ceramic composites ranging from MIEC membranes to nuclear waste immobilization will be discussed.

2:30 PM

(EMA-S4-002-2016) Preparation of Proton Conductor for Pure Hydrogen Separation from Coke Oven Gas

H. Konishi*[1]; H. Ono[1]; 1. Osaka University, Japan

The $SrZr_{1-x}Y_xO_{3-\alpha}$ of proton conductor was prepared by normal sintering and SPS methods in order to separate pure hydrogen gas from H_2-containing mixed gases at high temperature. The $SrZr_{1-x}Y_xO_{3-\alpha}$ obtained by normal sintering at 1580°C for 10 h and SPS at 1500°C for 3 min was found to be single phase of perovskite structure. The relative density of $SrZr_{1-x}Y_xO_{3-\alpha}$ obtained by SPS at 1400 and 1500°C was over 95 %. Furthermore, the relative density increased with sintering temperature and time of SPS. The proton conductivity of $SrZr_{1-x}Y_xO_{3-\alpha}$ of SPS increased with sintering temperature, and was higher than one of normal sintering under wet 10 % H_2 and Ar gases atmosphere. On the other hand, the proton conductivity of $SrZr_{1-x}Y_xO_{3-\alpha}$ of SPS under the simulated coke oven gas atmosphere was equivalent to one under 50 % H_2 and Ar gases atmosphere. Furthermore, the structure of $SrZr_{1-x}Y_xO_{3-\alpha}$ was chemically stable under the simulated coke oven gas atmosphere. The applied voltage (V_{appl}) at 1273 K under the simulated coke oven gas atmosphere under 50 % H_2 and Ar gases atmosphere using $SrZr_{1-x}Y_xO_{3-\alpha}$ was equivalent to one under 50 % H_2 and Ar gases atmosphere, but the electrode polarization (V_{appl}-iR) was higher.

2:45 PM

(EMA-S4-003-2016) Electrical Properties of Lanthanum Silicate-Based Oxygen-Excess-Type Ionic Conductors

A. Mineshige*[1]; T. Nishimoto[1]; A. Heguri[1]; H. Hayakawa[1]; T. Yazawa[1]; 1. University of Hyogo, Japan

Lanthanum silicate ($La_{9.33+x}Si_6O_{26+1.5x}$, LSO) is one of the candidates as an electrolyte material used in intermediate-temperature SOFCs. Introducing excess oxygen by additional La incorporation, cation doping into its Si-site, and firing at very high temperature (1973 K) are important to enhance conductivity, although the specimen fired at 1973 K is chemically unstable. In this study, its conducting properties were investigated in detail aiming at obtaining highly conductive and chemically stable LSO specimen. Solid-state reaction was employed to prepare specimens with the composition of $La_{10}(Si_{5.8}Al_{0.2})O_{26.9}$. After mixed raw powders were calcined and pulverized, they were fired at various temperatures (T_f). Ionic conductivity was measured with a DC four probe method. The conductivity largely enhanced as T_f increased. Those of specimens were quite low when T_f was lower than 1773 K due to lower sample density. Although dense structure was obtained at $T_f \geq$ 1873 K, conductivities for the specimens with T_f =1873 and 1923 K were still low because La_2SiO_5 phase was coexisted with the LSO phase owing to its La-excess composition. On the other hand, the specimen fired at 1973 K was single phase LSO, and exhibited high conductivity. In addition, it was found that LSO specimen with high chemical stability as well as high conductivity could be successfully obtained with a small amount of iron addition.

3:00 PM

(EMA-S4-004-2016) High performance solid oxide electrolysis cells with hierarchically porous Ni-YSZ support electrode

L. Lei*[1]; Y. Chen[2]; T. Liu[3]; Y. Wang[3]; F. Chen[1]; 1. University of South Carolina, USA; 2. Georgia Institute of Technology, USA; 3. Wuhan University, China

To improve the electrochemical performance of solid oxide electrolysis cells (SOECs), hierarchically porous Ni-YSZ substrates were fabricated by freeze-drying tape casting method. Sponge-like porous substrates were fabricated using the traditional dry-pressing fabrication method for comparison. Microstructure characterization using SEM, mercury intrusion, 3D X-ray microscopy and gas permeability indicates that for the Ni-YSZ substrates, high porosity and low tortuosity factor are beneficial for gas diffusion. The electrochemical tests show that the SOECs with hierarchically porous Ni-YSZ substrate display much higher performance both in steam electrolysis mode (1.3 V, 0.95 A cm^{-2}) and co-electrolysis mode (1.3 V, 0.85 A cm^{-2}) at 750 ºC. Compared with the sponge-like porous Ni-YSZ substrates, the advantages of hierarchically porous Ni-YSZ substrates are more obvious in the SOEC mode than in the SOFC mode due to the slower diffusion of H_2O and CO_2, compared with H_2.

3:15 PM

(EMA-S4-005-2016) "Eel-ectrifying" Membranes: Toward the development of biomimetic, ion-based energy storage

E. Spoerke*[1]; L. Small[1]; A. Martinez[1]; D. Wheeler[1]; V. Vandelinder[1]; G. Bachand[1]; S. Rempe[1]; 1. Sandia National Laboratories, USA

In an effort to identify alternative technologies needed to meet the ever-growing demand for safe, high power, high energy density electrical energy storage, we have turned to the electric eel for inspiration. Utilizing the relatively simple concept of controlling ion concentration gradients across cellular membranes, these remarkable organisms are capable of repeatedly generating and discharging 1 Ampere of current at over 600V! This presentation will describe our efforts to create a simplified mimic of this concept based on actively creating, maintaining, and releasing ion concentration gradients across synthetic membranes. In particular, it will explore how combinations of natural protein-based ion pumps, programmable nanopore functionalization, and even advanced copolymer chemistries may be employed to control the active, rectified transport of ions in synthetic systems to generate and discharge electrical energy. Continued advances toward this biomimetic approach may ultimately lead to the development of new highly scalable and inherently robust alternative ion-based energy storage technologies. Sandia National Laboratories is a multi program laboratory managed and operated by Sandia Corporation, a wholly owned subsidiary of Lockheed Martin Corporation, for the U.S. Department of Energy's National Nuclear Security Administration under contract DE-AC04-94AL85000.

Processing and Microstructure Effects on Ion Conduction II

Room: Caribbean B
Session Chair: Erik Spoerke, Sandia National Laboratories

4:00 PM

(EMA-S4-006-2016) Grain-boundary resistance in yttrium-doped barium zirconate: influence of fabrication process (Invited)

S. Ricote*[1]; D. Clark[2]; N. Sullivan[1]; W. Coors[2]; 1. Colorado School of Mines, USA; 2. CoorsTek, USA

Yttrium-doped barium zirconate ($BaZr_{1-x}Y_xO_{3-d}$, BZY) is the most-studied high-temperature proton-conducting ceramic because of its stability in CO_2- and H_2O-containing atmospheres and its satisfactory bulk conductivity. However, the development of BZY-based devices is hindered by the presence of resistive grain boundaries. The blocking character of the grain boundaries has been explained by the space-charge layer model; low protonic-conductivity is a result of a positively charged grain-boundary core that creates a surrounding depletion layer for protons. The validity of this model has only been proven by indirect methods such as conductivity measurements under bias. In this work, atom probe tomography is used to quantify the chemical composition of the grain boundaries of several BZY specimens prepared by different processes. For the first time, we show direct proof of the positively charged grain-boundary core through the accumulation of oxide-ion vacancies. The results highlight the significant impact of the fabrication process on the resistive behavior of the BZY grain boundaries, which can have largely variable chemistries. Solid-state reactive sintering is the most-attractive fabrication method of those examined: it leads to a large-grained microstructure with the least-resistive grain boundaries, while reducing the sintering temperature and the number of fabrication steps.

4:30 PM

(EMA-S4-007-2016) Probing Ionic Transport Mechanisms in Y-doped Barium Zirconate

J. Ding*[2]; E. Strelcov[2]; G. Veith[2]; C. Bridges[2]; J. Balachandran[2]; P. Ganesh[2]; S. Kalinin[2]; N. Bassiri-Gharb[1]; R. Unocic[2]; 1. Georgia Institute of Technology, USA; 2. Oak Ridge National Lab, USA

Barium zirconate (BZO) has been widely studied as electrolyte in proton-conducting solid oxide fuel cells (PT-SOFCs), due to its high proton conductivity and excellent chemical stability at intermediate temperatures (500-700 °C). Previous work has concentrated on the conduction mechanisms and ionic transport in BZO; however, the role of defects, such as yttrium dopant and oxygen vacancies, on the proton transport, especially on the nanoscale and atomic scale, is still under debate. Here, we explore the ionic dynamics in pure and yttrium doped BZO (Y-BZO) films using energy discovery platforms, a synergy of nanofabricated device and in-situ characterization methods under controllable external stimuli. Through time resolved Kelvin probe force microscopy (tr-KPFM), the local potential in both the space and time domains is obtained, enabling analysis of local proton transport dynamics on the 10^{-2} to 10^2 s scale as a function of temperature and Y concentration. The activation energy increases with increasing dopant concentration, which is explained by the lattice distortion effect from the dopant clustering via density

functional theory. Simulation of ion transport through finite element method allows for creation of a physical model consistent with observed phenomena, and establishing of the dynamic characteristics of the process, including proton mobility and diffusivity.

4:45 PM

(EMA-S4-008-2016) Sodium ion conductivity and scaling effects in NASICON thin films prepared via chemical solution deposition

J. Ihlefeld*[1]; W. Meier[1]; E. Gurniak[1]; M. Blea-Kirby[1]; M. Rodriguez[1]; B. McKenzie[1]; A. McDaniel[1]; 1. Sandia National Laboratories, USA

We will present a methodology for preparing $Na_{1+x}Zr_2Si_xP_{3-x}O_{12}$ (sodium super ionic conductor, NASICON) thin films via a chemical solution deposition approach. Compositions spanning x=0 to x=1 were investigated with crystallization temperatures ranging from 750 °C to 800 °C. Increasing processing temperature resulted in increased ionic conductivity. Increasing silicon content was not accompanied by a significant increase in sodium-ion conductivity; the highest ionic conductivities were measured in films with an x=0.25 composition and not the expected x=1 composition. Conversely, it was observed that grain size had a strong effect on the measured ionic conductivities and that this superseded expected composition trends. This notwithstanding, the ionic conductivities measured exceed those of common lithium ion conductors and open possibilities for thin film solid-state sodium ion batteries. Sandia National Laboratories is a multiprogram laboratory operated by Sandia Corporation, a wholly owned subsidiary of Lockheed Martin Company, for the United States Department of Energy's National Nuclear Security Administration under contract DE-AC04-94AL85000.

S5. Multifunctional Nanocomposites

Multifunctional Nanocomposites IV

Room: Coral B

Session Chair: Junwoo Son, Pohang University of Science and Technology(POSTECH)

2:00 PM

(EMA-S5-019-2016) Metal to insulator transition in ultrathin complex-oxide heterostructures (Invited)

A. Janotti*[1]; 1. University of Delaware, USA

The two-dimension electron gas at the interface of complex oxides (*e.g.* $LaAlO_3/SrTiO_3$ and $GdTiO_3/SrTiO_3$) display distinctive characteristics, such as high charge densities (of the order of 10^{14} electrons/cm^2), distributed over a few unit cells near the interface. Combined with the localized nature of the Ti *d* orbitals that compose the conduction-band states, these properties lead to interesting physical phenomena that involve a strong interplay between electron-electron interaction and lattice distortions. In this talk we discuss results of first-principles calculations for the evolution of the electronic structure of complex oxide heterostructures as a function of the thickness of the $SrTiO_3$ layer. For thick layers, we find a 2DEG with a density of 1/2 electron per unit-cell area per interface within the $SrTiO_3$ layer. However, once the $SrTiO_3$ layer thickness is reduced to below three layers, we find that the electrons localize on every second interface Ti atom, giving rise to a charge-ordered Mott-insulating phase. This onset of localization is analyzed in terms of the electron density in the $SrTiO_3$ layer and octahedral distortions at the interface. We compare our results to experimental results available for $GdTiO_3/SrTiO_3$ heterostructures.

2:30 PM

(EMA-S5-020-2016) Thickness and Strain Effect on the Magnetic Properties of Epitaxial $Nd_{0.5}Sr_{0.5}CoO_3$ Thin Films

S. Cheng*[1]; M. Liu[1]; G. Hu[1]; L. Lu[1]; S. Mi[2]; C. Jia[1]; 1. Xi'an Jiaotong University, China; 2. Xi'an Jiaotong University, China

$Nd_{0.5}Sr_{0.5}CoO_3$(NSCO) thin films with various thickness were epitaxially fabricated on (001) $LaSrAlO_4$(LSAO), (001) $LaAlO_3$(LAO) and (001) (La,Sr)(Al,Ta)O_3(LSAT) substrates by using a KrF excimer pulsed laser deposition system. High resolution X-ray diffraction and TEM were used to characterize the structure of NSCO films; and the magnetic properties of films were measured by a Quantum Design Physical Property (PPMS-9) measurement system. All the NSCO films show excellent single crystalline quality and atomic sharp interface. It can be observed that NSCO films on LSAT substrates were under in-plane tensile strain while films on LSAO and LAO substrates were under in-plane compressive strain. Both film thickness and strain exhibit significant effect on the magnetic properties of NSCO films. The out-of-plane magnetization can be enhanced by out-of-plane tensile strain while the in-plane compressive strain will suppress the in-plane magnetization. Moreover, Curie temperature of the NSCO films dropped with the film thickness decreasing due to finite size effect; on the other hand it could also be enhanced by in-plane compressive strain. It indicates that controlling the strain and thickness of the films is an effective method to tune the magnetic properties of epitaxial NSCO thin films.

2:45 PM

(EMA-S5-021-2016) Dynamic Hydrogenation of Hexagonal WO_3 Epitaxial Thin Films with Open Tunnels

J. Park*[1]; J. Son[1]; 1. POSTECH, The Republic of Korea

Tungsten trioxide, which is best known material for smart windows and water splitting, exhibits various polymorphs depending on the synthesis processing condition. Different from the typical ReO_3-type polymorphs, metastable hexagonal WO_3(h-WO_3) has different arrangement of WO_6 octahedron, exhibiting 3.67Å diameter open tunnel along c-axis. Due to this mesoporous structure, alkali metal ions or water moleculces can be diffused and incorporated in this hexagonal window. Moreover, atomic hydrogen is known to be absorbed in h-WO_3 up to 0.5, but electronic phase transition as a function of hydrogen contents are not experimentally confirmed via hydrogen intercalation process. In this presentation, we show reversible structural and electronic phase transition of epitaxial h-WO_3 thin films by hydrogen intercalation through open tunnel in h-WO_3 with nano-sized Pt catalyst. At first, epitaxial h-WO_3(0001) thin films were successfully grown on YSZ(111) substrate by pulsed laser deposition. Interestingly, as more hydrogen is incorporated, in-plane lattice parameter expands and out-of-plane lattice parameter contracts. It is inferred that the hydrogen is diffused along the open tunnel, but captured in trigonal cavity based on the Raman spectroscopy analysis. We will discuss structural and electronic change of hydrogenated h-WO3 thin films in the context of diffusion and stability of hydrogen in h-WO_3.

3:00 PM

(EMA-S5-022-2016) Reversible phase transition of hydrogen sponge in multi-valent VO_2 epitaxial thin film

H. Yoon*[1]; M. Choi[2]; T. Lim[2]; H. Kwon[1]; K. Ihm[3]; J. Kim[1]; S. Choi[2]; J. Son[1]; 1. Pohang University of Science and Technology, The Republic of Korea; 2. Korea Institute of Materials Science, The Republic of Korea; 3. Pohang Accelerator Laboratory, The Republic of Korea

Hydrogen, the smallest and the lightest one among atomic elements, is reversibly incorporated into the interstitial site of vanadium dioxide (VO_2), a $3d^1$ correlated metal oxide undergoing metal-insulator transition at ~ 68 °C, and then induces dramatic electronic phase transition. It is widely reported that hydrogen stabilizes the metallic phase in low doping regime, but the understanding of hydrogen in high doping regime is very limited so far due to the

difficulty of heavy hydrogenation. Here, we present that hydrogenation can be achieved up to two hydrogen atoms per VO_2 unit cell, and hydrogen is reversibly absorbed into and released out of VO_2 without destroying the lattice framework due to the low temperature annealing process. More importantly, this massive hydrogenation process allows to elucidate phase transition of vanadium oxyhydride (H_xVO_2), remarkably demonstrating two-step insulator (VO_2) — metal (H_xVO_2) — insulator (HVO_2) phase transition using in-situ electrical measurement. Based on synchrotron X-ray measurement and first principles calculations, the unprecedented insulating HVO_2 with $3d^2$ configuration is attributed to highly doped electrons via hydrogenation process in conjunction with lattice expansion. Our finding opens up the potential application for novel hydrogen storage and the possibility of reversible and dynamic control of topotactic phase transition in VO_2.

3:15 PM

(EMA-S5-023-2016) Wafer-scale growth of VO_2 thin films using a combinatorial approach

H. Zhang*[1]; R. Engel-Herbert[1]; 1. Pennsylvania State University, USA

VO_2 is one of the prototype metal-insulator-transition (MIT), which has been intensively studied due to the wide range of potential applications in electronic and optical devices in its thin film form. The functional property – the resistivity change across the MIT – has been found highly sensitive to valence state variations, requiring extensive calibration series stabilize the desired valence state of vanadium. In this talk we present a new thin film growth approach that allows for a precise valence state control using a combinatorial technique enabling the growth of high quality VO_2 thin films on wafer scale. By creating an oxygen activity gradient across the wafer, a continuous valence state library is established, enabling a rapid identification of the optimal growth condition. The superior control over the valence state of vanadium allows to grow high quality VO_2 thin films on 3-inch sapphire substrates. Wafer-scale metrology results will be presented that highlight the high uniformity of VO_2 thin films achieved across the wafer. RF switches were fabricated and revealed one order higher cut-off frequency than state-of-the-art traditional semiconductor based devices, demonstrating that 'electronic grade' transition metal oxide films can be realized on a large scale using a combinatorial growth approach, which can be extended to other multivalent oxide systems.

4:00 PM

(EMA-S5-024-2016) Many-body effects and band structure of the transparent oxide semiconductors In_2O_3 and SnO_2 (Invited)

M. Feneberg*[1]; 1. Otto-von-Guericke University Magdeburg, Germany, Germany

Transparent oxide semiconductors like cubic In_2O_3 and rutile SnO_2 can serve as platform for plasmonic applications in the infrared and visible part of the spectrum. They serve as contact layers for optical devices or may be used as material of choice for transparent electronics. Engineering of their properties is possible by doping. However, many-body interactions between charged particles alter the band structure compared to the intrinsic material. Here, recent achievements in understanding band structure parameters like effective electron masses, absorption onsets and their doping dependency are discussed. Spectroscopic ellipsometry from the mid-infrared (~30meV) into the vacuum-ultraviolet (~30eV) spectral region over three orders of magnitude is applied to determine dielectric tensor components. Analysis of the dielectric function in the infrared yields phonon frequencies and plasmon contributions from which the effective electron mass as a function of carrier density is obtained. In both materials, the conduction band is strongly nonparabolic. In the ultraviolet part of the spectrum, Burstein-Moss effect and bandgap renormalization have a strong influence on the behavior of the fundamental absorption onset. A quantitative description of these properties will be presented both for the isotropic case (cubic In_2O_3) and for the anisotropic case (rutile SnO_2).

4:30 PM

(EMA-S5-025-2016) Dielectric Screening and Optical Absorption in In_2O_3 and Ga_2O_3 from First Principles

J. Varley[2]; A. Schleife*[1]; 1. University of Illinois at Urbana-Champaign, USA; 2. Lawrence Livermore National Laboratory, USA

Transparent conducting materials such as indium oxide, In_2O_3, and gallium oxide, Ga_2O_3, are highly desirable for transparent electronics, photovoltaics, and optoelectronics. Both are wide-band gap semiconductors with high transparency and can be doped such that their electrical conductivity is large enough for device applications. However, the influence of screening on the electron-hole interaction and optical absorption is poorly understood and is difficult to access directly in experiment. We recently computed optical absorption spectra across a large photon energy range, using the Bethe-Salpeter equation to include excitonic effects. A state-dependent scissor shift is used to closely reproduce hybrid functional results for single-particle band structures, while meeting the challenging convergence criteria necessary for optical spectra. Our accurate theoretical-spectroscopy results for optical spectra allow us to discuss the influence of excitons across a large spectral range. We provide a qualitative understanding of optical anisotropy in monoclinic β-Ga_2O_3 near the absorption edge and at high photon energies. Our spectra, that are directly comparable to experiment, show that a first-principles description accurately predicts optical properties of complex, technologically relevant materials, which is critical for successful computational materials design.

4:45 PM

(EMA-S5-026-2016) Semiconducting oxides - From material design to basic devices (Invited)

H. von Wenckstern*[1]; 1. Universität Leipzig, Germany

Research on semiconducting oxides, triggered by the extraordinary material properties of crystalline but amorphous thin films as well, boosted in recent years and resulted in first commercial applications like transistors used in the backplane of flat-panel displays or transparent electrodes of touch panels or thin film solar cells. Potential applications of semiconducting oxides include transparent electronics, flexible circuitry, power electronics, diluted magnetic semiconducting layers, chemical and bio sensors, visible-blind, solar-blind and quantum well infrared photodetectors. In this talk, we will discuss material design of semiconducting oxides via creation and analysis of material libraries, which are realized by deposition methods allowing a controlled lateral variation of the chemical composition of oxide thin films. Examples are detailed for amorphous zinc-tin oxide layers for which the cation ratio has major influence on e.g. charge carrier transport properties or the rectifying properties of Schottky contacts and *pn*-heterodiodes. Further, we will address the development of wavelength selective, narrow bandwidth, visible-blind photodetector arrays and present first results on solar-blind detectors. Finally, properties of the group III sesquioxides and their alloys are introduced and devices based thereon are reviewed.

5:15 PM

(EMA-S5-027-2016) Semiconducting Ga_2O_3 layers grown by metal organic vapor phase epitaxy (Invited)

M. Baldini*[1]; M. Albrecht[1]; K. Irmscher[1]; R. Schewski[1]; G. Wagner[1]; 1. Leibniz Institute for Crystal Growth, Germany

Gallium oxide is one of the most emerging compound among transparent semiconducting oxides, thanks to its distinctive physical properties. The most stable monoclinic β-phase is characterized by a large bandgap (E_g=4.8 eV), an extremely high breakdown field (8 MV/cm) and a widely tunable *n*-type conductivity (10^{16}-10^{19} cm^{-3}). The most promising application fields of β-Ga_2O_3 are high power devices and solar blind UV photodetectors. In both cases, β-Ga_2O_3 is supposed to outperform actual devices based on SiC and AlGaN thanks to a higher breakdown voltage, an enhanced

UV-transparency and the availability of cheap and high quality bulk material. For the realization of such applications, β-Ga_2O_3 layers with the highest crystalline quality are required. By using metal organic vapor phase epitaxy, we demonstrated the coherent growth of semi-insulating homo-epitaxial β-Ga_2O_3 layers and revealed a dramatic improvement of their crystalline perfection through the surfactant effect of In. A reproducible n-conductivity, in the range $5x10^{17}$-$2x10^{18}$ cm^{-3}, was obtained by using an alternative Ga precursor that in the literature is known to lead to a lower C incorporation. The electron mobility, with a maximum value of 40 cm^2/Vs, showed a peculiar decrease at low free carrier concentrations explained by the scattering of free charge carriers at stacking errors, identified as the main crystallographic defects of the layers.

S6. Computational Design of Electronic Materials

Materials by Design: Electronic Materials I

Room: Mediterranean A
Session Chair: Mina Yoon, Oak Ridge National Laboratory

2:00 PM

(EMA-S6-001-2016) Relaxor behavior and electrocaloric effect of Na1/2Bi1/2TiO3: Insights from computer simulations (Invited)

K. Albe*[1]; 1. Technical University Darmstadt, Germany

Na1/2 Bi1/2 TiO3 (NBT) and its solid solutions with other lead-free perovskite materials have attracted significant interest for applications in actuators, sensors, and transducers due to their excellent piezoelectric properties. Moreover, they have been recently discussed for applications in solid state refigeration, because of a significant negative electrocaloric effect (EVE). The physical reasons for the relaxor behavior and the negatice ECE are, however, unclear. In this contribution, I will first present a method based on *ab initio* calculations to predict compositions at morphotropic phase boundaries in lead-free perovskite solid solutions. This method utilizes the concept of flat free energy surfaces and involves the monitoring of pressure-induced phase transitions as a function of composition. Then the kinetics of octahedral tilt transitions is investigated for transitions between tetragonal, rhombohedral and orthorhombic tilts in cation configurations with [001]- and [111]-order and discussed in the context of polar nanoregions, which are the cause of the experimentally observed relaxor behavior of NBT.

2:30 PM

(EMA-S6-002-2016) High thermoelectric figure of merit as a counterindicated property of matter: Transport theory as a guide for resolving this conundrum (Invited)

D. J. Singh*[1]; 1. University of Missouri, Columbia, USA

Thermoelectric efficiency is governed by a figure of merit, ZT, which has no known thermodynamic limit (infinite ZT yields Carnot efficiency). However, as will be discussed, the ingredients needed for high ZT, specifically high thermopower, high electrical conductivity and low thermal conductivity, do not generally occur together, and in fact the standard models for semiconductors to not yield insights into how to obtain high ZT. Here these contradictions are discussed from the point of view of transport theory and first principles calculations and a strategy for overcoming them is presented along with some results for specific materials.

3:00 PM

(EMA-S6-003-2016) First principle prediction of semiconducting/metallic phase transitions in Transition Metal Dichalcogenides: Coupled Electron and Strain effects

B. Ouyang*[1]; J. Song[1]; 1. McGill Univesity, Canada

The existence of semiconductor to metal transitions within several monolayer VI transition-metal dichalcogenides (TMDs) has opened gates to manipulate related devices by phase engineering. The flourish of phase engineering techniques can be categories as charge engineering (intercalation, electron doping, etc.) and/or strain engineering. In this work, coupled electron doping and strain effects were investigated employing first-principles density functional theory (DFT) calculations. For each TMD system, with the lattice strain and electron density treated as state variables, the energy surfaces of different phases were computed and the correspondent phase diagrams were constructed. These diagrams assess the competition between different phases and predict conditions of phase transitions for the TMDs considered. Meanwhile, the interplay between lattice deformation and electron doping was identified to originate from the deformation induced band shifting and band bending. Based on our findings, much lower electron doping density is required for inducing phase transition with coupled strain effects. These findings lead to the potential design scheme of more controllable phase engineering by combining electron gating and elastic strain.

3:15 PM

(EMA-S6-004-2016) Identification of metastable ultrasmall titanium oxide clusters using a hybrid optimization algorithm

E. Inclan*[1]; D. Geohegan[2]; M. Yoon[2]; 1. Georgia Institute of Technology, USA; 2. Oak Ridge National Lab, USA

Nanostructured TiO_2 materials have interesting properties that are highly relevant to energy and device applications. However, precise control of their morphologies and characterization are still a grand challenge in the field. Using a hybrid optimization algorithm we theoretically explored configuration spaces of energetically metastable TiO_2 nanostructures. Our approach is to minimize the total energy of TiO_2 clusters in order to identify the structural characteristics and energy landscape of plausible $(TiO_2)_n$ (n = 1-100). The results were compared against known physical structures and numerical results in the literature as well as our experimentally synthesized structures. A new method to measure computational effectiveness is proposed using a regression on known structures. This scheme defines effectiveness as the ability of an algorithm to produce a set of structures whose energy distribution follows the regression as the number of $(TiO_2)_n$ increases without specifying an exact distribution to allow for flexibility between approaches. The hybrid algorithm is shown to reproduce the known structures up to n = 5, and retains good agreement with the regression up to n = 25. For n > 25, the structures continue to increase in stability. This work is supported by the U.S. Department of Energy, Office of Science, Basic Energy Sciences, Materials Sciences and Engineering Division.

Materials by Design/Interface driven Functional Materials

Room: Mediterranean A
Session Chair: Ghanshyam Pilania, Los Alamos National Lab

4:00 PM

(EMA-S6-005-2016) Information-driven approach to materials discovery and design (Invited)

T. Lookman*[1]; 1. Los Alamos National Lab, USA

Some of the outstanding challenges in information-driven materials design include identifying key features, guiding the next experiment to aid the learning process, dealing with rather small data sets and incorporating domain knowledge to make better predictions. By using examples on materials classes such as perovskites and alloys related to classification and regression problems, I will emphasize the need for an adaptive feedback loop to find materials with targeted properties. Examples include finding low thermal dissipation NiTi based shape memory alloys.

4:30 PM

(EMA-S6-006-2016) Band-gap and Band-edge Engineering of Multicomponent Garnet Scintillators (Invited)

C. Stanek*[1]; S. Yadav[1]; B. Uberuaga[1]; C. Jiang[2]; M. Nikl[3]; 1. Los Alamos National Laboratory, USA; 2. Thermo-Calc Software, USA; 3. Institute of Physics, Academy of Sciences of the Czech Republic, Czech Republic

Complex doping schemes in $RE_3Al_5O_{12}$ (RE=rare earth element) garnet compounds have recently led to pronounced improvements in scintillator performance. Specically, by doping lutetium and yttrium aluminate garnets with gallium and gadolinium, the band-gap is altered in a manner that facilitates the removal of deleterious electron trapping associated with cation antisite defects. After a brief review of initial studies of the effect of substitutional dopants on defect chemistry and band gap, recent results using density functional theory (DFT) and hybrid density functional theory (HDFT) to closely examine the effect of dopants on conduction and valence band edge levels will be reported. Two sets of compositions (based on $Lu_3B_5O_{12}$ where B = Al, Ga, In, As, and Sb; and $RE_3Al_5O_{12}$, where RE = Lu, Gd, Dy, and Er) will be used to illustrate the effect of dopants on band edges. These results indicate that certain dopants can be used to selectively modify only the conduction band minimum or the valence band maximum and demonstrate an approach to quickly screen the impact of dopants on the electronic structure of scintillator compounds, identifying those dopants which alter the band edges in very specic ways to eliminate both electron and hole traps responsible for performance limitations.

5:00 PM

(EMA-S6-007-2016) First-Principles Predication of Two-Dimensional Electrides

W. Ming*[1]; M. Yoon[1]; 1. Oak Ridge National Laboratory, USA

Two-dimensional (2D) electrides have recently received increasing interest due to the promise for electron emitter, surface catalyst and high-mobility electronic devices. However, they are very limited in a few layered alkaline-earth nitrides and rare-earth carbides. Here, we extend the possibility of 2D electrides by structure predication, using density functional theory calculation in conjunction with particle swarm optimization algorithm. Simple-element compounds A2B (A/B = alkali metals/halogen, or A/B = alkaline-earth metals/VA, VIA, VIIA nonmetals) and AB (A/B = alkaline-earth metals/halogen), which have nominal imbalanced oxidation numbers, are investigated. We find several new 2D electrides out of 90 candidates, and uncover that the stabilization of layered structure, which is required for the success of 2D electrides, strongly depends on the relative size of cation, in such a way that it has to be of similar or larger size than the anion in order to sufficiently screen the repulsion between the excess electrons and anions. We additionally identify the experimental conditions of temperature and chemical potential where the predicted 2D electrides are stabilized against the decomposition into compounds with balanced oxidation numbers. Our results will shed light on searching for new electrides and understanding on design principles of electrides for practical applications.

5:15 PM

(EMA-S6-008-2016) Designing quantum spin defects in ceramic materials for scalable solid-state quantum technologies (Invited)

H. Seo*[1]; 1. The University of Chicago, USA

Although quantum mechanics has enabled astounding advances in semiconductor technology, such technologies still do not fully exploit several aspects of quantum physics, such as entanglement. It is expected that a second revolution in semiconductor technology will stem from the successful control and implementation of entanglement and other exotic features of quantum physics. In this talk, we discuss a material platform that may lead to new types of quantum electronics building upon mature semiconductor microelectronic technologies: solid-state quantum bits (or qubits) realized using electronic spins bound to atom-like point defects in crystals. First, we will present our recent work on the quantum decoherence dynamics of divacancy spin qubits in silicon carbide using cluster correlation expansion theory. In collaboration with experiment, we found that the coherence time of the divacancy qubit is even longer than that of the nitrogen-vacancy center in diamond and we explained its microscopic origin. In the second part of the talk, we will describe our work on the exploration of new quantum defect spins in piezoelectric aluminum nitride. We used hybrid density functional and GW many-body perturbation calculations and we predicted that the negatively charged nitrogen vacancy under strain is a strong candidate for a defect spin qubit in AlN.

S8. Interface Structure, Orientation, and Composition: Influence on Properties and Kinetics

Interface Structure and Properties

Room: Mediterranean B/C

Session Chair: David McComb, The Ohio State University

2:00 PM

(EMA-S8-007-2016) Metal- Dielectric Interfaces: Temporal Evolution Under Applied Bias (Invited)

E. C. Dickey*[1]; A. Moballegh[1]; L. Chen[2]; J. Wang[2]; H. Huang[2]; 1. North Carolina State University, USA; 2. Pennsylvania State University, USA

The design of electrode interfaces is an important aspect of the overall properties and performance of electroceramic devices, as the electrochemical boundary conditions affect the transport of ionic and electronic carriers across the metal-ceramic interface. Once the device is in service, the externally applied voltages induce electromigration processes in the ceramic, and the resulting spatio-temporal changes in chemistry lead to an evolution in device properties. Often these types of phenomena control device reliability and lifetime. This talk will focus on the particular issue of electromigration of point defects on local interface chemistry and transport properties, and the influence of the electrochemical boundary conditions on these processes. Particular attention will be given to recent experimental studies on single-crystal TiO_2 [Acta Materialia, 86 (2015) 352-360], $SrTiO_3$ and $BaTiO_3$. A combination of electrical transport and electron microscopy analyses help provide insight into the interface evolution from the atomistic to micrometer length scale. This work was sponsored by the National Science Foundation under grant DMR-1132058 and AFOSR under grant FA9550-14-1-0067.

2:30 PM

(EMA-S8-008-2016) Impact of space charge on grain growth in perovskite ceramics: growth stagnation, solute drag and intrinsic defects (Invited)

W. Rheinheimer*[1]; F. Lemke[1]; M. J. Hoffmann[1]; 1. Karlsruhe Institute of Technology, Germany

In ceramic materials, grain boundaries are typically charged; consequently different intrinsic or extrinsic (solutes) defects form a space charge layer at the boundaries. If such a boundary migrates at low driving forces, the concentration profile of defects follows the migration and the boundary is dragged by the diffusion of defects. This effect is known as solute drag. However, for high driving forces, the interface breaks away from the space charge and moves without defect diffusion and drag. This study shows that in perovskite ceramics a drag effect exists, which is similar to solute drag, but in contrast no external defects are needed. Solely intrinsic defects (i.e. cation vacancies) seem to be responsible. This assumption bases on different growth stagnation effects in perovskite ceramics: for $SrTiO_3$, grain growth was found to stagnate at a temperature dependent critical grain size. This stagnation can be correlated with the intrinsic defect concentration: a decreasing oxygen partial pressure results in a decreasing drag effect. According to the defect

chemistry of perovskites this correlates with a decreasing strontium vacancy concentration. On the other hand, external defects (e.g. iron dopants) result in very strong stagnation effects. Based on these findings all stagnation effects are explained by an intrinsic drag effect similar to solute drag.

3:00 PM

(EMA-S8-009-2016) Characterization of grain boundary disconnections in general grain boundaries in $SrTiO_3$

H. Sternlicht*[1]; W. Rheinheimer[2]; M. J. Hoffmann[2]; W. D. Kaplan[1];
1. Technion, Israel; 2. Institute of Applied Materials, Karlsruhe Institute of Technology, Germany

General grain boundaries (GBs) in $SrTiO_3$ were found to contain steps along the boundary planes. The steps are likely correlated to the mechanism of grain boundary motion in $SrTiO_3$. These steps were found to lie along the same crystallographic planes regardless of the annealing temperature or atmosphere, even if the measured GB mobility is drastically different. It was shown that the steps also had a dislocation component, creating overall grain boundary disconnections. General GBs in polycrystalline $SrTiO_3$ and GBs between a single crystal diffusion bonded to polycrystalline $SrTiO_3$ were characterized using aberration corrected transmission electron microscopy (TEM) combined with exit wave reconstruction. While the steps tend to appear along the same crystallographic planes, the dislocations vary between different boundaries, and have no consistent structure and density. The atomistic termination of the steps tends to vary as well, yielding many possible terminations and step-chemistry.

3:15 PM

(EMA-S8-010-2016) Surface and interface composition in LAO/STO hetero-interface

H. Zaid[2]; M. Berger[2]; D. Jalabert[3]; M. Walls[4]; R. Akrobetu[1]; N. Goble[1]; X. Gao[1]; W. Lambrecht[1]; A. Sehirlioglu*[1]; 1. Case Western Reserve University, USA; 2. Mines ParisTech, Centre des Matériaux, France; 3. Univ. Grenoble Alpes, France; 4. CEA, France

$LaAlO_3$/ $SrTiO_3$ (LAO/STO) hetero-interfaces are of-interest due to observation of unexpected phenomena at the interface including tunable 2D conductivity, superconductivity and magnetic scattering. A great number of physical and chemical factors have been hypothesized to create these unique observations at the interface; however neither is necessarily exclusive of each other. Therefore, quantification of all parameters is crucial to understand the extent each factor contributes to both the presence/absence and the magnitude of the 2D conductivity. Presented here is how the local chemistry at the interface affects the local strain and how the surface chemistry can play a role on the electrical conductivity at the interface. The techniques include medium energy ion spectroscopy (MEIS) and X-ray Photoelectron Spectroscopy (XPS). The intermixing of both the A- and B-site cations have been quantified and related to in-plane strain with atomic resolution. The surface adsorbed species have been identified, quantified and was related to electrical properties. The results show both the need for quantification of parameters and the complex nature of these interfaces.

4:00 PM

(EMA-S8-011-2016) Characterizing ordering phenomena at the atomic scale through high-resolution electron microscopy and simulation (Invited)

B. D. Esser[1]; R. E. Williams[1]; D. W. McComb*[1]; 1. The Ohio State University, USA

Aberration corrected scanning transmission electron microscopy (STEM) has become a powerful tool for studying the atomic structure of materials in order to establish structure-property relationships. The increasing availability of state-of-the-art STEMs has resulted in efforts to push the limits and retrieve 3-dimensional information about a material from 2D images. Doing so has the potential to significantly improve the way materials are characterized by accessing structural, chemical, and electronic properties with the highest resolution. The applications of this are vast including cation ordering in oxide materials, localized defects at interfaces and other boundaries, site-specific solute segregation within defects, etc. While the prospects of such studies are very appealing, there are still many physical phenomena within the microscope that need to be better understood to be fully quantitative. Chief among these is the interaction of the electron probe with a material and the effect of probe channeling on image contrast and spectroscopic intensity. Theory-based simulations are critical in order to better understand these data. Through the combination of experimental and theoretical techniques, the meaning of resolution in the STEM can be greatly expanded.

4:30 PM

(EMA-S8-012-2016) Effect of grain boundary energy and mobility anisotropy on the coarsening kinetics of highly twinned microstructure (Invited)

M. Tang*[1]; 1. Rice University, USA

FCC metals such as Cu and Ni alloys often contain significant amount of twin Σ3 and multiply twinned (e.g. Σ9, Σ27) grain boundaries in microstructures, which can be further enhanced by grain boundary engineering. These special boundaries often show large contrast to random boundaries in their energy and mobility values. We study the effect of such grain boundary character dependence of boundary energy and mobility on the grain growth kinetics. Phase-field simulations reveal that the special boundary fraction alone is not a sufficient indicator of the coarsening behavior of the grain boundary network. Instead, the connectivity of random boundaries in the network has considerable influence on grain growth. By comparing two types of microstructures with different random boundary connectivity, it is found that the relative special boundary population is not stable and continues to decline during coarsening when random boundaries form a continuous sub-network in the microstructure. In contrast, when the connectivity of random boundaries is broken, the special boundary fraction increases with time, which results in a lower grain growth rate. The modeling results indicate that breaking the random boundary network is a necessary condition for obtaining grain boundary engineered microstructures that are resistant against thermal coarsening.

5:00 PM

(EMA-S8-013-2016) Dominance of Interface Chemistry over the Bulk Properties in Determining the Electronic Structure of Epitaxial Metal/Perovskite Oxide Heterojunctions

P. Sushko*[1]; Y. Du[1]; M. Gu[1]; T. Droubay[1]; S. Hepplestone[2]; H. Yang[3]; C. Wang[1]; N. Browning[1]; S. Chambers[1]; 1. Pacific Northwest National Lab, USA; 2. University College London, United Kingdom; 3. University of Oxford, United Kingdom

We show that despite very similar crystallographic properties and work function values in the bulk Fe and Cr, thin films of these metals on Nb:SrTiO3(001), an oxide semiconductor of considerable current interest, exhibit very different structures and heterojunction electronic properties. This difference arises because of variations in interface chemistry. Body-centered cubic Cr(001) nucleates epitaxially on $SrTiO_3$(001) and forms a low-resistance Ohmic contact. Examination of STEM images reveals a clear presence of Cr^{3+} ions at interstitial sites within the first few atomic layers of $SrTiO_3$. Ab initio simulations demonstrate that in-diffused metal ions can act as anchors for the epitaxial metal films, increasing adhesion, and modifying the electronic properties so as to metalize the interface and preclude Schottky barrier formation. In contrast, Fe/$SrTiO_3$ forms a disordered interfacial layer and a Schottky barrier with a barrier height of 0.50 eV. In-diffused Fe exhibits a +2 oxidation state and occupies Ti sites in the perovskite lattice, resulting in negligible charge transfer to Ti, upward band bending, and Schottky barrier

formation. These results are attributed to the difference in the dominant defects reaction pathways at the film/substrate interface.

5:15 PM

(EMA-S8-014-2016) Structure of the Equilibrated Ni(111)-YSZ(111) Solid-Solid Interface

H. Nahor*[1]; W. D. Kaplan[1]; 1. Technion - Israel Institute of Technology, Israel

The stability of metal films on oxide surfaces is important for the performance of devices such as solid oxide fuel cells (SOFCs) and thermal barrier coatings (TBCs). Ni-YSZ serves as an anode material in SOFCs. During SOFC operation, the metal-ceramic interface is subjected to high temperatures and a reducing atmosphere, which can lead to coarsening of the Ni nanoparticles, which decreases the number of three-phase boundaries. The three-phase boundaries (Ni/YSZ/fuel-gas) are essential for catalytic activity which controls the electrical properties. A better understanding of the equilibrated Ni-YSZ interfacial structure and energy can lead to improved adhesion and long-term stability of SOFCs. In this work, solid-state dewetting of continuous Ni films deposited on the (111) surface of yttrium stabilized zirconia (YSZ) was used to produce equilibrated Ni particles, and the solid-solid interface structure was determined using aberration corrected transmission electron microscopy (TEM). The ~150nm thick Ni films were annealed at 1350°C (0.94 T_m) in Ar+H_2 (99.9999%) at a partial pressure of oxygen of 10^{-20} atm for 6 hours. TEM of equilibrated particles was conducted to analyze the structure at the interface, and revealed that despite the 31% lattice mismatch between Ni and YSZ, the interface is semi-coherent and a two dimensional network of misfit dislocations was identified.

5:30 PM

(EMA-S8-015-2016) Effect of Top Electrode Material on Radiation-Induced Degradation of Ferroelectric Thin Films

S. Brewer*[1]; M. Paul[2]; K. Fisher[3]; J. Guerrier[4]; J. L. Jones[4]; R. Rudy[6]; R. G. Polcawich[6]; E. Glaser[5]; C. Cress[5]; N. Bassiri-Gharb[1]; 1. Georgia Institute of Technology, USA; 2. Woodward Academy, USA; 3. Riverwood International Charter School, USA; 4. North Carolina State University, USA; 5. Naval Research Laboratory, USA; 6. US Army Research Laboratory, USA

The large dielectric, piezoelectric and pyroelectric response of ferroelectric thin films has drawn a substantial interest over recent years for use in millimeter-scale robotics, in which the ferroelectric material fulfills multiple functionalities such as sensing, actuation, energy harvesting, mechanical logic, etc. Of specific interest are applications in dangerous or difficult-to-reach locations such as nuclear power plants and aerospace. This work addresses the mechanisms of radiation interaction with ferroelectric $Pb[Zr_{0.52}Ti_{0.48}]O_3$ thin films deposited on platinized silicon wafers, with IrO_2 or Pt top electrodes. All samples were irradiated with 2.5 Mrad (Si), using a ^{60}Co gamma radiation and the dielectric and electromechanical response were characterized before and after irradiation. Samples with IrO_2 electrodes generally showed less degradation of dielectric properties compared to samples with Pt electrodes. Pinching in polarization-electric field hysteresis loops and formation of secondary peaks in C-V curves were observed only in samples with metallic top electrodes. The electromechanical response of the samples was substantially more stable for the oxide electrodes than samples with Pt top electrode. The quantitative results will be discussed in terms of ion-blocking or ion-conducting electrode materials and possible approaches for "self-healing," radiation-hard devices.

5:45 PM

(EMA-S8-016-2016) Energetics of All Metal Oxide Junctions

K. Rietwyk*[1]; D. Keller[1]; H. Barad[1]; A. Ginsburg[1]; K. Majhi[1]; A. Anderson[1]; A. Zaban[1]; 1. Bar-Ilan University, Israel

During the 1990s a major breakthrough in thin film technologies was achieved with the application of metal oxide buffer layers between organic/polymer layers and metal electrodes. This improved the energy level alignment between the layers, resulting in a drastic enhancement in the performance of a range of devices. There has since been growing interest in active metal oxide layers, due to their high abundance, stability, and low-cost processing. Consequently, metal oxides are more frequently grown as adjacent layers in thin film devices. However, the underlying mechanisms that determine the energetics across all metal oxide interfaces have yet to be extensively investigated. To address this shortcoming we have developed an innovative depth profiling method. Exploiting the proven combinatorial metal oxide growth techniques we deposit a metal oxide layer with a thickness gradient onto a homogeneous metal oxide layer. Depth profiling is then achieved by laterally scanning the energetics across the sample using scanning Kelvin probe, air photoemission and UV-Vis optical analysis and correlating the measured properties of the layer to the thickness. From this an entire band diagram of the entire active depth of the junction can be developed. To demonstrate the power of this technique we will provide a complete band diagram of the TiO_2-Co_3O_4 heterojunction which has recently shown promise in all oxide photovoltaics and water splitting.

S9. Recent Developments in Superconducting Materials and Applications

Electronic Structure and Superconductivity Mechanism

Room: Pacific

Session Chairs: Xingjiang Zhou, National Lab for Superconductivity; Gang Wang, Institute of Physics, Chinese Academy of Sciences

2:00 PM

(EMA-S9-019-2016) Searching Genes of Unconventional High Temperature Superconductors (Invited)

J. Hu*[1]; 1. Institute of Physics, CAS, China

We discuss two emergent principles, which are called as the correspondence principle and the selective magnetic pairing rule, to unify the understanding of both cuprates and iron-based superconductors. These two principles provide an unified explanation why the d-wave pairing symmetry and the s-wave pairing symmetry are robust respectively in cuprates and iron-based superconductors. In the meanwhile, the above two principles explain the rareness of unconventional high Tc superconductivity, identify necessary electronic environments required for high Tc superconductivity and finally serve as direct guiding rules to search new high Tc materials. We predict that the third family of unconventional high Tc superconductors exist in the compounds which carry two dimensional hexagonal lattices formed by cation-anion trigonal bipyramidal complexes with a d^7 filling configuration on the cation ions. Their superconducting states are expected to be dominated by the d+id pairing symmetry and their maximum Tc should be higher than those of iron-based superconductors. Verifying the prediction can convincingly establish the high Tc superconducting mechanism and pave a way to design new high Tc superconductors.

2:30 PM

(EMA-S9-020-2016) New approaches for enhancing T_c (Invited)

M. Osofsky*[1]; J. Prestigiacomo[1]; C. Krowne[1]; R. Soulen[2]; H. Kim[1]; E. Clements[1]; G. Woods[3]; H. Sikanth[3]; I. Takeuchi[4]; V. Smolyaninova[5]; B. Yost[5]; K. Zansder[5]; T. Gresock[5]; S. Saha[4]; R. Greene[4]; I. Smolyaninov[6]; 1. Naval Research Laboratory, USA; 2. Retired, USA; 3. University of South Florida, USA; 4. University of Maryland, USA; 5. Towson University, USA; 6. University of MAryland, USA

For conventional superconductors, the superconductive critical temperature can be characterized by the coupling strength, l=NV where N is the single particle density of states and V is an attractive

potential. The search for new superconductors with high T_c often involves searching for materials with enhanced N. In this presentation we explore an alternative approach the entails enhancing V. We will discuss two methodologies, metamaterial engineering and proximity to the metal-insulator transition (MIT). Metamaterials are artificial materials built from conventional microscopic materials in order to engineer their properties in a desired way. We recently used the metamaterial approach to dielectric response engineering to increase the T_c of a composite superconductor-dielectric metamaterial. Specifically, an increase of the critical temperature of the order of 0.15 K compared to bulk tin has been observed for tin/barium and strontium titanate nanoparticle composites. We also analyze several other promising geometries that can enable the optimization of the metamaterial superconductor properties. We also demonstrate empirically that several disparate classes of superconductors share a common phase diagram $T_c(r)$ where r is a coordinate characterizing the distance to the MIT. This phase diagram may be explained by explicitly incorporating the novel properties of the MIT in V. These results can be used to optimize T_c for any system with an MIT.

3:00 PM

(EMA-S9-021-2016) Observation of strong electron pairing on bands without Fermi surfaces in $LiFe_{1-x}Co_xAs$ (Invited)

T. Qian*[1]; 1. Institute of Physics, Chinese Academy of Sciences, China

In conventional BCS superconductors, the quantum condensation of superconducting electron pairs is understood as a Fermi surface instability, in which the low-energy electrons are paired by attractive interactions. Whether this explanation is still valid in high-Tc superconductors such as cuprates and iron-based superconductors remains an open question. In particular, a fundamentally different picture of the electron pairs, which are believed to be formed locally by repulsive interactions, may prevail. Here we report a high-resolution angle-resolved photoemission spectroscopy study on $LiFe_{1-x}Co_xAs$. We reveal a large and robust superconducting gap on a band sinking below the Fermi level on Co substitution. The observed Fermi-surface-free superconducting order is also the largest over the momentum space, which rules out a proximity effect origin and indicates that the order parameter is not tied to the Fermi surface as a result of a surface instability.

4:00 PM

(EMA-S9-022-2016) Quantitative Determination of the Pairing Interactions in High Temperature Superconductors (Invited)

X. Zhou*[1]; 1. National Lab for Superconductivity, China

A profound problem in modern condensed matter physics is discovering and understanding the nature of the fluctuations and their coupling to fermions in cuprates which lead to high temperature superconductivity and the associated strange metal behaviors. Here we will report the quantitative determination of the attractive effective interactions in the (d)-wave pairing symmetry as well as their repulsive counterpart in the full symmetry of the lattice, made possible by laser-based angle-resolved photoemission measurements with unprecedented accuracy and stability. Our results concern the pivotal issues in the problem so that a valid theory should lead to results in qualitative and quantitative agreement with them. *Work in collaboration with Jin Mo Bok, Jong Ju Bae, Wentao Zhang, Junfeng He, Yuxiao Zhang, Li Yu, Han-Yong Choi and Chandra M. Varma.

4:30 PM

(EMA-S9-023-2016) Weyl semi-metals and Weyl superconductors (Invited)

X. Dai*[1]; 1. Institute of Physics, Chinese academy of sciences, China

The basic electronic structure of Weyl semi-metals will be introduced with some typical materials including the TaAs family. The possible superconducting phases in the Weyl semi-metal systems will then be discussed and classified according to their topological features. We find that the exchange interaction combined with the inversion symmetry breaking terms will probably lead to the topological superconductivity phase in such systems.

5:00 PM

(EMA-S9-024-2016) Electron-pair state in crystal: a missing piece in solid-state theory (Invited)

G. Hai*[1]; 1. University of Sao Paulo, Brazil

Electronic band-structure in solid-state theory is based on single-electron states. It is known that the single-electron energy levels of periodically organized individual atoms form energy bands in a crystal. In fact, individual electron pairs also exist in atoms and ions such as the negative hydrogen ion H- and helium atom. The quantum state of an electron pair is different in its nature from the single-electron state bacuase of the strong correlation between the two paired electrons. The electron pair localizes closely to the positive charge of the nucleus and does not form a valence with other atoms. In this talk, we show that the electron-pair states from individual atoms may survive in a two-dimensional crystal. When the amplitude of the crystal potential is larger than a certain value, a metastable electron-pair band arises between the two lowest single-electron energy bands at low electron density. Based on the single-electron and electron-pair band structure, we demonstrate that the many-particle exchange-correlation corrections renormalize the energy bands and stabilize electron pairs for certain electron-pair and hole densities. Therefore, depending upon the crystal potential and free carrier densities, there may exist energy band of electron pairs and, consequently, a many-particle system consisting of electron pairs and holes in a two-dimensional crystal.

5:30 PM

(EMA-S9-025-2016) A BCS-like model for heavy fermion and cuprate superconductivity (Invited)

Y. Yang*[1]; 1. Institute of Physics, Chinese Academy of Sciences, China

Dual (simultaneously localized and itinerant) behavior is a general property of strongly correlated electrons and has been experimentally established in both high T_c cuprate and heavy fermion superconductors. They may both be described as Kondo lattices and exhibit characteristic two-fluid behaviors. Paring quasiparticles are naturally born out of interacting local moments and the pairing glue has been in many cases identified as quantum critical spin fluctuations, so that the exchange coupling seems to set the fundamental scale for the superconducting transition temperature T_c. This suggests a common mechanism for the high T_c nature in both materials. I will extend previous spin fluctuation calculations in cuprate superconductivity to propose a simple BCS-like expression for heavy fermion superconductivity that parameterizes the effective frequency-dependent quasiparticle interactions in terms of their unusual normal state properties. I will show that there are two key elements that determine the magnitude of T_c. The model provides a quantitative explanation of the measured pressure-induced variation in T_c in the "hydrogen atoms" of unconventional superconductivity, $CeCoIn_5$ and $CeRhIn_5$, and predicts a similar dome structure for other heavy electron quantum critical superconductors. Similar results may be applied to understand the cuprate superconductors.

S11. Advanced electronic Materials: Processing, structures, properties and applications

Advanced Electronic Materials: Piezoelectric I

Room: Indian

Session Chairs: Dragan Damjanovic, Swiss Federal Institute of Technology in Lausanne - EPFL; Andrew Bell, University of Leeds

2:00 PM

(EMA-S11-024-2016) 3-Atom Model Parameters in Lead-free and Lead-based Piezoelectric Materials (Invited)

A. J. Bell*[1]; 1. University of Leeds, United Kingdom

The recently proposed 3-atom model for describing electromechnical properties of ionic solids has been applied to a range of classical and lead-free piezoelectric materials, providing analysis of properties in terms of an effective ionic charge and the asymmetry of the interatomic force constants. Specific cases in which trends have been examined include (i) PZT ceramics across the MPB; (ii) alkali metal niobates and tantalate single crystals; (iii) PMN-PT type crystals as a function of poling direction and phase and (iv) barium titanate single crystal as a function of temperature. For single crystals, the asymmetry in the force constants is dominant in determining the values of the piezoelectric charge coefficient and the electromechanical coupling coefficient, whilst in ceramics the effective charge plays a stronger role in increasing the charge coefficient in relation to the dielectric anisotropy of the constituent crystals. The results are consistent with our current understanding of how polarization rotation close to phase instabilities leads to high piezoelectric coupling. However, understanding how the model parameters depend upon composition for intrinsic behaviour is still at the start of the learning curve.

2:30 PM

(EMA-S11-025-2016) Emergence of electro-mechanical coupling in complex materials (Invited)

D. Damjanovic*[1]; 1. Swiss Federal Institute of Technology in Lausanne - EPFL, Switzerland

The term electro-mechanical coupling describes several phenomena including piezoelectricity, electrostriction, and flexoelectricity. While in each case the electro-mechanical coupling can be described by simple equations which relate electrical (electric field, polarization) and mechanical (strain, stress) functions, the experiments usually show strong deviations from expected ideal behaviors. These deviations are often termed "extrinsic" contributions. Examples are domain switching which can give electro-mechanical response that is in some accepts qualitatively similar to that of electrostriction and domain wall motion which can behave as piezoelectricity. To complicate the matter, the term is sometimes used even in the cases when a "contribution" is comparable to or even much larger than the effect itself. The mutual interaction of different contributions is most often not well understood and may lead to surprising effects, such as negative longitudinal piezoelectric effect in PVDF. Perhaps the least understood are electro-mechanical phenomena that are observed in materials that exhibit strain-gradients. Such phenomena are naturally attributed to flexoelectricity, but most often without rigorous proofs. In this talk several examples of such emergent electro-mechanical coupling in complex materials will be discussed.

3:00 PM

(EMA-S11-026-2016) Extraordinary High T_c PZT-based Relaxed Single Crystal Thin Films

K. Wasa*[1]; 1. Yokohama City University, Japan

Ferroelectric thin films with high Curie temperature T_c and high piezoelectric coupling factor are fascinated for a high temperature piezoelectric MEMS. $Pb(Zr,Ti)O_3$ (PZT)-based ferroelectric ceramics exhibit high coupling, but the T_c is not high, i.e. $T_c < 400$ºC. Higher T_c PZT- based thin films will be much acceptable. Based on a strain engineering, it is commonly understood the in-plane biaxial strained PZT-based thin films exhibit enhanced T_c in the laminated composite structure. However, thickness of the PZT thin films will be limited below a critical thickness typically < 50nm. When the thickness of the piezoelectric thin films exceeds the critical value, the piezoelectric thin films will show relaxed structure. The T_c of the relaxed piezoelectric based thin films, thickness > the critical thickness, is believed to be the same to bulk T_c. However, we have found, a sort of relaxed epitaxial single crystal thin films of PZT-based thin films, typically 1~3mm, including intrinsic PZT and ternary perovskite $Pb(Mn,Nb)O_3$-PZT exhibits extraordinary high T_c, T_c = ~600ºC. These PZT-based thin films exhibit 2nd order ferroelectric behavior with highly self-polarization *P*r, *P*r = 80-100mC/cm^2. Present enhanced T_c phenomena are based on high quality heteroepitaxial growth process. The possible mechanism of the enhanced T_c behavior is discussed.

3:15 PM

(EMA-S11-027-2016) Potential of gehlenite single crystals for piezoelectric sensor applications

H. Takeda*[1]; K. Takizawa[1]; K. Yoshida[1]; T. Hoshina[1]; T. Tsurumi[1]; 1. Tokyo Institute of Technology, Japan

Calcium aluminate silicate, gehlenite, $Ca_2Al_2SiO_7$ (CAS) single crystals were characterized to disclose their potentials for piezoelectric sensor applications. An electrical charge induced by stress was properly detected under pseudo combustion environment in the engine cylinder at 700 ºC. The uniaxial compressive strength as mechanical properties of the CAS crystal were enough for combustion sensor application. All material constants consisting two piezoelectric d_{ij}, two dielectric e_{ij}, and six elastic compliance s_{ij} moduli of CAS crystal was successfully determined using resonanse-antiresonance method. Temperature dependence of these moduli was also determined between -30 ºC and 120 ºC. As temperature increased, the d_{14} value decreased but the d_{36} value increased. This result offers hope to us searching zero coefficient of coupling factor for acoustic application.

Advanced Electronic Materials: Piezoelectric II

Room: Indian

Session Chairs: Zuo-Guang Ye, Simon Fraser University; Clive Randall, Penn State University

4:00 PM

(EMA-S11-028-2016) Piezoelectric and Dielectric Multilayer Components (Invited)

C. Randall*[1]; 1. Penn State University, USA

Components for high temperatures and high voltages that are applicable for power electronic applications continue to evolve. Here we outline some new dielectrics and some new compositional approaches to designing robust dielectric materials. We also consider the details of their degradation and breakdown mechanisms. The basic dielectric materials are based upon weak relaxor materials, paraelectric materials, and antiferroelectrics. There are also applications within these areas that make multilayer piezo transformers important. We will have a brief discussion on cofired multilayer piezoelectric transformers.

4:30 PM

(EMA-S11-029-2016) Rediscovering PZT through Single Crystal Studies (Invited)

Z. Ye*[1]; 1. Simon Fraser University, Canada

Lead zirconate-titanate solution, $Pb(Zr_{1-x}Ti_x)O_3$ [PZT], and related materials are undoubtedly the most widely used electroceramics in a wide range of technological applications. However, despite decades'

effort, its local structure and anisotropic properties, and the origin of its enhanced piezoelectric performance near the morphotropic phase boundary (MPB) still remain poorly understood. Recently, thanks to our capability to grow PZT single crystals and the availability of advanced characterization and analytical techniques, such as piezoresponse force microscopy, spherical aberration-corrected transmission electron microscopy, high-resolution neutron total scattering and diffuse scattering and pair-distribution function (PDF) analysis, we have gained new insights into the *complex local structure, atomic scale polarization rotation, nano-scale domain structure, intricate phase transition and critical behaviour, and tri-critical points in PZT. These results have provided a better understanding of* the relationship between micro-/nanoscopic structure and macroscopic functional properties not only for this important class of materials, but also for the other piezo-/ferroelectric materials in general.

5:00 PM

(EMA-S11-030-2016) Ubiquitous Magneto-Mechano-Electric (MME) Generators for wireless sensor network driving (Invited)

J. Ryu*[1]; D. Jeong[2]; S. Choi[1]; W. Yoon[1]; J. Choi[1]; J. Kim[1]; B. Hahn[1]; C. Ahn[1]; D. Park[1]; 1. Korea Institute of Materials Science, The Republic of Korea; 2. Inha University, The Republic of Korea

Magnetoelectric (ME) composites exploit the product property of magnetostriction and piezoelectricity. The ME effect is the result of multiple energy transduction starting from magnetic energy to mechanical energy and finally to electrical energy, i.e, magneto-mechano-electric (MME) transduction. In this presentation we report the energy harvesting performance of self-biased ME laminate composite with anisotropic piezoelectric single crystal fiber composites (SFC) and magnetostrictive Ni plate. The flexibility of SFC represents high compliance of the sample and it is ideal for achieving low resonance frequency in cantilever structure. Flexibility also imparts durability and ability to apply increased strain magnitudes. Ni can be easily self-biased and generates linear strain response in low level magnetic field environment. ME properties and MME generator performance were evaluated under 60 Hz low level magnetic noise to clarify the performance metrics and illustrate the uniqueness of this architecture. In addition, we demonstrate the energy harvesting from the real power line for vacuum pump and 60 LEDs lighting under the weak magnetic field of 700 mT at 60 Hz. Furthermore, this MME harvester can operate wireless sensor networks (WSN) composed of TI-MSP430-CC2500 module.

5:30 PM

(EMA-S11-031-2016) Sol-gel grown PMN-PT films for tunable bulk acoustic wave resonators

M. Spreitzer*[1]; S. Kune[1]; D. Suvorov[1]; 1. Jozef Stefan Institute, Slovenia

This work examines the synthesis and characterization of $Pb(Mg_{1/3}/Nb_{2/3})O_3$-$PbTiO_3$ thin films using the sol-gel method for FBARs sensor applications. In order to determine the influence of the coordination chemistry on the formation of the perovskite the conditions of the reagents were systematically varied. As a source of Mg-precursor $Mg(CH_3COO)_2{\times}4H_2O$, $Mg(AcAc)_2{\times}2H_2O$ and $Mg(NO_3)_2{\times}6H_2O$ were applied to reduce the concentration of the undesired pyrochlore phase that forms in addition to the perovskite phase. $Pb(NO_3)_2$, $Pb(CH_3COO)_2$, $Pb(PVP)_2$ and $Pb(AcAc)_2$ were used as a source of Pb. A pyrochlore-free $Pb(Mg_{1/3}/Nb_{2/3})O_3$-$PbTiO_3$ film was formed when the steric hindrance of the Pb precursor was increased. Thus, $Pb(PVP)_2$ and $Pb(AcAc)_2$ were shown to be effective in the formation of pyrochlore-free thin films. It was observed that during the direct casting of the film on the Pt (111) substrate the film grows preferentially in the (100) direction. A predominant change in the growth direction from (100) to (111) was achieved by the initial casting of a thin, TiO_2 undercoat. The prepared films were dense and crack-free. The phase composition of the thin films was characterized by means of X-ray diffraction (XRD), whereas the morphology and the thickness of the thin films were studied with scanning electron microscopy (SEM).

Friday, January 22, 2016

Plenary Session

Plenary III

Room: Indian

8:40 AM

(EMA-PL-003-2016) Power Semiconductors

T. Detzel*[1]; 1. Infineon Technologies Austria AG, Austria

Power semiconductors have become key innovation drivers in many technological areas of modern society. Efficient generation and use of electricity will be crucial in order to supply a growing population with electric power while preserving natural resources. Modern power semiconductors ensure feeding electricity from renewable energy sources, such as solar or wind, into the grid with low losses and provide efficient voltage conversion at different stages up to the point of use in any electrical appliance. In addition, power devices render cars more fuel efficient and enable electric mobility as well as advanced public transportation based on electric traction. This plenary talk will provide a deeper insight into different technologies, products, and applications of advanced power semiconductors. The main goal of power semiconductor research is the reduction of the area specific on-state resistance and switching losses as well as increasing corresponding breakdown voltage. A particular focus will be on novel semiconductor materials, such as Gallium Nitride (GaN), required for revolutionary developments aiming at ever increasing power density and efficiency. The main benefit of the wide band gap semiconductor GaN originates from its high electrical breakdown field and superior electron mobility compared to silicon, allowing very compact and fast switching devices. The advantageous use of GaN and its exciting material development will be discussed.

S4. Ion-conducting Ceramics

Ion Conductors for Energy Storage

Room: Caribbean B

Session Chair: Kyle Brinkman, Clemson University

10:00 AM

(EMA-S4-009-2016) Solid State Batteries for Automotive Applications (Invited)

V. Anandan*[1]; A. Drews[1]; 1. Ford Motor Company, USA

The Li-ion battery is the preferred energy storage device for a wide range of applications ranging from handheld devices to electric vehicles (EVs). Though Li-ion batteries offer better performances than other commercial battery technologies, some aspects of their performance are not sufficient for EVs. For example, current Li-ion batteries do not have sufficient energy density to provide long range (500 miles) for an EV in a reasonable packaging volume. Because these batteries contain flammable liquid electrolytes, providing high safety while increasing the number of batteries becomes increasingly difficult. Therefore, new battery technologies are needed for future automotive applications that provide better safety and energy density without compromising other performance parameters. The most widely researched next generation technologies are solid state batteries (SSB), Li-air, and Li-S batteries. Among these, SSB have substantial advantages for the automotive application because of their high volumetric energy density and better inherent safety. Despite its promise, development has been hindered by several issues from material chemistry level to battery fabrication process. This presentation will: 1) Review some of the competing battery

technologies; 2) Feasibility analysis of SSB with respect to the automotive application; 3) Development of oxide based solid electrolytes; 4) Issues and challenges in developing practical SSB.

10:30 AM

(EMA-S4-010-2016) A facile method for the synthesis of the $Li_{0.3}La_{0.57}TiO_3$ solid state electrolyte (Invited)

G. Cao*[1]; 1. University of Washington, USA

We report a facilemethod for the synthesis of $Li_{0.3}La_{0.57}TiO_3$ by forming a coagulated precursor solution which contains Li^+, La^{3+}, and TiO_2 nanoparticles mixed highly homogeneously. The grain of the synthesized $Li_{0.3}La_{0.57}TiO_3$ are comparable to the values in literature for the material prepared by other methods. The lithium ionic conductivities of $Li_{0.3}La_{0.57}TiO_3$ produced using this method are on the order of 10^{-4} S cm^{-1} for single crystalline grains and 10^{-5} S cm^{-1} for the bulk material. The conductivities are comparable to the values reported in literature for the material synthesized using a solid state reaction or sol–gel method. In addition to the synthesis of $Li_{0.3}La_{0.57}Ti_{O3}$, the coagulated solution method is also thought of as an extendable approach for the fabrication of other multi-element oxides with the capability to easily and consistently control the stoichiometric composition of the material.

11:00 AM

(EMA-S4-011-2016) Defect Driven Titania Anode for Secondary Sodium and Lithium Batteries

K. A. Smith*[1]; H. Xiong[1]; J. Wharry[1]; D. P. Butt[1]; 1. Boise State University, USA

Titanium dioxide has much potential for future rechargeable battery systems, but the increasing demands for next generation energy storage systems calls for increased energy and power density, improved safety, longer lifetime and lower cost. Recent studies have suggested that enhanced electrochemical energy storage may be achievable by producing intentional structural defects within the oxide materials, but this has yet to be thoroughly explored for lithium and sodium ion battery systems. In this study titania nanotubes were synthesized via electrochemical and processed to create either oxygen or titania vacancies. The resulting materials were structurally characterized then deployed as the anode in a coin-type half-cell to determine the electrochemical properties such as specific capacity and operating voltage. Results from these studies will be discussed.

11:15 AM

(EMA-S4-013-2016) Conductivity, Mechanical Properties, and Stability of $Li_7La_3Zr_2O_{12}$ Solid State Electrolytes (Invited)

C. R. Becker*[1]; J. B. Wolfenstine[1]; J. L. Allen[1]; J. Sakamoto[2]; 1. US Army Research Laboratory, USA; 2. University of Michigan, USA

Solid state electrolytes (SSEs) confer several advantages over conventional lithium ion batteries: improved high temperature performance, increased safety, enhanced cycle life, and larger capacity. In a solid state battery, there is nothing to catch fire, metallic lithium can be used as an anode, and conductivity improves as temperature increases. At room temperature however, few SSEs offer large enough ionic conductivity to be viable. One of the more promising SSE materials based on the garnet structure is cubic $Li_7La_3Zr_2O_{12}$ (LLZO). High Li-ion lattice conductivity LLZO can be obtained by substituting some of the Zr sites with super valent cations such as Ta or Nb. Through the use of hot-pressing, near theoretical density can be obtained which results in low grain boundary resistance and high total Li-ion conductivity. DC polarization measurements confirm negligible electronic conductivity. Evaluation of the mechanical properties of LLZO reveal that the elastic modulus is high enough to prevent Li dendrite formation during cycling, possess adequate strength, but suffers from low fracture toughness. Up to relatively high temperatures, LLZO appears stable against lithium metal. Preliminary cycling data at room temperature reveals dendrites are not formed as long as the current density is not too great. These results along with means to improve them will be presented.

11:45 AM

(EMA-S4-014-2016) Understanding the ionic conductivity enhancement in lithium conducting garnets

M. M. Ahmad*[1]; 1. King Faisal University, Saudi Arabia

Ceramic/inorganic Li+ solid electrolytes have been proposed for the development of solid-state Li+ batteries. Li5La3M2O12 (M= Ta, Nb) Li+ conducting garnets are promising candidates as solid electrolytes. However, the ionic conductivity of these materials is in the 10^-6 S/cm, which is low for practical applications. Conductivity enhancement could be achieved by chemical substitutions on La or M sites such as in Li6La2BaTa2O12, Li5+2xLa3M2-xAxO12 (A= trivalent cations) and Li7La3Zr2O12 with conductivity values up to ~10^-4 S/cm. The increased conductivity is attributed to the increased concentration of mobile Li+ with increasing Li+ content. Here, with appropriate analysis of the conductivity spectra at different temperatures of several garnet phases, we show that Li+ conductivity enhancement is due to the enhanced mobility of Li+ rather than the concentration of mobile Li+. The enhanced mobility is due to the re-distribution of Li+, so that the occupancy of Li+ in tetrahedral sites decreases and the occupancy of Li+ in octahedral sites increases with increasing Li+ content. This re-distribution process creates more vacant tetrahedral sites available for Li+ diffusion. We suggest that, chemical substitutions on Li sites by divalent or trivalent cations will create more vacancies, leading to increased conductivity.

S5. Multifunctional Nanocomposites

Multifunctional Nanocomposites V

Room: Coral B

Session Chair: Aiping Chen, Los Alamos National Lab

10:00 AM

(EMA-S5-028-2016) Impurity and defect effects on phonon transport in complex oxides: Impact on thermal conductivity and tehrmal boundary conductance (Invited)

P. E. Hopkins*[1]; 1. University of Virginia, USA

The types of impurities that are common complex oxide classes of materials can lead to large, and controllable changes in phonon scattering rates, and therefore thermal properties. In this talk, I will discuss 3 projects in which we highlight the role of nanoscale defects on the thermal conductivity of complex oxides and the thermal boundary conductance (or Kaptiza conductance) across corresponding metallized interfaces. First, I will show results demonstrating the role of stoichiometry on the thermal conductivity of LaVO3 and oxygen vacancies on the thermal conductivity of TiO2. Both the defects from changing the composition of the solid solution and from increasing oxygen vacancies have pronounced roles on changing the thermal conductivity. Secondly, I will demonstrate the role that point defects and oxygen vacancies have on the thermal boundary conductance across metal/SrTiO3 and metal/TiO2 interfaces, along with the role that electric field have on manipulating this thermal boundary conductance. Finally, I will discuss the intertwined role among mass/alloy scattering, ferroelastic domain scattering, and thermal boundary conductances in Pb[ZrxTi1-x]O3 thin films through the experimental demonstration of an electric field controlled phonon thermal switch.

10:30 AM

(EMA-S5-029-2016) The Transport Properties of Dislocations in the Perovskite-Oxide $SrTiO_3$ (Invited)

R. A. De Souza*[1]; 1. RWTH Aachen University, Germany

The one-dimensional lattice defects known as dislocations are widely believed to provide short-circuit paths for diffusion in crystalline materials. In this contribution I will present recent work that we have been doing on characterizing and understanding mass transport processes along dislocations in the perovskite-type oxide $SrTiO_3$. I will focus on experimental studies of oxygen diffusion along the periodic array of dislocations that constitutes a low-angle tilt grain boundary. Isotope penetration profiles obtained by Secondary Ion Mass Spectrometry (SIMS) indicated no evidence of fast diffusion along the dislocation array. I will also present complementary results obtained from atomic-level studies of point-defect processes by means of static lattice simulations. Combining all results and literature reports, I will present a comprehensive and consistent picture of the transport properties of dislocations in $SrTiO_3$. Finally I will describe the consequences for memresistive devices.

11:00 AM

(EMA-S5-030-2016) Electronic Transport in Oxygen Vacancy Doped Epitaxial $BaSnO_3$: Doping, Mobility, and the Insulator-Metal Transition (Invited)

K. Ganguly[1]; J. Walter[1]; P. Ambwani[1]; P. Xu[1]; A. Prakash[1]; J. Jeong[1]; A. Mkhoyan[1]; B. Yang[1]; A. Goldman[1]; B. Jalan[1]; C. Leighton*[1]; 1. University of Minnesota, USA

$BaSnO_3$ has recently been identified as a high room temperature mobility (> 300 $cm^2V^{-1}s^{-1}$ in bulk) wide gap semiconductor with much potential for oxide electronics. Although progress with thin films has been significant, there remain open questions with respect to optimal dopants, mobility limits, transport mechanisms, and the interplay with defects. In this presentation we first summarize a study of the microstructure, morphology, and stoichiometry of undoped $BaSnO_3$ on $SrTiO_3$(001), $LaAlO_3$(001) and MgO(001), using high pressure oxygen sputter deposition. Optimized conditions result in single-phase, relaxed, close to stoichiometric films, with substrate-dependent dislocation density. We then demonstrate vacuum annealing as a facile route to *n*-doped $BaSnO_{3-d}$, leading to electron density up to 5.0 x 10^{19} cm^{-3}, resistivity down to 3 mΩcm, and room (low) temperature mobility of 35 (45) $cm^2V^{-1}s^{-1}$. At equivalent electron densities this in fact exceeds the mobility reported for La or Sb doping. Temperature and magnetic field dependent transport measurements *vs*. reduction temperature and thickness will then be discussed. These have allowed us to probe the insulator-metal transition and weak localization in $BaSnO_3$, exposing important correlations with microstructure, and providing insight into mobility limiting factors.

11:30 AM

(EMA-S5-031-2016) Nanoscale heat transport in complex oxide thin films and superlattices (Invited)

J. Ravichandran*[1]; 1. University of Southern California, USA

Thin film growth of high quality heterostructures and superlattices has led to observations of exotic phenomena, and the realization of several device applications. Until recently, growth of heterostructures, with sharp interfaces and low defect density, has been the domain of conventional semiconductors. Recently, such advances have been extended to other materials such as oxides, particularly complex oxides. Much of the applications of such advances have focused on electronic, dielectric and/or optical effects. Most thermal transport phenomena have been considered classical until the widespread employment of nano/microscale heat transport measurement techniques in the past few decades. I will first review the evolution of oxide thin film growth techniques and the advances in material properties specifically thermal properties in complex oxide thin films. I will discuss two cases, where nanoscale thermal transport has enabled new insights into oxide materials. First, I will show an example, where thermal transport can act as a probe for material quality in oxide heterostructures. In the second part, I will show that perovskite superlattices are a model system to observe a crossover from incoherent to coherent phonon transport, which has been elusive in other semiconductor superlattice systems. This observation opens up opportunities to control thermal transport using coherent phonons.

12:00 PM

(EMA-S5-032-2016) TaOx thin films for resistance switching memory applications

F. Kurnia[2]; D. Kim[1]; B. Lee[1]; C. Liu*[1]; 1. Hankuk University of Foreign Studies, The Republic of Korea; 2. The University of New South Wales, Australia

In this work we discuss the resistance switching properties of TaOx thin films prepared by pulsed laser deposition on $Pt/TiO_2/SiO_2/Si$ substrates. We found that only those grown at room temperature showed stable resistance switching. From Pt/TaOx/Pt structure, unipolar resistive switching behaviors with and without a forming process were both observed, showing an opposite relationship between the reset current and the resistance of the low resistance state. Through I-V analysis, we proposed different evolution processes of the conducting filaments (CFs) for the forming-free and forming-required RS behaviors. From the Cu/TaOx/Pt structure, unipolar resistive switching (URS) and bipolar resistive switching (BRS) behaviors were observed depending on the compliance current. A non-reversible transition from the URS to a BRS mode occurred when the compliance current was increased to 10mA. Detailed analysis of the electrical properties in each resistance state of both switching modes revealed that the permanent transition of the switching mode was induced by the formation of stronger conductive filaments consisted of Cu metals within the TaOx thin film. Furthermore, both URS and BRS modes were governed by the formation and rupture of conductive filaments, whereas the rupture of these filamentary paths in the BRS mode was proposed due to both Joule heating and electric field effects.

S6. Computational Design of Electronic Materials

Materials by Design: Electronic Materials II

Room: Mediterranean A

Session Chair: Wolfgang Windl, Ohio State University

10:00 AM

(EMA-S6-009-2016) Correlating structure and function for nanoparticle electrocatalysts (Invited)

G. Henkelman*[1]; 1. University of Texas at Austin, USA

Metal nanoparticles of only ~100-200 atoms are synthesized using a dendrimer encapsulation technique to facilitate a direct comparison with density functional theory (DFT) calculations in terms of both structure and catalytic function. Structural characterization is done using electron microscopy, x-ray scattering, and electrochemical methods. Combining these tools with DFT calculations is found to improve the quality of the structural models. DFT is also successfully used to predict trends between structure and composition of the nanoparticles and their catalytic function for reactions including the reduction of oxygen and the oxidation of formic acid. This investigation demonstrates some remarkable properties of the nanoparticles, including facile structural rearrangements and nanoscale tuning parameters which can be used to optimize catalytic rates.

10:30 AM

(EMA-S6-010-2016) Theoretical Investigation of Silicon-based Materials with Exceptional Optoelectronic Properties (Invited)

B. Huang*[1]; 1. Beijing Computational Science Research Center, China

Silicon is an extremely important electronic material in technological fields, but it is not a good optoelectronic material. In the last few decades, researchers have heavily studied the structural and electronic properties of silicon in order to improve its optical absorption in the visible light range using analyses of metastable silicon phases, silicon-based alloys, and silicon-based superlattices. In this talk, I will present our recent theoretical efforts on searching and designing new silicon phases, from bulk to 2D silicon and silicon phosphides, with exceptional optoelectronic properties.

11:00 AM

(EMA-S6-011-2016) Predictive bandgap engineering in 2H transition metal dichalcogenides through inherent interface coupling

B. Ouyang*[1]; J. Song[1]; 1. McGill Univesity, Canada

VI transition-metal dichalcogenides (TMDs) have attracted enormous research efforts because of their distinguished electronic properties. One unique feature of TMDs is the polymorphism. This feature brings the interesting possibility of the inherent TMD heterostructures where different phases are coupled through interfaces. Employing density functional theory (DFT) calculations, we systematically examined the electronic coupling between 2H-MX2 with its polymorphic phases in bilayer inherent heterostructures. We found that the interface coupling, augmented by lateral strain, can greatly modify the band structure of the 2H phase, inducing indirect-to-direct bandgap transition. We further showed that the effects of strain bandgap can be well predicted by the deformation potential theory. Predictive diagrams were then constructed to map the indirect/direct bandgap regimes with various planar strains, for different type of interface coupling. The present study provides great insights towards bandgap engineering in TMD-based devices.

11:15 AM

(EMA-S6-012-2016) Uncovering the physics and chemistry of complex oxide surfaces (Invited)

R. Mishra*[1]; 1. Washington University in St. Louis, USA

Perovskite surfaces provide fertile ground for the discovery of novel electronic and magnetic phenomena. In this work, we combine scanning transmission electron microscopy imaging and electron energy loss spectroscopy (EELS) with density functional theory (DFT) based calculations to reveal the physics and chemistry of the surfaces of two distinct perovskite superlattice systems. In the first part of the talk, we study the surface of a $(LaFeO_3)_m/(SrFeO_3)_n$ heterostructure. Using STEM/EELS, we observe a reduction in the oxidation state of Fe from Fe^{3+} in the bulk to Fe^{2+} at the surface over a length of ~5 unit cells. By combining the STEM results with DFT calculations, we show that the surface is terminated with FeO_4 tetrahedra instead of the FeO_6 octahedra as present in the bulk. This surface reductions results in an exotic phase where the surface layer displays a half-metallic ferromagnetic behavior, while the bulk remains antiferromagnetic and insulating, similar to the class of topological insulators. In the last part of the talk, we will show the implications of surface termination on the two-dimensional electron gas present at the interface of n-type SrTiO3/ $LaAlO_3$ films.

11:45 AM

(EMA-S6-013-2016) Electronic and Magnetic Properties of Transition-Metal Oxide Nanocomposites: A Tight-Binding Modeling at Mesoscale (Invited)

Y. Tai[1]; J. Zhu*[1]; 1. Los Alamos National Laboratory, USA

Transition metal oxides (TMOs) exhibit many emergent phenomena ranging from high-temperature superconductivity and giant magnetoresistance to magnetism and ferroelectricity. In addition, when TMOs are interfaced with each other, new functionalities can arise, which are absent in individual components. In this talk, I will present an overview on our recent efforts in theoretical understanding of the electronic and magnetic properties TMO nanocomposites. In particular, I will introduce our recently developed tight-binding modeling of these properties arising from the interplay of competing interactions at the interfaces of planar and pillar nanocomposites. Our theoretical tool package will provide a unique capability to address the emergent phenomena in TMO nanocomposites and their mesoscale response to such effects like strain and microstructures at the interfaces, and ultimately help establish design principles of new multifunctionality with TMOs. This work was carried out under the auspices of the National Nuclear Security Administration of the U.S. Department of Energy at Los Alamos National Laboratory (LANL) under Contract No. DE-AC52-06NA25396. It was supported by the LANL LDRD Program, and in part by the Center for Integrated Nanotechnologies a U.S. DOE Office of Basic Energy Sciences user facility.

12:15 PM

(EMA-S6-014-2016) Creating Two-Dimensional Electron Gas in Nonpolar/Nonpolar Oxide Interface via Polarization Discontinuity: First-Principles Analysis of CaZrO3/SrTiO3 Heterostructure

K. Yang*[1]; S. Nazir[1]; J. Cheng[1]; 1. University of California San Diego, USA

The perovskite-based oxide heterostructures (HS) are attracting increasing interests because of their novel interfacial properties such as the interfacial superconductivity and ferromagnetism that are drastically different from those of the corresponding bulk materials. One example is the formation of the high-mobility Two-Dimensional Electron Gases (2DEG) at TiO2-terminated interface in the polar/nonpolar LaAlO3 /SrTiO3 (LAO/STO) HS system. Compared to the great success of generating 2DEG in the LAO/STO system via the polar discontinuity, there have been few reports on the possibility to produce the 2DEG in the perovskite oxide HS using the polarization. Herein, I will talk about the strain-induced polarization and resulting conductivity in the nonpolar/nonpolar CaZrO3/SrTiO3 (CZO/STO) heterostructure (HS) system by means of first-principles electronic structure calculations. We found that the lattice-mismatch-induced compressive strain leads to a strong polarization in the CZO film, and as the CZO film thickness increases, there exist an insulator-to-metal transition. These findings open a new avenue to achieve 2DEG (2DHG) in perovskite-based HS systems via polarization discontinuity.

S9. Recent Developments in Superconducting Materials and Applications

Applications and related Material issues including Wire Properties

Room: Pacific

Session Chairs: Timothy Haugan, Air Force Research Lab; Charles Rong, U.S. Army Research Laboratory

10:00 AM

(EMA-S9-026-2016) Advanced Superconducting High-T_c Magnetic Applications (Invited)

F. N. Werfel*[1]; U. Floegel-Delor[1]; 1. Adelwitz Technologiezentrum GmbH (ATZ), Germany

ATZ Corp. produces more than 1 ton HTS material per year. Bulk superconductors can trap up to 1.5 T at 77 K and more than 17 T at lower temperatures. The principal advantage of (HTS) magnet technology relates to the absence of any physical contact. We discuss the principles of MAGLEV interaction of rotational and linear applications and the technology involved in realizing it. The technical

requirements are demonstrated at a 10 kWh/ 250 kW flywheel energy storage system. Linear magnetic levitation trains attract great interest in the low-noise transportation. Similar challenges in design and construction of magnetic trains are discussed. Robust HTS vacuum cryostats allow a one-day train operation. Three different MAGLEV demonstrator train concepts using ATZ's HTS components with magnetic forces up to 6 t in Brazil, China and Germany are compared. We investigate and report about the possible influence of particle irradiated YBCO bulks being for several months in space. Within the German space mission program started in 2014 earth magnetic field interaction with a HTS device is measured and investigated. We compare expected models with present experiments on the International Space Station (ISS). The experiments on the ISS are extended to the end of 2016.We expect new electromagnetic shielding results for future long range space missions.

10:30 AM

(EMA-S9-027-2016) The HTS Coated Conductor Roebel cable on route to first applications (Invited)

W. Goldacker*[1]; 1. Karlsruhe Institute of Technology, Germany

Roebel cables from coated conductors provide special features as retained field anisotropy of transport critical currents in fields and very good bending ability. They are the candidate for HTS magnets, in particular insert magnets for advanced accelerator dipoles as for the planned upgrade of LHC at CERN due to their high engineering current density. Both the cable design and properties and the magnet design need to be adapted to the special features of the selected application. We present the status of knowledge obtained during the fabrication of suitable Roebel cable modifications for the dipole insert magnet, the characterization of the properties as anisotropy, bending ability and achieved transport currents and the development of technical features as the impregnation with resins. We present the status of options as filament structures in the strands for reduced AC losses and finally the first applications in windings.

11:00 AM

(EMA-S9-028-2016) Persistent Critical Current Characteristics with Closed Superconducting Loops Made Out of RE123 Coated Conductors (Invited)

C. Rong*[1]; J. D. Miller[2]; G. A. Levin[3]; P. N. Barnes[1]; 1. U.S. Army Research Laboratory, USA; 2. Naval Surface Warfare Center Carderock Division, USA; 3. Florida Institute of Technology, USA

We will report recent experimental observations of persistent current in closed loops made out of the currently manufactured coated conductors. Data was taken in the range of 23K to 38K with the persistent current being induced by field cooling the loops and then turning off the external field. The relaxation rate in this temperature range is very low and these results suggest that coated conductors can be considered as a viable option for persistent current applications such as energy storage, MRI magnets, magnetic levitation, as well as magnets for motor/generator. We also measured the values of the *persistent critical current* as determined by a slow warming of the loops and monitoring the magnetic field created by the circulating current. These values will be compared with the *resistive critical current* usually specified by the manufacturers. The characteristics of the *persistent critical current* could be a new criteria to evaluate the quality and performance of the coated conductor, in addition to a single value of the *resistive critical current.*

11:30 AM

(EMA-S9-029-2016) Fatigue Properties of IBAD-MOCVD REBa2Cu3O7-x

S. Rogers*[1]; J. Schwartz[1]; 1. North Carolina State University, USA

REBa2Cu3O7-x coated conductors show promise for use in a multitude applications, including high-field magnets, energy storage devices, motors, generators, and power transmission systems. Many of these applications are AC systems and thus the fatigue properties of the conductor must be well understood. Previous studies have determined the performance of REBCO tapes under single cycle loads, but an understanding of the fatigue properties is lacking. Here the fatigue behavior of 4 mm wide IBAD-MOCVD REBCO on Hastelloy substrate conductors is reported. Strains up to 0.5% and up to 100,000 cycles are considered. Failure modes are investigated via microstructural study.

11:45 AM

(EMA-S9-030-2016) Electric Aircraft and Future Need for Cryogenic/Superconducting Components and Drivetrains (Invited)

T. J. Haugan*[1]; G. Panasyuk[2]; 1. Air Force Research Lab, USA; 2. UES Inc., USA

New technologies are available for increasing the efficiency or lowering the cost of transportation, that are well-known in the automotive industry, including Hybrid-electric-vehicle (HEV), battery-electric-vehicle (BEV) and Liquid Hydrogen Fuel Cell (LHFC), and Liquid Natural Gas (LNG). The increase of energy efficiencies can very significantly up to 2-3x or more from the use of non-combustion energy sources and 'smart' energy management including brake regeneration. The use of these technologies is increasingly being realized for aircraft propulsion in the last 5 years, and has been successfully implemented in 2 and 4 passenger aircraft. This paper will summarize recent progress in this field for aircraft, and present the unique properties of cryogenic/superconducting machines and the positive impacts they can have for hybrid-electric or all-electric propulsion in the future for 10-500 passenger aircraft and 1-50 MW power drivetrains. The studies will compare properties of cryogenic systems and components to Cu-wire or conventional based systems. Acknowledgments: Air Force Office of Scientific Research (AFOSR), and the Aerospace Systems Directorate of The Air Force Research Laboratory (AFRL/RQ).

12:15 PM

(EMA-S9-031-2016) AC Loss in High-Temperature Superconducting (HTS) Tapes in a Stator Environment Measured by the Calorimetric Method

N. Gheorghiu*[1]; J. P. Murphy[2]; M. D. Sumption[3]; M. Majoros[3]; E. W. Collings[3]; T. J. Haugan[4]; 1. UES, Inc., USA; 2. University of Dayton Research Institute, USA; 3. Ohio State University, USA; 4. AFRL/WPAFB, USA

Measuring the AC loss in HTS materials as well as understanding the underlying mechanisms is important for designing power devices such as motors and generators. For this study, a new apparatus measures AC loss with a calorimeter mounted in the stator environment of a generator/motor where a 0.6 T peak AC magnetic field is produced by an 8-pole rotor at frequencies up to 400 Hz. The apparatus exposes samples to an AC magnetic field, both synchronously and asynchronously, and allows measurements at very high sweep rates $Bf \leq 240$ T/s, i.e., about 10× higher than achieved by more standard techniques. Measurements can be done with applied field only, or in field and the HTS tapes (ReBCO) samples also carrying DC or AC currents. The calorimetric method used is based on the mass boil-off of liquid nitrogen at 77 K. The apparatus' calibration is done on both known resistors and also Cu-tape standards, and results compared to the AC loss expected from the standard theory. (Y,Gd)-Ba-Cu-O HTS tapes and cables with different architectures are measured and analyzed, and compared to AC loss measured in a standard set up with a pure unidirectional sinusoidal field. Our results agree within 5% of each other as well as with Brandt theory. Acknowledgements: This work was supported by The Air Force Office of Scientific Research (AFOSR) and the Aerospace Systems Directorate.

12:30 PM

(EMA-S9-032-2016) Superconducting Joint between (RE) $Ba_2Cu_3O_{7-x}$ Coated Conductors via Electric Field Sintering

C. Jensen*[1]; M. Li[1]; J. Schwartz[1]; 1. North Carolina State University, USA

One of the most promising commercially produced high temperature superconductors is (RE)$Ba_2Cu_3O_{7-x}$ in the film of a coated conductor on a Ni-alloy substrate. Its high critical current and mechanical strength make it promising for many applications. Yet the inability to create low-cost superconducting joints has long been one of the barriers in the use of (RE)$Ba_2Cu_3O_{7-x}$ tapes for applications which require long lengths of superconductor. Current joining techniques utilize thermally driven diffusion, which is difficult to accomplish in the c-direction of YBCO, or a non-superconducting solder. These approaches often require impractical processing conditions and yield low-resistance joints at best. However, several groups have shown that the application of an electric field during annealing can reduce the processing temperature required to produce diffusion in ceramics; this technique is known as electric field assisted sintering. Here, we investigate the use of an electric field to reduce the temperature and time required to create direct contact joints between the superconducting (RE)$Ba_2Cu_3O_{7-x}$ conductors. We present a study which produces joints using a range of sintering pressures, times, and atmospheres. The critical current, magnetic behavior, and microstructure of the joints were then characterized using low temperature four-point probe measurements and electron microscopy.

S10. Emerging functionalities in layered-oxide and related materials

Synthesis and Characterization

Room: Mediterranean B/C

Session Chair: Serge Nakhmanson, University of Connecticut

10:00 AM

(EMA-S10-001-2016) Mixed-metal fluorocarbonates as Deep UV NLO Materials: Synthesis, Characterization, and Properties (Invited)

T. Tran*[1]; S. Halasyamani[1]; J. He[2]; J. Rondinelli[2]; 1. University of Houston, USA; 2. Northwestern University, USA

New deep ultraviolet (DUV) non-linear optical (NLO) materials - KMgCO3F, RbMgCO3F, and Cs9Mg6(CO3)8F5 - have been synthesized and characterized. The achiral non-polar acentric materials are SHG active at both 1064 and 532nm. In addition, the materials exhibit a short UV cut-off - below 200nm. The materials exhibit three dimensional crystal structures with corner shared Mg(CO3)F polyhedra. Electronic structure calculations reveal that the denticity of the carbonate linkage, monodentate or bidendate, to the divalent cation is a useful parameter for tuning the transparency window and achieving the sizable SHG response.

10:30 AM

(EMA-S10-002-2016) From Layers to Scrolls – Layer Construction and Peapod Formation through the Manipulation of Niobium Oxides (Invited)

J. B. Wiley*[1]; 1. University of New Orleans, USA

Various layered niobates are open to topochemical manipulation. Layered perovskites for instance can be receptive hosts for oriented construction of metal-nonmetal layers (e.g. transition-metal halides, alkali-metal halides and alkali-metal chalcogenides). Recently we have developed methods for the insertion of oxygen species into these hosts resulting in the assembly of alkali-metal hydroxide layers. The compound $(Rb_2OH)LaNb_2O_7$ for example is made by a two-step intercalation method involving sequential reductive and oxidative intercalation steps. In another layered niobate system, $K_4Nb_6O_{17}$, we are able to manipulate these systems to create organized nanocomposites. Here a series of peapods structures are prepared by taking advantage of the scrolling tendency of these materials on exfoliation to capture preformed nanoparticles. In one example, iron oxide nanoparticles (Fe_3O_4) can be readily entrapped to make Fe_3O_4@ hexaniobate peapods.

11:00 AM

(EMA-S10-003-2016) 2-D to 3-D: Assembly of oxide nanosheets into 3-D monoliths

T. A. Gubb*[1]; T. Hey[1]; S. Misture[1]; 1. Alfred University, USA

A subset of layered ceramics can be successfully ion-exchanged and exfoliated using soft chemical approaches at or near room temperature. Herein, the solid-state synthesis, ion-exchange, and exfoliation of niobate and titanate ceramics to form suspensions of nanosheets is detailed and discussed. Of particular interest is the colloidal behavior of exfoliated nanosheets, which includes gelation, flocculation and liquid crystal formation. Suspension properties may be controlled by stabilizing electrolytes including alkali and transition metal salts, pH, nanosheet concentration, and temperature. We find distinct regions where the nanosheets form gels, liquid crystals, and 3-D edge-to-face floccules. The latter are of high interest for functional device applications, including electrochemical intercalation and sensors, because of their high surface areas of 200-300 m^2/g. The paper will demonstrate tailoring specific surface area and pore size distribution of dried 3D mesostructures. Lastly, we show that the oxide nanosheet assemblies are robust in high temperature applications, with good microstructural stability up to ~700°C for niobate and titanate nanosheets.

11:15 AM

(EMA-S10-004-2016) X-ray total scattering analysis of MnO_2 nanosheet assemblies

P. C. Metz*[1]; P. Gao[1]; T. Hey[1]; S. Misture[1]; 1. Alfred University, USA

Understanding the atomic structure of nanosheet materials is complicated by the inherently large surface to volume ratio, extensive stacking disorder, and complex surface chemistry. Robust characterization of disordered layered materials is of broad interest in electrochemical applications, and we report a new approach to modeling distributions of stacking defects to access the nano and mesoscales. As demonstrated in Birnessite-derived MnO_2 nanosheet systems, the local chemical environment and surface speciation effect changes in the Mn oxidation state that are linked to defects and structural distortions in the sheets. We use X-ray total scattering to probe the mesostructure and the atomic disorder of MnO_2 nanosheets perturbed by different aqueous treatments and leading to doubling of the electrochemical charge storage – to above 300 F/g. Application of large supercells and distributions of stacking defects within the formalisms of the software DISCUS and DIFFaX results in statistical defect models that provide the foundation for defect engineering in oxide nanosheets that are disordered on the mesoscale. Preliminary analyses of electrostatically assembled and dried MnO_2 nanosheets indicate some measure of restacking. The stacking behavior shows fractional intersheet translations distributed around {m/3, n/3} rather than a turbostratic configuration, and becomes increasingly ordered with heat treatment temperature.

11:30 AM

(EMA-S10-005-2016) Materials By Design: Superconducting Polymorphs Through Kinetic Control of Solid-state Chemistry (Invited)

J. R. Neilson*[1]; 1. Colorado State University, USA

A grand challenge in materials research revolves around controlling structure-property relationships to achieve desired properties, so-called "materials by design." The discovery and design of new superconducting materials has remained particularly enigmatic: not only do we lack universal structure-property relationships, but

we also lack the ability to synthesize metastable materials predicted to have desirable properties. We show how kinetic control of the synthetic reaction pathway can produce metastable, high-pressure polymorphs of superconducting metal chalcogenides, but without the use of pressure; this commences a new paradigm for materials by design.

12:00 PM

(EMA-S10-006-2016) Local epitaxial growth of layered oxides on isostructural polycrystals using combinatorial substrate epitaxy (Invited)

P. Salvador*[1]; G. Rohrer[1]; W. Prellier[2]; 1. Carnegie Mellon University, USA; 2. ENSICAEN, Universite de Basse-Normandie, France

Layered oxides in the $A_2B_2O_7$ and A_2BO_4 families exhibit a rich array of functional properties, including ferroelectricity, superconductivity, magnetoresistance, and mixed ionic and electronic transport. Most epitaxial film growth of these materials have been carried out on (110) or (100) perovskite single crystals, resulting in films oriented with their layered directions normal to the substrate plane. This represents an incredibly narrow range of epitaxial synthesis space. To open the door to epitaxial stabilization of new materials using more idealized substrates for comlex materials, and to wider ranges of strain engineering, we have been exploring growth of both families on various isostructural polycrystalline substrates that are not available in single-crystal form, such as $Sr_2Nb_2O_7$ and Sr_2TiO_4. The local epitaxial growth of films was investigated to determine phase formation and preferred epitaxial orientation relationships (*ORs*), further developing the high-throughput synthetic approach called Combinatorial Substrate Epitaxy (*CSE*). Most *CSE* films grow in a grain-over-grain fashion and, depending on the growth conditions, and in one of a relatively few *ORs*. The fabrication of metastable $A_2B_2O_7$ titanates and the dependence of *ORs* on composition for A_2BO_4 oxides will be presented to highlight the potential of *CSE* for designing complex layered oxides.

S11. Advanced electronic Materials: Processing, structures, properties and applications

Advanced Electronic Materials: Dielectrics II

Room: Indian

Session Chairs: Ian Reaney, University of Sheffield; Xiang Ming Chen, Zhejiang University

10:00 AM

(EMA-S11-032-2016) A Crystal-Chemical Framework for Relaxor versus Normal Ferroelectric Behavior in Tetragonal Tungsten Bronzes (Invited)

I. M. Reaney*[1]; 1. University of Sheffield, United Kingdom

Tetragonal tungsten bronzes (TTBs), an important class of oxides known to exhibit ferroelectricity, undergo complex distortions, including rotations of oxygen octahedra, which give rise to either incommensurately or commensurately modulated superstructures. Many TTBs display broad, frequency-dependent relaxor dielectric behavior rather than sharper frequency-independent normal ferroelectric anomalies, but the exact reasons that favor a particular type of dielectric response for a given composition remain unclear. In this contribution the influence of incommensurate/commensurate displacive modulations on the onset of relaxor/ferroelectric behavior in TTBs is assessed in the context of basic crystal-chemical factors, such as positional disorder, ionic radii and polarizabilities, and point defects. We present a predictive crystal-chemical model that rationalizes composition–structure–properties relations for a broad range of TTB systems.

10:30 AM

(EMA-S11-033-2016) Ferroelectric transition, low-temperature dielectric relaxations and their structural origins of $Ba_5RTi_3Nb_7O_{30}$ (R=La, Nd and Sm) tungsten bronze ceramics (Invited)

X. Chen*[1]; X. Zhu[1]; M. Mao[1]; K. Li[1]; X. Liu[1]; 1. Zhejiang University, China

Ferroelectric transition and low-temperature dielectric relaxations were determined for $Ba_5RTi_3Nb_7O_{30}$ (R=La, Nd and Sm) tungsten bronze ceramics together with their structural origins. The typical relaxor nature was observed for $Ba_5LaTi_3Nb_7O_{30}$, and the normal ferroelectric transition was determined for $Ba_5NdTi_3Nb_7O_{30}$ and $Ba_5SmTi_3Nb_7O_{30}$, while a low-temperature dielectric relaxation was detected for all compositions. The incommensurate modulation was observed in both $Ba_5LaTi_3Nb_7O_{30}$ and $Ba_5NdTi_3Nb_7O_{30}$ at room temperature, while there was a transition from incommensurate tilted structure to commensurate superstructure for $Ba_5NdTi_3Nb_7O_{30}$ with decreasing temperature. The incommensurate and commensurate modulations were determined by the *A*-site occupancy of Ba and R cations. The *A*-site disorder resulted in larger incommensurability parameter *d* and the diffusion of the satellite reflection spots. The effect of *A*-site disorder on the coupling between long-range dipolar order and the commensurate modulation was also discussed. The obvious ferroelectric 180° domains with spike-like shape parallel to *c* axis were observed for $Ba_5NdTi_3Nb_7O_{30}$, while no macro ferroelectric domain was determined for $Ba_5LaTi_3Nb_7O_{30}$.

11:00 AM

(EMA-S11-034-2016) Phase Formation and Microstructure Development of $(1-x)BaTiO_3$ - $xBi(Zn_{0.5}Ti_{0.5})O_3$

M. A. Kuzara*[1]; A. Mattern[1]; D. Hook[2]; G. Tutuncu[3]; G. Brennecka[1]; 1. Colorado School of Mines, USA; 2. CoorsTek Technical Ceramics, USA; 3. Brookhaven National Laboratory, USA

The purpose of this study was to elucidate the reaction pathways during calcination and sintering of $(1-x)BaTiO_3 - xBi(Zn_{0.5}Ti_{0.5})O_3$ ceramics in an effort to better understand the effects of phase formation, site occupancy, and cation diffusion kinetics on both phase formation and microstructural development. Phase formation was analyzed through laboratory and synchrotron X-ray powder diffraction across the full processing temperature range. The diffraction studies allowed identification of intermediate phase formation during calcination, as well as multiple reactions at elevated temperatures. Chemical heterogeneity was observed in microstructures of sintered pellets obtained through scanning electron microscopy (SEM) and chemical maps obtained through energy dispersive spectroscopy (EDS). SEM and EDS also revealed a relationship between calcination conditions (and therefore the phases present) in the powder and the density and phase formation of the sintered pellet. When studying systems with complex phase diagrams and wildly different cation diffusion kinetics, it is especially important to remember that processing steps can profoundly affect phase formation, microstructure development, and diffusion kinetics, which in turn affect resultant properties.

11:15 AM

(EMA-S11-035-2016) Functionally graded tunable multilayer capacitors

H. Song*[1]; D. Maurya[1]; S. Priya[1]; 1. Virginia Tech., USA

Tunable capacitors have attracted great deal of attention for their potential applications in wireless technologies. In present work, we report a novel method to achieve enhanced the tunability (> 100%) with lower loss tangent (< 5%) in a discrete component over a frequency regime of 1 – 5MHz. To achieve high volume efficiency of the tunable capacitor, novel high dielectric compositions $[0.975BaTi_{1-y}SnyO_3–0.025Ba(Cu_{1/3}Nb_{2/3})O_3$, (y = 0.04 ~ 0.08)] were developed. By adjusting the elemental composition, high dielectric permittivity (~9000) and small dielectric losses (~ 0.5 %) were achieved in these materials. These high dielectric constant materials

had grain size in submicron regime, which is important for achieving the high volume efficiency and the enhanced dielectric strength. Moreover, the curie temperature of these compositions can be easily tuned by changing Sn content in the matrix. The tunability of these compositions was found to be high near phase transitions. Here, we report functionally graded tunable multilayer capacitors based on the compositions having phase transitions around the room temperature. These tunable architectures were found to exhibit enhanced tunability (>100%) with small dielectric losses (<5%) over a wide temperature range around RT.

11:30 AM

(EMA-S11-036-2016) Electrical Heterogeneity and Anomalous Conductivity Behaviour in Reduced Titanates. (Invited)

D. C. Sinclair*[1]; M. Ferrarelli[1]; Z. Lu[1]; J. Dean[1]; I. M. Reaney[1]; 1. University of Sheffield, United Kingdom

Ceramic processing of titanate-based rutiles and perovskites at high temperature and/or low oxygen partial pressure can result in partial reduction of titanium from + 4 to +3 to give oxygen deficient and mixed Ti3+/4+ materials. This can result in significant levels of electronic or mixed ionic/electronic conduction that can be useful in the search for n-type thermoelectrics or electrode materials for solid oxide fuel cells, respectively. In many cases, surface reoxidation of mixed Ti3+/Ti4+ materials on cooling from the sintering temperature can be rapid whereas bulk re-oxidation is a much slower process and generates electrically heterogeneous (functionally graded) ceramics, many of which exhibit surface or internal barrier layer capacitance effects that generate high effective permittivity (e > 1000) effects and/or exhibit unusual low temperature (< 100 K) bulk conductivity with a very low activation energy, ~ 0.4 -0.7 meV. We present data on two titanate-based perovskite systems (magneto-electric EuTiO3 and thermoelectric La-doped SrTiO3) that have been processed under reducing conditions (eg 5 % H2 at ~ 1400 - 1500 C) and two that have been processed in air (CaCu3Ti4O12 and co-doped (In,Nb) TiO2) and discuss the spectrum of dielectric and/or conducting properties based on a variety of cooling/post-annealing conditions deliberately employed to generate electrically heterogeneous ceramics.

12:00 PM

(EMA-S11-037-2016) Transport properties of $BaTiO_3$-$Bi(Zn_{1/2}Ti_{1/2})O_3$ ceramics (Invited)

N. Kumar*[1]; D. Cann[1]; E. A. Patterson[2]; T. Frömling[2]; E. Gorzkowski[3]; 1. Oregon State University, USA; 2. Technische Universität Darmstadt, Germany; 3. Naval Research Laboratory, USA

Ceramics based on $BaTiO_3$-$Bi(Zn_{1/2}Ti_{1/2})O_3$ (BT-BZT) have been shown to exhibit excellent properties (relative dielectric constant > 1000, high breakdown strength) that enable the material to be used for high energy density and high temperature applications. Multilayer capacitors based on these have demonstrated energy densities approaching ~3 J/cm^3, which is superior to commercially available devices. However, similar to other Bi-perovskites, the defect chemistry needs to be fully understood before it can be fully exploited for capacitor applications. A significant (~2 orders of magnitude) improvement in the electrical resistivity was recently reported in these ceramics with addition of BZT, which was also accompanied by a change in the polarity of the majority charge carrier from p-type for BT to n-type for the BT-BZT solid solution. This points towards an unintended donor doping in BT-BZT ceramics. Even though there is no obvious mechanism for donor doping in these ceramics, the cause may be linked to the formation of an intermediate phase $BaBiO_3$ with Bi^{5+} on the B-site, the presence of oxygen vacancies being compensated by electrons, the loss of zinc and bismuth during processing, and other mechanisms. With the help of XPS, TGA with in-situ mass spectroscopy, EMF, O-18 annealing and other experiments, this presentation will include findings which help understand the underlying defect mechanisms in BT-BZT ceramics.

Advanced Electronic Materials: Electrocaloric, Thermoelectric and Devices

Room: Coral A

Session Chairs: Zdravko Kutnjak, Jozef Stefan Institute; Guangzu Zhang, Huazhong University of Science and Technology

10:00 AM

(EMA-S11-038-2016) Relaxor Ferroelectric Ceramics as a Working Body for an Electrocaloric Cooling Device (Invited)

Z. Kutnjak*[1]; U. Plaznik[2]; A. Kitanovski[2]; H. Ursic[1]; M. Vrabelj[1]; B. Malic[1]; B. Rozic[1]; 1. Jozef stefan Institute, Slovenia; 2. University of Ljubljana, Slovenia

The electrocaloric (EC) effect has attracted great interest for developing new cooling devices that have the potential to reach better efficiency than the existing cooling technologies. Recently, a revival of the EC effect has been triggered by the discovery of a giant EC temperature change of a few ten degrees in relaxor ferroelectric ceramic and polymer thin films. A review of recent ECE findings obtained in lead-based and lead-free perovskite ceramic relaxor materials including thick ceramic multilayers, substrate-free thick films, thin films, and liquid crystals will be given. The importance of microstructure, doping, and aging effects on the electrocaloric properties will be discussed. In addition, the recent advances in development of practical regenerator based cooling device utilizing PMN-10PT perovskite relaxor ceramics as active electrocaloric elements will be presented**.** The experimental testing of the cooling device demonstrates the efficient regeneration and establishment of the temperature span between the hot and the cold sides of the regenerator, exceeding several times the EC temperature change within a single PMN-10PT ceramic plate.

11:00 AM

(EMA-S11-040-2016) Giant Electrocaloric Effect in Polymer Nanocomposites with Nanostructured Ceramic Fillers (Invited)

G. Zhang*[1]; Q. Li[2]; S. Jiang[1]; Y. Zeng[1]; Q. Wang[2]; 1. Huazhong University of Science and Technology, China; 2. Pennsylvania State University, USA

We designed the ferroelectric nanocomposites as a new class of electrocaloric (EC) materials that are solution-processable and display pronounced ECE. Firstly, we created solution-processed EC materials based on the ferroelectric polymer nanocomposites consisting of BST nanoparticles and boron nitride nanosheets. The composites exhibit remarkable room-temperature ECE, including a giant cooling energy density of 129.2 MJ m^{-3} and temperature change of 50.5 °C. Subsequently, we found that not only the composition, but also the microstructure of the ceramic fillers play an important role in improving the ECE of the composites. By substituting PMN-PT for BST acted as the nanofillers, the composites exhibit significantly enhanced ECE in a wide temperature range (0-60 °C). Besides, compared to the polymer composites composed of ferroelectric nanoparticles, nanocubes and nanorods, the composites consisting of nanowires exhibit much higher breakdown and EC strengths as a direct consequence of the high aspect ratio of nanofillers, and consequently, greater ECE. The excellent ECE features of the polymer nanocomposites, together with simplicity in preparation and scalability in size and shape, open up new perspectives for development of light, compact and environmentally friend solid-state devices with high cooling power as alternatives to the presently existing cooling technologies.

11:30 AM

(EMA-S11-041-2016) Thermal Impact of Point Defect Migration and Buildup at TiO_2-Electrode Boundaries

B. F. Donovan*[1]; D. Long[2]; A. Moballegh[2]; E. C. Dickey[2]; P. E. Hopkins[1]; 1. University of Virginia, USA; 2. North Carolina State University, USA

The dielectric breakdown process involves the buildup of mobile point defects at the electrode-dielectric interface. In our study, we

will cause migration of Ti interstitials in TiO_2 with a DC bias and measure the changes in thermal conductance across the TiO_2-anode boundary throughout the breakdown process. We will use advanced time domain thermoreflectance analysis techniques to judge the impact of the defect buildup and relate the changes in thermal properties to the characteristics of dielectric breakdown. We anticipate a significant reduction in phonon mobility near the interface due to the higher concentration of point defects. This process is likely to compound over time and lead to accelerated breakdown due to thermal runaway.

11:45 AM

(EMA-S11-042-2016) Fabrication and Characterization of PLZT Films for Advanced Power Inverters in Electric Drive Vehicles

B. Balachandran*[1]; B. Ma[1]; T. H. Lee[1]; S. E. Dorris[1]; 1. Argonne National Laboratory, USA

Future availability of high-temperature power inverters will advance the market share for highly fuel-efficient, environmentally friendly electric drive vehicles (EDVs). An integral part of vehicle power inverters is the DC buss capacitor, which has a significant influence on inverter lifetime, reliability, cost, and temperature of operation. Advanced power inverters require capacitors that operate under high voltage conditions at under-hood conditions and yet have minimal footprint. Lead lanthanum zirconate titanate (PLZT) capacitors have the greatest potential for volume reduction. A high-rate aerosol deposition (AD) process is being developed at Argonne to produce thick PLZT films with desirable high voltage properties. The AD process can produce dense films at room temperature without a need for high temperature sintering. Recently we demonstrated that a ≈8-µm-thick PLZT film on aluminum-metallized polyimide substrate can be deposited in less than 20 minutes by the AD process. Films deposited by the AD process exhibited dielectric constant of ≈80 at 300 V bias, dielectric loss <2%, mean breakdown voltage of ≈1000 V, and temperature-dependent properties suitable for advanced power inverters. Results of our work will be presented in this talk. Work is supported by the U.S. Department of Energy, Vehicle Technologies Program.

12:00 PM

(EMA-S11-043-2016) Temperature Sensing at the Micro and Nano Scales

X. Huo*[1]; G. Li[1]; S. Xu[1]; 1. Peking University, China

To sense temperatures at the micro/nano-scales is always a technical challenge. As non-contact method usually needs complicated optical setup and has a relatively low resolution, contact method still takes an important portion in many applications. We have observed an unexpected thermoelectric size effect, showing the absolute Seebeck coefficient of metallic thin-film stripes decreases with width in the range of 3-100µm. This was repeatedly observed in more than 10 different metals, including Ni, Cr, Pd, Pt, W, etc. Based on this effect, we have developed dual-beam temperature sensors made from a single metallic thin film. By using arrays of these sensors, we have obtained 2D maps of local temperatures in a small area. We have developed multiplexier circuits to record signals from 5x5, 10x10 arrays and obtained nearly real-time 2D temperature maps with a time delay of only tens of seconds. We have utilized EBL technique to fabricate dual-stripe thermal sensors with a total width under 1µm, a sensitivity of 0.5-2.2 µV/K and a resolution of 0.1-0.5 K. We also fabricated the sensor array on an ultrathin flexible Parylene-C substrate with a thickness of 1-10µm for measuring temperatures of curved surfaces. With the merits of simple structure and flexible choice of materials, the novel single-layered dual-beam sensors may find practical applications in MEMS, lab-on-a-chip and flexible electronic devices.

12:15 PM

(EMA-S11-044-2016) Syntheses of large-scale, high-quality 2D wide-band-gap semiconductor nanosheets for high-performance deep ultraviolet photo detectors

P. Feng*[1]; E. Li[1]; M. Rivera[1]; O. Resto[1]; A. Aldalbahi[2]; 1. UPR, USA; 2. Department of Chemistry, Collage of Science, King Saud University, Saudi Arabia

We report on our new approach to quick synthesis of large-scale, high-quality 2D wide-band-gap semiconductor (boron nitride and silicon carbide) nanosheets for development of deep UV photoconductive detectors. The focus of our studies is on electrical and electronic properties, as well as sensitivity, response and recovery times, and repeatability of the detectors. Raman scattering spectroscopy, X-ray diffraction (XRD), scanning electron microscope (SEM), transmission electron microscopy (TEM), and electrometers were used to characterize the synthesized BN and SiC photoconductive sheet materials. Based on the synthesized BN and SiC sheet materials, deep UV detector is designed, fabricated, and tested. High sensitivity, quick time responsivity less than 0.5 ms has been achieved. Effects of dopant concentration, thickness of sheets on the properties of prototypic photodetectors are also discussed.

S4. Ion-conducting Ceramics

Oxygen Conducting Ceramics and Films

Room: Caribbean B

Session Chair: Collin Becker, US Army Research Laboratory

1:30 PM

(EMA-S4-015-2016) Magnetic and High Temperature Phase Transformations of Ca-doped Lanthanum Ferrites (Invited)

D. P. Butt*[1]; 1. Boise State University, USA

This research looks at the stability of a specific family of $La_xA_{1-x}FeO_{3-y}$ materials being piloted and have shown great promise for use as membranes in gas seperation processes. These electronic-ionic conductors will be expected to survive for years under highly reducing as well as oxidizing conditions, under pressure, thermal stresses, and to temperatures approaching 1000°C. Using a combination of diffraction and electron microscopy, dilatometry, magnetometry, and thermal analysis methods, the phase relations and stability of $La_xA_{1-x}FeO_{3-y}$ membrane materials were assessed. Structural modeling and Reitfeld refinement were used to assess atomic positions of atoms and vacancies in order to determine the mechanisms of thermally and environmentally induced structural phase transformations. A pseudobinary phase diagram will be presented as well as a discussion of the kinetics of phase transformations and reversible oxygen uptake processes.

2:00 PM

(EMA-S4-016-2016) Strain control of oxygen stoichiometry and ionic conduction in epitaxial perovskites (Invited)

H. Lee*[1]; 1. Oak Ridge National Laboratory, USA

Functional ionic defects, such as oxygen vacancies, in perovskite oxides play a central role in the performance of many advanced energy technologies, including solid-oxide fuel cells, rechargeable batteries, and oxygen-separation membranes. We have explored strain-mediated oxygen vacancy formation and migration in $SrCoO_{3-\delta}$ "oxygen sponges" and layered structures, including the brownmillerite $SrCoO_{2.5}$ and the Ruddlesden-Popper Sr-doped La_2CuO_4. From these materials, we find unanimously that the oxygen vacancy activation and oxygen ion conduction in oxide films are very sensitive to the sign and magnitude of epitaxial strain. Theoretical calculations confirm that the activation energy barrier for oxygen diffusion can be reduced by ~30% under only 2% tensile strain, whereas it is increased for compressive strain. This result indicates that tensile strain greatly enhances the oxygen activity, since it

has a much larger propensity to move oxygen in and out of the film than compressive strain. In this talk, we will present approaches to strain engineering in epitaxial multivalent transition metal oxides synthesized by pulsed laser epitaxy in order to control the oxygen vacancy concentration and improve oxygen ion conduction by epitaxial strain. *The work was supported by the U.S. Department of Energy, Office of Science, Basic Energy Sciences, Materials Sciences and Engineering Division.

2:30 PM

(EMA-S4-017-2016) Strain-Induced Control of Nano-Structuring and Fast Oxide Ion Transport in Thin $SrCrO_{3-x}$ Films

P. Sushko*[1]; Y. Du[1]; H. Zhang[1]; R. Colby[1]; M. Bowden[1]; S. Chambers[1]; 1. Pacific Northwest National Lab, USA

Oxygen vacancies are often present in complex oxides as point defects and their effects on the electronic properties on the host materials are typically uniform and isotropic. Exploiting oxygen deficiency in order to generate controllably novel structures and functional properties remains a challenging goal. We show that epitaxial strontium chromite films can be transformed, reversibly and at low temperature, from cubic, metallic perovskite $SrCrO_{3-x}$ (SCO) to rhombohedral, semiconducting $SrCrO_{2.8}$. As the concentration of oxygen vacancies in perovskite $SrCrO_{3-x}$ increases, the vacancies start to interact and, at x=0.2, aggregate giving rise to ordered two-dimensional (2D) arrays of {111}-oriented SrO2 planes interleaved between layers of tetrahedrally-coordinated Cr and separated by ~1 nm. First-principle calculations provide insight into the origin of the stability of such quasi-two-dimensional nanostructures and, consistently with the experimental data, predict that the barrier for O^{2-} diffusion along these nanostructures is approximately four times lower than that in the cubic $SrCrO_{3-x}$. While the diffusion activation energy is relatively independent on the substrate-induced strains, the stability of the 2D oxygen vacancy arrays varies, thus, providing an approach for controlling the stability of such structures and their stability.

2:45 PM

(EMA-S4-018-2016) Control of oxygen sublattice stability by strain in Ruddlesden-Popper films

T. Meyer*[1]; J. Petrie[1]; L. Jiang[1]; J. Lee[1]; M. Yoon[1]; J. Freeland[2]; T. Egami[1]; H. Lee[1]; 1. Oak Ridge National Laboratory, USA; 2. Argonne National Lab, USA

Modifications to the lattice structure, specifically lattice expansion, with increasing oxygen vacancy concentrations are reported often. However, the current understanding of the lattice behavior in oxygen-deficient films becomes questionable when considering compounds containing different atomic coordination or layering. Moreover, tensile strain has been found to stabilize oxygen vacancies in epitaxial films, which further complicates the interpretation of lattice behavior resulting from their appearance. Here, we present on the selective strain control of oxygen vacancy formation and resulting lattice responses in epitaxial films of the Ruddlesden-Popper phase, $La_{1.85}Sr_{0.15}CuO_4$. We find that preferential oxygen vacancy formation occurs within the equatorial position of the CuO_2 plane, which can be described by a drastically reduced Gibbs free energy for oxygen vacancy formation. Interestingly, this preferential oxygen vacancy formation leads to an unexpected lattice contraction. The strong strain coupling of oxygen nonstoichiometry and the unusual structural response can provide new understanding to the structure and property relationships of many other functional oxide materials. This work was supported by the U.S. DOE, Office of Science, Basic Energy Sciences, Materials Sciences and Engineering Division.

S5. Multifunctional Nanocomposites

Multifunctional Nanocomposites VI

Room: Coral B

Session Chair: Aiping Chen, Los Alamos National Lab

1:30 PM

(EMA-S5-033-2016) Mesoscale Interfacial Dynamics in Magnetoelectric Nanocomposites (Invited)

D. Viehland*[1]; J. Li[1]; Z. Wang[1]; 1. Virginia Tech, USA

Both heterostructural and vertically integrated two phase ME epitaxial thin layers have been fabricated by various deposition methods. With regards to vertically integrated nanostructures, our investigations have shown various phase architectures of self-assembled $BiFeO_3$-$CoFe_2O_4$ (BFO-CFO) thin films on differently oriented $SrTiO_3$ (STO) and $Pb(Mg_{1/3}Nb_{2/3})O_3$-xat%$PbTiO_3$ (PMN-x%PT) substrates. CFO forms segregated square, stripe, and triangular nanopillars embedded in a coherent BFO matrix on (001)-, (110)- and (111)-oriented substrates, respectively. Nanostructures with an aspect ratio of up to 5:1 with a prominent magnetic anisotropy were obtained on both (001) and (110) substrates along out-of-plane and in-plane directions. Magnetic easy axis rotation from in-plane to out-of-plane directions was realized through aspect ratio control. These studies established a detailed relationship of magnetic anisotropy with specific shapes and dimensions of ordered magnetic arrays. The results suggest a way to effectively control the magnetic anisotropy in patterned ferromagnetic oxide arrays with tunable shape, aspect ratio, and elastic strain conditions of the nanostructures. Using an epitaxial engineering approach, many different types of nanostructures are possible. It offers the ability to change the balance of terms in the free energy by which to tune the magnetic anisotropy via shape and also by electric field.

2:00 PM

(EMA-S5-034-2016) Giant magneto-resistance in epitaxial $ZnO:La_{0.7}Sr_{0.3}MnO_3$ nanocomposites

W. Pan*[1]; J. Ihlefeld[1]; P. Lu[1]; S. R. Lee[1]; 1. Sandia National Laboratories, USA

A great deal of research has been carried out in oxide material systems. Among them, ZnO and $La_{0.7}Sr_{0.3}MnO_3$ (LSMO) are of particular interest due to their superb optical properties and colossal magneto-resistive effect. In this talk, we will report our recent results of magneto-transport studies in self-assembled, epitaxial $ZnO:La_{0.7}Sr_{0.3}MnO_3$ nanocomposite films. The epitaxial LSMO/ZnO phase-separated nanocomposites were prepared by rf magnetron sputtering on (001) $LaAlO_3$ single crystalline substrates. X-ray diffraction analysis showed that the LSMO phase was cube-on-cube epitaxial on the substrate and the ZnO phase possessed a nominal [11-20] texture. AC-STEM imaging and EDS chemical mapping were used to characterize these ZnO/LSMO composite films. Compositional analysis indicates mutual solubility between ZnO and LSMO, and compositional variation across the ZnO/LSMO interfaces. In our magneto-transport studies, a giant negative magneto-resistance was observed at low temperatures and high magnetic fields, reaching almost 700% at a magnetic field of 5 Tesla at 70K. This giant magneto-resistance decreases with increasing temperatures, to ~ 15% at 200K. We believe that this giant magneto-resistance is related to variations in the orientation of the ZnO pillars and self-organization of the pillars into quasi-periodic percolated domains within our ZnO/LSMO nanocomposites.

2:15 PM

(EMA-S5-035-2016) Energy-efficient magnetization reversal in multiferroic nanostructures (Invited)

J. Hu*[1]; T. Yang[1]; J. Wang[1]; C. Nan[2]; L. Chen[1]; 1. Pennsylvania State University, USA; 2. Tsinghua University, China

In multiferroic nanostructures, magnetization can be switched (e.g., via strain) with an electric voltage rather than a current, dissipating much less energy. This can be exploited for energy-efficient magnetic and spintronic devices. However, voltage-driven reversal of uniform magnetization has not yet been experimentally demonstrated. In this talk, we report our recent theoretical predictions of achieving voltage-driven uniform magnetization reversal in multiferroic nanostructures through three different approaches, hoping to provide useful guidance to experiments.

2:45 PM

(EMA-S5-036-2016) Towards Magnetocaloric Response Over A Broad Temperature via Ferromagnetic Bilayers

D. Xue*[1]; A. Chen[1]; Q. Jia[1]; T. Lookman[1]; 1. Los Alamos National Lab, USA

The magnetization instabilities at the ferromagnetic phase transition can be utilized to enhance properties such as magnetocaloric effect (a magnetic field induced temperature change) and magnetoresistance (a magnetic field induced resistance change). A drawback is that these enhancements occur within a narrow temperature range near the phase transition, while a wide operational temperature range is highly desired for practical devices. Therefore, in the present study, we propose a method to enlarge the temperature range of magnetocaloric and magnetoresistance effects via bilayer structure. We combine two ferromagnetic materials with different transition temperatures, $La_{0.8}Sr_{0.2}MnO_3$ and $La_{0.7}Ca_{0.3}MnO_3$, on a STO(001) substrate. By varying the thickness of the individual layers, the enhancement of magnetocaloric and magnetoresistance effects at individual ferromagnetic phase transition can be combined, resulting in good response over a wide temperature range.

3:00 PM

(EMA-S5-037-2016) UV photoluminescence and cathodoluminescence from Gd^{3+} in $YAlO_3$ thin films

Y. Shimizu*[1]; K. Ueda[1]; H. Takashima[2]; Y. Inaguma[3]; 1. Kyushu Institute of Technology, Japan; 2. National Institute of Advanced Industrial Science and Technology (AIST), Japan; 3. Gakushuin University, Japan

Gd^{3+} as UV luminescence center shows sharp luminescence attributed to 4f-4f transition at approximately 310 nm. Recently, we found that Gd^{3+} doped and Gd^{3+}-Pr^{3+} co-doped $YAlO_3$ powders show UV photoluminescence (PL) of Gd^{3+}. In this study, we prepared thin films of Gd^{3+} doped and Gd^{3+}-Pr^{3+} co-doped $YAlO_3$ and investigated not only PL but also cathodoluminescence (CL) of the films, aiming for future application of thin film-type luminescence devices. Thin films of Gd^{3+} doped and Gd^{3+}-Pr^{3+} co-doped $YAlO_3$ were deposited on $LaAlO_3$ (001) single crystal substrates by pulsed laser deposition method and the films were annealed in air. XRD patterns and FE-SEM images revealed that the films were epitaxial thin films with smooth surfaces. Gd^{3+} doped and Gd^{3+}-Pr^{3+} co-doped $YAlO_3$ showed UV PL of Gd^{3+} on host excitation at 157 nm. Under excitation at 216 nm, which correspond to Pr^{3+} 4f-5d transition energy, Gd^{3+}-Pr^{3+} co-doped $YAlO_3$ also showed UV PL of Gd^{3+} through energy absorption by Pr^{3+} and energy transfer from Pr^{3+} to Gd^{3+}. Under electron irradiation, Gd^{3+} doped and Gd^{3+}-Pr^{3+} co-doped $YAlO_3$ showed UV CL of Gd^{3+}. The CL intensity of Gd^{3+} doped $YAlO_3$ was more intense than that of Gd^{3+}-Pr^{3+} co-doped $YAlO_3$. This is probably because CL excitation energy absorbed by $YAlO_3$ host was concentrated at Gd^{3+} in Gd^{3+} doped $YAlO_3$, whereas the energy was transferred to Pr^{3+} as well as Gd^{3+} in Gd^{3+}-Pr^{3+} co-doped $YAlO_3$.

3:45 PM

(EMA-S5-038-2016) Spatially-resolved mapping of enhanced oxygen ion conduction in Sm-doped CeO_2-$SrTiO_3$ vertical nanocomposite films (Invited)

S. Yang*[1]; S. Lee[2]; J. Jian[3]; W. Zhang[3]; P. Lu[4]; Q. Jia[5]; H. Wang[3]; T. Noh[6]; S. Kalinin[1]; J. MacManus-Driscoll[2]; 1. Oak Ridge National Laboratory, USA; 2. University of Cambridge, United Kingdom; 3. Texas A&M University, USA; 4. Sandia National Laboratories, USA; 5. Los Alamos National Laboratory, USA; 6. Seoul National University, The Republic of Korea

Fast oxygen ion transport at reduced temperature is highly desirable in many oxide-based electrochemical devices, including solid oxide fuel cells (SOFCs), catalysts, and memristors. While huge ion conductivity has been demonstrated in planar heterostructure films, there has been often considerable debate over the origin of the conductivity enhancement, in part because of the difficulties of direct probing buried ion transport channels. Here, we present nanoscale investigation of oxygen ion transport in vertical heteroepitaxial Sm-doped CeO_2 (SDC)-$SrTiO_3$ (STO) films using scanning probe microscopy (SPM). The ionic conductivity of SDC-STO nanocomposite film is higher by one order of magnitude than plain SDC films. By using SPM, we show that only the SDC nanopillars have high oxygen ion conductivity, while the surrounding STO matrix showed negligible conduction. Furthermore, the fast ion-conducting channels are not exclusively restricted to the interface but rather reside in the whole volume of the high crystalline SDC nanopillars. This work highlights that direct spatially-resolved mapping of oxygen ion conduction at the nanoscale is essential to verify the underlying mechanism of ionic conductivity enhancement. In addition, this work offers a pathway to realize spatially localized fast ion transport in oxides of micrometer-thickness.

4:15 PM

(EMA-S5-039-2016) Enhanced performance of triboelectric nanogenerator by compositing high dielectric nanoparticles into sponge PDMS film

J. Chen*[1]; H. Guo[1]; C. Hu[1]; 1. Chongqing University, China

Modification of the organic triboelectric film plays a critical role in enhancing the output performance of triboelectric nanogenerator (TENG). In this paper, a high output performance composite sponge PDMS film based triboelectric nanogenerator (CS-TENG) is fabricated by optimizing both the dielectric properties and the porosity of the tribo-layer through a feasible filling and removing method. The influence of dielectricity on the output performance is discussed experimentally and theoretically, which indicates that both the surface charge density and the charge transfer ratio have the proportional relationship with the relative permittivity of the tribo-layer. By combining the enhancement of permittivity and produce of pores in the PDMS film, the charge density of 20 nC cm^{-2}, open circuit voltage of 338 V, and power density of 7.38 W m^{-2} at working frequency of 2.5 Hz are obtained with the optimized film consisting of 10% $SrTiO_3$ nanoparticle (~20 nm) and 15% pores by volume, which gives over 5-fold power enhancement compared with the nanogenerator based on pure PDMS film. This work provides a new and effective way to enhance the performance of TENG inside the material other than only to modify the surface properties.

4:30 PM

(EMA-S5-040-2016) CuO Nanostructures Synthesised by Chemical Bath Deposition (CBD) on Seed Layers Deposited by SILAR and CSP Methods

C. M. Muiva*[1]; K. Maabong[2]; C. Moditswe[1]; 1. Botswana International University of Science and Technology, Botswana; 2. University of Botswana, Botswana

Cupric oxide (CuO) is a p-type semiconductor material with diverse applications in photovoltaic and photo-thermal energy conversion, catalysis, gas sensing, lithium ion battery technologies and magnetic storage. CuO nanostructures have been synthesised by a simple

chemical bath deposition (CBD) method on seed layers deposited by successive ionic layer adsorption and reaction (SILAR) and chemical spray pyrolysis (CSP) techniques. Fourier transform infrared spectroscopy (FTIR) and EDS studies showed that the synthesised product was CuO. All the XRD peaks observed were indexed to pure monoclinic phase of CuO and no peaks corresponding to other crystalline phases or Cu and $Cu(OH)_2$ impurities were observed. The main diffraction peaks at 2θ equals to 35.54° and 38.76° were assigned to (002) and (111) planes of monoclinic CuO respectively. The broadening of the XRD peaks showed that the samples were nanosized. The average grain sizes evaluated on the basis of Debye-Scherrer method were found to be 12.9 nm and 32.1 nm for the film deposited on SILAR and CSP seed crystals respectively. The lattice parameters slightly deviated from the standard values implying that the film was under strain. `The films were mainly absorbing in the visible and UV regions with an optical band gap of 1.72 and 1.55 eV for a sample deposited on SILAR and CSP seed layers respectively.

S6. Computational Design of Electronic Materials

Low Dimensional Systems

Room: Mediterranean A
Session Chair: Emmanouil Kioupakis

1:30 PM

(EMA-S6-015-2016) Computational Discovery of Novel 2D Materials for Optoelectronic and Spintronic Applications (Invited)

R. G. Hennig*[1]; 1. University of Florida, USA

The rapid rise of novel 2D materials, presents the exciting opportunity for materials science to explore an entirely new class of materials. This comes at the time when mature computational methods provide the predictive capability to enable the computational discovery, characterization, and design of 2D materials and provide the needed input and guidance to experimental studies. I will present our data-mining and genetic algorithm approaches to identify novel 2D materials with low formation energies and show how unexpected structures emerge when a material is reduced to sub-nanometers in thickness. We discovered several 2D materials in the families of group III-V compounds and group-II oxides with promising properties for electronic devices and identify suitable substrates that stabilize these materials. In the families of group-III monochalcogenides and transition metal dichalcogenides we identify several 2D materials suitable for photocatalytic water splitting. For several transition-metal chalcogenide compounds ferromagnetic order emerges at temperatures accessible to experiments. This opens the opportunity to investigate the interplay of magnetic order and reduced dimensionality and may provide materials for spintronics applications. Our results provide guidance for experimental synthesis and future searches of materials suitable for energy technologies and electronic devices.

2:00 PM

(EMA-S6-016-2016) Interfaces between one-atom-thick materials and metals:
Indications to the interpretation of scanning tunneling spectroscopy (Invited)

C. Park*[1]; B. G. Sumpter[1]; M. Yoon[1]; 1. Oak Ridge National Laboratory, USA

Nowadays, atomic-resolution images of two-dimensional materials are routinely generated by the scanning tunneling microscopy (STM). Due to the one-atom thickness, the substrate can affect the tunneling current significantly in a nontrivial way. For example, it is phenomenologically known that the scanning tunneling spectroscopy map (dI/dV) of graphene on metal substrate has quite different shape from the density of states of it. The lateral heterojunction between graphene and boron nitride where well-defined one-dimensional boundary states emerges [Nature Communications 5, 5403 (2014)], provides an idea platform for the origin of this discrepancy by comparing the tunneling current of metallic and insulating materials with the same condition. In this talk, two peculiar observations of STM measurement will be explained with the first-principles simulations; 1) The apparent height difference between the two which is related with the different strength of dipole layers along the normal direction and 2) the similar amount of tunneling currents which indicates the dominant contribution to them comes from the metallic substrate. For the latter reason, the true position of atoms can be different from the atomic-resolution image obtained by the tunneling current map.

2:30 PM

(EMA-S6-017-2016) Indiene 2D Monolayer: Theoretical Study of a New Nanoelectronic Material

S. K. Gupta*[1]; D. Singh[3]; I. Lukacevic[2]; Y. Sonvane[3]; 1. St. Xavier's College, Ahmedabad, India; 2. University J. J. Strossmayer,, Croatia; 3. S.V. National Institute of Technology,, India

One atom thick monolayer nanostructures consisting of group III, IV and V elements are drawing ever more attention for their extraordinary electronic properties. Through first principles calculations, we systematically investigate structural and electronic properties of the corresponding indium monolayers in three dierent allotropic forms: planar, puckered and buckled. Our study shows that planar and buckled allotropes are stable and show metallic and semiconducting behavior, respectively. Their stability and electronic properties cannot be easily correlated to those of similar elemental monolayer structures. Van-Hove singularity is observed in the electronic density of states which could lead to an increase in the electronic conductivity, opening paths to new electronic applications. Strain engineering is applied in order to determine the changes in the electronic behavior and band gap properties. Planar allotrope remains metallic under both compressive and tensile strain, while buckled allotrope changes from an indirect semiconductor to a semimetal. Our study demonstrates that the indiene nanostructures possess diverse electronic properties, tunable by strain engineering.

2:45 PM

(EMA-S6-018-2016) Vibrational Mode Lifetimes: New Insights (Invited)

M. Daw*[1]; 1. Clemson University, USA

We discuss a practical, new method for calculating vibrational mode lifetimes in insulating solids. The approach is based on a recursion method analysis of the Liouvillian. In practical terms, the calculation is accomplished by evaluating ensemble averages of specific operators, meaning that the entire calculation is to be done with Monte Carlo, given a means of calculating energies and forces. We discuss the results of evaluating this method for both simple lattice models and more realistic interatomic potentials. This technique makes possible the calculation lifetimes for even complex materials and complex structures. Using this method, we have identified some modes in Si- and Ge-based clathrates that have unusually short lifetimes; we make comparison to available Raman data. The authors acknowledge support from the Dept. of Energy under grant DE-SC0008487.

3:15 PM

(EMA-S6-019-2016) Anisotropic spin transport and strong visible-light absorbance in few-layer SnSe and GeSe

G. Shi*[1]; E. Kioupakis[1]; 1. University of Michigan, USA

Similar to TMDs, several IV-VI compounds including GeSe and SnSe also crystallize in layered structures with weak bonding between the layers. In this work, we perform first-principles calculations based on density functional theory and many-body perturbation theory to analyze the electronic and optical properties

of few-layer SnSe and GeSe. The fundamental band gaps are found to be direct in single-layer and double-layer GeSe, but indirect in SnSe few-layer structures. Our analysis reveals that the interplay of spin-orbit coupling with the symmetry of the monolayer structures results in anisotropic spin-orbit splitting of the bands that can find applications in directionally dependent spin-transport devices. We also found that the optical absorbance in the visible range is high for the few-layer structures, reaching values as high as 47% for bilayer SnSe with a thickness of just 1 nm. Our results suggest that few-layer SnSe and GeSe are promising materials for ultra-thin-film flexible photovoltaic applications with an upper limit to the conversion efficiency that rivals the record efficiencies of organic and dye-sensitized solar cells.

High-throughput/Multiscaling Calculations

Room: Mediterranean A

Session Chairs: Richard Hennig, University of Florida; Andre Schleife, University of Illinois at Urbana-Champaign

4:00 PM

(EMA-S6-020-2016) First-principles Simulations of Electronic Excitations and Ultrafast Real-time Dynamics in Semiconducting Oxides (Invited)

A. Schleife*[1]; 1. University of Illinois at Urbana-Champaign, USA

High-performance super computers nowadays allow for predictive accuracy of quantum-mechanical computational approaches to study material properties. At the same time, these codes need to scale well on hundreds of thousands of processors to exploit leadership-class machines and to deal with the complexity of novel materials. This talk focuses on a first-principles description of electronic excitations and ultrafast atto-second dynamics. These effects are omnipresent in materials and their accurate description is crucial for computational design of electronic materials. Cutting-edge first-principles techniques will be discussed that accomplish predictive theoretical spectroscopy of electronic excitations. These techniques yield deep insight into quasiparticle and excitonic effects and optical absorption, e.g. for lanthanum-aluminum oxide and hafnium oxide. Using computed spectra in multi-scale Maxwell modeling allows us to understand materials properties on the meso-scale. This talk will also describe how Ehrenfest molecular dynamics provides accurate insights from first principles into ultrafast real-time dynamics of electrons under particle-radiation conditions. Using high-performance super computers we apply these approaches to magnesium oxide and indium phosphite, in order to explore these materials for energy harvesting and radiation-hard applications.

4:30 PM

(EMA-S6-021-2016) Pyroelectric and Electrocaloric Properties of Ferroelectric Ceramics: A Mesoscopic Modeling Perspective (Invited)

P. Alpay*[1]; 1. University of Connecticut, USA

Electrothermal interconversion energy sources have recently emerged as viable means for primary and auxiliary solid state cooling and power generation. Electrocaloric and pyroelectric responses describe converse effects, wherein an adiabatic change in temperature occurs in response to an applied electric field, or a change in the electric polarization occurs in response to a change in temperature. Here, we use a nonlinear thermodynamic model based on Landau-Ginzburg-Devonshire formalism to analyze the electrothermal properties of ferroelectric ceramics such as $BaTiO_3$ and $PbTiO_3$. Taking into account that such materials are usually employed in thin film form, we provide a thorough analysis of the electrical and mechanical boundary conditions. We show that internal stresses that develop due to lattice mismatch or during processing can have a significant influence on the electrothermal properties. Using the theoretical tools, we also compute the pyroelectric and electrocaloric responses of multilayer ferroelectric heterostructures. We demonstrate that by adjusting internal electrical fields through changing relative thicknesses in a multilayer ferroelectric construct, electrothermal properties can be significantly enhanced.

5:00 PM

(EMA-S6-022-2016) First-principles High-throughput Screening for Doped-ZnO

K. Yim*[1]; J. Lee[1]; H. Nahm[2]; S. Han[1]; 1. Seoul National University, The Republic of Korea; 2. Institute for Basic Science, The Republic of Korea

Zinc oxide (ZnO) has been receiving lots of attentions for its potential in electronic and optoelectronic and magnetic applications. As a transparent conducting oxide (TCO), ZnO is wide-direct band gap materials and also has high mobility. However, intrinsic carrier concentration of ZnO is not large enough as an electronic material. To utilize ZnO for conductors in electronic devices, the material should be heavily doped. For example, heavy doping of Al has achieved n-type conductivity with $\rho \sim 10^{-4}$ Ωcm which is comparable to ITO. Despite extensive studies on certain dopants for ZnO, exact defect types of all possible dopants are still unknown. To screen optimal dopants for specific applications, we develop an in-house automatization code to search the most stable doping configurations for each dopant using density functional theory calculation. Our algorithm automatically identify the possible doping sites including substitutional sites, interstitials and split-interstitials with various charge states and calculate the formation energies of each doping configuration. As a result, we can obtain formation energies of the stable defect types, transition-levels, magnetic moments, and carrier concentrations at a various conditions. Using the automatization code, we obtain database of 60 elements as dopants and identify intriguing doping types that have not been reported.

5:15 PM

(EMA-S6-023-2016) First Principles screening of Transparent Conducting Oxides Using aMoBT

A. Faghaninia*[1]; M. T. Sullivan[1]; D. I. Becker-Ricketts[1]; C. S. Lo[1]; 1. Washington University in St. Louis, USA

Accurate ab initio electronic transport models can facilitate high throughput screening of semiconductor materials. Previous such attempts on transparent conducting oxide (TCO) materials have focused on their average effective mass, due to the simplicity and speed of such calculations. The effective mass calculation is often simplified by basing it solely on the shape of the band extrema. Although the approximate effective mass gives a valuable prediction of material performance, it lacks sufficient complexity for accurate calculation of electronic properties, especially in degenerate semiconductors. In particular, electron-phonon interactions, which limit the mobility at room temperature, are ignored. Here we employ an *ab initio* transport Model in the Boltzmann Transport (aMoBT) framework, which accurately predicts the electrical mobility and conductivity of both n-type and p-type semiconductors. We screen more than 70 promising TCOs that were pre-screened using the average effective mass, and rank them based on their conductivity, as limited by ionized impurity scattering and electron-phonon scattering mechanisms. We now report the most promising candidates from each of the n- and p-type semiconductors, and assert the utility of aMoBT, as incorporated into an automated atomistic calculation framework, in designing new materials for solar cell applications

5:30 PM

(EMA-S6-024-2016) Enhancing magnetoelectric coupling in multiferroics via temperature mediated mechanism (Invited)

C. Chang[1]; B. Mani[1]; S. Lisenkov[1]; I. Ponomareva*[1]; 1. University of South Florida, USA

Magnetoelectric coupling in multiferroics is very attractive for many innovative applications such as four-state logic in a single device, magnetoelectric random access memories, electrically controlled exchange bias devices. Unfortunately, in most of the known

multiferroics this coupling is too weak to allow for technological applications. We propose an unusual route to a robust enhancement of magnetoelectric coupling via thermally mediated mechanism. Such mechanism couples magnetization to the electric field (polarization to the magnetic induction) indirectly by taking advantage of pyromagnetic and electrocaloric (pyroelectric and magnetocaloric) properties of the material. This approach was tested in both direct and indirect first-principles-based simulations and revealed that a significant enhancement of magnetoelectric coupling could be achieved. In particular, we predict a four order of magnitude enhancement of magnetoelectric coupling in the most celebrated multiferroic $BiFeO_3$. From thermodynamics point of vew, the thermally mediated magnetoelectric effect is quantified by an isentropic rather than isothermal magnetoelectric response.

S10. Emerging functionalities in layered-oxide and related materials

Properties and Theory/Simulation

Room: Mediterranean B/C

Session Chairs: Edward Gorzkowski, Naval Research Lab; Bharat Jalan, University of Minnesota

1:30 PM

(EMA-S10-007-2016) High temperature dielectric properties of c-axis oriented bismuth layer-structured dielectric films prepared on Si and Glass substrates using nanosheets buffer layer (Invited)

H. Funakubo*[1]; J. Kimura[1]; I. Takuwa[1]; M. Matsushima[1]; T. Shimizu[1]; H. Uchida[2]; T. Shibata[3]; M. Osada[3]; T. Sasaki[3]; 1. Tokyo Institute of Technology, Japan; 2. Sophia University, Japan; 3. National Institute for Material Center, Japan

Uniaxially (001)-oriented $CaBi_4Ti_4O_{15}$ films with various film thicknesses were prepared on (100)$_c$$SrRuO_3$/$Ca_2Nb_3O_{10}$ nanosheet/glass and (100)$_c$$SrRuO_3$/$Ca_2Nb_3O_{10}$ nanosheet/(100)Si substrates to realize a high-temperature adaptor capacitor. As the film thickness decreases down to 50 nm, the out-of-plane lattice parameters decrease, while the in-plane lattice ones increase due to the in-plane tensile strain for (001)-oriented $CaBi_4Ti_4O_{15}$ films prepared on (100)$_c$$SrRuO_3$/$Ca_2Nb_3O_{10}$ nanosheet/glass. However, the relative dielectric constant (e_r) at room temperature exhibits a negligible degradation as the film thickness decreases down to 50 nm, suggesting that e_r of (001)-oriented $CaBi_4Ti_4O_{15}$ is less sensitive to the residual strain. The capacitance density increases monotonously with decreasing film thickness and is stable against temperature changes from room temperature to 400 °C irrespective of film thickness. Moreover, $Ca_2Nb_3O_{10}$ nanosheets play an important role for prepared uniaxially (001)-oriented films that result in the stable dielectric properties against the temperature and the scaling down of the film thickness. This research was partially covered by foundation for the MEXT Elements Strategy Initiative to Form Core Research Center.

2:00 PM

(EMA-S10-008-2016) Octahedral tilting in layered perovskites – Factors that lead to polar space groups (Invited)

P. Woodward*[1]; A. Sharits[1]; 1. Ohio State University, USA

Ruddlesden-Popper (RP) phases are layered analogs to the three dimensional perovskite structure. In 3D perovskites one of the most important structural distortion mechanisms involves tilts of corner connected octahedra. Whereas our understanding of octahedral tilting in 3D perovskites is quite mature, octahedral tilting in RP phases is complicated by the presence of both 9- and 12-coordinate A-site cations. In this talk I will summarize our efforts to understand and control octahedral tilting in layered perovskites, specifically n = 2 Ruddlesden-Popper phases. This is more than a scientific curiosity because certain tilt patterns lead to polar structures that are potentially of interest for their pyroelectric, ferroelectric and multiferroic properties. I will also discuss the synthesis and crystal structures of $CaRE_2Sc_2O_7$ and $SrRE_2Sc_2O_7$ (RE = La, Pr, Nd) RP phases.

2:30 PM

(EMA-S10-009-2016) Intentional defects in 2-D birnessite MnO_2 to improve supercapacitor performance

P. Gao*[1]; P. C. Metz[1]; T. Hey[1]; S. Misture[1]; 1. Alfred University, USA

2-D birnessite MnO_2 nanosheets were successfully modified by reduction treatments to double the electrochemical capacitance to values in excess of 300 F/g. The nanosheets were prepared by solid state sintering of the parent K-Mn-oxide, followed by ion-exchange and exfoliation. MnO_2 nanosheet suspensions were flocculated to assemble 3-D porous nanostructures, and finally subjected to reduction treatments to generate surface defects. SEM images demonstrate porous structures assembled from ultra-thin 2-D MnO_2 nanosheets with the birnessite structure that have high surface area. XPS, XANES and high energy X-ray PDF analyses indicated an increase in the Mn^{3+}/Mn^{4+} ratio with partial reduction of MnO_2 nanosheets, where the Mn^{3+} cations shift from the plane of the 2-D nanosheet to the nanosheet surface. This defect geometry is likely to create more active surface sites that can promote sodium ion intercalation. Electrochemical measurements showed that the charge storage capacitance increased from about 150 F/g to over 300 F/g when we intentionally reduced the MnO_2 nanosheets to form out-of-plane Mn ions, and the charge transfer resistance decreased from ~18 Ω to ~3 Ω correspondingly. These experimental results demonstrate that self-assembled 3-D porous MnO_2 nanostructures are of commercial value when engineered to optimize their defect structures.

2:45 PM

(EMA-S10-010-2016) Engineering the Properties of Perovskite-Based Sn Oxide Transparent Conductors (Invited)

D. J. Singh*[1]; 1. University of Missouri, Columbia, USA

Recent experimental results have shown that doped n-type BaSnO3 may be a useful high performance transparent conductor based on abundant elements. In particular, it has a favorable combination of good mobility and optical transparency, although the band gap of below 3 eV is slightly smaller than usually desired. BaSnO3 is a cubic perovskite and is a member of a class of Sn-based oxides including SrSnO3, ferroelectric ZnSnO3 and Ruddlesden-Popper phases. Remarkably the band gaps and other properties vary strongly among these compounds and in addition there are exceptionally strong strain dependencies of the electronic and optical properties. Here an overview of the strain and structure dependent properties of n-type Sn(IV) oxides in this family are presented along with various strategies, such as dimensional reduction, for improving these materials.

3:45 PM

(EMA-S10-011-2016) The Aurivillius phases as potential multiferroics: a view from first principles (Invited)

C. Ederer*[1]; 1. ETH Zurich, Switzerland

Aurivillius phases exhibit a naturally-layered crystal structure with robust ferroelectric properties that allows to incorporate a variety of magnetic cations. However, the reported physical properties and magnetic ordering temperatures of "multiferroic" Aurivillius phases vary considerably, even for closely related compositions. Here, we focus on $Bi_5FeTi_3O_{15}$ (BFTO) as a prototypical Aurivillius phase containing magnetic ions. We use first principles calculations and Monte Carlo simulations to establish the intrinsic properties of BFTO, and discuss the general suitability of Aurivillius phase materials as potential multiferroics. We address a possible site preference of the Fe^{3+} cation in BFTO, calculate the spontaneous electric polarization, and investigate the effect of epitaxial strain. We calculate the strength of the magnetic coupling and perform Monte Carlo simulations to estimate magnetic ordering temperatures. We discuss possible routes to obtain robust magnetic properties at high temperatures in Aurivillius phases by varying composition

and the number of perovskite-like layers. Furthermore, we discuss the mechanism underlying the ferroelectricity in Aurivillius phases by focusing on 2-layer systems based on $SrBi_2Ta_2O_9$. We study the coupling between polar and non-polar modes in these systems, and discuss our results in light of the general concept of "hybrid improper ferroelectricity".

4:15 PM

(EMA-S10-012-2016) Electrocaloric effects in layered oxides with easy polarization rotation

J. Mangeri[1]; K. Pitike[1]; P. Alpay[1]; S. Nakhmanson*[1]; 1. University of Connecticut, USA

We have recently predicted existence of Goldstone-like excitations — manifested through easy in-plane polarization rotations — in some Ruddlesden-Popper-type layered oxides. Here we study electrocaloric response in one of such systems for a wide range of applied epitaxial strains. That is accomplished by constructing a Landau-Ginzburg thermodynamic potential for the system from the results of our previous DFT calculations and analyzing its behavior for both amplitudon and phason types of polarization switching.

4:30 PM

(EMA-S10-013-2016) The origins of Goldstone-like polar distortions in perovskite-oxide multilayers

K. Pitike[1]; L. Louis[1]; S. Nakhmanson*[1]; 1. University of Connecticut, USA

Here we report on our investigations of electronic-structure-based underpinnings of Goldstone-like excitations — and the associated apparent loss of crystalline anisotropy with respect to polar distortions — in epitaxial perovskite-oxide slabs. This is accomplished by examining the behavior of individual atomic planes and tracking evolution of their properties as they are stacked back into a slab. We demonstrate that proper combinations of active (polar) and bracing (non-polar) layers, in conjunction with the right amount of strain to make the polar-state energy wells along (100) and (110) directions about the same magnitude, are needed to induce Goldstone-like excitations, while the presence of lone-pair active ions within the polar layers is not always required.

S11. Advanced electronic Materials: Processing, structures, properties and applications

Advanced Electronic Materials: Lead- free Piezoelectrics

Room: Indian

Session Chairs: Jing-Feng Li, Tsinghua University; Hijime Nagata, Tokyo University of Science

1:30 PM

(EMA-S11-045-2016) $CaZrO_3$-Modified (K,Na)NbO_3-Based Lead-Free Piezoceramics with Enhanced Thermal Stability and Fatigue Resistance (Invited)

J. Li*[1]; K. Wang[1]; F. Yao[1]; 1. Tsinghua University, China

Research progress achieved in the last decade after Saito's work has further confirmed the promising potential of (K,Na)NbO_3 -based (KNN) lead-free piezoelectric ceramics, although more studies are still required for large-scale industrial applications. Temperature sensitivity of piezoelectric properties has been recognized as one of the drawbacks of KNN-based ceramics as compared with lead-containing counterparts, but we found that a high piezoelectric strain up to 0.16 % over a wide temperature range could be achieved in $CaZrO_3$-modified Li/Ta co-doped KNN ceramics. Our work also has shown that the electric-field-induced strain exhibits excellent fatigue resistance regardless of electric loading forms. Such good properties that are indispensable for piezoelectric actuators could be well explained in association with the ferroelectric domain structure and phase evolution under electrical field.

2:00 PM

(EMA-S11-046-2016) High power piezoelectric characteristics of $(Bi_{1/2}Na_{1/2})TiO_3$-based solid solutiona system and their demonstration for ultrasonic aaplications (Invited)

H. Nagata*[1]; 1. Tokyo University of Science, Japan

Recently, many high-power piezoelectric ceramic devices, such as ultrasonic motors and piezoelectric transducers, have been developed so far. Important piezoelectric constants for obtaining high vibration velocity are both piezoelectric strain constant d and mechanical quality factor Q_m. In this situation, we investigated lead-free piezoelectric ceramics, $(Bi_{0.5}Na_{0.5})TiO_3$ (BNT)-based solid solution systems, such as below. $(Bi_{1/2}Na_{1/2})TiO_3$-$(Bi_{1/2}Li_{1/2})TiO_3$-$(Bi_{1/2}K_{1/2})TiO_3$ ternary system $(Bi_{1/2}Na_{1/2})TiO_3$-$(Bi_{1/2}Li_{1/2})TiO_3$-$BaTiO_3$ ternary system Then, some specific compositions in BNT-based systems show relatively high d and Q_m, Thus, they seem to be good candidates for high-power piezoelectric devices realizing a large-amplitude and a linear stability against vibration velocity. Then, we tried to demonstrate ultrasonic motors and ultrasonic nebulizers by using BNT-based solid solution systems and investigate electrical properties. For example, the ultrasonic motors we fabricated by some BNT ceramics were successfully rotated under the large amplitude driving around the resonance frequency. The maximum rotation-speeds of BNT-based ternary systems were lower than that in PZT but higher than that in BNT ceramic. From these results, BNT-based solid solution systems are one of good candidates for high-power piezoelectric applications.

2:30 PM

(EMA-S11-047-2016) Potassium-Sodium Niobate (KNN)–Based Piezo-/Ferroelectric Single Crystals

Z. Ye*[1]; J. Y. Wong[1]; N. Zhang[1]; 1. Simon Fraser University, Canada

The development of lead-free materials to replace lead-based piezo-/ferroelectrics has been intensified for obvious health and environmental reasons. $(K_{1-x}Na_x)NbO_3$ (KNN) solid solution is an interesting lead-free system as it has a high Curie temperature.It is also known to have a variety of oxygen octahedral tilts depending on K/Na ratio, especially in the Na-rich region. There are discrepancies in the Na-rich end as to whether it is of orthorhombic or monoclinic symmetry at room temperature. Thus, single crystals of KNN are needed to provide a better understanding on its structure. In this work, single crystals of $K_{0.1}Na_{0.9}NbO_3$ (KNN) and $0.98K_{0.8}Na_{0.2}NbO_3$ – $0.02LiNbO_3$ (KNN-LN) have been grown using a high-temperature solution growth method with K_2CO_3 and B_2O_3 as flux. Polarized light microscopy was used to study the Na-rich KNN crystals, and the phase diagram on the Na-rich end of the (1-x)$KNbO_3$ - x$NaNbO_3$ solid solution has been updated. With the intention of addressing the issue of composition segregation, a modified vapour transport equilibration technique has been developed and demonstrated to be a viable approach to increase the Li-content in the KNN-LN crystals. In addition, a new ternary solid solution of $y(K_{0.5}Na_{0.5})NbO_3$ – (1-y) $[(1-x)Bi_{0.5}K_{0.5}TiO_3$ – $xBaTiO_3]$ has been synthesized in the form of ceramics with compositions of y = 0.96 to y = 0.98 and its partial phase diagram has been established.

2:45 PM

(EMA-S11-048-2016) Field-induced structural diversity at the morphotropic phase boundary in $(Na_{1-x}K_x)_{0.5}Bi_{0.5}TiO_3$ perovskite solid solution

D. Suvorov*[1]; 1. Jozef Stefan Institute, Slovenia

Structural diversity of the $Na_{0.5}Bi_{0.5}TiO_3$ – $K_{0.5}Bi_{0.5}TiO_3$ perovskite solid-soultion system at the morphotropic phase boundary was studied by different in-situ diffraction methods. Electron diffraction of the $Na_{0.5}Bi_{0.5}TiO_3$ – $K_{0.5}Bi_{0.5}TiO_3$ (NBT – KBT) system, performed on mechanically thinned dimple-ground and ion-milled samples,

indicates that crystal structure of the perovskite solid solution on the KBT side changes from untilted polar tetragonal (P4mm) for KBT to in-phase tilted polar tetragonal (I4mm) in the vicinity of morphotropic boundary (0.8NBT – 0.2KBT). Furthermore imaging of individual grains of thus prepared thin foils with morphotropic composition exhibit well-defined lamellar domains characteristic for tetragonal structure in this system. On the contrary X-ray powder diffraction of morphotropic composition predominantly indicates presence of rhombohedral crystal structure. The XRD and TEM experiments suggest that in its "virgin" state the 0.8NBT – 0.2KBT solid solution exhibits pseudocubic crystal structure with nanosized rhombohedral and tetragonal polar regions that can be converted to either long-range ordered polar rhombohedral or tetragonal phase by mechanical operations such as grinding or polishing. To further study the phenomenon we employed in-situ electric field and uniaxial stress X-ray diffraction experiments.

3:00 PM

(EMA-S11-049-2016) A first-principles study of phase transition order in $Ba_xSr_{1-x}TiO_3$ solid solution

S. Binomran*[1]; I. Kornev[2]; L. Bellaiche[3]; 1. King Saud University, Saudi Arabia; 2. Laboratoire SPMS, UMR 8580 du CNRS, Ecole Centrale Paris, France; 3. University of Arkansas, USA

Most ferroelectric materials undergo a structural phase transition from a high- temperature non-polar (paraelectric) phase into a low-temperature polar (ferroelectric) phase. The temperature at which the transformation takes place is called the Curie point or the Curie temperature (and is usually denoted as T_c). The transition usually leads to strong anomalies in the dielectric, elastic and other properties of the material. Having such a property, ferroelectrics play a major role in technological applications. The aim of this work is thus to gain a deep understanding of phase transitions and to determine the nature of the critical behavior in BST system via the use of the first-principles-based effective Hamiltonian scheme combined with an efficient Monte Carlo technique. In particular, we aim to find out the tricritical point at which the system is at the border between first-order and second-order transitions of BST systems. By taking the advantages of the Wang-Landau algorithm that it can provide the free-like energy (A) and the internal energy (U), we can reveal the order of the phase transition: As a matter of fact, a first-order transition exhibits two minimum in the A-vs-U curve for temperatures close to Tc, while a second-order transition only has one minimum. This work is supported by the National Plan for Science, Technology and Innovation under the research project No. 11-ADV-1498-2.

Advanced Electronic Materials for Energy Storage

Room: Indian

Session Chairs: Rudeger (Derek) Wilke, Sandia National Laboratories; Eugene Furman

3:45 PM

(EMA-S11-050-2016) Fringing Field Effect on Ultrathin Glass Dielectrics (Invited)

J. Gao[2]; D. Kwon[2]; E. Furman*[2]; M. Lanagan[2]; B. Akkopru Akgun[2]; B. Balachandran[1]; S. Garner[3]; 1. Argonne National Laboratory, USA; 2. Pennsylvania State University, USA; 3. Corning Incorporated, USA

Ultrathin, flexible glass will be a strong competitor to polymers for the next generation of dielectrics to be used in extreme environments, such as capacitors for power converters in electric vehicles. The energy density is proportional to permittivity, which is obtained from capacitance measurement. In general, the capacitance value of a practical capacitor configuration is larger than that calculated from the conventional capacitance expression due to the fringing field effect. For example, in case of the parallel plate capacitor, the electric field does not end abruptly at the edge of the plates. Instead, a fringing field exists outside the plates, curving from one to the other. Thus, the practical capacitance is the sum of ideal capacitance (C_i) and fringing capacitance (C_f). In this work, the effects of fringing field on capacitance of ultrathin glass (100mm thick Corning® Willow® Glass) are systematically investigated with experimental measurements and numerical simulations. The fringing field effect on capacitance (C_f/C_i) increases as the area of the electrode diminishes, but it does not change very much among different electrode shapes. The fringing field effect on capacitance (C_f/C_i) is inversely proportional to the frequency of applied field, but it has no monotonous change as a function of the applied voltage.

4:15 PM

(EMA-S11-051-2016) Multi-layer Glass Capacitors with High Dielectric Energy Density

R. H. Wilke*[1]; H. J. Brown-Shaklee[1]; R. Johnson[1]; 1. Sandia National Laboratories, USA

Alkali-free glasses show immense promise as a potential high dielectric energy density storage material. Commercially available alumino-borosilicate compositions exhibit high breakdown strengths (exceeding 1000 MV/m), low loss (tan d < 0.01), modest relative permitivities (5-7), high dielectric energy storage densities (35 J/cc), and enhanced temperature stability up to 180 °C. In order to take advantage of the intrinsic properties of these materials it is necessary to develop processing and packaging strategies for fabricating devices with appreciable capacitance values. By utilizing the glass, rather than air or insulating fluid, to define the edge margins, significant improvements in the working energy density of the capacitor can be achieved. Sandia National Laboratories is a multi-program laboratory managed and operated by Sandia Corporation, a wholly owned subsidiary of Lockheed Martin Corporation, for the U.S. Department of Energy's National Nuclear Security Administration under contract DE-AC04-94AL85000.

4:30 PM

(EMA-S11-052-2016) Nanoscale Mapping of Current Transport Pathways

Y. Kutes[1]; J. Luria[1]; A. Moore[3]; E. Stach[4]; N. Padture[2]; B. D. Huey*[1]; 1. University of Connecticut, USA; 2. Brown University, USA; 3. Colorado State University, USA; 4. Brookhaven National Laboratory, USA

It is crucial to be able to investigate transport pathways in advanced electronics in order to optimize their design, processing, and functionality. One common approach is conducting atomic force microscopy, which has long been implemented for measuring currents in semiconductors and interconnects. By performing such measurements during in situ illumination, photocurrent transport can also be mapped and investigated spectroscopically. However, measurements with CdTe solar cells reveal not just extensive variations in local photovoltaic performance for distinct grains and grain boundaries, but also a strong sensitivity to the presence of planar defects such as stacking faults and twins. Similar studies on $MAPbI_3$ molecular perovskites also identify unexpectedly strong inter, and intra, granular variations. Comparing these results with local TEM, as well as macroscale performance measures, ultimately provides valuable insight into the profound structure-property relationships even down to the nanoscale. This suggests several pathways towards improving thin film solar cell systems, but the method and approach is more generally applicable to a wide range of transport measurements in nano- and micro- structured advanced electronic materials.

4:45 PM

(EMA-S11-053-2016) Visible Light Absorption in Semiconducting Ferroelectric Perovskites Designed for Photovoltaic Applications

L. Wu*[1]; A. R. Akbashev[2]; D. Imbrenda[2]; J. E. Spanier[1]; P. K. Davies[1]; 1. University of Pennsylvania, USA; 2. Drexel University, USA

The bulk photovoltaic effect (BPE) in ferroelectric materials has been extensively studied for both its underlying physics and

applications in solar energy conversion. Perovskite solid solutions in the $[KNbO_3]_{1-x}[BaNi_{1/2}Nb_{1/2}O_{3-d}]_x$ (KBNNO) system were recently shown to lower the bandgap of the parent $KNbO_3$ end member and promote photocurrent generation across the solar spectrum. In this work, we explored the responses of new acceptor-doped and donor-acceptor co-doped $BaTiO_3$ ferroelectrics. While partial substitution of Ti by acceptor ions promotes strong visible light absorption it also stabilizes the hexagonal polymorph of $BaTiO_3$. To promote formation of a ferroelectric polymorph and induce the BPE in $BaTiO_3$-based ferroelectrics, a series of annealing and quenching procedures was used to stabilize the tetragonal form of the acceptor-doped $BaTiO_3$ while retaining strong visible light absorption. The absorption intensity of donor-acceptor co-doped $BaTiO_3$ in the 400 nm to 800 nm range also responded to alterations in the ratio of acceptor to donor ions. Bulk ceramic specimens were used as targets for the fabrication thin films by pulsed laser deposition. The photocurrent measurements, phase stability and photovoltaic response of the bulk and thin film specimens will be discussed.

5:00 PM

(EMA-S11-054-2016) Energy storage materials with nano-encapsulated inclusions of a low-melting metal

A. Abraham*[1]; E. Dreizin[1]; M. Schoenitz[1]; 1. New Jersey Institute of Technology, USA

Metal based energy storage materials (ESM) have advantages of high thermal conductivity and high strength. One of the main challenges in designing such materials is to contain the low-melting metal, serving as an energy storage medium, upon its heating. Containment of liquid metals is difficult; often bulk containers are used, limiting the types of manufactured structures. Here, an ESM is prepared and characterized with low-melting metal inclusions encapsulated in thin inert oxide shells within a more refractory (metal/ceramic matrix) material. Bi is selected as a low-melting metal. Similarly, Sn, In, or other low melting metals can be used. Bi inclusions are encapsulated in Al2O3 shells within an Al/Al2O3 matrix. ESM is prepared by annealing of a precursor composite manufactured by ball milling. Final ESM is a powder, which is readily consolidated. Both, thermal and mechanical stability are presented. ESM is compared to two reference composites without encapsulation. Molten Bi is redistributed within the reference material at the surface. Encapsulated Bi remains inside the composite matrix even after the Bi melting point is substantially exceeded. Materials with and without nano-encapsulated Bi behave qualitatively different upon mechanical loading at different temperatures. The material with encapsulated inclusions is much stronger than its counterpart, with nominally the same bulk composition.

Author Index

G

H

I

J

K

Author Index

L

M

N

O

Author Index

2016

The American Ceramic Society
www.ceramics.org

Meetings & Expositions of THE AMERICAN CERAMIC SOCIETY

JANUARY 24 – 29
40TH INTERNATIONAL CONFERENCE AND EXPO ON ADVANCED CERAMICS AND COMPOSITES (ICACC'16)
Hilton Daytona Beach Resort/Ocean Walk Village
Daytona Beach, FL USA

MARCH 29 – 31
ST. LOUIS SECTION/RCD 52ND ANNUAL SYMPOSIUM
St. Louis, MO USA

APRIL 7 – 11
INTERNATIONAL COMMISSION ON GLASS XXIV INTERNATIONAL CONGRESS 2016
Shanghai, China

APRIL 17 – 21
MATERIALS CHALLENGES IN ALTERNATIVE & RENEWABLE ENERGY (MCARE 2016)
Hilton Clearwater Beach Resort
Clearwater, FL USA

APRIL 24 – 26
5TH CERAMIC LEADERSHIP SUMMIT, IN CONJUNCTION WITH CERAMICS EXPO (CLS 2016)
Cleveland, OH USA

APRIL 26 – 28
2ND CERAMICS EXPO
Cleveland, OH USA

MAY 2 – 4
STRUCTURAL CLAY PRODUCTS DIVISION
North Canton, OH USA

MAY 22 – 26
GLASS & OPTICAL MATERIALS DIVISION MEETING (GOMD 2016)
The Madison Concourse Hotel and Governor's Club
Madison, WI USA

JUNE 26 – JULY 1
9TH INTERNATIONAL CONFERENCE ON HIGH TEMPERATURE CERAMIC MATRIX COMPOSITES (HTCMC 9)
Toronto Marriott Downtown Eaton Centre Hotel
Toronto, Ontario Canada

JULY 11 – 13
7TH ADVANCES IN CEMENT-BASED MATERIALS (CEMENTS 2016)
Northwestern University
Evanston, IL USA

JULY 28 – JULY 31
INNOVATIONS IN BIOMEDICAL MATERIALS AND TECHNOLOGIES
Rosemont Hyatt
Chicago, IL USA

JULY 31 – AUGUST 5
GORDON RESEARCH CONFERENCE ON CERAMICS AND SOLID STATE STUDIES
Mount Holyoke College
MA USA

AUGUST 21 – 26
INTERNATIONAL CONGRESS ON CERAMICS (ICC6)
Dresden, Germany

OCTOBER 23 – 27
MATERIALS SCIENCE & TECHNOLOGY 2016, COMBINED WITH ACERS 118TH ANNUAL MEETING (MS&T16)
Salt Palace Convention Center
Salt Lake City, UT USA

H																	He
Li	Be											B	C	N	O	F	Ne
Na	Mg											Al	Si	P	S	Cl	Ar
K	Ca	Sc	Ti	V	Cr	Mn	Fe	Co	Ni	Cu	Zn	Ga	Ge	As	Se	Br	Kr
Rb	Sr	Y	Zr	Nb	Mo	Tc	Ru	Rh	Pd	Ag	Cd	In	Sn	Sb	Te	I	Xe
Cs	Ba	La	Hf	Ta	W	Re	Os	Ir	Pt	Au	Hg	Tl	Pb	Bi	Po	At	Rn
Fr	Ra	Ac	Rf	Db	Sg	Bh	Hs	Mt	Ds	Rg	Cn	Uut	Fl	Uup	Lv	Uus	Uuo

Ce	Pr	Nd	Pm	Sm	Eu	Gd	Tb	Dy	Ho	Er	Tm	Yb	Lu
Th	Pa	U	Np	Pu	Am	Cm	Bk	Cf	Es	Fm	Md	No	Lr

Now Invent.™